

Cranfield University

Cranfield University at Silsoe

NSRI

M.Sc. by Research  
2005

Dirk Ansorge

Comparison of Soil Compaction below  
Wheels and Tracks

Supervisor:

Prof. Richard J. Godwin

19<sup>th</sup> of October 2005

This thesis is submitted in partial fulfillment of the requirements for the Degree of Master of Science by Research.

ProQuest Number: 10832236

All rights reserved

INFORMATION TO ALL USERS

The quality of this reproduction is dependent upon the quality of the copy submitted.

In the unlikely event that the author did not send a complete manuscript and there are missing pages, these will be noted. Also, if material had to be removed, a note will indicate the deletion.



ProQuest 10832236

Published by ProQuest LLC (2018). Copyright of the Dissertation is held by Cranfield University.

All rights reserved.

This work is protected against unauthorized copying under Title 17, United States Code  
Microform Edition © ProQuest LLC.

ProQuest LLC.  
789 East Eisenhower Parkway  
P.O. Box 1346  
Ann Arbor, MI 48106 – 1346

## ABSTRACT

This study investigated the effect of high axle loads carried on self propelled wheels and tracks on soil bulk density, soil deformation, rut depth, and penetrometer resistance under controlled laboratory conditions. Furthermore pressure distribution below a three and a two idler track was measured. A brief field study was also conducted to compare the results gained under laboratory conditions.

The benefit of the "Terra Trac" driving systems compared to wheel type systems was clearly shown in uniform and stratified soil conditions. Soil deformation was reduced to 50 % for the tracks compared to the wheels at an overall load of 12 t and 10.5 t, respectively. Penetrometer resistance showed a very high resistance close to the surface for the tracks. In uniform soil conditions there was no significant increase in penetrometer resistance compared to the control below 400 mm depth.

Reducing the inflation pressure to half the recommended inflation pressure reduced soil deformation by 25 %. Three passes of a tire increased soil density by 20 % compared to a single pass.

The three idler track showed only a 50 % increase in pressure from the front to the rear sprocket compared to a 100 % increase for the two idler track. Single peaks in pressure below each idler were less pronounced for the three idler track. Unfortunately the advantage in the pressure distribution for the three idler track did not lead to significant improved behavior concerning soil compaction.

The advantage of a tracked combine compared to a wheeled combine is also shown in field measurements. The root system of oil seed rape in former track ruts is more developed than in former wheel ruts.

Soil physical properties after the passage were compared to the predictions of two models. The tendency was correct, however the real values were largely offset.

## TABLE OF CONTENTS

ABSTRACT .....	I
TABLE OF CONTENTS .....	II
LIST OF FIGURES .....	V
LIST OF TABLES .....	VII
NOMENCLATURE .....	VIII
1 INTRODUCTION .....	2
2 PROJECT DESCRIPTION .....	3
3 LITERATURE REVIEW .....	4
3.1 Soil Compaction .....	4
3.2 Soil Compaction – Consequences .....	7
3.3 Tracks compared to Wheels .....	9
3.4 Loosening Soil Compaction .....	12
3.5 Conclusions .....	13
4 EXPERIMENTAL OVERVIEW .....	14
4.1 Laboratory Studies .....	14
4.1.1 Soil Compaction Below Pulled Wheels .....	14
4.1.2 Soil Compaction Below Self Propelled Tracks and Wheels .....	14
4.1.3 Multi Pass Effect and Pressure Distribution .....	15
4.2 Field Studies .....	16
4.2.1 Tracks vs. Wheels (2004 – 2005 Crop Season) .....	16
4.2.2 Tracks vs. Wheels (2005 Harvest) .....	16
5 DETAILS OF LABORATORY STUDIES .....	19
5.1 Soil Conditions .....	19
5.2 Tire and Tracks .....	20
5.3 Description of the Measurement Devices .....	20
5.3.1 Dry Bulk Density .....	20
5.3.2 Rut Characteristics .....	21
5.3.3 Soil Displacement .....	22
5.3.4 Cone Penetration Resistance .....	29
5.3.5 Draught Force Measurement and Slip Measurement .....	32
5.3.6 Profile .....	33

5.3.7 Pressure Transducer .....	33
5.4 Single Wheel Tester .....	33
5.5 Statistical Analysis .....	35
6 RESULTS AND DISCUSSION OF RESULTS .....	36
6.1 Soil Compaction caused by towed Wheels .....	36
6.1.1 Penetration Resistance Results .....	37
6.1.2 Soil Displacement .....	38
6.1.3 Dry Bulk Density .....	41
6.1.4 Rut Depth .....	42
6.1.5 Rolling Resistance .....	43
6.2 Soil Compaction Caused by Driven Wheels and Tracks .....	43
6.2.1 Penetration Resistance .....	43
6.2.2 Soil Deformation.....	47
6.2.3 Average Dry Bulk Density .....	51
6.2.4 Rut Characteristics .....	53
6.3 Soil Compaction in Stratified Soil Conditions.....	55
6.3.1 Penetration Resistance .....	55
6.3.2 Soil Deformation.....	58
6.3.3 Dry Bulk Density .....	59
6.3.4 Rut characteristics.....	60
6.4 Multi Pass Effect .....	61
6.4.1 Penetrometer Resistance .....	61
6.4.2 Soil Deformation.....	62
6.4.3 Dry Bulk Density .....	63
6.4.4 Rut Characteristics .....	63
6.5 Pressure Distribution Below Tracks and the 800 mm Section Tire .....	64
6.6 Field Measurements .....	65
6.6.1 Tracks vs. Wheels (2004 – 2005 Crop season).....	65
6.6.2 Tracks vs. Wheels in Harvest Season 2005 .....	73
7 SOIL COMPACTION MODELS – APPLICATION AND DISCUSSION .....	76
7.1.1 O’Sullivan’s Model.....	76
7.1.2 SOCOMO a SOil COMpaction MOdel: .....	81
8 DISCUSSION OF RESULTS .....	86
8.1 Soil Compaction Below Wheels and Tracks.....	86
9 CONCLUSIONS.....	91
10 FURTHER REQUIREMENTS AND PRACTICAL SUGGESTIONS.....	93
11 BIBLIOGRAPHY .....	94

---

12	ACKNOWLEDGEMENTS .....	105
13	APPENDIX.....	106
13.1	Data of Soil Compaction Studies .....	106
13.1.1	Average Penetrometer Resistance .....	106
13.1.2	Soil Profile Pictures .....	114
13.1.3	Average Soil Displacement Diagrams .....	121
13.2	Single Wheel and Track Test Frame (submitted as M.Sc. Thesis at University of Hohenheim) .....	128

## List of Figures

<b>Figure 1:</b>	Relationship between soil dry density and dry matter of corn crop yields.....	8
<b>Figure 2:</b>	Pressure distribution below a tracked tractor during ploughing .....	10
<b>Figure 3:</b>	Drawing of field layout and combine harvester tracks .....	18
<b>Figure 4:</b>	Proposed soil profile for stratified soil conditions.....	20
<b>Figure 5:</b>	Talcum powder stripes in preparation in the soil bin included.....	23
<b>Figure 6:</b>	Vertical cut in soil bin showing white talcum dots and across the soil bin .	23
<b>Figure 7:</b>	Draw string transducer on frame in soil bin.....	25
<b>Figure 8:</b>	2 <sup>nd</sup> Replication of vertical cut for the 800 mm section width tire run .....	26
<b>Figure 9:</b>	2 <sup>nd</sup> Replication of tire with section width 800 mm run at 1.25 bar and.....	26
<b>Figure 10:</b>	Movement of position of talcum powder points during the 900/10.5/1.9 ....	27
<b>Figure 11:</b>	Movement of position of talcum powder points during the multi pass .....	28
<b>Figure 12:</b>	Movement of position of talcum powder points during the t3/12 .....	28
<b>Figure 13:</b>	Example penetrometer resistance across the soil bin .....	30
<b>Figure 14:</b>	Average of the left and right hand side together in the soil bin.....	31
<b>Figure 15:</b>	Average of curves 4+7 and 5+6 from <b>Figure 11</b> .....	32
<b>Figure 16:</b>	Single wheel tester over soil bin with a 900 mm section width tire inside...	34
<b>Figure 17:</b>	Average penetrometer resistance vs. depth for towed tires .....	37
<b>Figure 18:</b>	Soil Displacement vs. depth on low and medium soil bearing capacity .....	39
<b>Figure 19:</b>	Relative decrease from initial to final layer thickness .....	40
<b>Figure 20:</b>	Penetrometer resistance below tracks and tires including control .....	44
<b>Figure 21:</b>	Average penetrometer resistance vs. depth for all tires .....	44
<b>Figure 22:</b>	Penetrometer resistance below tracks including control and LSD .....	46
<b>Figure 23:</b>	Vertical cut through soil with points of talcum powder .....	47
<b>Figure 24:</b>	Average position of the displaced talcum powder points .....	48
<b>Figure 25:</b>	Soil deformation for all devices including LSD at given depth .....	48
<b>Figure 26:</b>	Soil deformation for the tires .....	49
<b>Figure 27:</b>	Soil deformation for the two and three idler track .....	50
<b>Figure 28:</b>	DBD initially and finally measured .....	51
<b>Figure 29:</b>	Initial penetrometer resistance in soil bin preparation .....	56
<b>Figure 30:</b>	Initial and final penetrometer resistance on stratified soil conditions .....	57
<b>Figure 31:</b>	Initial and final penetrometer resistance on stratified soil conditions .....	57
<b>Figure 32:</b>	Soil deformation on stratified soil conditions .....	58

---

<b>Figure 33:</b>	Initial and final dry bulk density .....	60
<b>Figure 34:</b>	Penetrometer resistance initially, after 1 pass, 2 passes and 3 passes.....	61
<b>Figure 35:</b>	Vertical soil deformation after one and three passes of the 900/10.5/1.9.....	62
<b>Figure 36:</b>	Dry bulk density initially, after one pass and after three passes .....	63
<b>Figure 37:</b>	Pressure distribution .....	64
<b>Figure 38:</b>	Penetrometer resistance over depth .....	66
<b>Figure 39:</b>	Biomass for control, track and wheel rut .....	67
<b>Figure 40:</b>	Differences in inter row emergence of rape due to harvest .....	68
<b>Figure 41:</b>	Differences in inter row emergence of rape due to harvest .....	68
<b>Figure 42:</b>	Flowering rape field harvested with a tracked combine harvester .....	69
<b>Figure 43:</b>	Flowering rape field harvested with a wheeled combine harvester .....	70
<b>Figure 44:</b>	Root development down to C – horizon in former track rut center .....	71
<b>Figure 45:</b>	Differences in root development.....	72
<b>Figure 46:</b>	Plants with restricted root development in 100 mm distance .....	73
<b>Figure 47:</b>	Penetrometer resistance vs. depth for the tracks vs. wheels .....	74
<b>Figure 48:</b>	Dry bulk density for field measurements during harvest 2005.....	75
<b>Figure 49:</b>	$v$ vs. $\ln(p)$ – diagram.....	79
<b>Figure 50:</b>	Predicted vs. measured deformation.....	80
<b>Figure 51:</b>	Estimated pressure distribution below 680/10.5/2.2.....	83
<b>Figure 52:</b>	Estimated pressure distribution below 800/10.5/1.25.....	83
<b>Figure 53:</b>	Estimated combined failure area for 680/10.5/2.2.....	84
<b>Figure 54:</b>	Estimated combine failure area for 800/10.5/1.25.....	84



**LIST OF TABLES**

<b>Table 1:</b>	Wheels, tracks, and loads used in soil bin investigation .....	15
<b>Table 2:</b>	Wheel, track and loads used for stratified soil conditions .....	15
<b>Table 3:</b>	Cohesion and angle of internal friction for different dry bulk densities.....	19
<b>Table 4:</b>	Dry bulk density values for initial and final soil conditions.....	42
<b>Table 5:</b>	Rut parameters including pooled SE for 800/8.5/2.5t .....	42
<b>Table 6:</b>	Statistical summary of penetrometer resistance for self propelled tires .....	45
<b>Table 7:</b>	Statistical summary of penetrometer resistance for tracks .....	47
<b>Table 8:</b>	Dry bulk density for self propelled experiments.....	52
<b>Table 9:</b>	Rut depth, width, and area of tires and tracks including LSD .....	53
<b>Table 10:</b>	Rut depth in areas without lug influence .....	55
<b>Table 11:</b>	Contact patch geometry of the tires .....	55
<b>Table 12:</b>	Rut characteristics for stratified soil conditions .....	60
<b>Table 13:</b>	Rut Characteristics for the 900/10.5/1.9 after one, two and three passes .....	64
<b>Table 14:</b>	Contact area of tires estimated and measured.....	79

**NOMENCLATURE**

## Abbreviations:

CI	Confidence Interval
DF	Degrees of Freedom
GLM	General linear model
LSD	Least Significant Difference
n	Number of observations
p	Probability
SE	Standard Error
t	t-statistic

## Units:

h	Hour
J	Joule
l	Liter
m	Meter
m <sup>2</sup>	Square meter
m <sup>3</sup>	Cubic meter
mol	Mol equals $6.02 \cdot 10^{23}$ molecules
N	Newton
Pa	Pascal = [N/m <sup>2</sup> ]
ppm	Parts per million
s	Seconds

## Factors:

mega (M)	10 <sup>6</sup>
kilo (k)	10 <sup>3</sup>
centi (c)	10 <sup>-2</sup>
milli (m)	10 <sup>-3</sup>
micro (μ)	10 <sup>-6</sup>

## 1 INTRODUCTION

Cereal farmers are under significant pressure at the moment due to a reduction in product related subsidies and a low world market prize for cereals. As a consequence farmers have the options either to grow in size and raise productivity and lower costs or to shut down. A third possibility may develop when the subsidies are transferred from being product related to being field related in order to avoid a landscape which is not attractive to tourism as well as the people living in it. Therefore areas with a low agricultural productivity due to soil and / or climatic factors limiting the productivity might be run by farmers getting subsidies for maintaining a certain landscape and ecosystem rather than for producing a certain crop. Yet, as these are only plans at the moment, farmers have to rely on expansion and their productivity to ensure their income. In order to gain income with a given amount of producer goods productivity has to increase.

Productivity can either be gained by more efficient machinery using more sophisticated technology or as a result of using the economy of scales. When using the economy of scales approach machinery has to grow because the bigger the machinery the more efficient it can be used as the fixed costs stay constant per unit of product. One example would be if it was possible to replace two combine harvesters with one bigger machine. Then the farmer gained the economy of scales effect because of lower fixed costs (only one person, only one building and so on). Yet larger machinery tends to mean heavier machinery and the threat of soil compaction increases.

This threat has lead to a discussion about the limitation of wheel and axle loads of agricultural machinery allowed on fields in Germany. In discussion is a limit for wheel loads of 3t which would basically ban all harvest machinery from the fields. Yet according to Kirchmann and Thorvaldsson (2000) "Innovation, creative solutions and discoveries based on natural science will be helpful in the development of sustainable agriculture, but not methods based on dogmatism". In this context a mere wheel load restriction can not be the answer because it doesn't take important soil parameters into account.

Concerning soil compaction many studies have been carried out. The general outcome as well as the work being related to this study is summarized in the literature review.

## 2 PROJECT DESCRIPTION

The aim of the work reported in this thesis was to conduct an independent fundamental study into the effect on soil compaction of self propelled wheels and tracks, loaded to 10-12 t, on both uniform and stratified soil conditions.

The objectives are to determine:

1. The relative effect of a range of tire sizes and track specifications on changes to soil density, penetrometer resistance, soil deformation, and rut depth when loaded to the same overall weight.
2. The effect of the above on uniform and stratified soil conditions.
3. To make recommendations for future practical developments.

The pressure distribution below a track unit should be investigated using cylindrical pressure transducers and the results should be compared to the assumed distribution. Further investigations into multi pass effects of high axle load should be useful. Measurements with a tracked and a wheeled combine harvester in the field were to be done in order to validate the results from the soil bin investigations.

Throughout an extended literature review the author was not able to find investigations being done into an axle load higher than 10 t in laboratory conditions and most in - field investigations. Some investigations were using axle loads up to 20 t, but end at a soil depth of 300 – 400 mm and thus are not able to detect subsoil compaction. The investigation of both higher axle load and particularly subsoil compaction will be the main task in this thesis.

The study will be carried out at the National Soil Resource Institute at Cranfield University at Silsoe (CU@S).

### 3 LITERATURE REVIEW

This section reviews papers and articles on the general topic of soil compaction and its effects on yield and on methods to reduce or ameliorate soil compaction.

#### 3.1 Soil Compaction

There are many definitions of soil compaction, however the most appropriate one in context with this work was given by the Soil Science Society of America (1996). According to them soil compaction is “the process by which the soil grains are rearranged to decrease void space and bring them into closer contact with one another, thereby increasing bulk density”.

The relationship between dry bulk density and mean normal stress as well as shear stress was shown by Vanden Berg, (1966). Basic work concerning stress distribution in the soil due to surface loadings was done by Soehne (1958). According to him soil stress close to the surface is determined by the inflation pressure whereas soil stress in deeper layers depends upon the amount of wheel load. Smith and Dickson (1990) supported these findings.

Under the definition of soil compaction given above any force applied to a soil exceeding its initial strength therefore causes soil compaction. Initial soil strength in civil engineering can be calculated according to the bearing capacity equation given by Terzaghi and Peck (1967). Under agricultural circumstances this equation is not easy to use as the necessary parameters are difficult to identify and can be highly variable over the area of a field. Soil strength or bearing capacity at a given soil water content depend on soil structure, organic matter content, and particle size distribution as these are affecting internal friction and cohesion. Assuming there is only one soil type in a field, these soil parameters can be regarded as being normally fairly uniform within a field and over time as these parameters do not change within a soil type. But they depend on soil water content, too. Water content may vary within a field and over time, resulting in different cohesion values thereby changing soil strength. Therefore calculating bearing capacity and predicting the occurrence of soil compaction is not reliably possible, although there are models available (Gassman et al., 1989; Bailey et al., 1995; O’Sullivan et al., 1999; Berli et al., 2003; Horn

and Fleige, 2003; Mouazen et al., 2003; Podt et al., 2003; van den Akker, 2004). The amount to which a tire at given load and soil conditions causes soil compaction depends on its carcass stiffness, inflation pressure, diameter and section width. The more flexible the carcass, the more load is carried by the rolling surface and not on the edges of the carcass. Lower inflation pressure increases contact area and increases tire flexibility. The larger the diameter of a tire or the wider it is, the larger its foot print becomes which increases the area carrying the load. As a consequence inflation pressure can be reduced resulting in a decreased contact pressure and thus less compaction. Much work showing the connection between soil compaction and inflation pressure was done in Auburn, Alabama at the National Soil Dynamics Laboratory by Raper and his colleagues (Raper et al., 1995; Raper et al., 1993; Raper et al., 1993; Bailey et al., 1993, Way et al., 1996). Their findings support the results from earlier work done by Raghavan et al. (1976). A smaller section width can reduce soil compaction when the area lost thereby is made up by a bigger wheel diameter (Bekker, 1956, Hakanson et al., 1988). In addition wheel slip increases soil compaction as soil particles are sheared against each other and thereby pores are diminished more effectively than without slip (Davis et al., 1973).

So the principal mechanical parameters are understood. For a detailed explanation of soil mechanics and soil dynamics refer to Gill and Vanden Berg (1968) and McKyes (1985). Yet the conclusions on appropriate inflation pressure as well as axle load for given soil conditions and their causing of significant soil compaction vary from author to author. Two examples are:

1. Beet et al. (2000) state that with an inflation pressure of 100 kPa (1 bar) up to 16.5t axle loads are acceptable for all soil conditions as agricultural soils can withstand this without excessive rut formation and/or subsoil compaction. On dry soil the acceptable pressure is even 150 kPa (1.5 bar) for up to 12.5t axle load, however an inflation pressure of 200 kPa (2 bar) is too high for all conditions.
2. Load recommendations in Sweden are 6t for a single axle and 8t for a tandem axle in order to keep the maximum of soil compaction within the top 40cm. Merely with an inflation pressure smaller than 80 kPa (0.8 bar) more load would be acceptable (Eriksson et al., 1974).

In field measurements soil compaction could not be detected below a combine harvester in the subsoil for moist conditions because it was already compacted by previous field work (Dickson, 1994). These findings are supported by Hadas (1994) who states that many data suggesting soil compaction can be interpreted differently and thus are showing other influences than soil compaction affecting measured parameters in fields. The author refers to both a high natural variability in measured dry bulk density which was ignored in one particular paper.

Yet Arvidsson et al. (2001) and Trautner and Arvidsson (2003) detected soil compaction by measuring soil displacement and penetrometer resistance caused by axle loads of 20 t of a sugarbeet harvester. Yavuzcan et al. (2004) detected soil compaction, e.g. increase in dry bulk density and reduced porosity down to 0.3 – 0.4 m in normal field conditions during sugarbeet harvest with similar loads as were used previously in southern Germany.

While there are disagreements and discussions about the intensity of soil compaction and its connection with axle load as well as inflation pressure, there is agreement that increasing load or contact surface results in deeper located soil compaction for the same contact pressure (Soane et al., 1981 and Grecenko, 2003). In laboratory conditions this can be proven, yet in the field it is much more difficult due to inherent soil structure, macropores, and soil water content (Hadas, 1994).

There is as well an ongoing discussion about establishing limits for axle loads and contact pressures. While improved efficiency in the short term is an interest of the farmer, long term productivity as well as the reduction of negative impacts of crop production on the environment is a concern for the society as a whole and thus should be discussed on a large scale (Hakansson and Medvedev, 1995). A summary of proposals for inflation pressure, contact area pressure, and wheel load is given by Alakakku et al. (2003). Keller and Arvidsson (2004) come to the conclusion, that soil stress is a function of wheel load, wheel arrangement, tire inflation pressure, contact stress distribution, and soil conditions. Therefore it depends on the particular tire properties and it is not a simple function of axle load and total vehicle load. Thus these authors are driving towards the same direction as Alakakku et al. (2003) in their summary of proposals and against the establishment of mere axle load limitations.

### 3.2 Soil Compaction – Consequences

As already mentioned in the definition of soil compaction the first consequence is an increase in bulk density due to the pores which are lost or at least reduced in volume in the process of compaction. Due to the reduced porosity infiltration rate is reduced and as a consequence surface run off may happen and cause soil erosion. This is especially dangerous during the time when no plants cover soil and no roots support its strength (Young and Voorhees, 1982). By reducing the pore volume soil conditions can become anaerobic as the oxygen / carbon dioxide exchange is retarded affecting crop growth conditions. This is a particular problem when the soil moisture content rises. Thereby physical properties change chemical properties of the soil as well and may cause nitrogen losses due to anaerobic conditions. Reduced porosity restricts root growth as well (Hakanson et al., 1988). Soane and van Ouwerkerk (1995) in their paper “Implications of soil compaction in crop production for the quality of the environment” gave a summarizing analysis of all the above. Yet, a recent publication by Shestak and Busse (2005) arrives at the conclusion that compaction alters soil physical properties but not the biological health of a soil. However, the work was done with very loose soil ( $0.8 - 1.4 \text{ g/cm}^3$ ) which came originally from a forest.

In this discussion one should not forget that some soil compaction is necessary for a good seedbed preparation in order to ensure good soil, nutrient, water, and thermal contact with the germinating seed. This carries all the way to the yield where for each species there is an optimum soil density for maximum yield. Is the density lower yield reduces, is it higher yield reduces as well (Soane, 1985). The particular relationship between corn crop yields and dry bulk density of the 0 – 200 mm layer of a sandy loam soil is shown in **Figure 1** by Negi et al. (1981). Hereby maximum yield is reached at about  $1.36 \text{ g/cm}^3$  dry bulk density. For both a higher and lower dry bulk density yield is reduced.



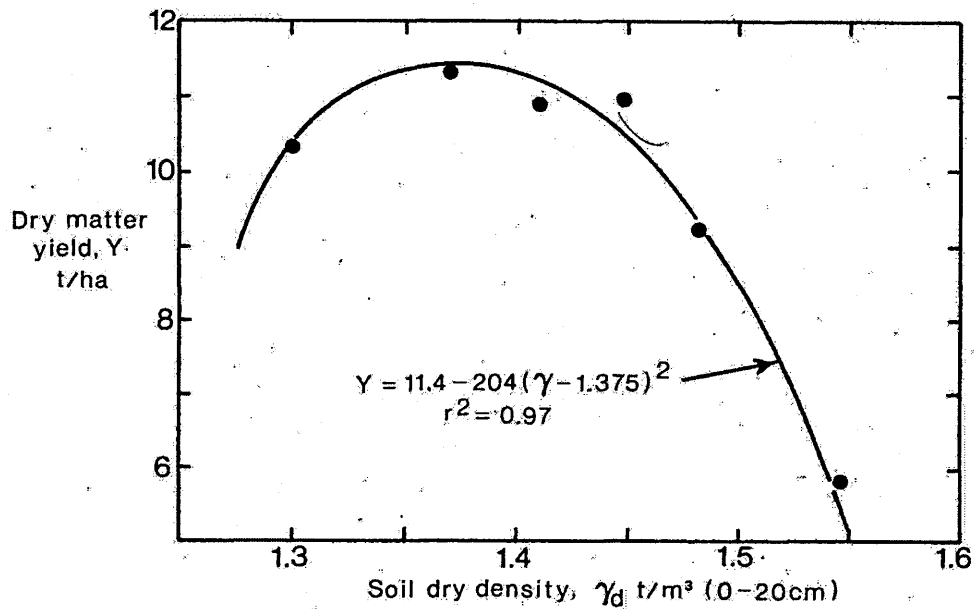


**Figure 1:** Relationship between soil dry density and dry matter of corn crop yields (Negi et al., 1981).

Not only plants are affected by soil compaction, but any subsequent tillage operation as well. A change in bulk density from 1.4 g/cm<sup>3</sup> to 1.65 g/cm<sup>3</sup> increases tractive resistance for ploughing from approximately 40 kN/m<sup>3</sup> to 90 kN/m<sup>3</sup>. This in turn increases fuel consumption for ploughing by 80% (Birkas et al., 1992). Chamen and Audsley (1993) confirmed the increase in energy demand due to soil compaction. Chamen (1996) found a higher energy efficiency for pulled tine implements than for power harrows as these were not able to produce a higher yield while consuming more energy.

As the necessary soil compaction mentioned above is easily achieved in normal field operations and often already exceeded, yields improve with a decrease in soil compaction. Chamen et al. (1988) detected a statistically significant greater yield in winter wheat for plots wheeled at 50 kPa than for normally wheeled plots at 250 kPa. Thus inflation pressure as well as tire load affect yield. In wet years yield differences are larger than in dry years as with increasing soil water content soil compaction increases as well. Findings by Vorhees (1986), Erbach et al. (1988), Hakansson et al. (1988), and Erbach et al. (1991) arrive at the same conclusion that reduced contact pressure increases yield. Using 10 and 20 t axle load in these investigations resulted in 9 % and 26 % yield reduction, respectively, compared to a standard treatment with no more than 5 t per axle (Voorhees and Lindstrom, 1983). Gameda et al. (1983) even reported 40% yield loss in an axle weight

range of 10 – 20t on clay soil. Yet on a silty clay loam Melvin et al. (1994) report less yield reduction by axle loads up to 18 t in maize than expected. In their study in central North America only one out of three compacted sites showed a significant reduction in yield after compaction and this only for one year after the compaction treatment. On one site soil may have been loosened again due to soil cracking. For all sites other yield limiting factors such as moisture stress may have had more influence than soil compaction, thereby diminishing the effect of soil compaction on yield.

In a review of soil compaction and its implications on crop growth and soil physical properties by Lipiec and Hatano (2003) indicators and methods used to quantify the effects of soil compaction on soil physical properties and crop growth are listed. The conclusion of their work states that more research needs to be done in relation to structural discontinuities caused by soil compaction and their implication on plant growth and physical soil conditions.

There are several reviews of soil compaction in literature, all summarizing the findings and work done at the time of publication as well as the inconsistent results mentioned above. (Soane, 1980; Soane et al., 1980/81; Soane et al., 1981; Soane, 1985; Soane and Ouwerkerk, 1994; Horn et al., 2000 and Hamza and Anderson, 2004). Especially Hamza and Anderson (2004) point out that ways have to be found to reduce soil compaction in order to maintain soil productivity and reduce soil deterioration. Soil compaction results from heavier machinery which is used in order to try to improve productivity but on the other hand, the machinery reduces productivity by soil compaction.

### **3.3 Tracks compared to Wheels**

Tracks are beneficial compared to wheels (Erbach, 1994). However, they can cause a higher soil compaction than ideally assumed for several reasons: a) calculated contact pressure is smaller than for a wheel, but applied for a longer time period; b) depending on the idler configuration and especially for track belts with inadequate tension non uniform pressure distribution may result which causes higher pressures under certain areas of the track and hence greater soil compaction c) vibrations from the engine and other machine parts

are better transmitted into the soil on tracks because of less efficient suspension (Culshaw, 1986; Erbach 2000).

Unequal weight distribution and changing actual weight distribution during heavy towing work have to be avoided in order to load the track evenly over the whole length. Otherwise contact pressure increases unnecessarily and causes more soil compaction than necessary (Weissbach, 2003; Keller et al., 2002; Tijink, 2000). The soil stress below the tracked tractor during ploughing used by Keller et al. (2003) is shown in **Figure 2**. The dashed line shows the pressure in the soil initially and the solid line after lowering the point of application of the draught force from the plough. It is interesting to note the difference in the average ground pressure for both settings. Calculating the approximate average ground pressure from the diagram it is 96 kPa initially and 76 kPa after the adjustment. Calculated average ground pressure is 43 kPa. The difference between the average calculated and measured ground pressure can be due to either non uniform load distribution across the belt or the pressure distribution in the soil itself. A mere offset in the pressure transducers might be another reason. However, the difference between the dashed and solid line is more difficult to explain as total machine weight did not change. So merely load transfer from the plough onto the tractor could have caused this difference. Unfortunately, the authors did not give enough information concerning plough settings to verify this. For combine harvesters pressure distribution is not as crucial as for tractors due to their different working requirements and because they are not designed to pull heavy implements.

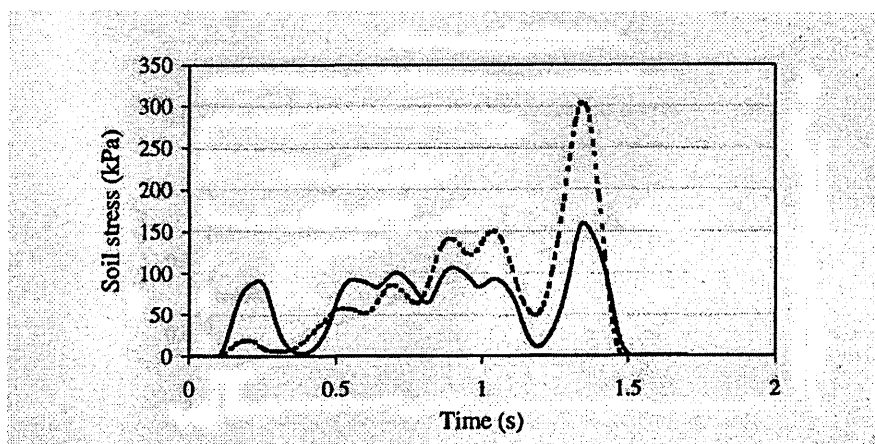


**Figure 2:** Pressure distribution below a tracked tractor during ploughing with original plough attachment (dashed line) and with a lowered attachment point (solid line) for the plough. (Keller et al., 2002).

The less rigid belt of rubber tracks is a big disadvantage compared to traditional steel track belts. For the use of tracked vehicles on the road belts have to be rubber to avoid damage to the surface and to increase driver safety and ride comfort. Yet on soft surfaces like soil, the problem of an uneven weight distribution below the rubber belt due to idler and belt configurations as well as belt tension is much higher than for steel tracks. A comparison by Brown et al. (1992) revealed an advantage of steel tracks compared to the tested rubber tracks in relation to reduced soil compaction. The results for rubber tracks in this investigation were intermediate between the ones from wheels and steel tracks, not significantly different from either. Further investigations showing the advantage of steel tracks compared to wheels were published by Reaves and Cooper (1960), Soane (1973), Taylor and Burt (1975), Janzen et al. (1985), Erbach et al. (1988), Erbach et al. (1991), and Kinney et al. (1992). For a 40t steel tracked excavator changes in precompression stress in topsoil could only be detected in very wet conditions. Subsoil conditions did not change in either dry or in very wet conditions (Berli et al., 2003). Steel bogie tracks on a trailer are beneficial compared to wheels according to Bygden et al. (2004). Yet, no differences between a steel tracked and a wheeled tractor were reported by Burger et al. (1983) and Burger et al. (1985). The authors conclude that other machine related factors than contact pressure had a large influence on the results.

Campbell et al. (1988) found a greater cone penetrometer resistance after using a wheeled tractor compared to a rubber - tracked machine having 24% higher total mass. Comparisons between a wheeled and a rubber tracked tractor by Pagliai et al. (2003) showed less soil density change and penetrometer increase in the top 100 mm for the wheeled tractor, less for the tracked vehicle between 100 – 200 mm depth and no difference between either at a depth of 200 – 400 mm. This was supported by the results of Servadio et al. (2001) and Brown et al. (1992). Servadio et al. (2001) found lower penetrometer resistance in the top 200 mm and a higher one between 200 – 400 mm depth for a wheeled tractor when compared to a rubber tracked tractor. Brown et al. (1992) found more compaction in the top 125 mm for wheeled tractors compared to tracked tractors, but below 125 mm differences were minimal.

Blunden et al., (1994) could not detect significant penetrometer resistance differences at 500 mm depth between a wheeled and a rubber belted tractor. Between 400 and 500 mm the wheeled tractor produced 0.03 MPa less penetrometer resistance. These results are in-

interesting as the wheeled tractor weighed 18 t and the tracked one 15 t and the mean contact pressure below the tracked one was 25 % smaller. From the report it is not evident why the differences are so small. One reason might be an unequal pressure distribution below the track as reported by Weissbach, (2003), Keller et al., (2002) and Tijink, (2000).

These results, while true cannot be generalized, however, they show the increased importance in designing the frame carrying the rubber belts and transferring the weight compared to the frame of steel tracks. A summary of papers reporting advantages (Bashford et al., 1988 and Rusanov, 1991) or disadvantages (Blunden et al., 1994) of tracks as far as soil compaction is concerned is given by Alakukku et al. (2003) as well.

Comparing traction of a wheeled equipment and a tracked equipment results in a higher coefficient of traction for the track. Maximum traction is at 6-8 % slip for a track compared to 15 – 20 % slip for a wheel (Culshaw and Dawson, 1987) which are in agreement with the findings reported by Taylor and Burt (1975) and Bashford and Kocher (1999).

### 3.4 Loosening Soil Compaction

In order to loosen soil an implement has to be pulled or driven through it inducing soil failure. Normally a tine or tine – similar – implement is used therefore. Tines cause a crescent failure of the soil whereby soil shears at an angle of 45 degree down to the critical working depth which depends on tine geometry and can either be estimated (6 times the width of the tine in depth) or calculated according to Eq. 20 with the extensions of Eq. 21 to Eq. 23 in Godwin and Spoor (1977). Below this depth lateral failure occurs basically pushing the soil in front sideways. In context with the working efficiency crescent failure is much more efficient than lateral failure. The implications of tines geometry and soil conditions for the optimum soil loosening are discussed in detail by Spoor and Godwin (1978) The force necessary for a tillage implement can be calculated using prediction models developed by Godwin and O'Dogherty (2003).

In case a soil is deeply compacted and one wants to loosen it again, care has to be taken not to cause severe re-compaction again. Loosened subsoil is very sensitive to re-compaction. Re-compaction can only be avoided using very light machinery, controlled traffic or by deep loosening simultaneously with surface cultivation and drilling. In case one does

mouldboard ploughing after deep loosening significant recompaction can occur no matter whether tractor wheels operate in the furrow or on the surface (Soane et al., 1986). Practical suggestions for loosening soil compaction are given by Spoor and Godwin (1981).

Yet not all consequences of soil compaction in the topsoil can be alleviated with tillage implements. Arvidsson and Hakansson (1996) found an effect of topsoil compaction on yield up to five years even after annually ploughing when the whole field was trafficked initially.

### **3.5 Conclusions**

A significant volume of work has been conducted in the area of soil compaction and as a result the soil physical principles of soil compaction appear to be clear, but its real implications with the soil conditions are less so. The results depend on the soil conditions and the authors interpretation. Laboratory studies were limited to loads smaller than 5 t and no published results have been found on the performance of tracks in laboratory conditions. Therefore this study aims to provide a laboratory investigation into the effects of high axle loads on both wheels and tracks in controlled laboratory conditions in a soil bin. The findings in the soil bin laboratory will be compared to a limited number of field measurements.

## 4 EXPERIMENTAL OVERVIEW

### 4.1 Laboratory Studies

#### 4.1.1 Soil Compaction Below Pulled Wheels

In order to start to develop the experimental methodology whilst the driven single wheel/track test rig was under construction preliminary experiments were conducted using an undriven single tire rig with the following specifications:

- 8.5 t overall load
- 800 mm tire run with recommended inflation pressure (250 kPa = 2.5 bar)
- Bulk densities of 1.5 g/cm<sup>3</sup> and 1.3 g/cm<sup>3</sup> on a sandy loam

The analysis of soil compaction and deformation will be explained in section 4.1.2..

The aim of the preliminary investigations was to gain experience with these tires as well as data about the expected soil compaction and rut depth. Draught force for pulled wheels was recorded as well in order to gain information about the coefficient of rolling resistance.

#### 4.1.2 Soil Compaction Below Self Propelled Tracks and Wheels

Studies were conducted under controlled soil bin conditions at CU@S, with each measurement replicated three times for the uniform and stratified soil conditions. Testing details for uniform conditions are shown in **Table 1**. For these investigations a driven single tire/track rig had to be built (see 5.4) as all available ones did not meet the specifications and rebuilding these would have been more difficult and expensive.

The effects of tire and track loads will be determined by changes in:

- a. Soil deformation
- b. Soil bulk density and porosity by direct sampling
- c. Soil penetration resistance by use of a 30° cone penetrometer

d. Rut depth measured with a profile meter

The results of the uniform soil conditions were analyzed and field conditions were surveyed. These results were discussed with Claas and decisions made concerning the used track and tire for the investigations in stratified soil conditions. The specifications are shown in **Table 2**. These investigations followed. Then a final data analysis and thesis preparation will follow.

**Table 1:** Wheels, tracks, and loads used in soil bin investigation for uniform soil conditions with 1.4 g/cm<sup>3</sup> dry bulk density

	680/85 R32 1939 mm Diameter	800/65 R32 1820 mm Diameter	900/65 R32 1935 mm Diameter	Two idler track	Three idler track
10.5 t	X	X	X	X	X
12 t				X	X

**Table 2:** Wheel, track and loads used in soil bin investigations for stratified soil conditions

	900/65 R32	Three idler track
10.5 t	X	
12 t		X

**4.1.3 Multi Pass Effect and Pressure Distribution**

One investigation concerning soil compaction after multi passes was done as well. Therefore the 900 mm section width tire passed three times over the surface. The analysis of soil physical properties was performed as described for single passes.

The pressure distribution below the three and two idler tracks was measured using two ceramic pressure transducers each embedded at the top of a 100 mm diameter aluminum



tube. These tubes were longitudinally integrated into the soil at 250 mm depth during the preparation for 12 t overall load run for the two track types and the 800 mm section width tire laden to 10.5 t. Thus when the tracks roll over the pressure transducers one gets the pressure distribution below each track.

## 4.2 Field Studies

### 4.2.1 Tracks vs. Wheels (2004 – 2005 Crop Season)

In 2004 wheat was harvested in two adjacent fields with a wheeled Lexion 480 (front tire size: 800/65 R32; rear tire size 600/70 R24) on one field and a tracked Lexion 480 (standard belt width, rear tire size 500/70 R24) on the other field at Roxhill Manor Farm of L.E. Barnes & Sons in Marston Moreteyne, Bedford MK43 0QG. The mass of the combines varied with the load in the corn tank. So front axle load was between 12 (empty corn tank) and 20 t (full corn tank) and rear axle load between 8 – 10 t. The fields are directly beside each other with identical soil type (clay; Chulkey Boulder Clay series), slope, and a size of approximately 45ha each. Oil seed rape was surface spread on both fields one day before harvest and is now used as plant growth indicator. In late April 2005 biomass and penetrometer resistance from track and wheel ruts and from the area between the ruts were sampled 3 and 30 times each respectively. Dry bulk density was measured once in the ruts at the surface and twice at 100 mm depth in each rut. Profiles were dug and roots excavated in the rut areas in order to trace differences in plant development. Photographs of plant growth in wheeled and tracked ruts and the surrounding crops were taken.

### 4.2.2 Tracks vs. Wheels (2005 Harvest)

The results gained under laboratory conditions were compared to field measurements with a tracked and a wheeled combine harvester (both Lexion 480) on identical soil conditions in harvest 2005. The soil type was a clay loam of the Ragdale series. This was conducted on the farm of Sam Fairs at Suffolk. Both combines were equipped similar to the ones mimicked in the laboratory. The tire size used was a 800/65 R32 tire on the front axle and

a 600 / 70 R24 on the back axle. The tracked machine was equipped with a standard belt of 635 mm width and a 500/70 – 24.2 rear tire.

On the field 4 plots are planned, in sequence:

- First plot is a combine with empty grain tank and normal tire pressure
- Second plot is a combine with full grain tank and normal tire pressure
- Third plot is a combine with full grain tank and half normal tire pressure
- Forth plot is a combine with empty grain tank and half normal tire pressure

For the tracked combine harvester only two plots are necessary as only one working condition concerning the tracks is possible.

Each plot will be at the end of the field close to the headland in order to allow the following movements: Drive the combine straight to the end of the field before the headlands, the moment the last wheat drops on the cutter bar turn 90 degrees away from the standing crop, thus front wheels go straight out of the field into the headland but without the rear wheels in the same track. For explanation see **Figure 3**. This is necessary to get straight wheel / track marks formed by only the front wheels/tracks.

The analysis included the measurement of cone penetration resistance (described in section 5.3.4), the measurement of rut characteristics (described in section 5.3.2), the measurement of soil bulk density (described in section 5.3.1) and a soil profile pit.

Penetration resistance measurements were replicated 10 times in each track. As a control each plot replication was randomly measured 10 times before being rolled. Rut characteristics were measured for each rut and soil bulk density was measured with three replications in the profile at the surface and at 250 mm.

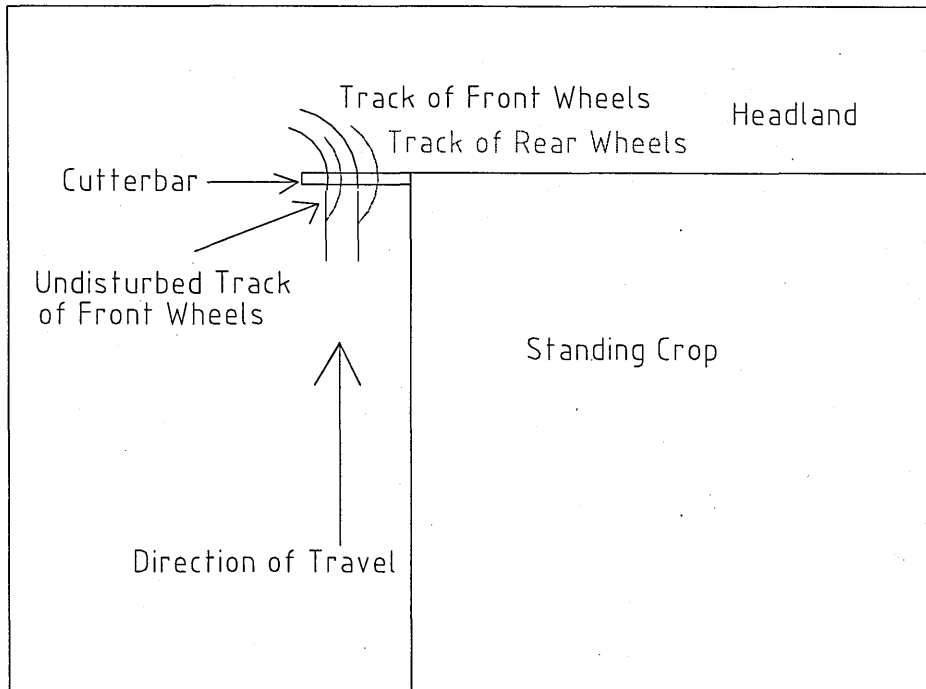


**Figure 3:** Drawing of field layout and combine harvester tracks

## 5 DETAILS OF LABORATORY STUDIES

### 5.1 Soil Conditions

In the soil bin a sandy loam soil, Cotterham series (King, 1969) was used. The exact particle distribution is 17.1% clay, 17.2% silt, and 65.7% sand. The sand fraction splits into 6.1% coarse sand, 34.9% sand, and 24.7% fine sand. Organic matter content of the soil is 4.1%. Cohesion and angle of internal friction for this soil depending on dry bulk density are shown in **Table 3** at a gravimetric water content of 8.2 %.

**Table 3:** Cohesion and angle of internal friction for different dry bulk densities

Dry Bulk Density [ $\text{g}/\text{cm}^3$ ]	Cohesion [ $\text{kN}/\text{m}^2$ ]	Angle of internal friction [°]
1.45	4.1	38.8
1.56	8.9	38.8
1.62	5.9	38.8

This soil is a standard soil type for investigation purposes and represents about a quarter of all arable soils in the UK and the world (Godwin, 1974). The average gravimetric soil water content during the experiments was about 10 % and kept constant during the investigation.

Soil bulk density was controlled by the amount of rolls per layer when preparing the soil. When preparing the soil bin from the bottom to the top, the soil processor places 65 mm deep layers of soil. Each layer is rolled to adjust soil density and wetted on top to maintain a constant soil moisture content before placing the next layer on top. Uniformity of soil moisture content is given according to measurements.

Uniform soil conditions were prepared by rolling each layer once for low bearing capacity and twice for medium bearing capacity. Stratified soil conditions were set up as follows: A 4 roll ( $\sim 1.5 \text{ g}/\text{cm}^3$ ) bin preparation in the subsoil (450 mm height), then a 6 roll ( $\sim 1.6 \text{ g}/\text{cm}^3$ ) bin preparation mimicking a plough layer (100 mm height) and this plough layer being covered by a 2 roll ( $1.4 \text{ g}/\text{cm}^3$ ) preparation (200 mm height). As shown in **Figure 4**.

Soil Bin

Soil Surface
1.4 g/cc
1.6 g/cc
1.5 g/cc

**Figure 4:** Proposed soil profile for stratified soil conditions

## 5.2 Tire and Tracks

All tires used were *Continental* harvester tires. Tire sizes are specified in **Table 1** with lug heights of 42 mm, 58 mm, and 55 mm for the 680, 800, and 900 section tire, respectively.

The two idler track is a standard track and the three idler track a prototype both from Claas Industrie Technik, GmbH, Germany. The two idler track has a belt having 63.5 mm lug height and the three idler track is equipped with a rubber belt with a lug height of 45 mm. Both belts are 635 mm wide.

## 5.3 Description of the Measurement Devices

### 5.3.1 Dry Bulk Density

Dry bulk density (DBD) was measured at depths of 0, 250 and 500 mm. This was conducted with three replications before and after each run in the middle of the track in the soil bin. A cylindrical ring was pushed into the soil and dug out. Then the surplus soil was carefully cut away with a knife. Afterwards the soil sample from the cylinder is put into a tin, weight was taken and the sample then placed into the drying oven for 48 h at 105° C.

The dry soil was weighed again. From the weight difference soil water content was calculated and from the given volume of the cylinder and the dry weight dry bulk density was calculated. Other methods for measuring DBD as well as other information can be found in Campbell (1994).

The following facts show that even a trained and experienced person can hardly reduce the measurement error to less than 4 %:

- 1.) With a volume of  $145613 \text{ mm}^3$  for an ideal cylinder with an internal length of 51.5 mm and an internal radius of 30 mm totally filled with soil the measurement would be correct. Yet with a slight deviation from the cylindrical shape leading to a reduction of 1 mm in diameter which would hardly be noticed, the volume would decrease by 3.3 %.
- 2.) By cutting off the soil from the top and bottom of the cylindrical ring, no soil particles can stick out in the end. Therefore where particles were sticking out beforehand a hole remains. These holes are only relevant for the sand fraction ranging from 0.1 mm to 2 mm. Therefore it can be assumed, that both ends of the cylinder are in average filled to 0.25 mm less in average. This would result in 1 % less volume than actually assumed.

### 5.3.2 Rut Characteristics

Rut deformation and rut area were measured using a profile meter. The profile meter with its rods was placed over the rut and the rods were lowered into the rut and fixed in their position. Then the device was taken out and the shape of the rut and thereby the area of disturbance was reproduced on a sheet of paper. The area on the paper was measured using a planimeter. This method gave the total area of deformation. Width of the rut as well as maximum depth were measured. All these measurement were done in three replications. For further information on rut measurements see Davies et al., 1973.

### 5.3.3 Soil Displacement

Soil is placed in layers into the soil bin and its displacement after a wheel or track ran over it can be traced in a vertical profile being cut afterwards. A different approach where no profiling is needed is taken by Way et al. (2005) who measure soil displacement using a linear motion potentiometer. The advantage of their approach is that it is easily possible to measure soil displacement in any direction, just depending on the orientation of the linear motion potentiometer. The disadvantage is the length of the linear motion potentiometer with 135.5 mm because this determines the measurement interval of the vertical displacement.

So far measurements of soil displacement at CU@S were done manually by measuring the position of the boundaries of the layers. Trein (1995) used a digital analysis program to analyze soil deformation from the position of color spots in pictures. However, the white color he used for laying white stripes into the soil in each layer was difficult to locate. The white lines in each layer appeared as white dots in the vertical cut through the soil.

For the analysis of soil compaction in the soil bin a faster and more precise method for recording soil displacement was of high necessity, particularly measuring the distance from each layer to the neighbouring layers as well as being able to record vertical movement. A new idea was to use talcum powder as its white color contrasts well with the soil and it does not alter soil properties and thus could be used in higher dosage without causing troubles in future investigations.

During the preparation of the soil on top of every second layer, approximately every 100 mm, talcum stripes were placed. Due to the high movement near the top they were placed in every layer. In total 7 layers were marked with white lines. The white lines were placed on top of the soil after the layer had been rolled and wetted. To produce the white lines 14 slots each 200 mm long and 6.25 mm wide were cut in a distance of 100 mm in a 3 mm thick plywood plate. The width of the plate and the marks are determined by the width of the roller in the soil processor for rolling the different layers. When the plate is placed on the soil talcum powder was strewn on it and brushed into the slots. Afterwards the plate was carefully removed in order not to disturb the white lines. Then the talcum powder lines were carefully covered with soil using a shovel. This procedure was repeated a few times

on top of each marked layer at different positions along the soil bin. Talcum powder lines and covering them is shown in **Figure 5**.

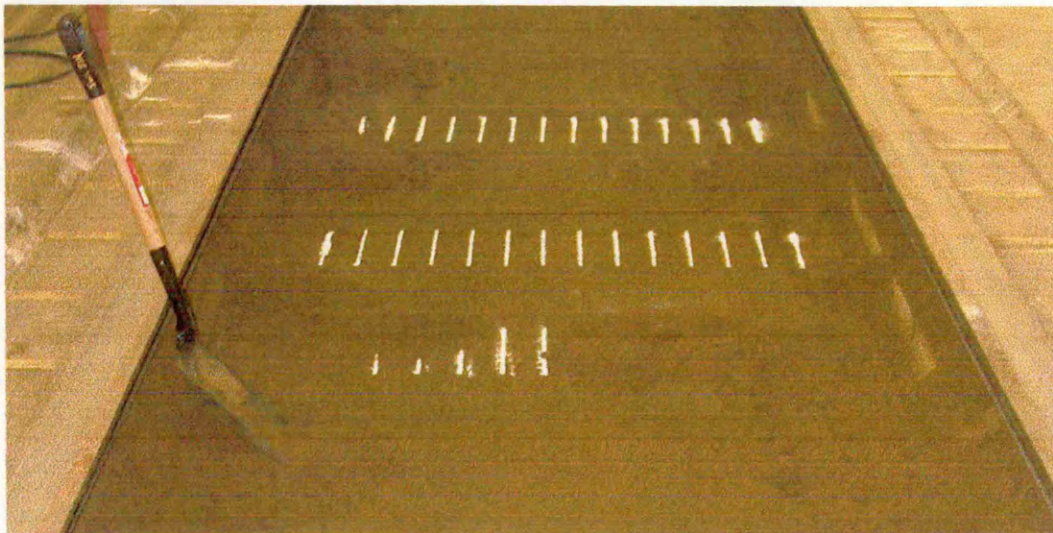


**Figure 5:** Talcum powder stripes in preparation in the soil bin included

One profile on undisturbed soil was used for reference and the others along the soil bin for the replicated disturbed measurements. When the preparation was finished, the surface load is applied and all necessary measurements on the surface are performed. These are followed by digging four vertical profiles, each at the position of the talcum powder lines. In the profile the lines appear as white dots in the soil as shown in **Figure 6**.

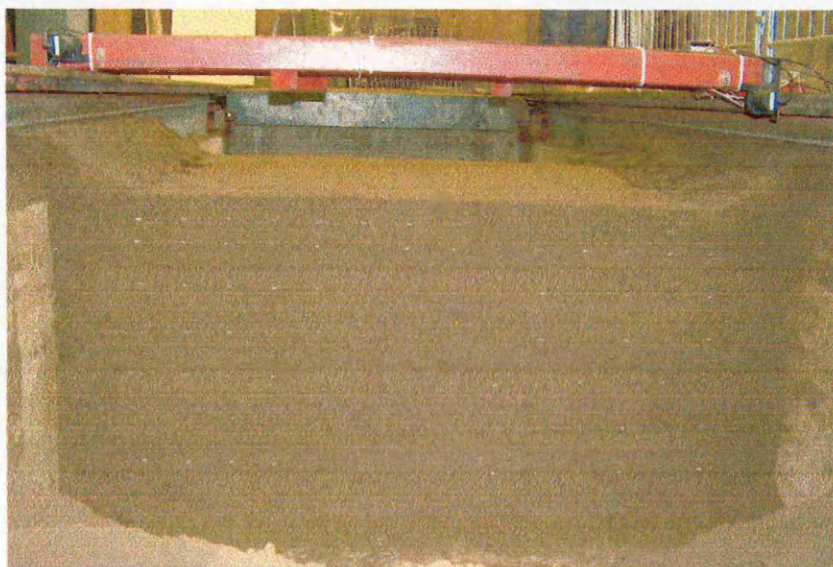


**Figure 6:** Vertical cut in soil bin showing white talcum dots and across the soil bin a frame with the draw string transducers



Two possible solutions were seriously contemplated for the process of digitizing the position of the white dots:

Firstly a computer program (e.g. Arc Map) could be used to localize the position of each white dot in a digital picture of the cut soil. A disadvantage of this method are the possible optical distortions in the digital picture.

Secondly draw string transducers could be employed in the soil bin. This means measurements are done by hand, however, they will be recorded digitally and processed in an Excel spread sheet.

For the analysis in this work draw string transducers with a battery power supply were chosen. In **Figure 6** they are shown on the frame above the soil bin.

The position in the profile of each dot is recorded using a frame with two connected draw string transducers. At the pin point both draw string transducers are connected. This pin point is moved subsequently to each mark and the coordinates are recorded automatically via a PMD 1208LS analog data logger with a USB output onto a laptop computer using Daisy Lab 7. The repeatability of the measurements is within +/- 1mm. The raw draw string transducer lengths are converted into coordinates of a position in the soil bin using the lengths  $x_l$  and  $x_r$  being pulled out of each draw string transducer and their distance  $a$  from each other at the fixed ends. With the cosine law depth and length position in the soil bin is then calculated according to the following equations (see **Figure 7** for explanations):

$$\cos \alpha = \frac{a^2 + x_r^2 - x_l^2}{2 * x_r * a} \quad \text{Eq. 1}$$

$$d = x_r * \sin \alpha \quad \text{Eq. 2}$$

$$l = x_r * \cos \alpha \quad \text{Eq. 3}$$

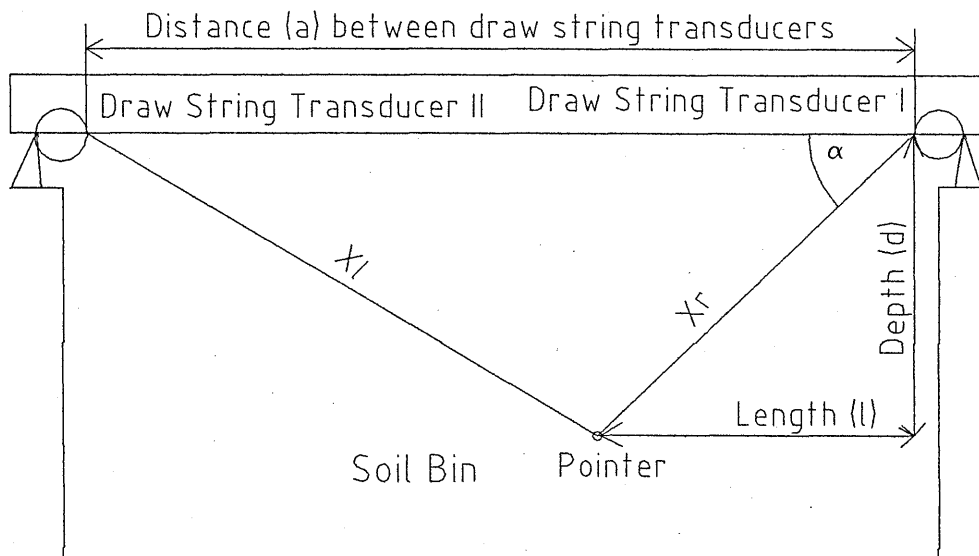


**Figure 7:** Draw string transducer on frame in soil bin

The accuracy of the measurement device was tested with a printed coordinate system on a poster simulating a soil bin profile, with the exact position of each point defined in a CAD drawing. The area was measured 5 times and afterwards all readings were statistically compared to the real values in horizontal and vertical distance with the resolution of the draw string transducers of 1 mm (least count) respectively. The standard errors in the vertical and horizontal direction were 1.1 mm and 2.0 mm, respectively.

This method provides the coordinates of each talcum powder dot and therefore the shape of the layer on which they are located. **Figure 8** shows a vertical cut through the soil showing displacement of the soil and talcum spots. One can as well see the boundaries between the single layers (which had earlier been used to measure soil displacement).



**Figure 8:** 2<sup>nd</sup> Replication of vertical cut for the 800 mm section width tire run at 1.25 bar and loaded to 10.5 t

The corresponding depth and length coordinates measured with the draw string transducers are shown in **Figure 9**.

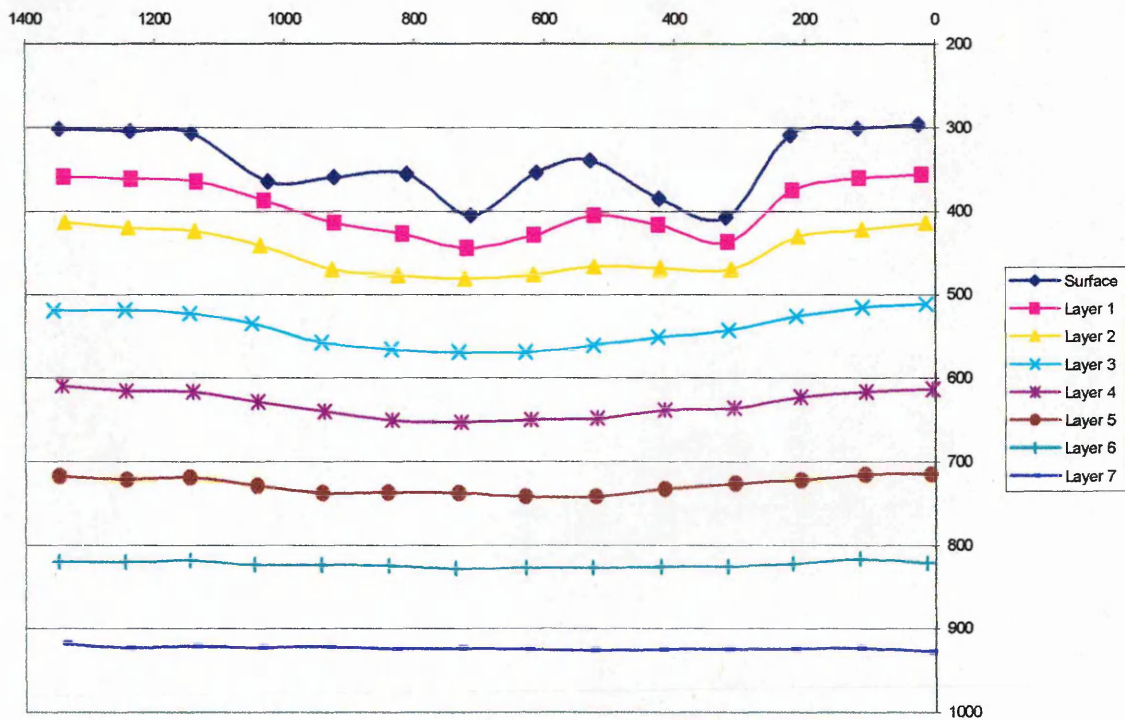


**Figure 9:** 2<sup>nd</sup> Replication of tire with section width 800 mm run at 1.25 bar and loaded to 10.5 t, measured talcum points.

In order to trace the movement of the talcum powder points diagrams like **Figure 10** were made. Here the arrows indicate the actual direction of soil displacement. Looking at **Figure 10**, it can be seen that there is also a horizontal displacement where the talcum powder points move horizontally from the center line on both sides.

The arrows at 920 mm depth pointing mostly to the right are caused by the variation with which the talcum powder board is placed in the soil bin in its horizontal position. The same is true for the other layers as well. Due to the fact that the talcum powder board was randomly aligned to either side of the soil bin during the preparation, resulting in 5 – 10 mm variation vertically, the arrows tend to point more to one side than to the other for a particular layer. However, the horizontal movement to the outside of the points themselves is still visible.

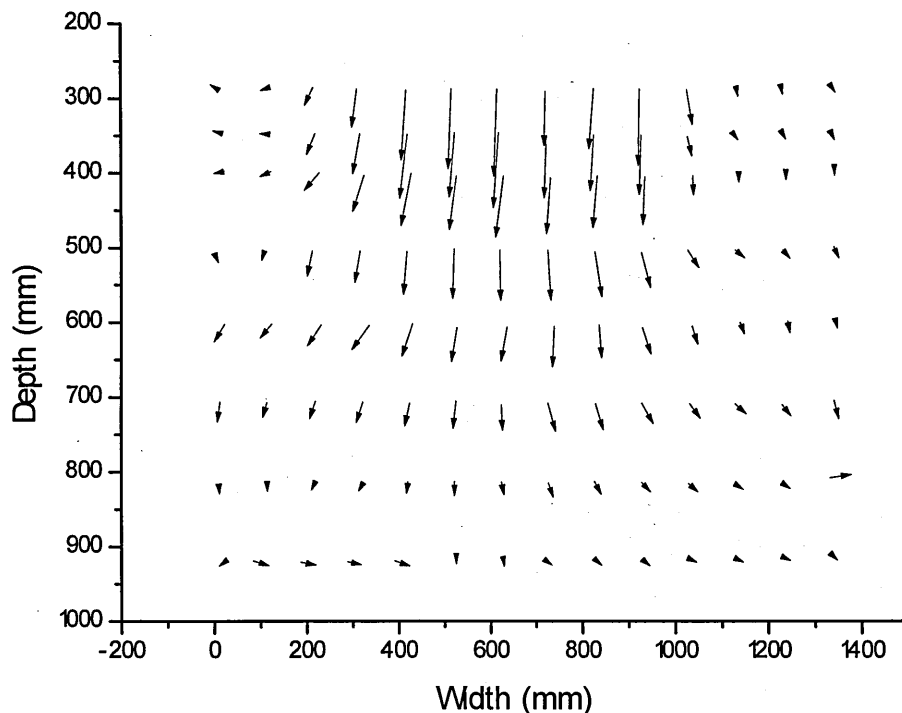


**Figure 10:** Movement of position of talcum powder points during the 900/10.5/1.9 experiment (section width [mm] / load [t] / inflation pressure [bar]). The length of the arrow equals the distance the soil moved.

This horizontal movement of the talcum powder points is caused by the soil moving along the path of least resistance. As a consequence one would expect larger horizontal movement after multi passes than after one pass. **Figure 11** shows the movement for the multi-pass experiment with the 900/10.5/1.9 where the soil movement happens to be unexpect-

edly vertical. Looking at the direction of the movement during the other experiments the tracks (in **Figure 12**) on soft soil conditions and the stratified soil conditions also show little horizontal movement.

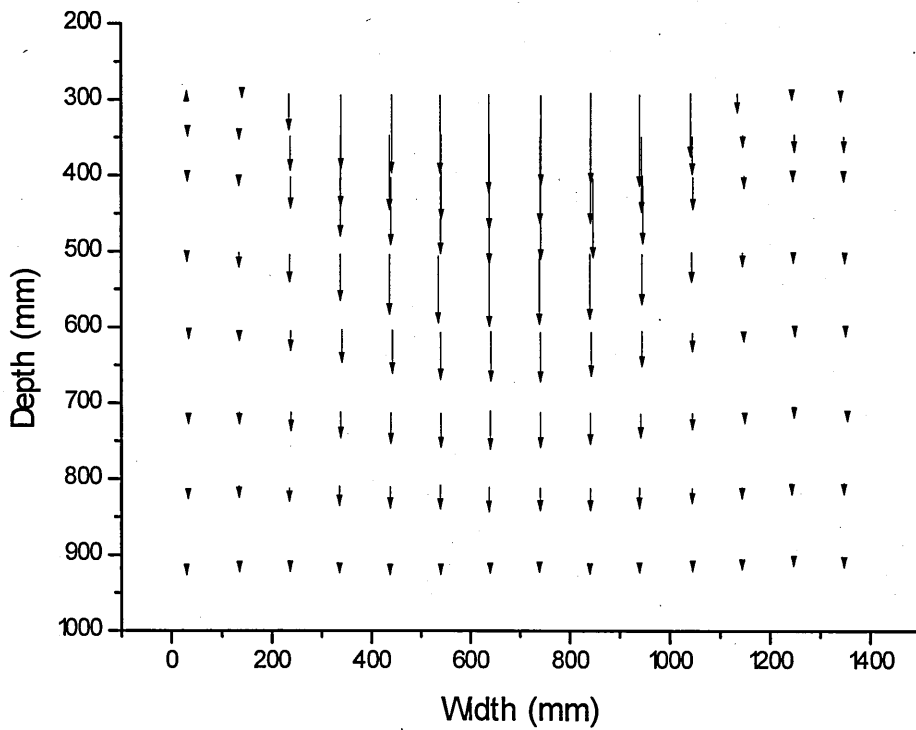


**Figure 11:** Movement of position of talcum powder points during the multi pass experiment with the 900/10.5/1.9

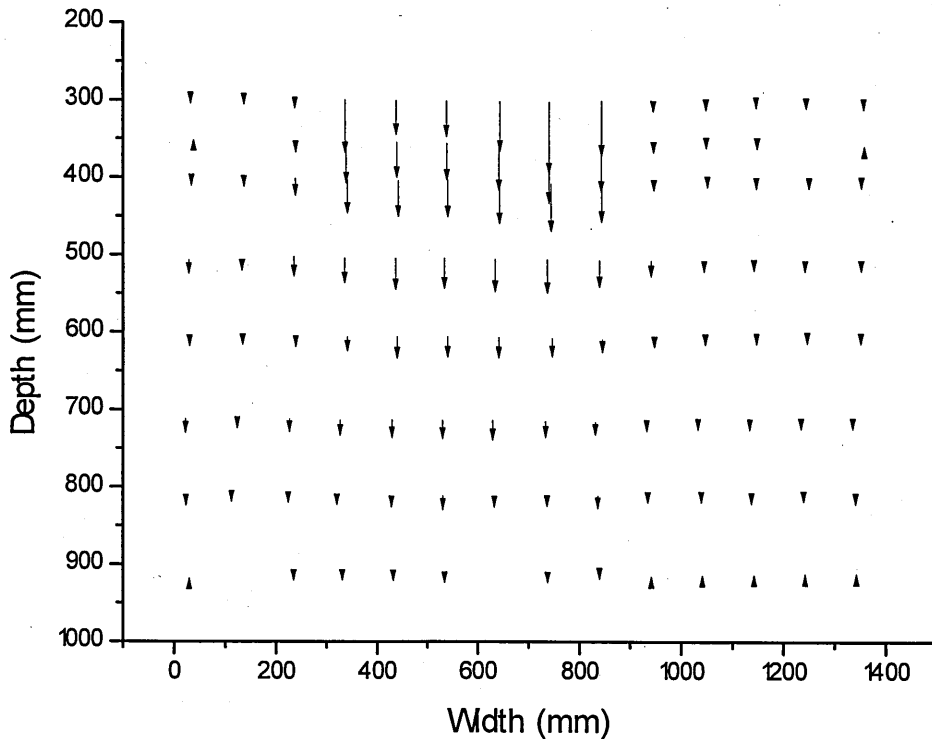


**Figure 12:** Movement of position of talcum powder points during t3/12 experiment

The arrows apparently missing in **Figure 12** are caused by a very small deviation between initial and final depth. Depth deviation is less than 0.5 mm and width deviation less than 5 mm between initial and final position for these points.

When looking at **Figure 10** and similar figures showing the direction of soil displacement a corridor in the central 300 mm was found with minimal horizontal deformation. Averaging the four points enclosing these 300 mm results in an average depth of each layer and thus provides a comparable number for all depths.

Doing this for the control as well as for the deformed layers and then subtracting the initial depth from the final depth of each layer reveals the total average vertical displacement for each layer. As one knows the initial distance  $i_0$  from the layers when they are prepared and the final distance  $i_1$  from the measurement below the rut it is possible to get the strain in each layer as well. The strain  $\varepsilon$  is the ratio between decrease in layer thickness to initial layer distance and is calculated according to Eq 4.

$$\varepsilon = \frac{i_0 - i_1}{i_0} \quad \text{Eq. 4}$$

### 5.3.4 Cone Penetration Resistance

Cone penetration resistance is the force required to push a 125 mm<sup>2</sup>, 30° cone into the soil. For detailed explanation see O'Connell, 1972. The data was automatically digitally recorded at every 10 mm depth and read as a .txt file which was then exported to Excel for further analysis. Data was plotted as resistance over depth for each 10 mm interval. Depth was referenced to the concrete base of the soil bin. So measurements were therefore conducted to the bottom of the bin discounting the final 50 – 100 mm as they will reflect the effect of the base. Thus a standard reference basis of depth exists for all measurements no matter where the actual soil surface was situated. Cone penetration resistance was measured at 10 places 120 mm apart across the soil bin resulting in a diagram as shown in **Figure 13** with three replications in both the disturbed and in the undisturbed area (as a check).

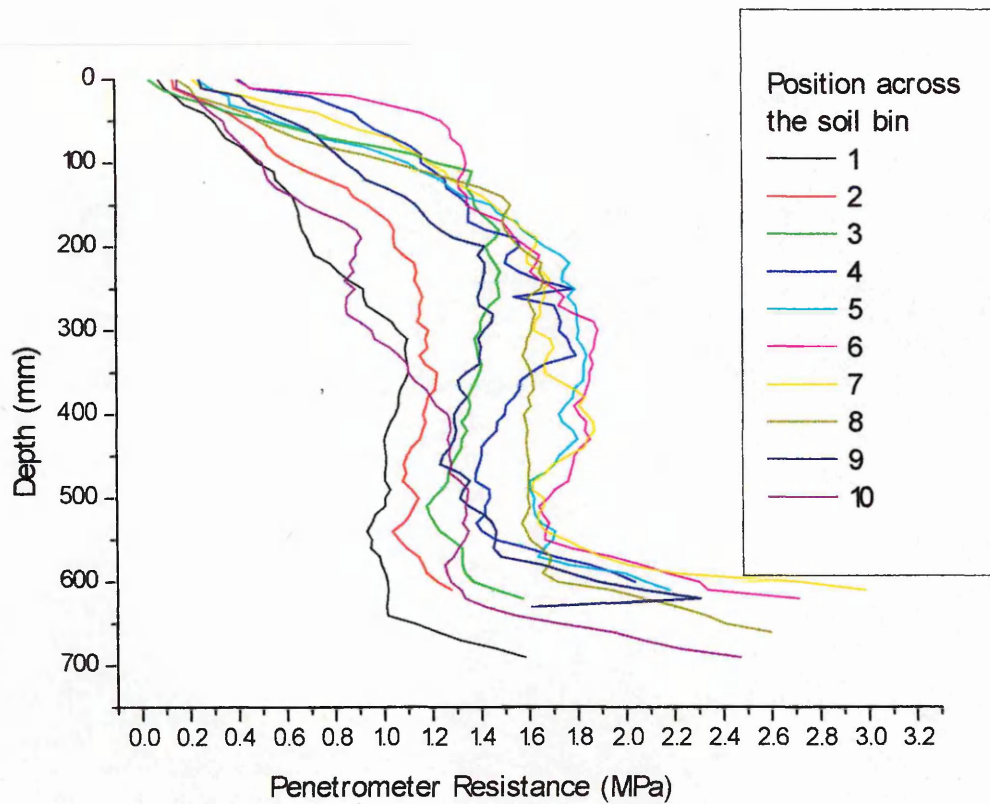


**Figure 13:** Example penetrometer resistance across the soil bin (here the 900 mm section width tire driven)

As it can be seen in the diagram above, there is a symmetry between the left (1, 2, 3, ...) and the right (10, 9, 8, ...) hand side of the soil bin with the highest values in the center (5 and 6). So basically the measurement taken at symmetrical positions relative to the center of the rut are close. This finding resulted in averaging the first (1) and the last (10), the 2<sup>nd</sup> and the 9<sup>th</sup>, the 3<sup>rd</sup> and the 8<sup>th</sup> and so on and produced the curves shown in **Figure 14**.

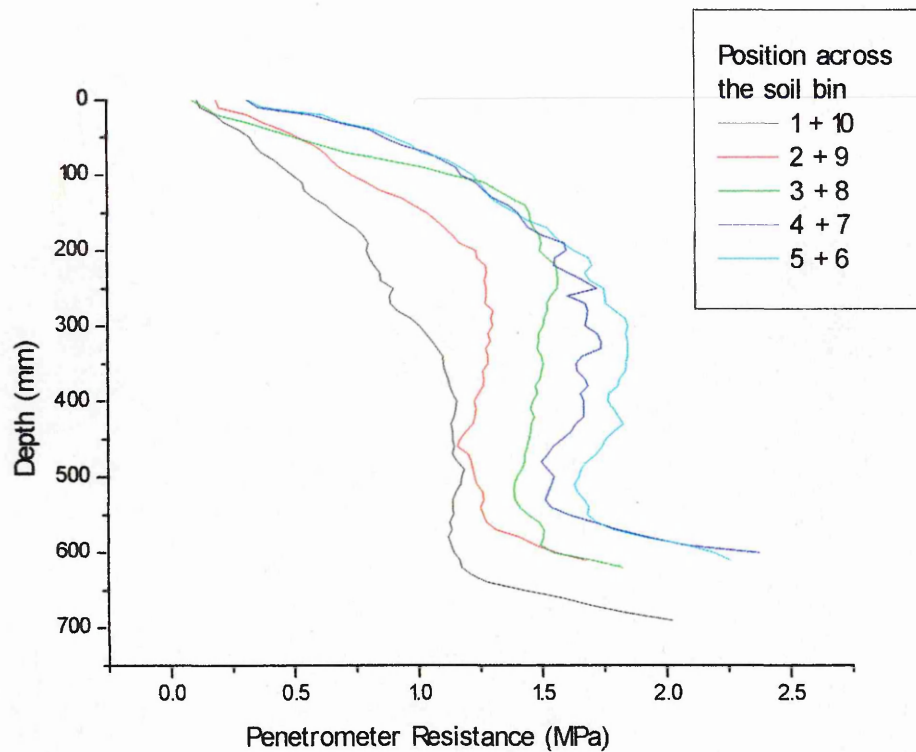


**Figure 14:** Average of the left and right hand side together in the soil bin

Looking at the shape of the curves in **Figure 14** shows the similarity of curves 4+7 and 5+6 which gave the possibility to average these two together and thus come up with one penetrometer resistance curve per tire representing the average of the center 4 points of measurements. This resulting curve is shown in **Figure 15**. For the control the center four measurements were averaged to one penetrometer resistance curve as well. So the same number of observations for both initial and final conditions was used.



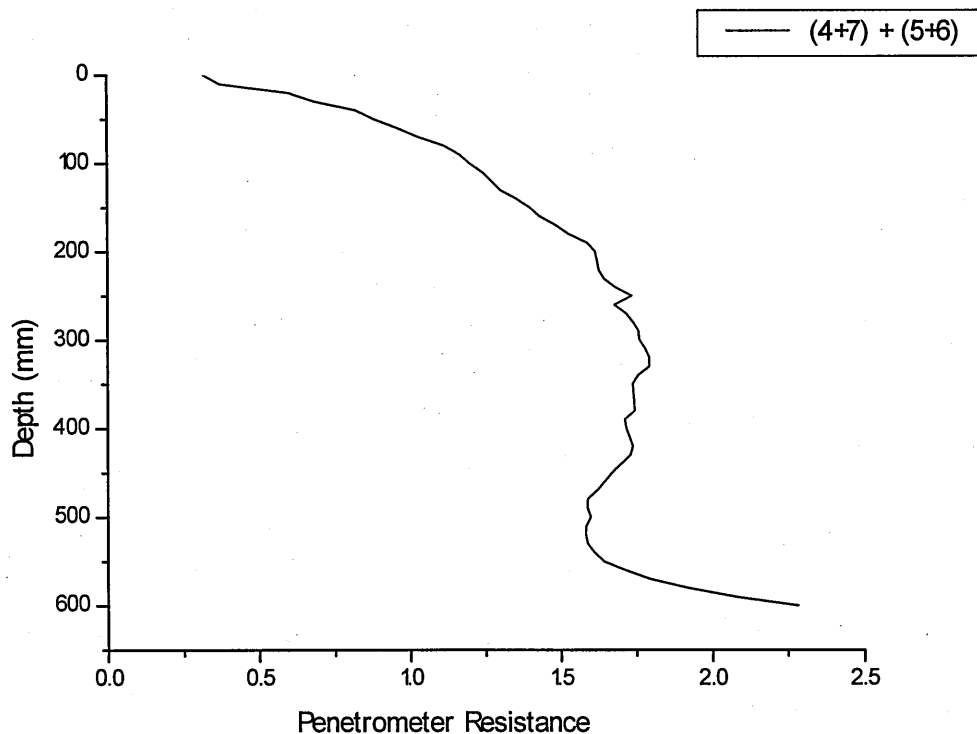


**Figure 15:** Average of curves 4+7 and 5+6 from **Figure 14**

In the in-field measurements the same replications were conducted across the wheel and track ruts. As check the untrafficked soil surface was also measured.

### 5.3.5 Draught Force Measurement and Slip Measurement

In the preliminary investigations when the non driven frame was used draught force was measured using an octagonal draught force transducer. For further explanations see Godwin (1975). Knowing the weight of the frame, load, and wheel as well as draught force rolling resistance can be calculated as the ratio of draught force to total weight.

In the main investigations slip was measured by recording both the rotational speed of the self propelled wheel or track and the true speed of the frame using a fifth wheel. For the exact assembly see Appendix 13.2..

### 5.3.6 Profile

In the in - field investigations a soil profile was dug to take soil samples and in order to investigate dry bulk density, soil water content, and root development below the surface. From the shape of the roots and their development conclusions on former soil displacement and thus on the existence of root growth restricting layers can easily be drawn (Spoor et al., 2003).

### 5.3.7 Pressure Transducer

Using ceramic pressure transducers embedded at the top of a 100 mm diameter aluminum tube the pressure exerted by the tracks when rolling over the soil was measured at 250 mm depth. The data was recorded at 50 Hz onto a laptop computer using Daisy Lab 7 software and a Doc Book for analog digital data processing. Detailed explanation and methodology will be published by Blackburn, Godwin, and Dresser in 2006. The transducers are available from the project "Trials to Identify Soil Cultivation Practices to Minimise the Impact on Archaeological Sites" project number BD1705 done for DEFRA. This is a project funded by DEFRA and English Heritage to investigate the effect of agriculture on buried archeology.

## 5.4 Single Wheel Tester

A further task in this project was to design a machine, which allows different loads to be applied onto a self propelled wheel or track, which can in turn be used to study soil compaction in the soil bin of the National Soil Resources Institute at Cranfield University. The design and construction of this single wheel tester was submitted to the University of Hohenheim, Department of Agricultural Engineering for acceptance as a Master of Science Thesis (see Appendix 13.2).

The rig constructed in this thesis and shown in **Figure 16** transfers a force onto a wheel or track axle by using a hydraulic ram. Therefore wheel or track loads can easily be changed as the load is a function of the pressure applied to the hydraulic ram. The hydraulic ram is

also used for lowering the wheel and track down to the surface of the soil bin as well as lifting it out again. Wheels and tracks can be exchanged or removed through the back of the frame of the rig. In this rig the loading weights for supplying the counterforce of the ram are spread over the frame and thus can remain in place when the wheels are changed. The wheels and tracks are self propelled using a hydraulic motor and pump driven by a combustion engine placed outside of the soil bin.

Forces and torques developing from the movement of the wheel and track are taken up by the linear bearing. This prevents any weight transfer as the linear bearing is essentially frictionless in the vertical direction.



**Figure 16:** Single wheel tester over soil bin with a 900 mm section width tire inside

Changing the equipment from wheels to tracks is achieved by removing the final reduction of the axle and replacing it with an adapter to compensate for the height difference and the different pitch circle diameters of the axle and the track. The height difference occurs as the axle stays in the same position for both wheel and track to ensure the same maximum

sinkage for both devices. The PTO shaft from the gear box to the track is also able to overcome the height difference as it can be operated at a maximum angle of 35 degree, whereas only 31 degrees are necessary to adapt to the track.

## **5.5 Statistical Analysis**

For statistical analysis SAS (statistical analysis software) was used (SAS, 2003) assuming a probability level of 0.05. This means that the probability for obtaining the tested result from a random population was less than 5%. Before the statistical analysis was conducted the normal distribution of data was verified. All parameters were analyzed using generalized linear models to determine whether there were significant differences between control and run, between single tires and tracks, and interaction over depth where parameters had been taken. To account for variances within the process of taking measurements covariance parameters were identified where appropriate on level of measurements and their replications. As measurements were taken in the same soil bin several times per run statistically they have to be treated as repeated unpaired measurements (Piepho et al., 2004). Normal probabilities were used for multiple comparisons as well because the standard errors of the different treatments were close together and differences are implicated by analyzing the data. This method is suggested by Nelder (1985).

## 6 RESULTS AND DISCUSSION OF RESULTS

This chapter reports both the detailed results, the statistical analysis of the data and a discussion of the results. The overall classification of this chapter in relation to the previous literature from chapter 3 follows in chapter 7 from which the ultimate conclusions will be drawn in chapter 8 .

The following experiments were conducted with the following self propelled wheels and tracks on uniform bearing capacity soil conditions as described in section 5.1.:

- 800 mm section tire loaded with 10.5 t and 2.5 bar inflation pressure; subsequently abbreviated to 800/10.5/2.5
- 800 mm section tire loaded with 10.5 t and 1.25 bar inflation pressure; 800/10.5/1.25
- 800 mm section tire loaded to 8.5t and 2.5 bar inflation pressure being towed; 800/8.5/2.5t
- 900 mm section tire loaded with 10.5 t and 1.9bar inflation pressure; 900/10.5/1.9
- 680 mm section tire loaded with 10.5 t and 2.2bar inflation pressure; 680/10.5/2.2
- two idler track loaded with 10.5 t; t2/10.5
- two idler track loaded with 12 t; t2/12
- three idler track loaded with 10.5 t; t3/10.5
- three idler track loaded with 12 t; t3/12

### 6.1 Soil Compaction caused by towed Wheels

The 800/8.5/2.5t on soft and medium soil conditions was used in this study.

### 6.1.1 Penetration Resistance Results

The variation in penetrometer resistance for the 4 readings over the central 300 mm of the tire with depth for a medium and soft bearing capacity soil both before (initial) and after (final) the passage of the 800/8.5/2.5t is shown in **Figure 17** together with the least significant difference (LSD) to compare two means at each depth. The LSD indicates the difference at a given depth by which two values have to be separated to be regarded as statistically different at the 95 % - probability level.

The data shows that the initial penetrometer resistance is significantly different between medium and low bearing capacity soils ( $p < 0.0001$ ) and that the increase between initial and final penetrometer resistance is also significant ( $p < 0.0001$ ) for both soils. There is also a significant difference between the penetration resistance of the two soils for the final condition for the soil surface to a depth of approximately 350 mm. The steep rise of the penetrometer resistance values at 700 mm depth is due to the penetrometer “sensing” the bottom of the soil bin.

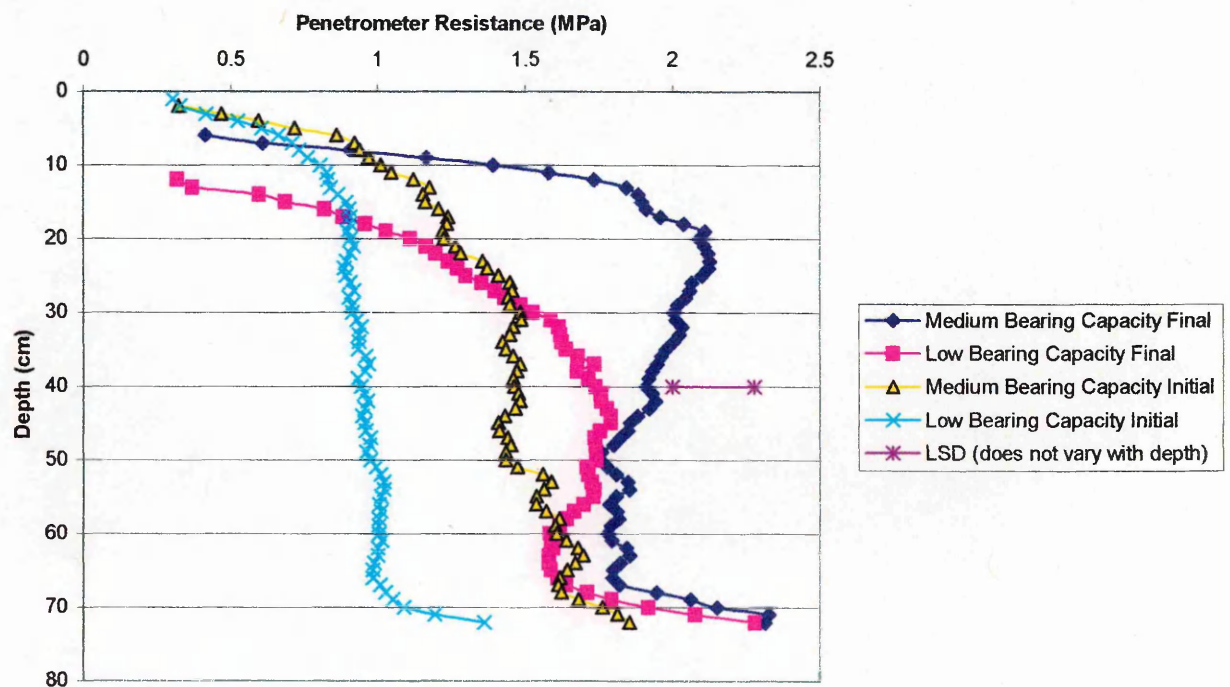


**Figure 17:** Average penetrometer resistance vs. depth for towed tires

Rut development can be seen from the beginning of the penetration resistance curve. The initial soil condition for medium and low bearing capacity show a uniform penetrometer resistance distribution over depth. The initial condition for the low bearing capacity is smoother than the one for the medium bearing capacity which may be due to slight fluctuations in strength from the surface rolling of the 50 mm deep layers. The peak at 200 mm depth for the final soil condition in the medium bearing capacity indicates that the soil is strong enough below to restrict further compaction. The increase in penetrometer resistance down to 350 – 400 mm for the final low bearing capacity indicates a compaction increasing over depth. It is interesting to note both final penetrometer resistances are very similar below 400 mm.

The penetrometer data averaged at the centre as explained in chapter 5.3.4 is shown in appendix 13.1.1 for the two soil conditions.

### 6.1.2 Soil Displacement

The average vertical soil displacement for the center six points per layer for medium and low bearing capacity (DBD 1.5 g/cm<sup>3</sup> and 1.3 g/cm<sup>3</sup>, respectively) caused with a 800/8.5/2.5t is shown in **Figure 18**. As explained in 5.3.3 every data point in **Figure 18** is the average of the central six talcum powder points of each layer. The displacement for the medium soil condition is significantly lower than for the soft soil condition ( $p = 0.0072$ ). For both soils the deformation decreases with depth and close to the bottom of the soil bin both curves approach each other.

For the average layer deformation diagram across the soil bin see appendix 13.1.3.

Two linear regression lines seem appropriate for the low bearing capacity soil conditions as they are properly able to explain soil deformation over depth with regression coefficients  $R^2 = 0.99$  and 1. Because the deeper part of the deformation lines of the low and medium bearing capacity soil conditions are similar, the decision was made to split up the linear regression lines for the low bearing capacity. For the medium soil conditions either a quadratic or two linear regressions can be fitted to the data. Overall the quadratic regression has a higher correlation coefficient,  $R^2 = 0.98$  compared to  $R^2 = 0.99$  and 0.89 for the two linear functions. Therefore the quadratic regression line seems more appropriate.

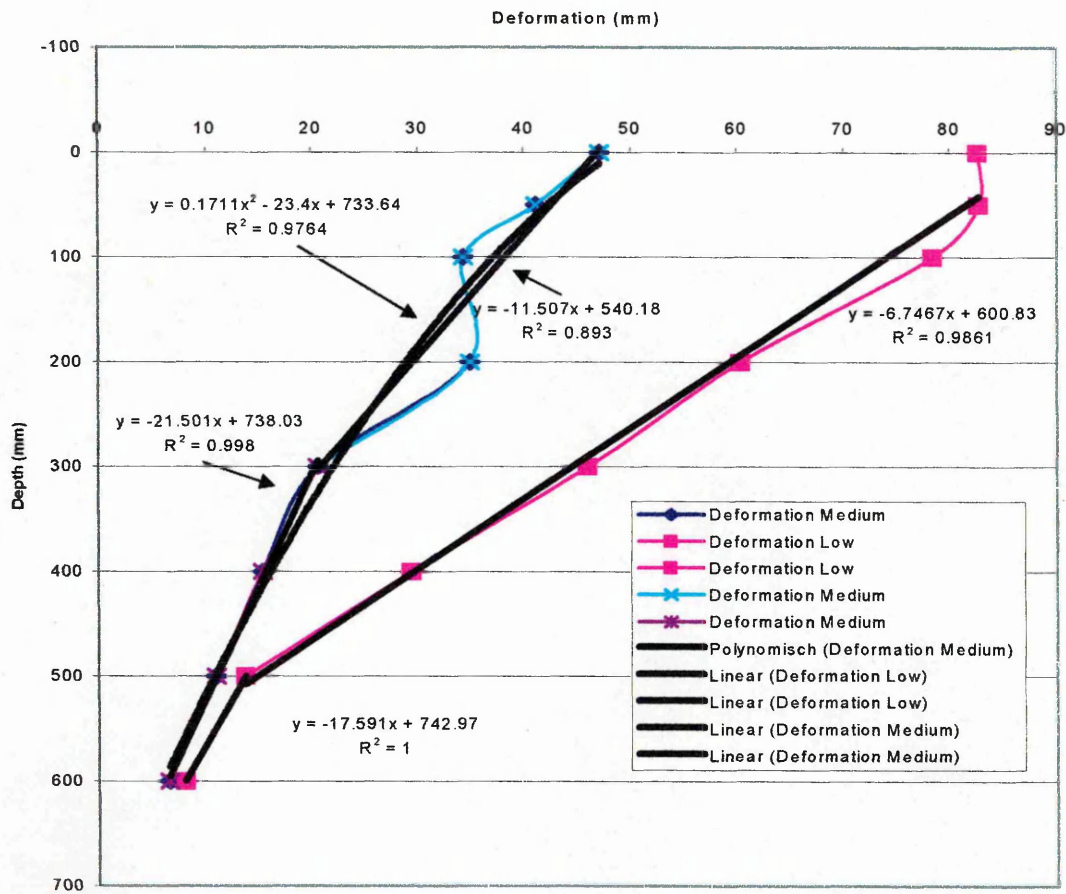


**Figure 18:** Vertical soil displacement vs. depth on low and medium soil bearing capacity for the 800/8.5/2.5t.

Soil strain of the measured data for the towed tire and both soil conditions is shown in **Figure 19**. The soil strain was determined by subtracting the final layer thickness from initial layer thickness, then divided by the corresponding initial layer thickness (see Eq. 4). The relative decrease in mm/mm is plotted vs. depth. The strain for the regression lines is shown as well. The strain is basically the differentiation of the regression lines and explaining strain as a function of depth.

Because of the steeper and more linear relationship in **Figure 18** the low bearing capacity shows a more pronounced and constant compaction over depth. The area between 200 mm depth to 500 mm depth is nearly uniformly compacted by a reduction of around 0.17 mm/mm or an increase in density of 17 %. The regression line shows an increase of 15 % down to 500 mm. Between 500 and 600 mm the increase is reduced to 5.5 %. The medium bearing capacity shows two peaks in compaction. The first in 100 mm depth and the sec-



ond at about 300 mm depth. This is due to seemingly non linearity in the medium soil at 100 mm – 200 mm depth shown in **Figure 18**. At lower depths the effect of compaction is reduced and more homogeneous. However, taking the differentiation of the squared regression into account for this soil condition the relative decrease seems to decrease with depth.

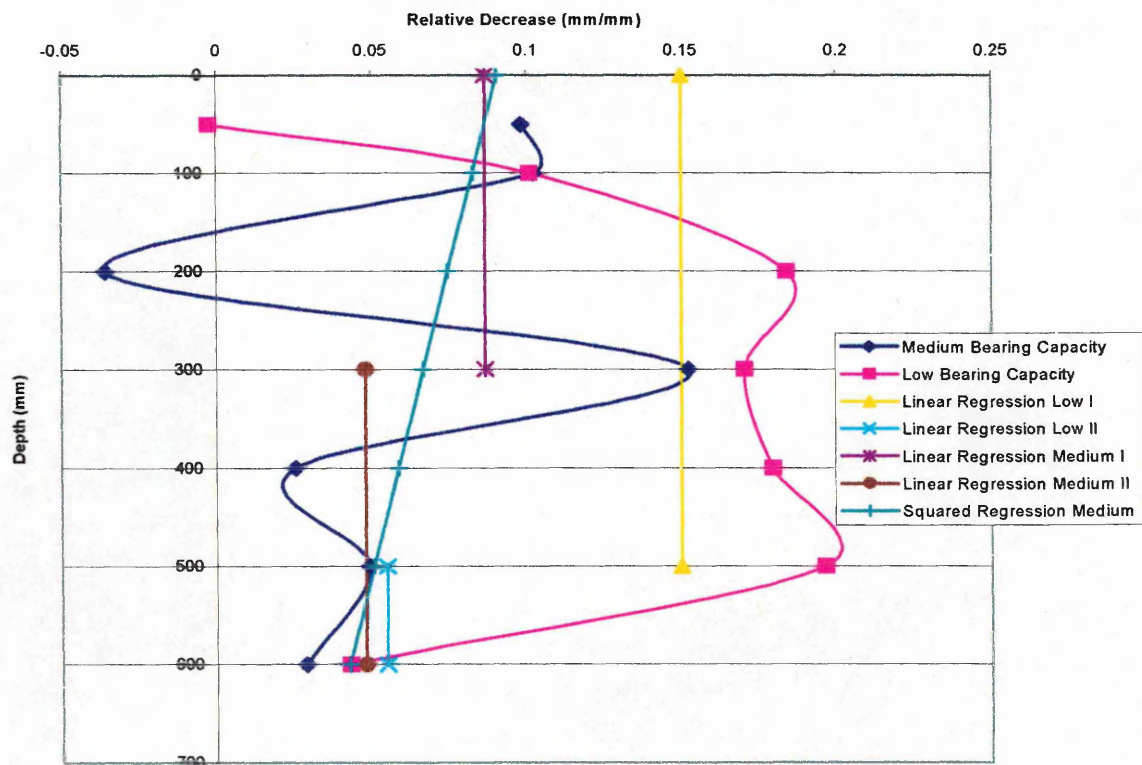


**Figure 19:** Relative decrease from initial to final layer thickness

The assumption of constant relative decrease for the medium soil condition does not seem to be as appropriate as the linear decrease. However, interesting to note is the similar relative decrease for both the medium and the soft soil conditions for the 2<sup>nd</sup> linear regression line. The relative decrease in layer thickness is 4.8 and 5.5 %. Whether the similar values at the bottom of the soil bin between medium and soft soil conditions are really meaning the soil would be strong enough to support the weight in the soft soil conditions or whether it is caused by the bottom influence of the soil bin is difficult to say. Yet it is interesting to note again that both soil conditions have the such a similar relative increase in their 2<sup>nd</sup> linear regression.

The relative decrease in the medium soil conditions shows a peak of compaction at about 300 mm depth. Thus in this case the soil appears to be strong enough to support most of the load above 400 mm depth. The peak of compaction at 100 mm depth appears to be at about the same value of 0.1 mm/mm relative decrease as for the soft soil conditions. Yet the fluctuation of the real relative decrease data around the line of linear decrease indicates the fact that the variation might be caused by mere noise of the measurements. Thus the relative decrease starts at 9 % and ends at about 4 %.

The peak in relative decrease for the medium soil condition corresponds with the depth of maximum penetrometer resistance very well. The peak in relative decrease at 300 mm depth is the average of the decrease in the layer initially being situated between 200 and 300 mm depth. Taking the displacement of about 35 mm from **Figure 18** into account for this layer the new position of the middle for this layer would be around 285 mm from the original surface. So the high penetrometer resistance below 200 mm corresponds with the soil displacement data. The force necessary to push a cone into the soil as done here, is more affected by the behavior of the soil somewhat deeper than immediately in front of the cone. For penetrometer resistance on soft soil conditions this conclusion can be supported as both the relative decrease as well as the penetrometer resistance show a uniform compaction between 210 mm down to 500 mm. Yet the large reduction in relative decrease found for the low bearing capacity below 500 mm cannot be found in penetrometer resistance. For the penetrometer resistance only a very small reduction occurs at 600 mm depth which is at the bottom of the last layer where soil displacement was measured.

### 6.1.3 Dry Bulk Density

The soil with medium bearing capacity had an average DBD of about  $1.54 \text{ g/cm}^3$  initially as well as finally. For the low bearing capacity initial DBD was  $1.33 \text{ g/cm}^3$  and finally  $1.50 \text{ g/cm}^3$ , thus an increase of about 13 %. This increase corresponds with the average increase shown in **Figure 19** for the low bearing capacity. The high variation and the resulting insensitivity using DBD as an indicator is already mentioned by Campbell (1994). In our case DBD changed with depth on soft soil condition. The highest value ( $1.63 \text{ g/cm}^3$ ) occurred at 250 mm depth. At the surface as well as at 500 mm depth statistically identical DBD ( $1.42 \text{ g/cm}^3$  and  $1.45 \text{ g/cm}^3$ ) were observed.

The data are summarized in **Table 4**.

**Table 4:** Dry bulk density values for initial and final soil conditions in towed wheels

All units are g/cm <sup>3</sup>	Soft Soil Conditions	SE	Medium Soil Condition	SE
Initial	1.33	0.019	1.55	0.07
Final (all)	1.50	0.042	1.56	0.03
Depth				
Surface	1.42	0.07	1.57	0.08
250 mm	1.63	0.06	1.56	0.02
500 mm	1.45	0.0002	1.56	0.09

#### 6.1.4 Rut Depth

**Table 5** shows the depth, width, and area of the rut created with the 800/8.5/2.5t including pooled SE for direct comparison of the means.

**Table 5:** Rut parameters including pooled SE for 800/8.5/2.5t

Soil Condition	Width (m)	Depth (m)	Area (m <sup>2</sup> )
Soft	0.85	0.12	0.0599
Medium	0.72	0.08	0.0267
Pooled SE	0.022	0.005	0.003

Statistically depth, width, and area are significantly smaller for the 800 tire on medium than on soft soil conditions. This was expected as soil with a higher bearing capacity, e.g. a higher initial DBD is less deformed when carrying same amount of load.

The smaller rut area, width and depth for the medium soil condition compared to the soft soil condition is in accordance with the amount of deformation caused on the two different treatments. The width of the rut is reduced due to less sinkage in medium soil condition which in consequence both reduce the rut area.

### 6.1.5 Rolling Resistance

On medium soil conditions the rolling resistance for the 800/8.5/2.5t was 9.28 kN with a standard error of 0.072 kN and on soft soil conditions draught force was 14.46 kN with a standard error of 0.063kN. Therefore the coefficient of rolling resistance for medium bearing capacity is 0.11 and 0.17 for medium and low bearing capacity, respectively. The low bearing capacity has a statistically significant higher (54%) rolling resistance.

The increase in rolling resistance from medium to soft soil conditions corresponds with the increase in soil deformation and rut. Due to the energy required for the process of deformation draught force and therefore rolling resistance has to increase when soil deformation increases.

## 6.2 Soil Compaction Caused by Driven Wheels and Tracks

All runs were done at approximately 10 % slip and approximately 3.6 km/h.

### 6.2.1 Penetration Resistance

The average of the central four penetrometer resistance readings over depth is shown in **Figure 20**, including both the undisturbed control as a mean over all experiments and LSD at a 95 % - probability level. The penetrometer data averaged at the centre as explained in chapter 5.3.4 is shown in Appendix 13.1.1 for each tire/track. The tire data is separately given in **Figure 21** and track data is shown in **Figure 22**. This demonstrates that tracks cause a higher penetrometer resistance than tires at the surface where it can easily be alleviated. For all tires the penetrometer resistance is higher in the subsoil (below 250 – 300 mm) than for tracks.

The 800/8.5/2.5t is also included in **Figure 21** because the measurements were taken in the same soil conditions. However, due to the different curvature it is not considered in the statistical comparison. One LSD is shown, which due to very similar SE does not vary very much with depth (SE is between 0.1366 and 0.1378 MPa thus the corresponding LSD between 0.279 and 0.282 MPa; in the diagram drawn as 0.28 MPa).

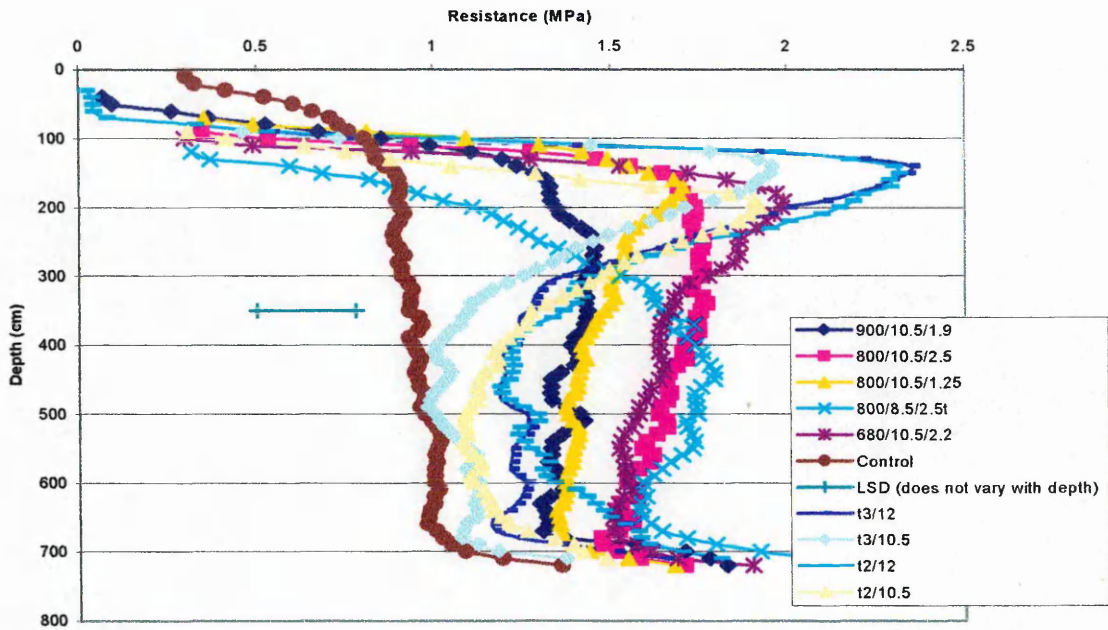


Figure 20: Penetrometer resistance below tracks and tires including control and LSD

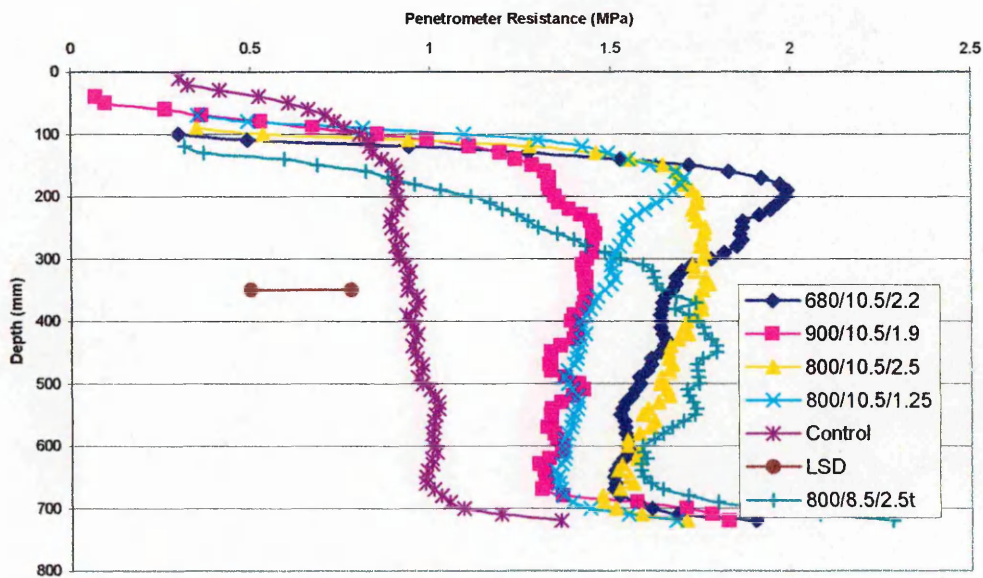


Figure 21: Average penetrometer resistance vs. depth for all tires on low bearing capacity

All of the curves are significantly different from the control. The 680/10.5/2.2 is statistically similar to the 800/10.5/2.5 ( $p$  – value = 0.987). The 800/10.5/1.25 is statistically identical with the 900/10.5/1.9 ( $p$  – value = 0.455). All other comparisons are different with  $p$ -values between 0.0068 for the 680/10.5/2.2 against the 900/10.5/1.9 to 0.040 for the 800/10.5/2.5 against the 800/10.5/1.25. Average penetrometer resistance, corresponding SE and degrees of freedom (DF) are shown in **Table 6**

**Table 6:** Statistical summary of penetrometer resistance for self propelled tires

Tire	Overall Average Penetrometer Resistance (MPa)	SE	DF
680/10.5/2.2	1.617	0.0845	25.2
800/10.5/2.5	1.615	0.0849	25.2
800/10.5/1.25	1.340	0.0838	24.8
900/10.5/1.9	1.245	0.0825	24.1
Control	0.883	0.0318	23.9

The different shapes of penetration resistance curves over depth are interesting to note. Only the 800/10.5/1.25 and 680/10.5/2.2 tire show a pronounced peak in penetrometer resistance close to the surface and a decline afterwards. The 900/10.5/1.9 as well as the 800/10.5/2.5 miss this pronounced peak in resistance close to the surface. For these resistance is constant with depth below 150 mm.

The grouping of the tire configurations (680/10.5/2.2 and 800/10.5/2.5 against the 900/10.5/1.9 and 800/10.5/1.25) indicates the relationship between contact area to penetrometer resistance. Tires with a larger contact area create less penetrometer resistance.

Due to the different curvature the 800/8.5/2.5t was not included in the statistical analysis. When comparing the shape of the curvature to the shape of the 800/10.5/2.5 it is very interesting that the lower load being pulled causes consistently higher penetrometer resistance at a depth between about 400 to 600 mm, although not statistically significant. The increase in penetrometer resistance at the surface is lower as well. Yet, it can not be concluded whether these differences are due to a smaller load or whether it is a slip effect as two parameters are different.

From **Figure 22** it can be seen that the shape and the values of the penetration resistance curve for the three idler and the two idler track at 12 t are very similar. At 10.5 t the curves have the same shape, however, the two idler track reaches the peak penetrometer resistance slightly greater depth.

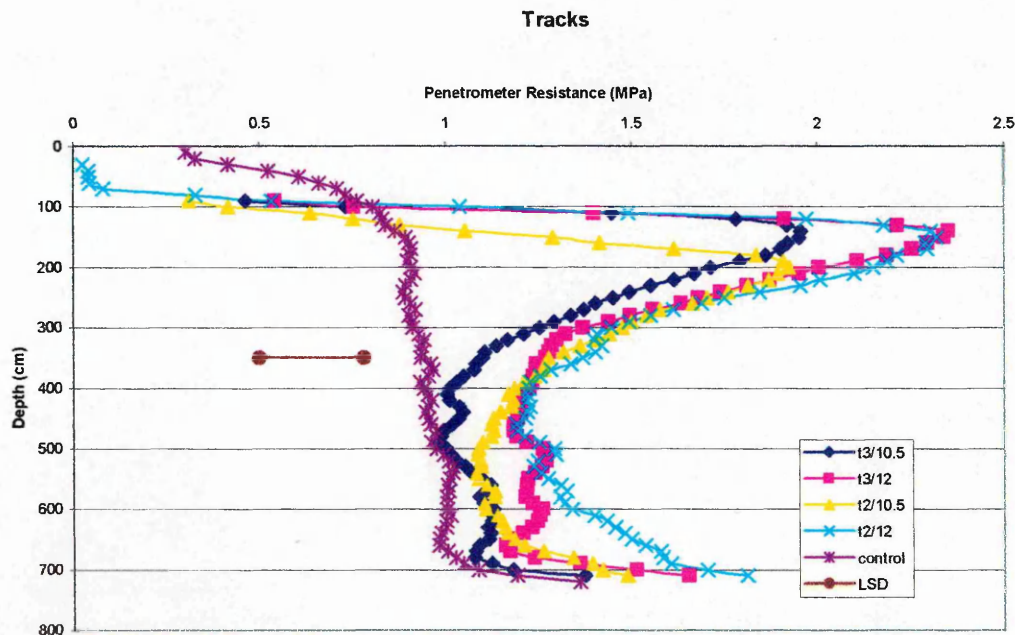


**Figure 22:** Penetrometer resistance below tracks including control and LSD

The very pronounced peak in penetrometer resistance close to the surface already mentioned before is obvious from this diagram. Statistically all tracks are the same because of the very similar shape and values. The only significant difference occurs in the depth between 100 and 200 mm between the 12 t and 10.5 t load. This is not enough to cause a significant difference when comparing the entire curves. Below 350 to 400 mm depth the final curves approach the initial condition strongly. As a consequence the difference between the final and initial conditions is merely significant for the t2/12, t2/10.5, t3/12 but not for the t3/10.5 over the entire depth.

In comparison to the wheels, tracks keep the change in penetrometer resistance very close to the surface. For the wheels, the peak penetrometer resistance is smaller, with the penetrometer resistance in the deeper layers being significantly higher than for tracks. Thus the advantage of tracks is the fact that these keep the soil compaction in layers close to the surface where it can be removed with shallower tillage operations.

**Table 7:** Statistical summary of penetrometer resistance for tracks

Track	Overall Average Penetrometer Resistance (MPa)	SE	DF
T2 10.5	1.189	0.1021	21.7
T2 12	1.212	0.1021	21.7
T3 10.5	1.0453	0.1027	21.9
T3 12	1.359	0.1007	21.4
Control	0.883	0.0318	23.9

### 6.2.2 Soil Deformation

Lines of white talcum powder were put into the soil during preparation in three replications and at a control position. A position of the cross section with the deformed white talcum powder lines is shown in **Figure 23**. Using the drawstring transducers this has been transformed into the soil deformation diagram as shown in **Figure 24**. A representative picture like **Figure 23** and the average displacement (**Figure 24**) for each test is shown in appendix 13.1.3 and 13.1.2, respectively.



**Figure 23:** Vertical cut through soil with points of talcum powder when the 900/10.5/1.9 had passed.



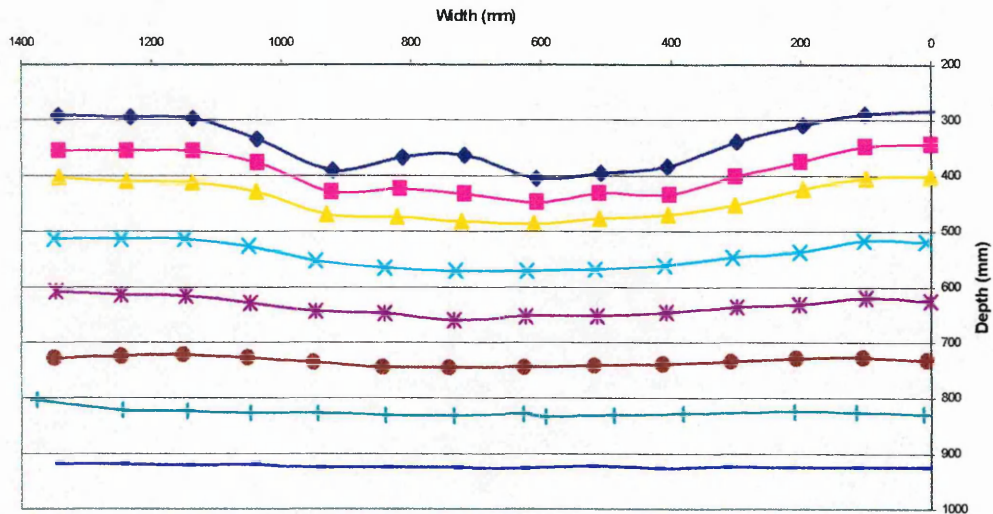


**Figure 24:** Average position of the displaced talcum powder points following the passage of the 900/10.5/1.9

**Figure 25** shows that the soil deformation for tires at standard inflation pressure is significantly greater than for tires at half the standard inflation pressure, which is significantly greater than the tracks.

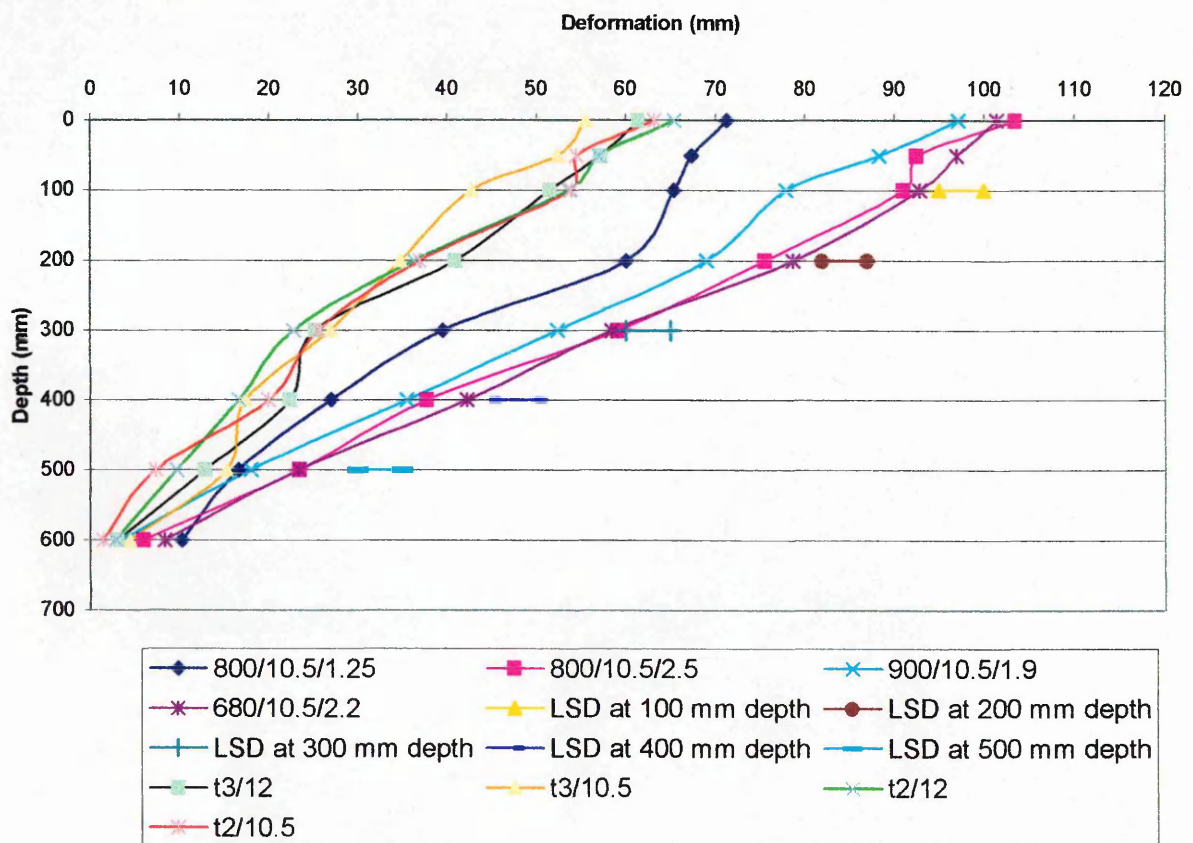


**Figure 25:** Soil deformation for all devices including LSD at given depth

**Figure 26** separates the tire data from the track data given in **Figure 27**. At the surface tires at normal inflation pressure cause about 100 mm of deformation which decreases to about 10 mm deformation at 600 mm depth. The tire at half inflation pressure starts at about 70 mm soil deformation in the surface and converges with the results of the other tires at 600 mm depth.

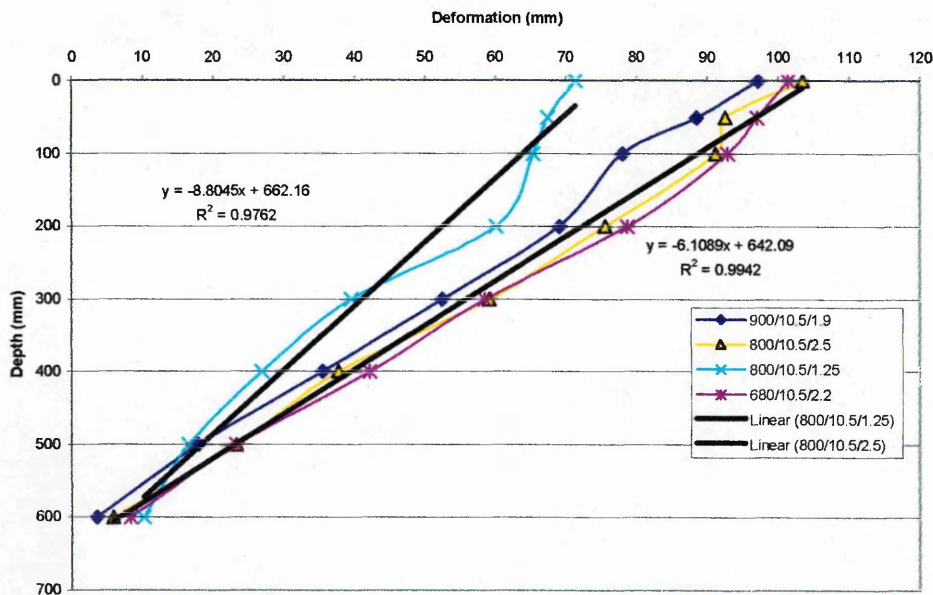


**Figure 26:** Soil deformation for the tires at normal working pressure and one at half inflation pressure (1.25 bar)

The nearly identical soil displacement caused by the 800/10.5/2.5 and 680/10.5/2.2 shown in **Figure 26** was very surprising. It would be expected just from looking at the section width that the 800/10.5/2.5 causes less soil displacement than the 680/10.5/2.2. However, due to tire properties like carcass stiffness, diameter (the 680 has a larger diameter, hence a greater length of contact patch giving a similar contact area as shown in **Table 11**) and necessary inflation pressure the smaller section width achieved this result. The 900/10.5/1.9 section width tire caused as expected (due to its width and inflation pressure) the least soil deformation at recommended inflation pressure. The 800/10.5/1.25 showed a significant decrease in soil deformation which can be achieved when using half the recommended inflation pressure. This is particularly interesting when looking at the penetrometer resistance results as there the 800/10.5/1.25 and the 900/10.5/1.9 cause the same final penetration resistance, yet in soil deformation they are significantly different from each other.

Significantly different is the 680/10.5/2.2 from the 800/10.5/1.25 and the 900/10.5/1.9 ( $p$  – values  $<0.0001$  and  $0.0003$ , respectively). The 680/10.5/2.2 tire is not significantly different from the 800/10.5/2.5 ( $p$  – values  $0.47$ ). The 800/10.5/2.5 itself is different from the 800/10.5/1.25 as well as the 900/10.5/1.9 (with  $p$  – values respectively  $<0.0001$ , and  $0.0038$ ). The 800/10.5/1.25 is significantly different from all tires as mentioned before and different from the 900/10.5/1.9 ( $p = 0.0002$ ). Taking the 800/8.5/2.5t into the same context as it has the same initial soil conditions, it is different from all except the 800/10.5/1.25.

**Figure 27** shows that the deformation of the soil caused by the tracks is about 60 mm deformation at the soil surface and decreases to about 5 mm deformation in 600 mm depth. As expected tracks at 12 t load cause more deformation than tracks at a 10.5 t load. However, these differences are not statistically significant.

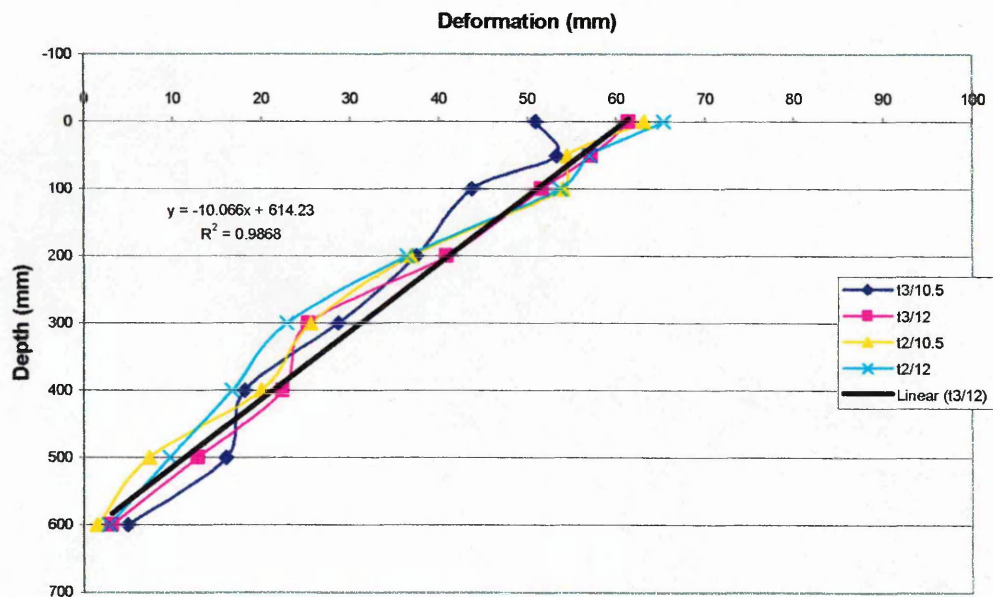


**Figure 27:** Soil deformation for the two and three idler track at corresponding tire load and at real tracked combine harvester working load

Transferring the equation of the regression line into deformation as a function of depth (instead of depth as a function of deformation which is given in the diagram) and differentiating these equations reveals the average increase in soil density over depth. Due to the high correlation coefficient a linear relationship between depth and deformation can be assumed. The correlation coefficient is between 0.99 to 0.97 for the three lines. For the tracks this reveals an average increase of 10 % in soil density, for the tire at half inflation

pressure this reveals an increase of about 12 % and for the tires at normal inflation pressure of 15 %.

Due to the very high correlation coefficient for the curves in **Figure 26** and **Figure 27** and as a result of the discussion of soil strain over depth from section 6.1.2 a linear relationship of deformation over depth is appropriate. Therefore the discussion in section 6.1.2 concerning the depth of maximum compaction and the non - linearity of soil compaction over depth is not repeated in this chapter. The only difference is the fact that only one linear regression line seems appropriate enough to fit each soil deformation line. Compared to section 6.1.2 the clear difference in slope between 500 to 600 mm depth and 0 to 500 mm depth can not be found in these curves for self propelled tires at a higher load. Linearity for soil strain seems appropriate for tracks as well. So using the linear regression lines as a function of soil deformation can describe the soil behavior satisfyingly.

### 6.2.3 Average Dry Bulk Density

There was no significant difference between soil bin preparations and hence all tests can be assumed to have been conducted in homogenous and nearly identical initial conditions. The data is shown in **Figure 28**.

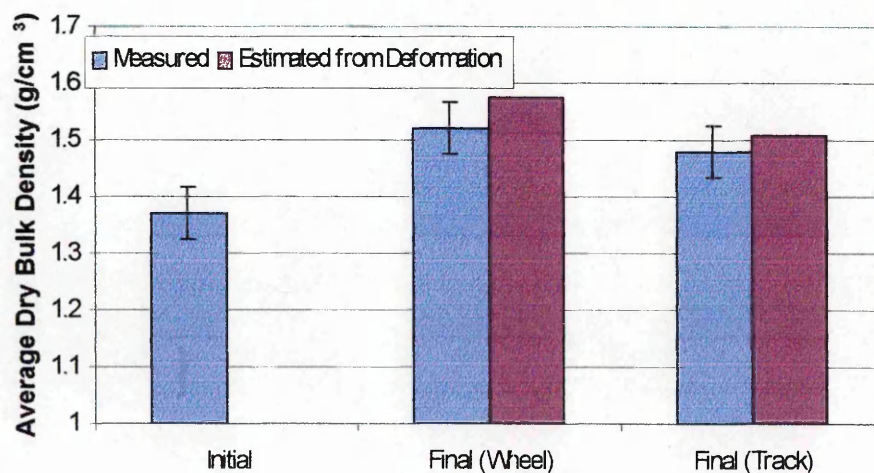


**Figure 28:** DBD initially and finally measured as well as expected for wheels and for tracks including 95% - confidence interval

The final measured dry bulk density (DBD) for both tires (1.52 g/cm<sup>3</sup>) and tracks (1.48 g/cm<sup>3</sup>) is significantly higher than initial DBD (1.37 g/cm<sup>3</sup>). The small difference between the wheel and track is also significantly different. All means are shown including a 95% - confidence interval (+/- 0.046 g/cm<sup>3</sup>). The statistical analysis (**Table 8**) of individual tires and tracks showed no significant effect on DBD.

This is a problem of the assessment of soil change with this method – as it is very insensitive. Campell (1994) discussed the difficulty in assessing soil compaction using dry bulk density in detail. The data given earlier in sections 6.2.1 and 6.2.2 has greater resolution. The increase in DBD for the tires is about 11 % and for the tracks about 8 %. These values support the increase in soil density calculated from the soil deformation in section 6.2.2. The calculated increase for tracks, tire at half inflation pressure and normal tire thereby was 10 %, 12 % and 15 %, respectively.

All DBD are numerically summarized in **Table 8**.

**Table 8:** Dry bulk density for self propelled experiments

Effect	Average of DBD (g/cm <sup>3</sup> )	SE	DF
680/10.5/2.2	1.56	0.0283	26.8
800/10.5/2.5	1.51	0.0255	18.7
800/10.5/1.25	1.55	0.0283	26.8
900/10.5/1.9	1.47	0.0283	26.8
T2 10.5	1.47	0.0282	26.8
T2 12	1.47	0.0283	26.8
T3 10.5	1.49	0.0283	26.8
T3 12	1.49	0.0283	26.8
Initial	1.37	0.0194	6.83
Final Wheel	1.52	0.0174	4.48
Final Track	1.48	0.0185	5.66

### 6.2.4 Rut Characteristics

The depth of the rut appears to depend on the inflation pressure and on the tire / track load. The higher both the load and inflation pressure, the deeper the rut depth becomes. For a detailed discussion of the rut depth and its connection to the measurement of soil deformation in the surface see the end of this chapter. The width of the rut is basically a function depending on the width of the tire / track belt. Thus the wider the tire and the less inflation pressure for the same load the wider the rut becomes. The area now is a function of load and inflation pressure. This would explain why the 680/10.5/2.2, 900/10.5/1.9 and the 800/10.5/2.5 at normal inflation pressure and load give similar results, and only results for the 800/10.5/1.25 differ from the others.

For detailed statistics concerning the question of identical and different values for each parameter and measurement see **Table 9**.

**Table 9:** Rut depth, width, and area of tires and tracks including LSD (due to slightly varying standard errors the range of LSDs is shown). Numbers not followed by the same letter (a – e) are statistically different.

Tire / Track	Max. Depth (m)	Max. Width (m)	Cross Sectional Area (m <sup>2</sup> )
680/10.5/1.9	0.127      a	0.760      a	0.060      a
800/10.5/2.5	0.110      b c	0.860      b	0.054      a
800/10.5/1.25	0.100      c d	0.917      b	0.040      b e f
900/10.5/1.9	0.123      a b	0.925      b	0.070      a
T2 10.5	0.102      c	0.707      c	0.031      d
T2 12	0.110      c	0.688      c	0.035      d e
T3 10.5	0.078	0.690      c	0.032      d
T3 12	0.092      c d	0.690      c	0.038      d f
LSD	0.012 – 0.0156	0.051 – 0.068	0.0072 – 0.011

The differences in rut depth, width, and area are less pronounced than penetrometer resistance and soil deformation. Therefore only taking a measurement of the rut and then trying to detect the tire causing least soil damage is not possible. Unfortunately, this finding is a

handicap for the interpretation of measurements of rut parameters as these can easily be taken in the field and are the most obvious parameters for farmers to look for on their fields.

When looking at the deformation in the surface caused by the different tires and tracks shown by the first point in **Figure 25**, then this is always less than the maximum rut depth discussed above. This is due to the way of measurement as rut depth is measured at the deepest point in the profile gained with the profile - meter. These deepest points were caused by the lugs. The deformation in the surface measured using the drawstring transducers is basically an average over 18 measurement points and therefore a representative average over rut depth caused by the mere tire / track body and the additional rut depth caused by the lugs. Therefore the soil deformation measurement is more reliable or for the rut depth several depth measurements at random positions across the rut would have to be taken which then basically would reveal the same results. To verify this assumption lug height and rut depth in areas without lug influence was measured and summed up. The data is shown in **Table 10**. The deformation in the surface (shown in **Figure 25**) is approximately in the middle between the depth of rut area without lugs and depths with lugs. Interestingly the difference between the maximum rut depth measured and the one calculated was always positive for the 800 mm section tire and both tracks, yet negative for the two other tires. This leads to the conclusion that the 800 mm section width tire and the tracks have a stiffer contact area than the other two tires. For the 680 and 900 mm section width tire the lugs seem to be pressed into the surface as the real rut is smaller than the one calculated.

**Table 11** shows the maximum length and width as well as the contact area of the static contact patch of the tires. The contact width follows the same rules as discussed at the beginning of this section and contact length is mainly influenced by the tire diameter and inflation pressure. The contact area is a result of both.

**Table 10:** Rut depth in areas without lug influence (Rdw); lug height of the different tires (L); the resulting maximum rut depth as the sum of Rdw and L (Rds); measured maximum rut depth (Rdm); difference (D) between Rdm and Rds.

Tire	Rdw (mm)	L (mm)	Rds (mm)	Rdm (mm)	D (mm)
680/10.5/2.2	85	52	137	127	- 10
800/10.5/2.5	52	52	104	110	+ 6
800/10.5/1.25	30	52	82	100	+ 18
800/8.5/2.5t soft	65	52	117	120	+ 3
800/8.5/2.5t medium	20	52	72	80	+ 8
900/10.5/1.9	80	55	135	123	- 12
T2 10.5	20	63	83	101	+ 18
T2 12	28	63	91	110	+ 19
T3 10.5	25	45	70	78	+ 8
T3 12	30	45	75	92	+ 17

**Table 11:** Contact patch geometry of the tires

Tire	Max. Width (m)	Max. Length (m)	Contact Area (m <sup>2</sup> )
680/10.5/2.2	0.69	1.2	0.69
800/10.5/2.5	0.78	0.96	0.62
800/10.5/1.25	0.9	1.3	0.98
900/10.5/1.9	0.9	1.2	0.94

### 6.3 Soil Compaction in Stratified Soil Conditions

#### 6.3.1 Penetration Resistance

Figure 29 shows the penetrometer resistance initially in the soil bin for the preparation of both the t3/12 and the 900/10.5/1.9. The penetrometer resistance in field condition with a plough layer is included as well. Thus it was possible to mimic real field conditions with a plough layer in the soil bin. The working depth from 0 – 200 mm depth shows the least



resistance, followed by the compacted plough layer between 200 – 300 mm depth and then less resistance in the subsoil from 300 – 700 mm depth. The only difference between field and soil bin conditions is the plough layer being 30 – 40 mm deeper in field conditions.

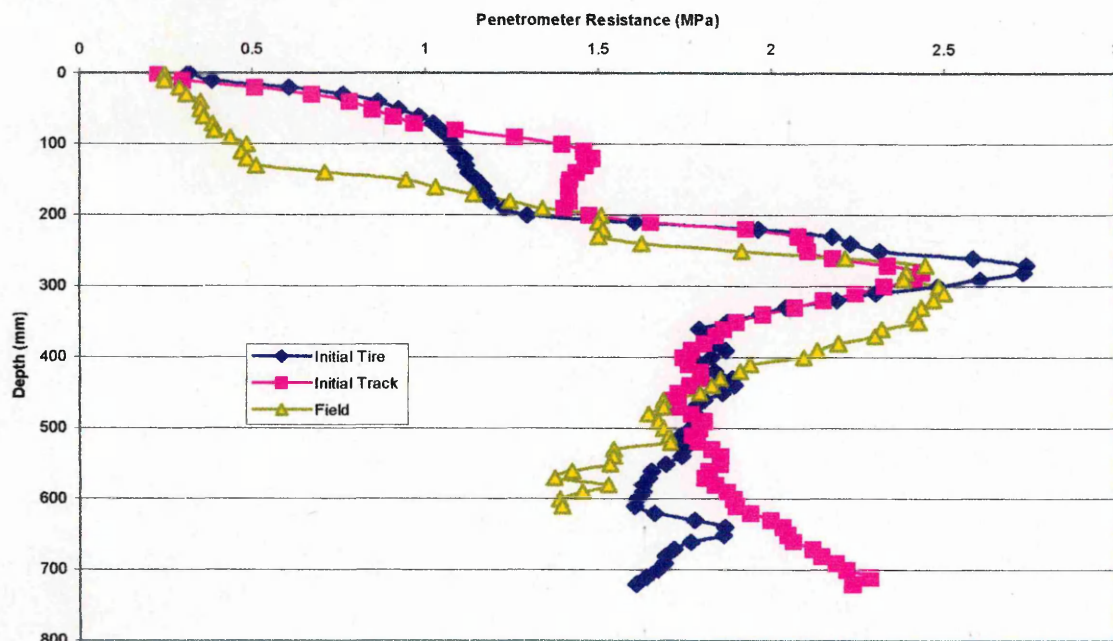


**Figure 29:** Initial penetrometer resistance in soil bin preparation as well as in real field conditions.

After the pass of the 900/10.5/1.9 penetrometer resistance is increased significantly. The initial and final curve is shown in **Figure 30**. The tire increased penetrometer resistance over the whole profile except the plough layer. The penetrometer resistance in the stratified soil conditions for the tire has a similar shape as in uniform conditions. The penetrometer resistance for the 900/10.5/1.9 on uniform soil conditions shown in **Figure 21** shows the same uniform higher penetrometer resistance as **Figure 30** except for the plough layer. In **Figure 30** the final penetrometer resistance (excluding the plough layer) is a near vertical line. The penetrometer resistance above and below the plough layer has the same average of approximately 2 MPa. It seems as if the plough layer has increased its thickness compared to the initial curve. When looking at the soil deformation in **Figure 32** this becomes clear, as this shows that the plough layer was pushed down into the weaker subsoil and this increases the thickness due to the new compact layer on top of the plough layer.

Penetrometer resistance initially and finally for the t3/12 in stratified soil conditions is shown in **Figure 31**. Again as before, the final curve shows the same principal behavior as on uniform soil conditions. There is the very pronounced peak close to the soil surface

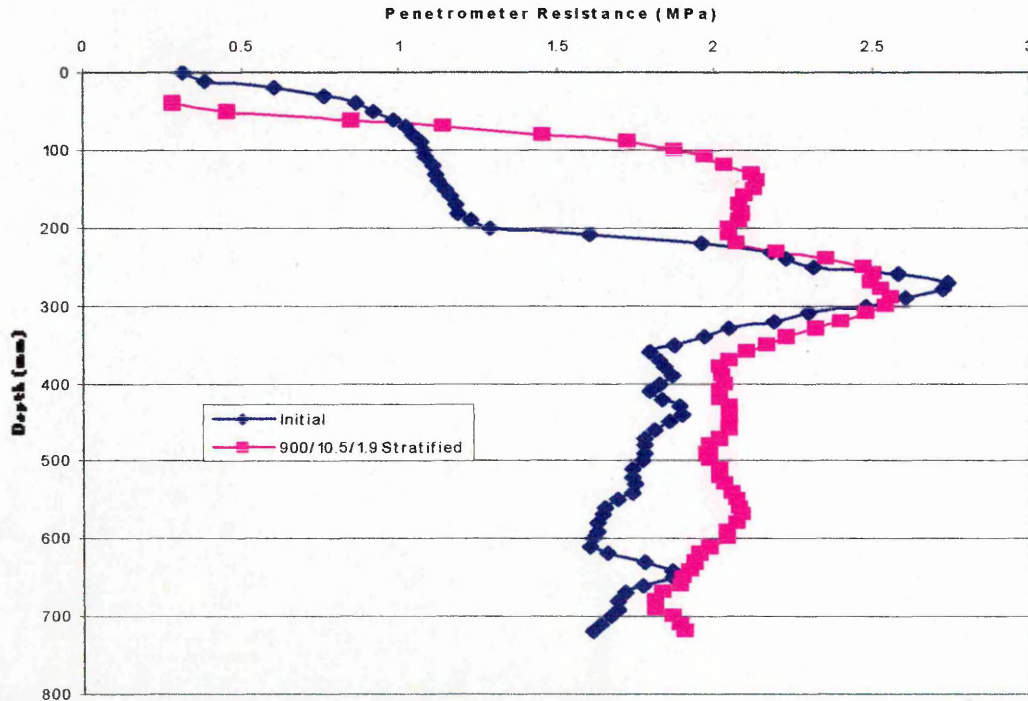


**Figure 30:** Initial and final penetrometer resistance on stratified soil conditions for the 900/10.5/1.9

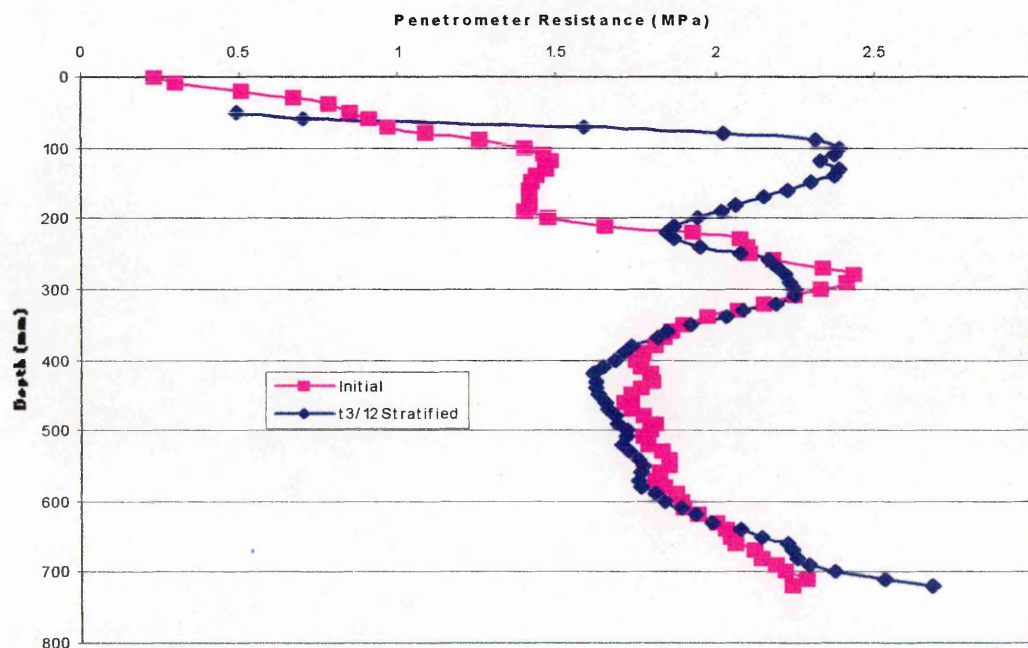


**Figure 31:** Initial and final penetrometer resistance on stratified soil conditions for the t3/12

followed by a reduction in penetrometer resistance. Thus the penetrometer resistance for the final condition merges with the initial condition in the working depth before the plough layer is reached. Once the final penetrometer resistance reaches the initial condition it remains at that value. There is therefore a significant increase in penetrometer resistance in the working depth for the track, yet before reaching the plough layer it is the same as initially.

Statistically penetrometer resistance for the track is significantly lower than for the tire on stratified soil conditions ( $p < 0.0001$ ) and both are different from their initial condition ( $p < 0.0001$ ).

### 6.3.2 Soil Deformation

Soil deformation over depth is shown in **Figure 32**. It includes the deformation of the 900/10.5/1.9, the 800/10.5/1.25 and t3/12 on uniform soil conditions and the 900/10.5/1.9 and t3/12 on stratified soil conditions. The overall deformation is largely reduced between the uniform and stratified soil conditions. This is due to the stronger soil conditions in the stratified soil conditions. At the surface the t3/12 and the 900/10.5/1.9 show nearly the same deformation, however at greater depths the soil strain behaves differently for the two

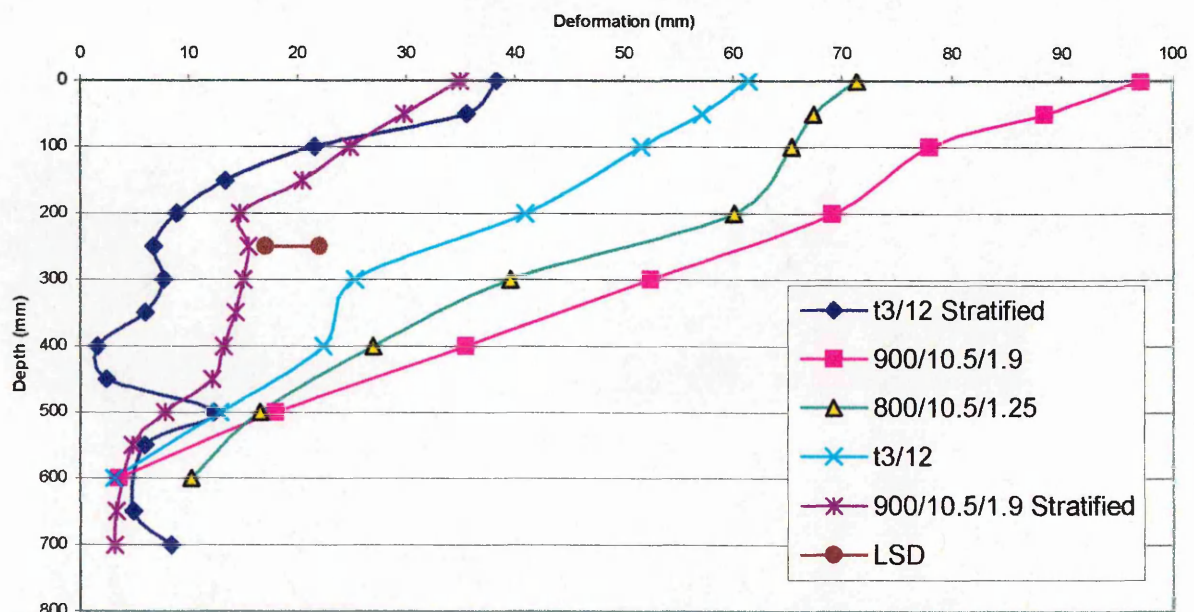


**Figure 32:** Soil deformation on stratified soil conditions for the 900/10.5/1.9 and the t3/12.

different treatments. The deformation of the t3/12 track is less at depth than the 900/10.5/1.9 tire. The lowest deformation for the track happens at 400 mm depth. Below this there is no deformation and the differences in the diagram have to be noise as there is no possibility that the initial and final layer is at the same depth at one depth and below it differs again. This has to be influenced by measurement and soil bin preparation errors (the only ones found during the whole project). The 900/10.5/1.9 tire, however, pushes the plough layer down into the weaker subsoil. It can be concluded that there is no change in deformation between 200 and 350 mm depth. Then deformation decreases again below 400 mm depth.

Statistically deformation for the t3/12. and the 900/10.5/1.9 on stratified soil conditions is significantly different ( $p = 0.0215$ ). LSD of 4.7 mm is shown in **Figure 32**, too.

### 6.3.3 Dry Bulk Density

**Figure 33** shows the initial and final dry bulk density for the working depth, plough layer and subsoil on the stratified soil conditions. At the bar of the initial DBD the 95 % - Confidence interval is included. As the CI overlaps with all means these are all the same. The reason for these large CI is the small sample size taken in stratified soil conditions due to only two soil bin preparations and thus only 6 measurements. The DBD in **Figure 28** is the average of 7 soil bin preparations and therefore the deviation is smaller and differences can actually be determined.

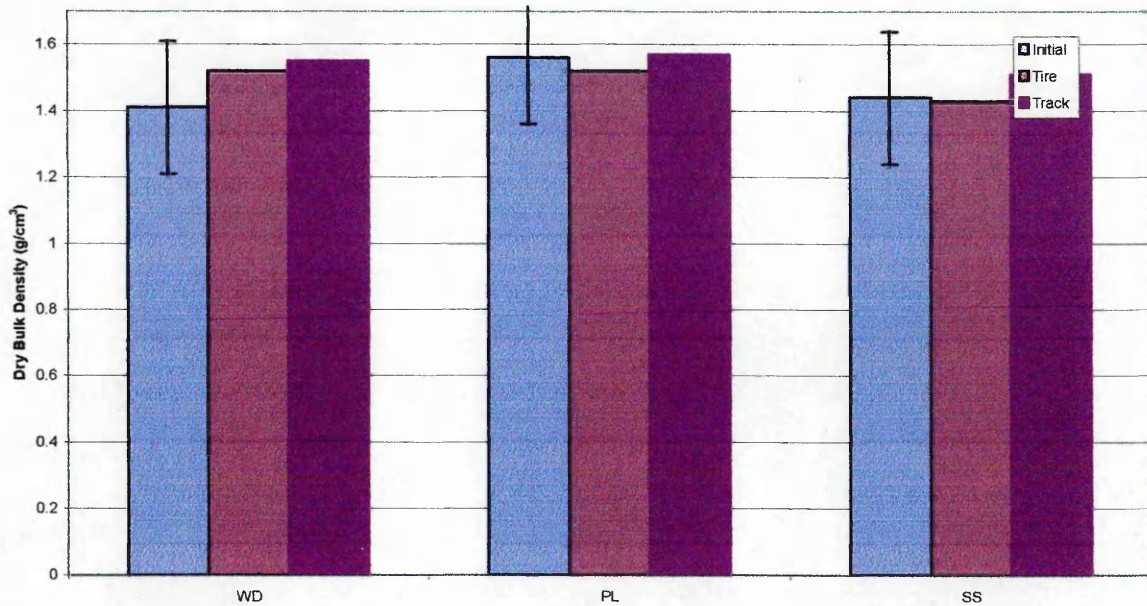


**Figure 33:** Initial and final dry bulk density in working depth (WD), plough layer (PL) and subsoil (SS)

#### 6.3.4 Rut characteristics

Rut characteristics are shown in most of the cross sectional area. Thus without the lugs there would be hardly a rut.

**Table 12.** Both treatments cause the same rut geometry apart from its width due to the different initial width. Therefore the differences seen in soil deformation in **Figure 32** and in penetrometer resistance in **Figure 30** and **Figure 31** between the t3/12 and 900/10.5/1.9 can not be detected by merely looking at the surface. The similar area is due to the lugs causing most of the cross sectional area. Thus without the lugs there would be hardly a rut.

**Table 12:** Rut characteristics for stratified soil conditions

	Max. Depth (m)	Max. Width (m)	Cross Sectional Area (m <sup>2</sup> )
Track	0.050	0.58	0.013
Tire	0.052	0.79	0.013

## 6.4 Multi Pass Effect

### 6.4.1 Penetrometer Resistance

Penetrometer resistance initially and after one, two, and three passes of the 900/10.5/1.9 tire on uniform soil conditions is shown in **Figure 34**. The resistance after the pass of the t3/12 is also shown.

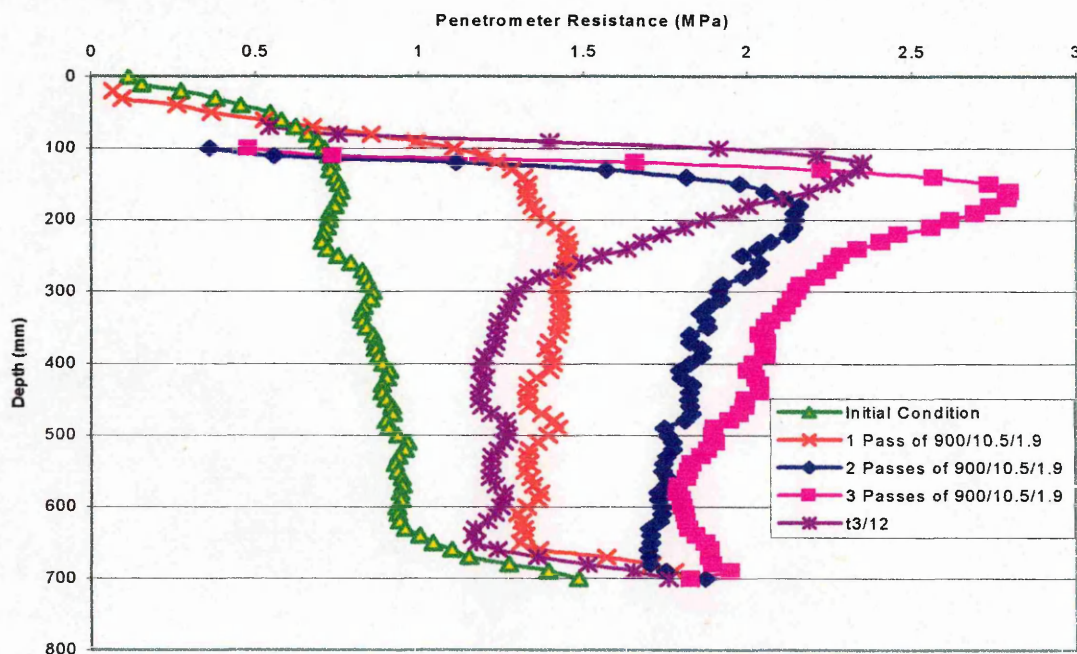


**Figure 34:** Penetrometer resistance initially, after one pass, two passes and three passes of the 900/10.5/1.9

After the first pass the soil is compacted uniformly over depth. Basically the penetrometer resistance increased from 0.83 MPa to 1.19 MPa. After the second pass a small peak in penetrometer resistance starts to develop close to the surface with a small reduction with depth. The average penetrometer resistance has increased to 1.60 MPa. After the third pass there is a pronounced peak in penetrometer resistance close to the surface and a greater reduction with depth. The curve has the shape of the penetrometer resistance below a track now. The average is increased to 1.84 MPa. However, the increase is higher close to the surface than at depth. To show the similarity in curvature after the pass of a t3/12 and three passes of a 900/10.5/1.9 the penetrometer resistance below a t3/12 is also included.

Increase in penetrometer resistance reduces with subsequent passes and finally shows a similar shape as after the pass of a track.

#### 6.4.2 Soil Deformation

The difference in soil deformation between one and three passes of the 900/10.5/1.9 is shown in

**Figure 35.** The deformation in the surface increased from about 95 mm deformation to about 115 mm deformation. The deformation at 600 mm depth increased from 10 to 15 mm deformation.

When differentiating the linear regression line of both curves, the average increase in density is about 15 % after one pass and 18 % after three passes. Therefore the two additional passes cause an overall increase of an additional 20 % in density. With correlation coefficients of more than 99 % linearity is justified.

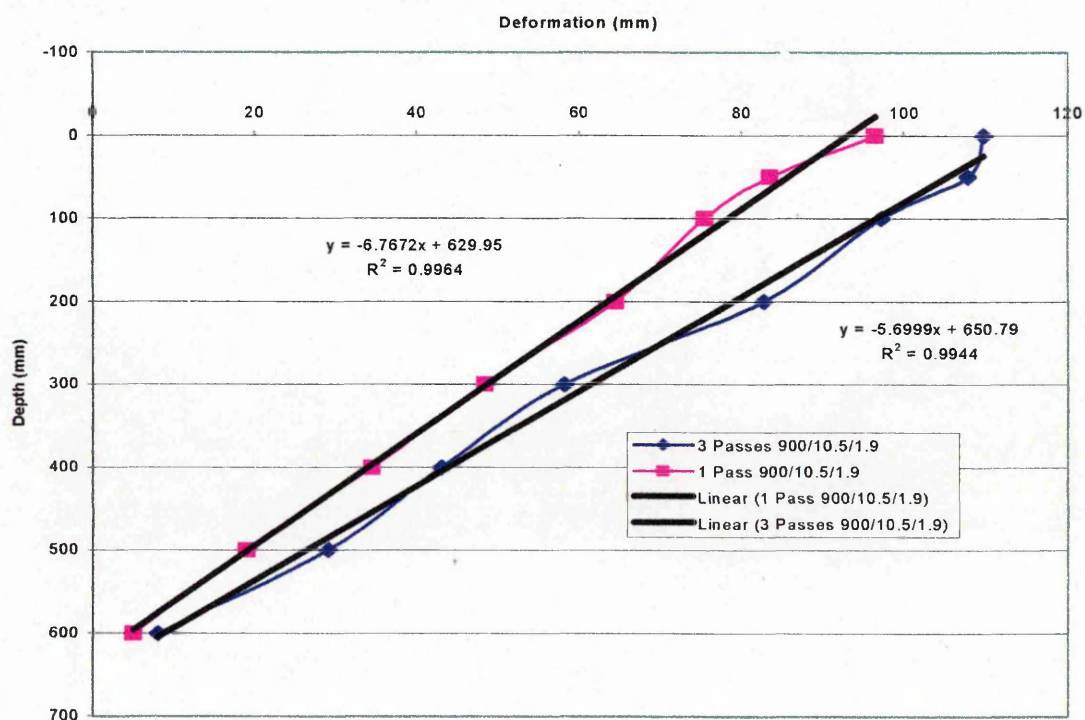


**Figure 35:** Vertical soil deformation after one and three passes of the 900/10.5/1.9

### 6.4.3 Dry Bulk Density

The measured and estimated (on basis of the initial DBD using the slope of the deformation curves) increase in DBD for one pass and three passes is shown in **Figure 36**. The measured DBD is the average of samples taken at three depths. Statistically all are different. DBD initially is  $1.38 \text{ g/cm}^3$ , after one pass  $1.52 \text{ g/cm}^3$  and after three passes  $1.61 \text{ g/cm}^3$  measured.

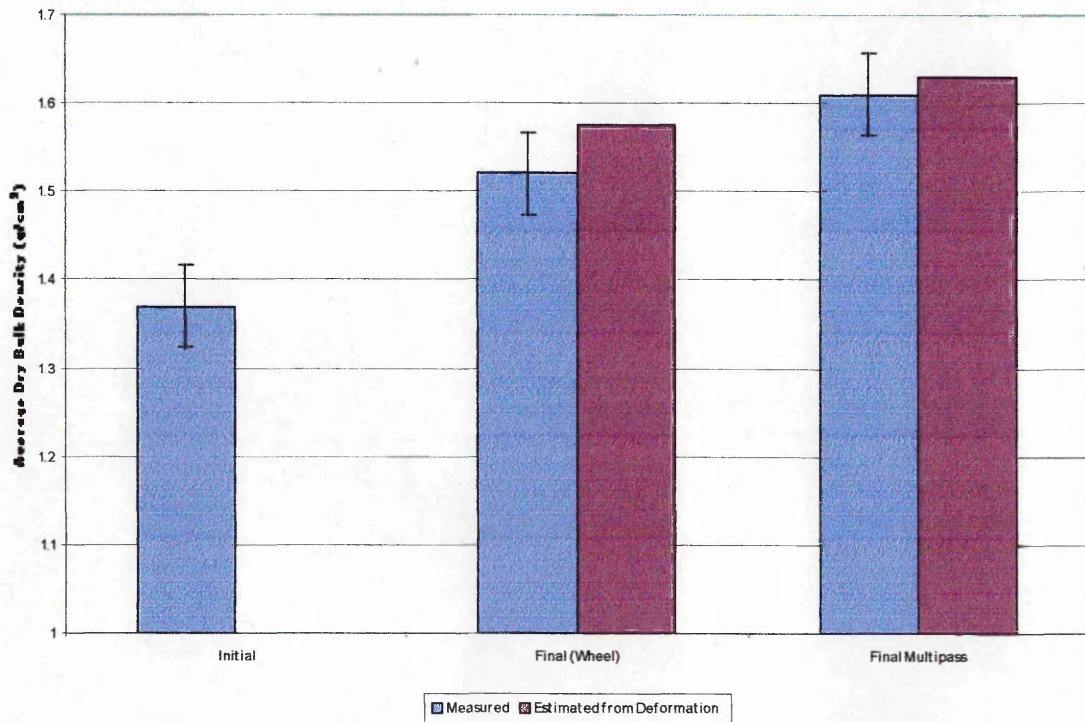


**Figure 36:** Dry bulk density initially, after one pass and after three passes of the 900/10.5/1.9

After one pass the increase in DBD is 11 % measured whereas it would be 15 % estimated from the deformation curves. After three passes the increase is 17 % and estimated it would be 18 %.

### 6.4.4 Rut Characteristics

With subsequent passes the maximum rut depth increases as well as the maximum width and the cross sectional area. Due to the lug influence being more reduced in subsequent



passes the area increases more than assumed when merely looking at the increase in maximum depth and width. Numbers followed by the same letter are statistically identical at the 5 % level.

**Table 13:** Rut Characteristics for the 900/10.5/1.9 after one, two and three passes

900/10.5/1.9	Max. Depth (m)	Max. Width (m)	Cross sectional area (m <sup>2</sup> )
1 <sup>st</sup> Pass	0.123 a	0.925 a	0.070 a
2 <sup>nd</sup> Pass	0.127 a b	0.963 a	0.080 b
3 <sup>rd</sup> Pass	0.135 b	0.970 a	0.089 c
LSD	0.04 – 0.07	0.06	0.007

### 6.5 Pressure Distribution Below Tracks and the 800 mm Section Tire

Using ceramic pressure transducers embedded at the top of a 100 mm diameter aluminum tube the data in **Figure 37** shows the difference in pressure distribution below the two and the three idler track in 250 mm depth with 12 t overall load. For comparison the pressure below the 800/10.5/2.5 is shown, too.

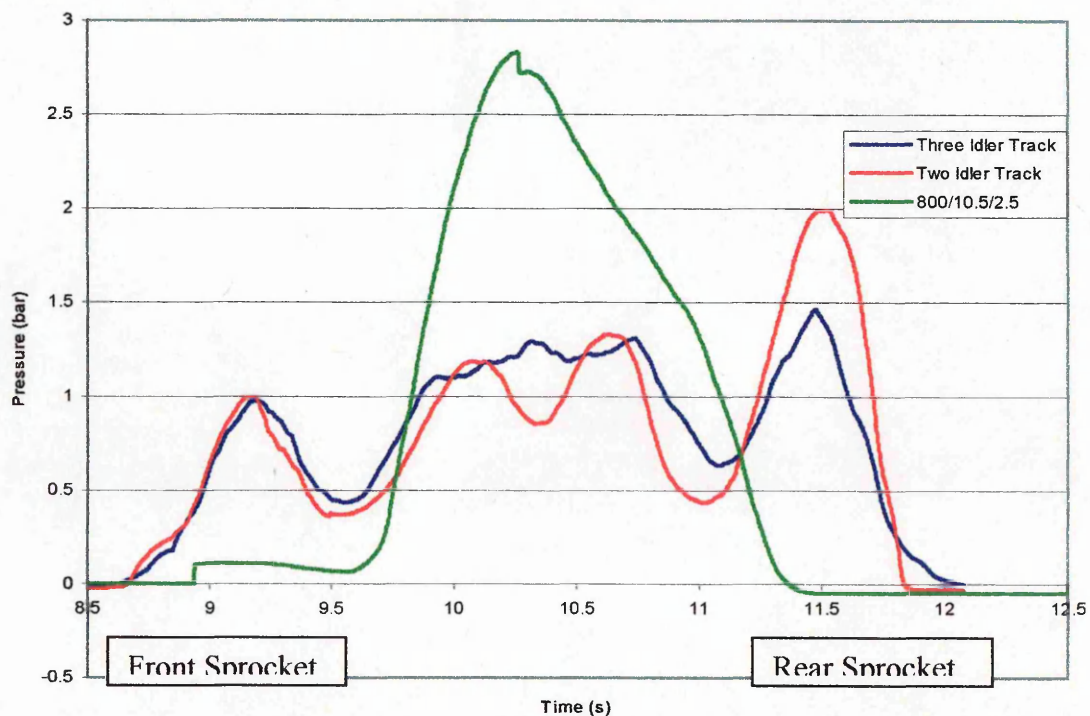


**Figure 37:** Pressure distribution below the three and two idler track in 250 mm depth

As expected the three idler track has a more uniform pressure distribution over the central idlers than the two idler track, where the effects of the individual idlers are more pronounced. However, the pressure from the rear sprocket is still higher than that of the front sprocket.

The difference in pressure between the front and the rear is about 100% for the two idler track whereas it is 45 % for the three idler track. Average contact pressure is about 0.81 bar below the three idler track and about 0.80 bar below the two idler track. The calculated contact pressure is 0.79 bar for an assumed contact length of 2.4 m and 0.86 bar for an assumed contact length of 2.2 m for the tracks. Therefore calculated and measured contact pressures are in approximate agreement with the estimated values.

The 800/10.5/2.5 has a peak pressure of about 2.7 bar, an average pressure of 1.61 bar and an average contact pressure of 1.68 bar estimated from the contact area and its load.

## **6.6 Field Measurements**

### **6.6.1 Tracks vs. Wheels (2004 – 2005 Crop season)**

Penetrometer resistance for a wheel rut and a track rut in a clay loam (Chulkey Bolder Clay) at Roxhill Manor Farm / Robert Barnes is shown in Figure 38. This shows a small but not statistically significant reduction in values for the tracks compared to the wheel.

The lack of significance could be due to the high gravimetric soil water content of 30%. This will also be affected by the natural variability and the small sample size. The critical issue is that for the depth range between 50 mm and 500 mm the track is always lower than the wheel.

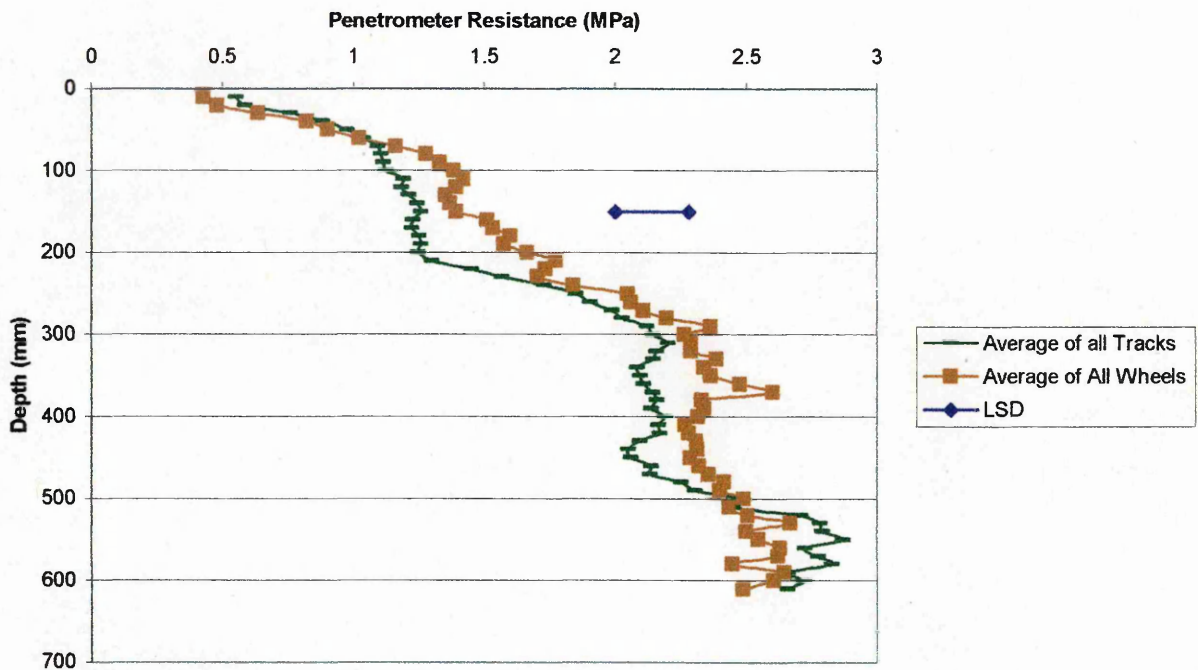


**Figure 38:** Penetrometer resistance over depth for average of track and wheel measurements in rape fields and LSD

Average gravimetric soil water content was 30% with a SE of 1.49%. DBD in the surface was lower than in 100 mm depth for the wheel rut as well as for the track rut, 1.21 and 1.36  $\text{g}/\text{cm}^3$  respectively. DBD in the track rut was higher than in the wheel rut, 1.34 and 1.24  $\text{g}/\text{cm}^3$  respectively. However, none of the differences was statistically significant due to the small sample size taken. Thus, the results from DBD give an idea of the circumstances in the field, but as already mentioned cannot be used to distinguish treatments.

A day before wheat harvest 2004 oil seed rape was broadcasted on the soil surface. Measurement of the oil seed rape biomass revealed a great difference between rut and within rut area at the end of April 2004. The average biomass for the track rut is 0.2 Mg/ha bigger than for the wheel rut. The results are shown in **Figure 39**. The difference is statistically significant between control and rut, but not between track and wheel rut. However, with a sample size of three taken only in one rut of each field statistical data would not be very reliable. The small sample size is due to a limited field study. Nevertheless these values correspond well with the pictures of flowering, growth and roots.

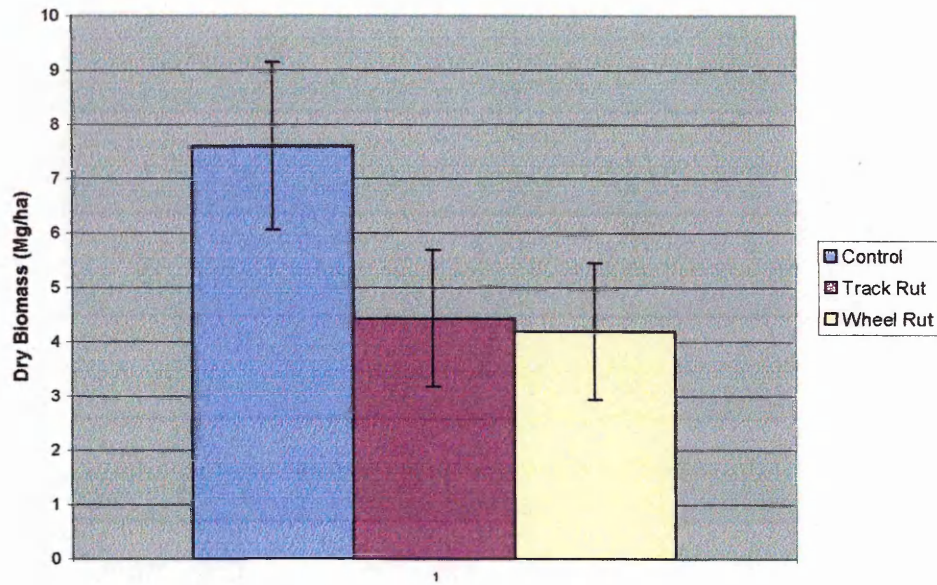


**Figure 39:** Biomass for control, track and wheel rut in rape including 95 - % CI

Looking at the plant growth in former wheel and track ruts the line of traveling of the tracked combine is shown in **Figure 40** and for the wheeled combine harvester in **Figure 41**. For the wheeled combine harvester the track width is clearly visible whereas for the tracked combine harvester more care has to be taken to distinguish between track and no track area.

The difference in flowering between **Figure 40** and **Figure 41** is due to the different slope exposure. The field harvested with the wheeled combine harvester is on a south facing slope, thus plants are slightly more developed than on the other field as this is basically flat. However, during the last years both fields had identical yields. So the little difference in emergence does not affect the overall final yield.



**Figure 40:** Differences in inter row emergence of rape due to harvest in the 2003 – 04 growing season with a tracked combine harvester (13. 04. 2005).



**Figure 41:** Differences in inter row emergence of rape due to harvest in the 2003 – 04 growing season with a wheeled combine harvester (13. 04. 2005).

Differences in rape flowering are detectable depending on the wheeling equipment of the combine harvester used in the previous harvest between (**Figure 42**) the field harvested with a tracked combine and (**Figure 43**) the field harvested with a wheeled combine harvester. The very pronounced crop depression in both pictures is due to the tramlines used for fertilizer and spray application. These tramlines are the same every year, so therefore the lines shown in the field can not be caused by last years tramlines.

When the second set of pictures (**Figure 42** and **Figure 43**) was taken 13 days later the differences were less pronounced. The smaller less pronounced tracks in the pictures are the ones from the combine harvester of the previous season. In **Figure 42** it can clearly be distinguished between the track marks from last year and the ones being caused by fertilizer and spray application. However, in **Figure 43** it is difficult to distinguish between the ruts being maintained by cultivation work and the ones not being used since last harvest. The rut in the middle of this picture for example is caused by the wheeled combine harvester in the previous season.

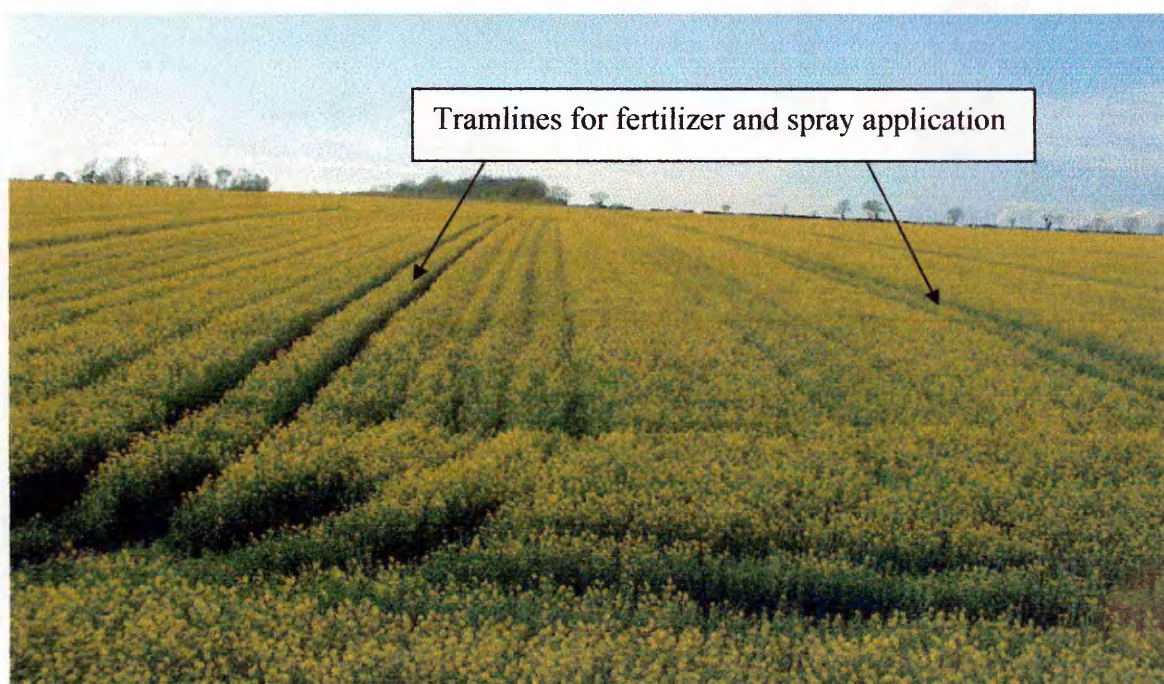


**Figure 42:** Flowering rape field harvested with a tracked combine harvester in the 2003 – 04 growing season (26. 04. 2005).

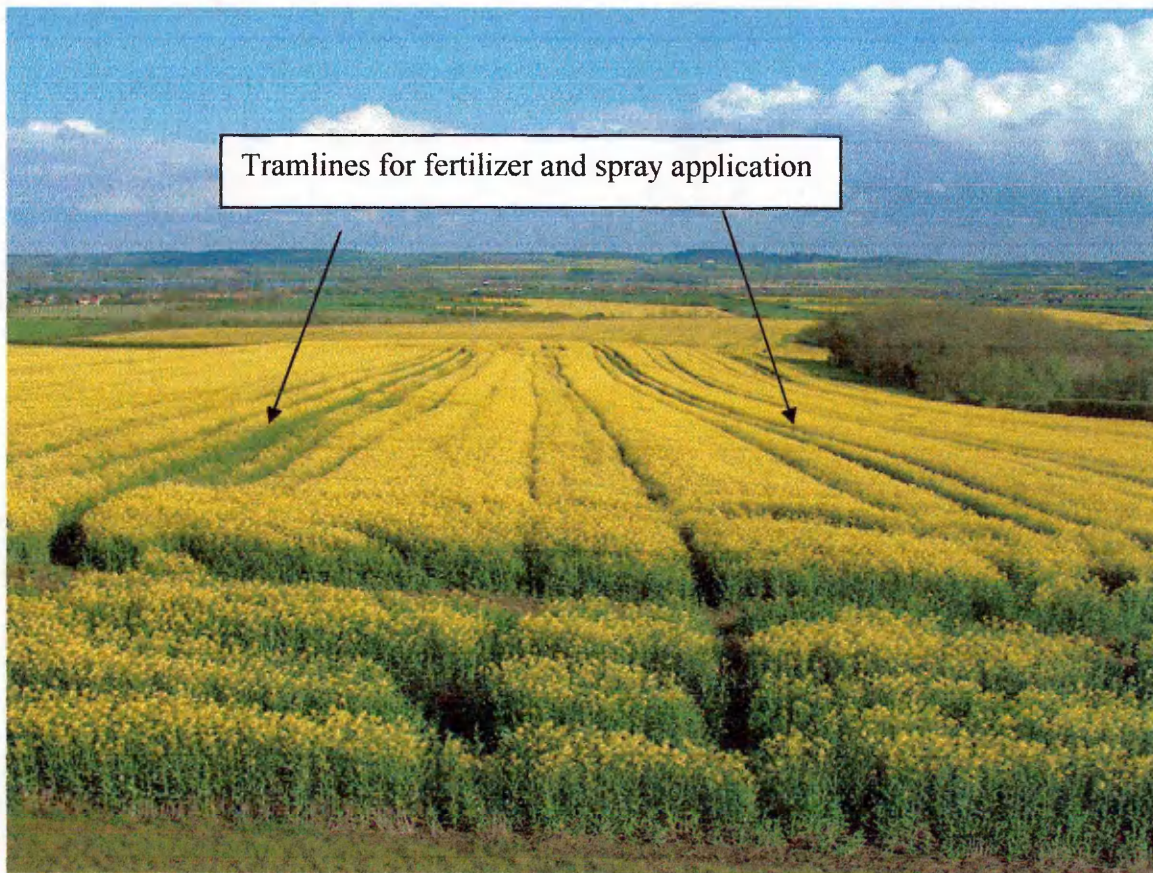


**Figure 43:** Flowering rape field harvested with a wheeled combine harvester in the 2003 – 04 growing season (26. 04. 2005).

The difference in flowering between both pictures is due to the exposition of the field slope again. The visible differences between both fields reduced over time.

An investigation of the root development below the wheel / track marks revealed differences in root length and characteristics of root growth between the two treatments. In the track rut plants are growing everywhere with a root development to a greater depth and more restricted in the center of the rut than on the outside as shown in **Figure 44**. Here the root of the plant close to the tape measure has developed to 250 mm. The root to the right shows a less pronounced development over depth, yet the root still penetrates the soil vertically.

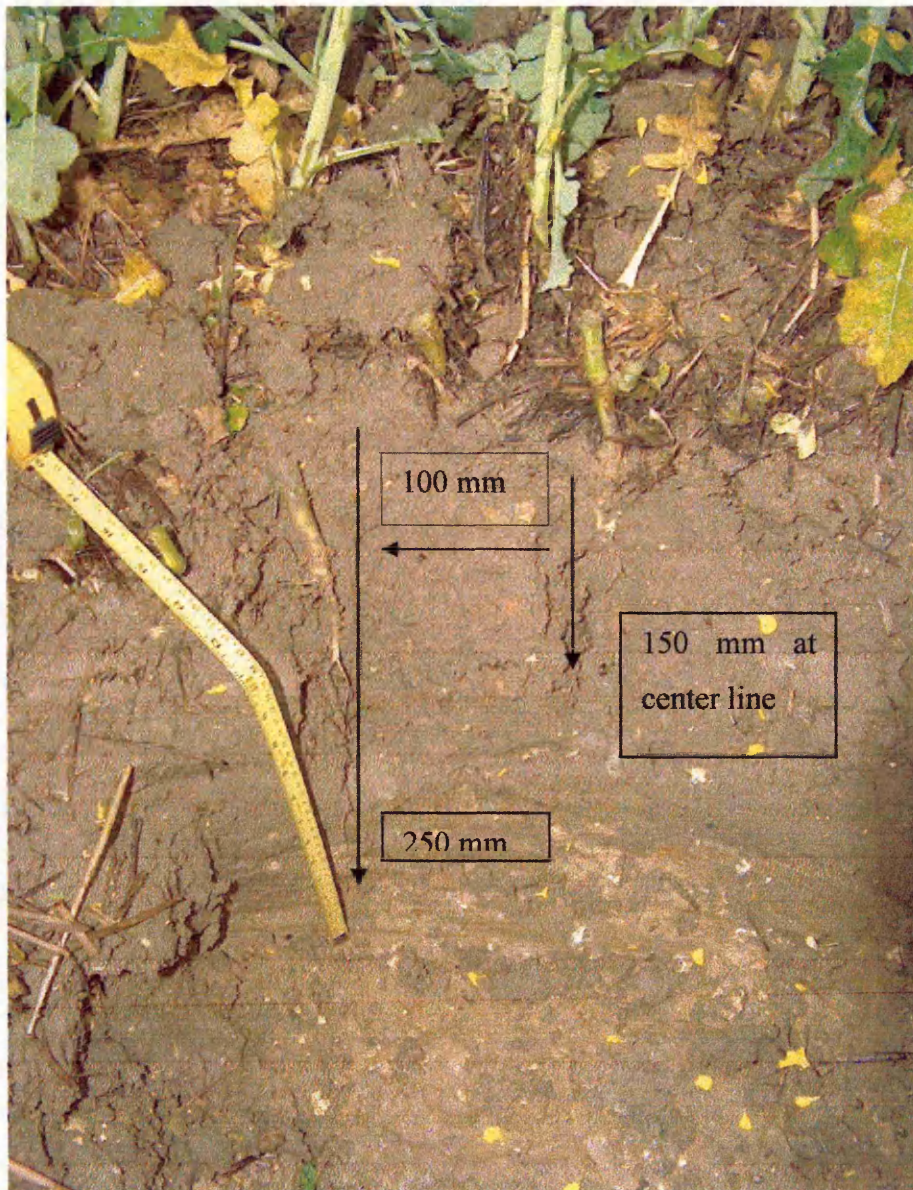


**Figure 44:** Root development down to C – horizon in former track rut center and 100 mm offset (26. 04. 2005).

In the wheel rut there are no plants in the center 200 mm of the rut (**Figure 46**). The first ones growing just have a pronounced root development very close to the surface like the one shown on the bottom of **Figure 45** but not at depth. Some roots grow more laterally than vertically.





**Figure 45:** Differences in root development between a plant 150 mm offset from the centerline (left) and one 250 mm offset from the centerline (right) in former wheel ruts (26. 04. 2005).

In **Figure 46** the restricted root development of plants 100 mm outside the center line of the wheel rut is shown. The plant on the right hand side shows a very pronounced root development at the surface. This is the plant shown on top in **Figure 45**. For the plant left to the center line in **Figure 46** the white roots are visible how they developed vertically instead of horizontally as usually expected.

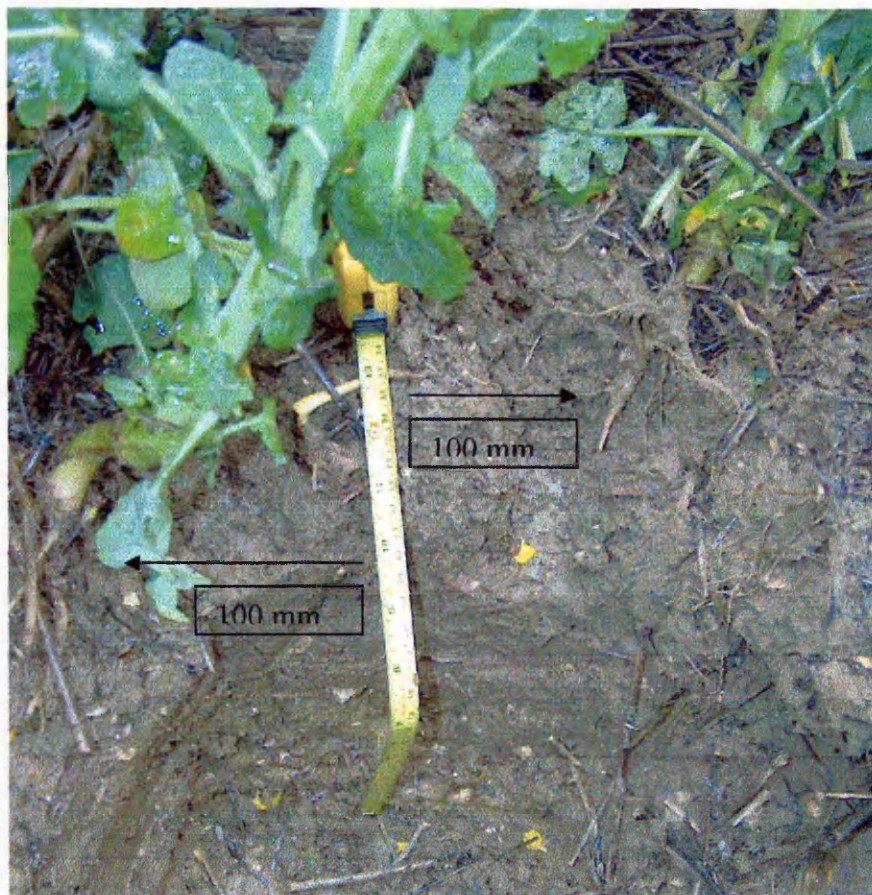


**Figure 46:** Plants with restricted root development in 100 mm distance from the center line in a wheel rut (26. 04. 2005).

### 6.6.2 Tracks vs. Wheels in Harvest Season 2005

Field measurements were done in a clay loam at the farm of Sam Fairs in Yoxford, Suffolk. Due to the harvest conditions measurements could only be made using the combine harvesters with empty grain tanks.

The penetrometer resistance results are shown in **Figure 47**. These include data for both initial and after the pass of a wheeled Lexion 480 and a tracked Lexion 480. The final penetrometer resistance reading was taken next to the initial penetrometer resistance reading in order to make sure initial and final reading are locally as close as possible. After the pass of the tracked combine harvester there is a small increase in penetrometer resistance in the top 80 mm below which the penetrometer resistance does not vary significantly from

the initial values. After the pass of the wheeled combine harvester the penetrometer resistance has significantly increased over the whole depth by approximately 0.8 MPa.

It must be reported, however, the penetrometer resistance for the control for the tracked combine harvester is 0.8 MPa greater than the wheeled. Therefore, although this soil was separated from that of the wheeled combine only 10 m it was significantly stronger in its initial condition. However, the penetrometer resistance for the wheeled combine exceeds both the track control and the final track reading. This is an indication of the effect of higher stresses below the wheeled combine, although it is statistically not significant.

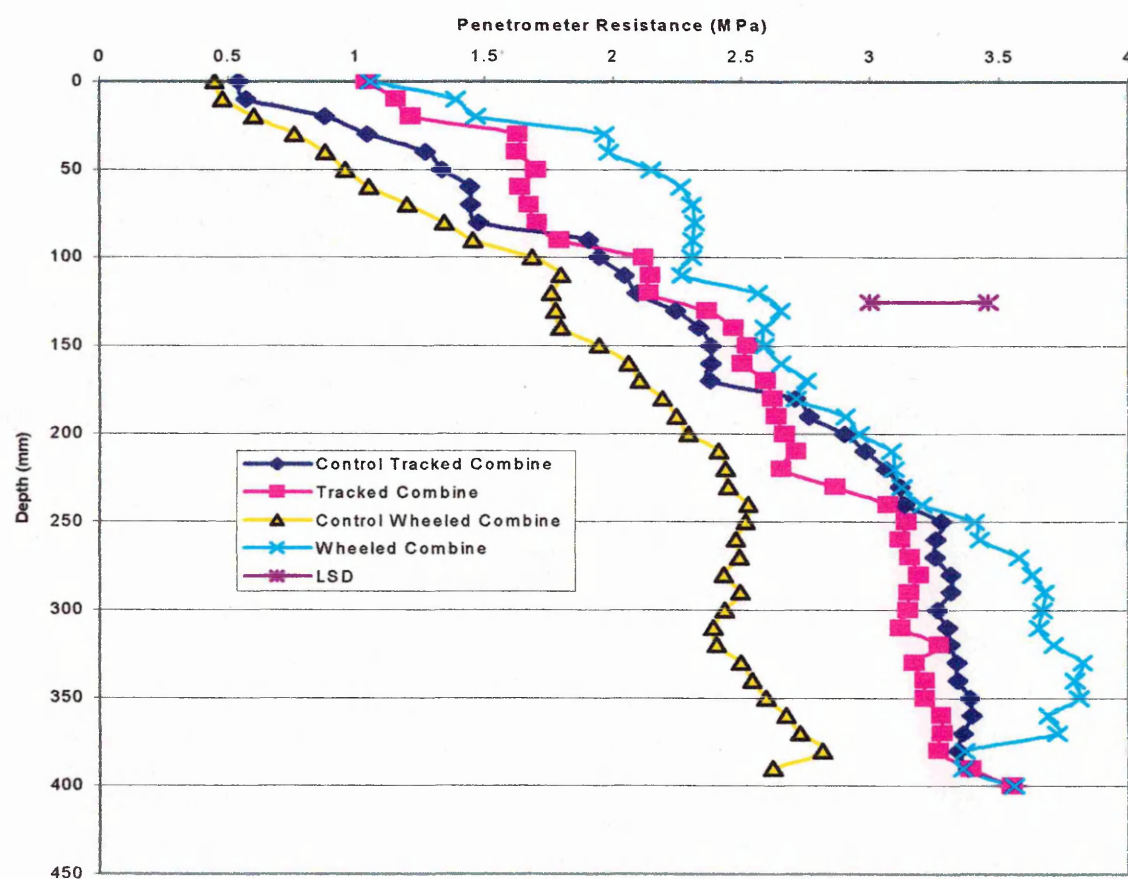


**Figure 47:** Penetrometer resistance vs. depth for the tracks and wheels in harvest 2005

Whilst the results of these studies are encouraging future studies need to consider field variability prior to driving over it. It also emphasizes the fact that initial and final places of measurements should be as close as possible together in field conditions.

DBD for both the initial and final soil conditions after the passage of the wheeled and tracked combine harvester is shown in **Figure 48** including a 95 % CI for the control. DBD varied slightly and not significantly around  $1.5 \text{ g/cm}^3$ . Soil moisture content was at 20 % which might have influenced DBD as many pores were partially water filled.

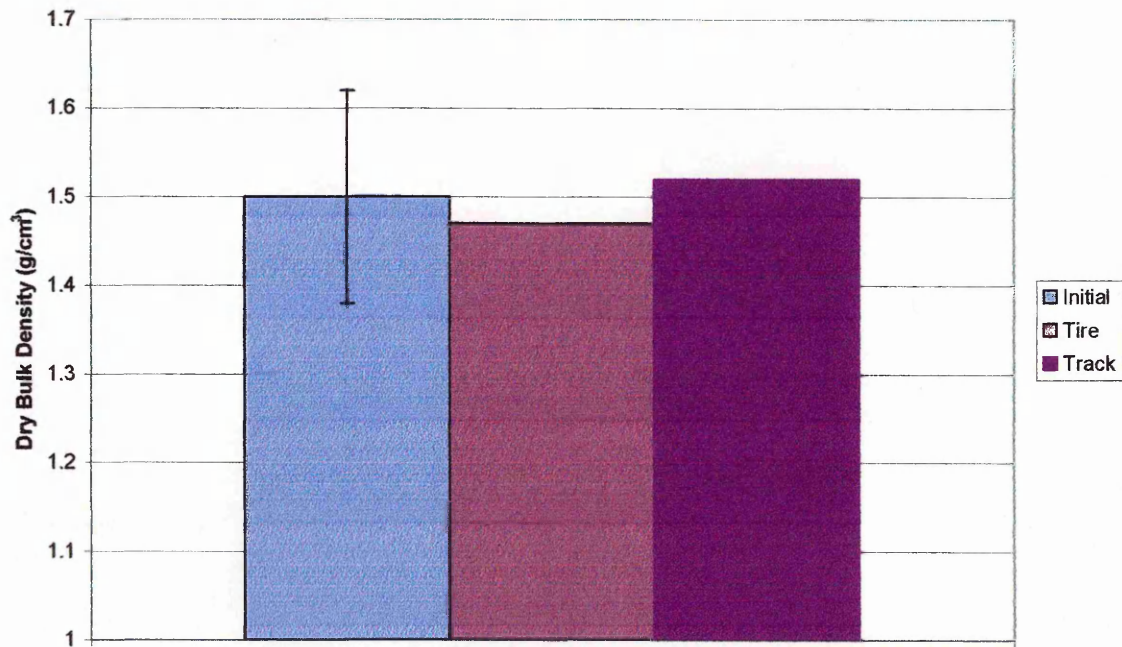


**Figure 48:** Dry bulk density for field measurements during harvest 2005 including 95% - CI

## 7 SOIL COMPACTION MODELS – APPLICATION AND DISCUSSION

In the following two models for soil compaction predictions are described and their output confronted with our measurements. The first is the soil compaction model by O'Sullivan et al., (1999) the second SOCOMO by van den Akker (2000).

### 7.1.1 O'Sullivan's Model

The soil compaction model by O'Sullivan et al. (1999) was used to estimate the size of the footprint and the increase in dry bulk density caused by tires. Tracks unfortunately could not be used directly as there was no option available.

The idea to increase the tire diameter until the contact area of the tire matches the contact area of the track worked in theory. The track with an assumed contact length of 2.2 m and a known contact width of 0.635 m results in 1.40 m<sup>2</sup> contact area. This could be matched with an imaginary tire of 4.75 m diameter, a width like the track of 0.635 m, and a theoretical inflation pressure of 0.8 bar which is the same as the average pressure below the track. Thereby the resulting contact area was 1.42 m<sup>2</sup>. Yet in practice it has not been possible because the program calculated correctly the contact area for a 4.75 m diameter tire with a width of 635 mm matching the contact area of the track but when running the program to calculate the increase in DBD it stopped because of an invalid tire diameter. Tire diameters are only valid up to 2 m.

The model is embedded as a macro in an excel spread sheet. At the beginning tire parameters, e.g. diameter, width, inflation pressure and type of tire (x-ply or radial) have to be given. Load has to be given in this step, too. Then the program calculates the estimated contact area. Multi passes can be achieved by adding several tires into the data table. Soil density and soil water profile have to be chosen as well as the soil type. From the given load, soil type and the profiles of soil water content and soil density over depth the program calculates the stress distribution on the assumed circular contact area. Then the Boussinesq equation (1885) for a point load in semi infinite space is used and integrated over the contact area. Froehlich's (1934) concentration factor is hereby included to account for

the different behavior of a soil in comparison to an ideal elastic medium. The mean normal stress is calculated according to Equation 4 from the paper by O'Sullivan et al., (1998) as the average of the mutually perpendicular major, intermediate and minor principle stresses. To get the necessary intermediate stress as well as the minor principle stress a regression equation was fitted with parameters depth, contact area and concentration factor. Hereby it is assumed on the basis of the work by Johnson and Burt (1990) that the stress ratios are independent of load.

The ratio  $\nu$  of solid particle density to dry bulk density is used to describe the compactness of the soil.

The virgin compression line expresses  $\nu$  as a function of the mean normal stress  $p$  in the following way:

$$\nu = N - \lambda_n \ln(p)$$

Eq. 5

with  $N$  being the ratio of solid particle density to dry bulk density at a pressure  $p = 1\text{kPa}$  and  $\lambda_n$  the so called compression index.

$N$  is obtained from gravimetric soil water content  $w$  and soil specific constants  $A$ ,  $B$  and  $C$  as follows:

$$N = A - B * (w - C)^2$$

Eq. 6

$\lambda_n$  is the constant slope in a  $\nu$  vs.  $\ln(p)$  – diagram. In such a diagram a pivot point with the coordinates  $(p_p; \nu_p)$  can be found around which the virgin compression line changes its slope. The slope ( $\lambda_n$ ) varies with soil water content due to  $N$  from Eq. 6. The coordinates of the pivot point vary with soil type:

$$\lambda_n = \frac{N - \nu_p}{p_p}$$

Eq. 7

When the soil is loaded with a certain pressure  $p$  for the first time it follows the virgin compression line (VCL) as shown in Eq. 5 to a certain point in  $v - \ln(p)$  space point on VCL. When the soil is unloaded afterwards it rebounds along a straight line with a smaller slope  $\kappa$ . The slope  $\kappa$  of the rebound line varies with water content, too.  $\kappa$  follows Eq. 8:

$$\frac{\kappa}{\lambda_n} = 0.119 - \frac{0.082 * w}{PL}$$

Eq. 8

where PL is a variable defined by Campbell, (1976).

Recompression again is assumed to happen along the same line as rebound until a yield stress is reached. Greater stresses than yield stress cause both non-recoverable and elastic deformations along a steeper line with a slope  $\kappa'$  equal to the geometric mean of  $\kappa$  and  $\lambda_n$ :

$$\kappa' = \sqrt{\lambda_n * \kappa}$$

Eq. 9

The separation  $m$  between yield line and VCL is 1.3 in units of  $\ln(p)$  and also called pre-consolidation stress.

The process described above can be traced in **Figure 49**.

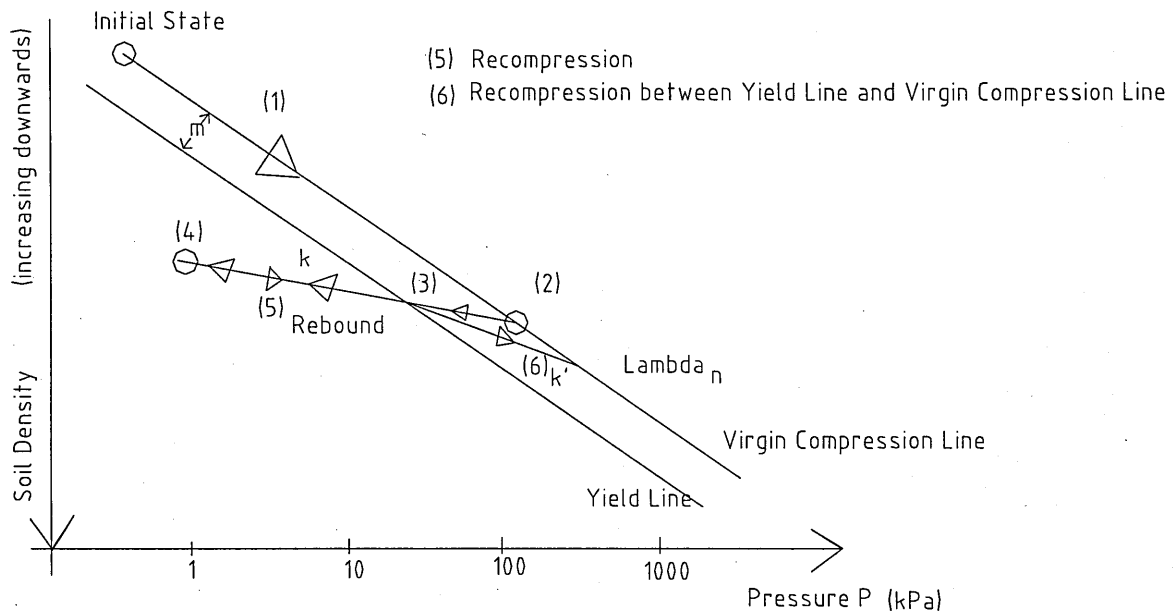


**Figure 49:**  $v$  vs.  $\ln(p)$  – diagram

The footprint estimation is good for the 680/10.5/2.2 and the 800/10.5/2.5 tires, yet underestimated for the 800/10.5/1.25 and the 900/10.5/1.9. Estimated and measured contact area as well as the deviation of the estimation from the measured area is given in **Table 14**.

**Table 14:** Contact area of tires estimated and measured

Tire	Estimated Area (m <sup>2</sup> )	Measured Area (m <sup>2</sup> )	Deviation (%)
680/10.5/2.2	0.72	0.69	4.2
800/10.5/2.5	0.67	0.62	7.5
800/10.5/1.25	0.77	0.98	- 27.3
900/10.5/1.9	0.80	0.94	- 17.5

The larger deviation between estimated and measured contact area for the 800/10.5/1.25 and the 900/10.5/1.9 might be due to the smaller inflation pressure compared to the two others and the disregarded effect of carcass stiffness.

Rut depth was underestimated. On average the estimation was about 0.019 to 0.016m. In reality it was 0.03 to 0.08 m when taking the inter lug rut depth, otherwise 0.10 to 0.127m when taking the lugs into account. One reason for this result might be the fact that the model does not account for lateral displacement of the soil. However, when looking at the soil deformation diagrams in Appendix 13.1.3 the lateral soil displacement can only ac-



count for a very small amount in soil displacement. Therefore ignoring lateral displacement can not be the only reason.

Taking the average increase in dry bulk density in the model, it was below 5 %, where as the measured increase with the talcum powder was averaged 15 % which corresponds with the measured increase in dry bulk density. At 500 mm depth compaction is calculated to be 1.8 %, but measured still about 15 %. For the stratified soil conditions the picture is similar. These results are illustrated as deformation over depth graph in **Figure 50**.

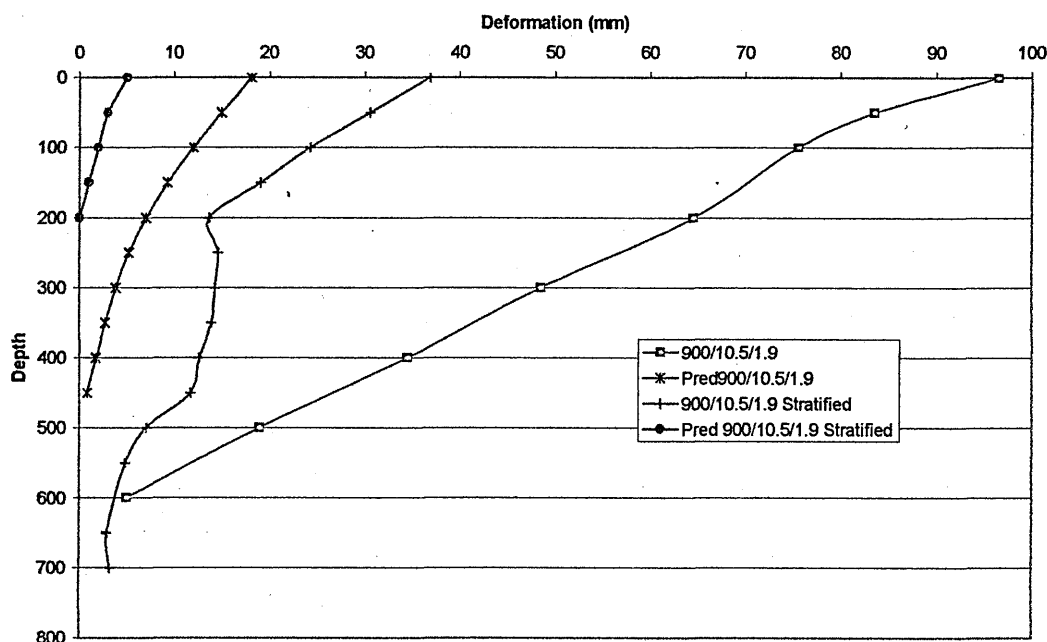


**Figure 50:** Predicted vs. measured deformation on uniform and stratified soil conditions for the 900/10.5/1.9

The effect of the loads on soil deformation in the model steadily decreases with depth. Thus highest soil compaction occurs at the top and little soil compaction occurs at 500 mm depth in the model, whereas in our investigations for the uniform soil with low bearing capacity a linear increase of density of about 15 % over the whole profile depth was detected.

Mimicking a concrete floor at the bottom of the soil bin changed the rut depth by 1mm but the average dry bulk density did not change at all. Thus it had basically no effect on compaction.

Further reasons for the correct trend yet incorrect real values might be:

- a) that the maximum weight with which the model was tested was 2.5 t and not 10 t
- b) the authors themselves did not claim the model to be realistic, but to be able to show the principles. As an application of the model a class room exercise is mentioned where just on paper the benefit of larger tire diameters and widths as well as less inflation pressure is shown.
- c) different soil properties, e.g. different cohesion and internal friction or  $\lambda_n$

The tendency of the results was correct apart from the tire at half inflation pressure. The authors themselves said that the model was designed to illustrate the principles which govern soil compaction e.g. increase in DBD. According to them the model was not designed to agree closely with field measurements and according to our experiments there are differences with the laboratory results.

### 7.1.2 SOCOMO a SOil COmpaction MOdel:

This model was developed by van den Akker and the latest description can be found in van den Akker (2004). The model is based on the theory of Boussinesq (1885) for the stress distribution in a homogenous isotropic semi – infinite solid mass due to a point load on the surface. In addition it includes the concentration factor proposed by Froehlich (1934) to account for not purely-elastic behavior. Socomo splits up the contact area in small single point loads according to Soehne (1953). The load on the tire can be chosen to be distributed uniformly, trapezoidally or parabolically over the contact area. It then calculates principal stresses for any given point in the soil by summing Boussinesq's solutions over all the point loads taking the concentration factor into account. Depending on preconsolidation stress soil compaction either happens at a given point or not.

Preconsolidation stress shows to which mechanical and hydraulic stresses the soil has been laden to in its history. Thereby indicating to which amount of stress the soil can be laden without further unrecoverable volume change (Baumgartl and Koeck, 2004). The preconsolidation stress can be found graphically, statistically or mathematically. A graphical

solution is to measure the distance from the virgin compression line to the yield line. O'Sullivan called this parameter  $m$  (section 7.1.1). This method was first described by Casagrande (1936). Dias Junior and Pierce (1995) determine the preconsolidation stress statistically from data describing the virgin compression and recompression line. The mathematical approach to determine the preconsolidation stress is described by Baumgartl and Koeck (2004).

The model assumes that no subsequent compaction occurs if the major principle stress  $S_1$  at any given point is smaller than the structural strength and the minor principle stress  $S_3$  equals:

$$S_3 = K_a * S_1 - 2 * C * \sqrt{K_a}$$

Eq. 10

where  $C$  is cohesion and

$$K_a = \tan^2\left(45^\circ - \frac{\varphi}{2}\right)$$

Eq. 11

with  $\varphi$  = angle of internal friction. Structural strength is given by precompression stress and preconsolidation load. These two conditions are called combined failure criteria

The output consists of tables with the major principle stresses at the considered cross section as shown in **Figure 51** and **Figure 52** for the 680/10.5/2.2 and 800/10.5/1.25, respectively. These are the mere stress distributions and do not indicate anything about changes in soil physical properties, e.g. combined failure.

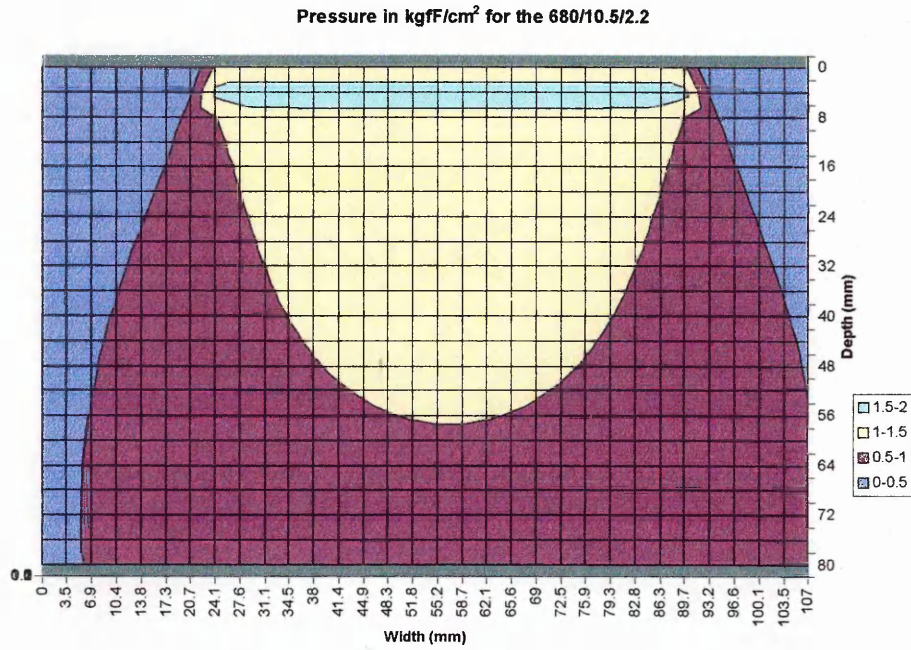


**Figure 51:** Estimated pressure distribution below 680/10.5/2.2 (van den Akker – model)

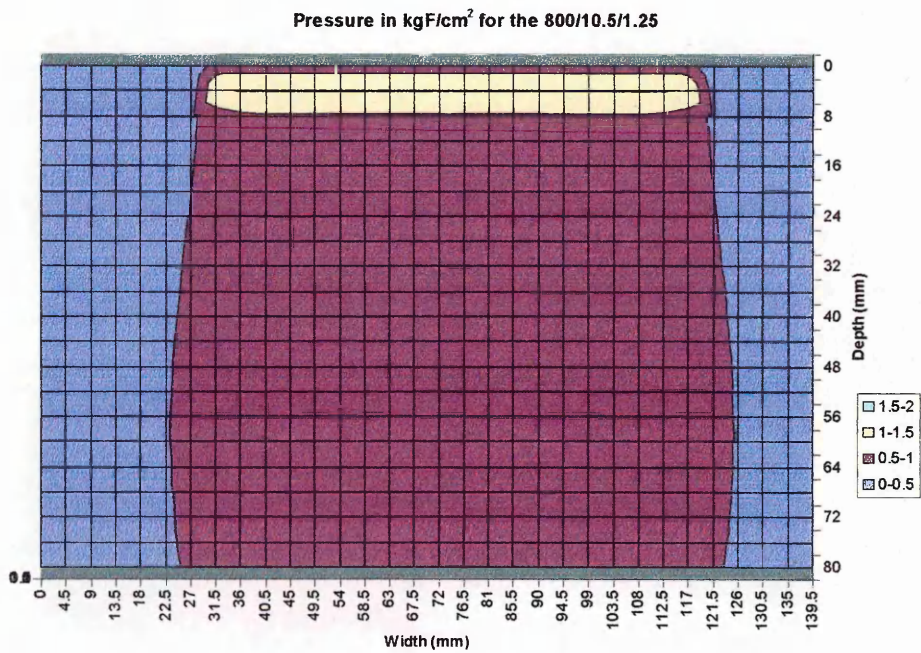


**Figure 52:** Estimated pressure distribution below 800/10.5/1.25 (van den Akker - model)

An excess of the combined failure criteria, e.g. changes in soil physical properties are indicated by letters as shown in **Figure 53** and **Figure 54**.

COMBINED FAILURE AREA 680/10.5/2.2

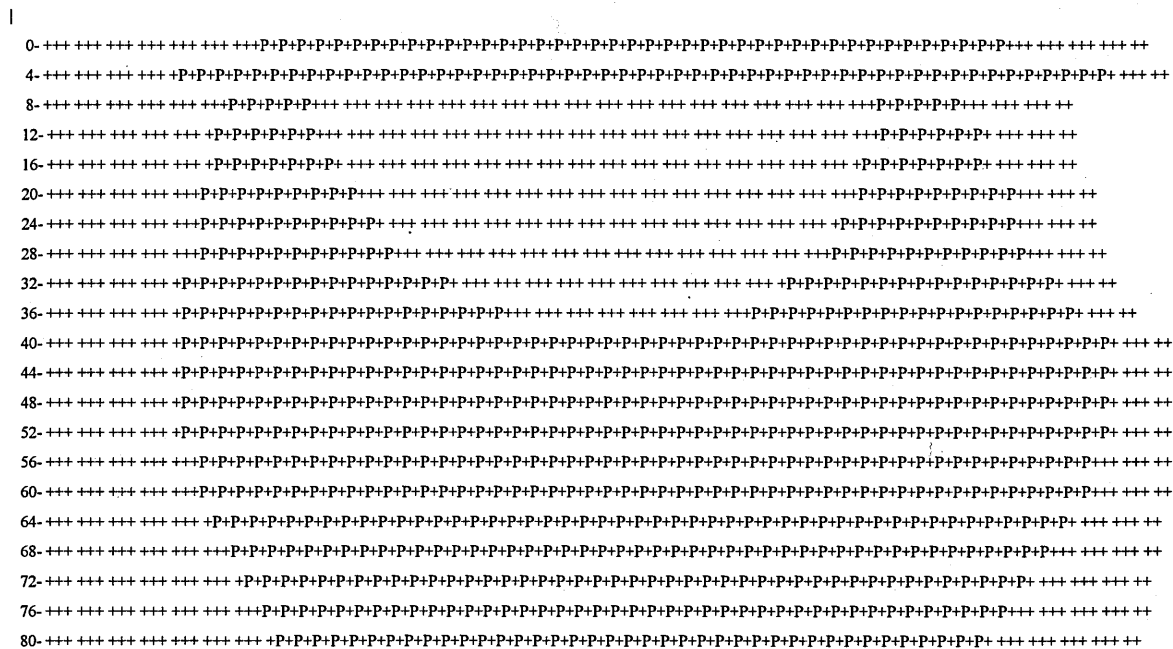


Figure 53: Estimated combined failure area for 680/10.5/2.2 (P = failure criteria exceeded)

COMBINED FAILURE AREA 800/10.5/1.25:

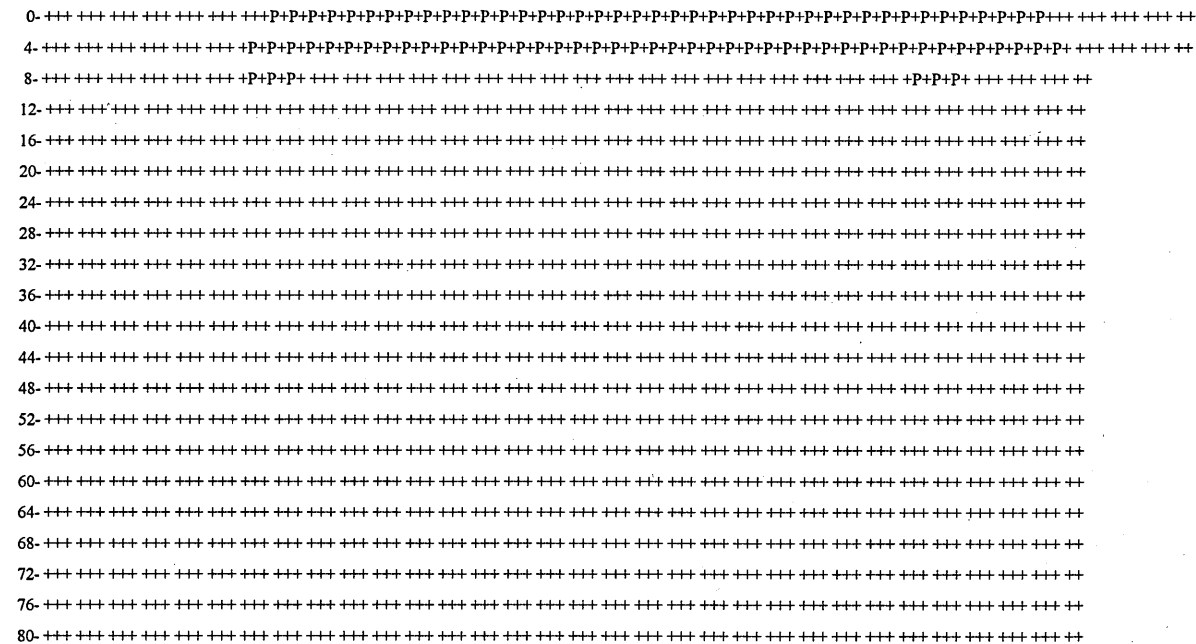


Figure 54: Estimated combine failure area for 800/10.5/1.25 (P = failure criteria exceeded)

Similarly to the results of this study the model estimates smaller stresses below the 800/10.5/1.25 than below the 680/10.5/2.2. The larger contact area results in smaller stresses in the soil. However, when comparing **Figure 53** and **Figure 54** with the area of combined failure, soil physical properties change for the 800/10.5/1.25 shown in **Figure 54** only in the top 100 mm. Whereas in this study both treatments changed soil physical properties down to at least 500 mm depth.

One reason for the different result might be a higher preconsolidation stress assumed in the model than in reality. Beside this, the author states that the model is particularly designed for the prediction of subsoil compaction as it is not applicable to describe the ensuing plastic deformation and does not permit large volume changes. In practice deformation and compaction of the generally loose topsoil by wheel loads is so high that the use of the model is not allowed under these conditions. So therefore volume changes might be too large in these soft soil conditions. Subsoil compaction can be predicted after the topsoil already has been compacted. Therefore rut depth must be estimated or measured to calculate the distance between the rut bottom and the topsoil – subsoil interface.

A remaining disadvantage of Socomo compared to the model by O'Sullivan et al. (1999) is that it is a black and white model. The combined failure criterion is either exceeded or not, i.e. soil physical properties either change or not. It does not estimate the magnitude of change as the model by O'Sullivan et al. (1999) does.

## 8 DISCUSSION OF RESULTS

### 8.1 Soil Compaction Below Wheels and Tracks

In general positive relationships were found between an increase in contact area and reduced soil compaction. A larger contact area of the tire caused less soil deformation and less increase in penetrometer resistance. Increasing the contact area by reducing inflation pressure has a positive effect, too. These results are in agreement with findings by Bekker (1956) and Hakanson (1988) and all the work done by Raper and his colleagues (Raper et al., 1995; Raper et al., 1993; Raper et al., 1993; Bailey et al., 1993, Way et al., 1996).

Considering rut geometry of the experiments 800/10.5/1.25, 800/10.5/2.5, and 800/8.5/2.5 it was shown that rut width increases with a decrease in inflation pressure and an increase in load. This agrees with the findings by Raper et al., (1995). In the case here cross section area for the 800/10.5/2.5 is significantly larger than the area of the 800/10.5/1.25. This does not support the findings by Raper et al., (1995) saying that the cross section area is not affected by inflation pressure because the change in rut width cancels out the gain due to reduced rut depth.

Typical cracks developing during compaction with an undriven wheel were found after the passage of the towed wheels. This behavior is explained in detail by Maciejewski and Jarzenbowski (2004). The influence of wheel slip on soil compaction cannot be determined from these studies as the towed wheels were loaded to less overall weight as well and thus two parameters changed at the same time.

Track load and depth of maximum soil compaction do not show a clear relation. Looking at the penetrometer resistance curves for the three idler track, higher load may cause slightly higher compaction at slightly deeper depth, but for the two idler track there is no difference (**Figure 20**). Therefore the influence of higher load and / or larger contact area on a deeper located maximum increase in soil density can not be assessed. This relation was shown by Soane et al. (1981) and Grecenko (2003). The most significant effect of the study was to record how close to the surface the maximum penetrometer resistance can be kept using tracks compared to tires. Therefore increasing the total contact length, yet keep-

ing the width nearly the same as the 680 mm section width tire and reducing the contact pressure by an increased contact area results in soil compaction close to the surface.

The multi pass experiment conducted in this study had an increase of 15 % after one pass and 18 % after three passes. This result is in agreement with the findings by Raghavan et al. (1976). However, the influence of subsequent passes is greater in their work. Initially dry bulk density is increased by 6 % after the first pass and reaches about 20 % increase after 10 passes. The difference might be due to weaker soil conditions in the soil bin of this study and to a higher sand content in the study by Raghavan et al. (1976) as they used sandy loam to sand with a moisture content of about 20 %.

The rubber tracks used in this study result in significantly smaller increase in penetration resistance and soil deformation compared to wheels, even with an overall load increase of 1.5 t. Therefore the overall finding that tracks are beneficial as compared to wheels from Erbach (1994) can be corroborated. In contrast to the findings by Brown et al. (1992) in which rubber tracked vehicles were intermediate to steel tracked and wheeled vehicles but not significantly different from either, here the advantage compared to tires can clearly be detected. The reason for this may be due to improved frame and belt tension for these track systems than for the ones used by Brown et al. (1992). The significantly reduced penetrometer resistance in the subsoil was not detected by Blunden et al. (1994), Pagliai et al. (2003) and Brown et al. (1992) when using tracks. Merely Servadio et al. (2001) found a smaller penetrometer resistance below a rubber belted tractor in 200 – 400 mm depth than for a wheeled tractor. No report was found reporting the reduced penetrometer resistance down to 650 – 700 mm.

The small section width and large contact area in total might be the reason for the good performance of the tracks compared to the tires. Tracks may behave like a tire with small section width and a large diameter. This would agree with Bekker (1956) and Hakanson (1988). These authors state that tires with a smaller section width can reduce soil compaction when the area lost thereby is made up with a bigger wheel diameter, e.g. a longer contact patch.

The increase in measured pressure from the front sprocket to the rear driving sprocket for the two as well as the three idler track is in agreement with the general increase found by



Keller et al. (2002) for a tracked tractor during ploughing. But in relation to the tractor the increase by 100 % and 50 % for the two and three idler track, respectively, is small. For the tractor it was nearly a 1000 % increase as shown due to higher traction forces. After adjustment of the point of draught force application the increase was reduced to 50 % and came into the range found below the tracks of a combine. The pressure curves below the tractor were shown in **Figure 2** and for the combine in **Figure 37**. It is supposed that with an adjustment of the weight application on the combine track a further balancing of the weight distribution under traction is possible and thus further improvement of the track behavior should be possible. Basically the idea is to apply the load approximately 100 mm offset from the center of the track frame towards the front of the combine. Thus when the combine is at rest, there is more load on the front sprocket than on the rear sprocket, yet under common traction requirements the load distribution is equal and results in the same weight of the front and rear sprocket. The difference in average pressure found by Keller et al. (2002) did not appear in this experiment. These authors got an approximate average pressure of 96 kPa initially and 76 kPa after the adjustment. The calculated average ground pressure was 43 kPa using machine weight and contact area. Possible reasons for the difference initially and after the adjustment are exemplified in section 3.3. The difference between the average pressure measured and calculated for the sensor used by Keller et al. (2002) and the agreeing results in section 6.5 of this study indicate unequal pressure distribution in the soil close to the surface. Keller et al. (2002) placed the sensors at 100 mm depth whereas in this study sensors were placed at 250 mm depth. Thus, the sensors used by Keller et al. (2002) may pick up differences across the contact patch which are equalized out at greater depth.

The fact that the pressure in the upper soil layers is determined by the specific pressure at the contact area and that the pressure in deeper soil layers depends upon the load (Soehne, 1958 and Smith and Dickson, 1990) can not be corroborated by this work. The tracks do have a higher overall load by 1.5 t in two runs, however, soil compaction e.g. all measured parameters are still significantly lower for the tracks than for the wheels. There is no significant difference in soil deformation and penetrometer resistance between any of the track runs. Therefore we cannot differentiate between the soil compaction caused by 10.5 t and by 12 t loads. The smaller increase in soil compaction for the tracks compared to the wheels is consistent with depth. However, the tracks should cause the same or even more soil compaction at deep layers when taking the facts mentioned by Soehne (1958) and

Smith and Dickson (1990) into account due to their same as well as higher overall load. But in fact the tracks cause consistently less soil compaction. One reason for this finding could be that the load used by Soehne (1958) and Smith and Dickson (1990) was merely a quarter of the loads used in these investigations and that for a higher load different rules apply. Smith and Dickson (1990) state that above a threshold value for the load of between 2.1 to 3.7 t soil compaction behaves differently. Yet as shown in this work it does change. Another reason for this behavior might be that the tracks used by Smith and Dickson (1990) were no real tracks, but merely a trailer with 5 axles surrounded by a tensionless belt.

The results from the 900/10.5/1.9 on stratified soil conditions agree with the findings from Arvidsson et al. (2001), Trautner and Arvidsson (2003) and Yavuzcan et al. (2004) who detected increases in soil density down to 0.3 – 0.4 m for wheeled sugar beet harvesters in field measurements. The subsoil conditions in the soil bin were insufficiently strong to resist the load without density change as found in field by Dickson (1994) on a previously compacted soil after passes with a combine harvester.

From field investigations of the growing season 2004 – 2005 the restricted root growth in ruts found by Hakanson et al. (1988) can be confirmed. Thereby the difference in root development between track and wheel rut is strongly pronounced with the advantage on the track side.

Comparing the decrease of soil deformation and penetrometer resistance from tires at normal inflation pressure to half inflation pressure to tracks the small influence of the tire size itself on soil compaction for high loads found by Gruber and Brokjans (1991) can be confirmed. Thus, equipping a heavy machine with tracks has more benefit than using larger tires or using central tire inflation systems. So taking into account that tire manufactures do not guarantee their tires when operated with lower than recommended inflation pressure and taking the additional cost of a central inflation pressure system into account, tracks are not more expensive and significantly better with regard to soil deformation and penetrometer resistance.

Tracked vehicles equipped with such a belt and frame system as the ones used in this investigation may be the answer to the requirements postulated by Hamza and Anderson

(2004). Taking the reduced soil compaction in deeper soil areas into account and ignoring the higher soil compaction close to the surface where it can easily be alleviated tracks may be the answer to maintain high yields in agricultural systems relying on heavy farm machinery in order to maintain and even increase productivity.

The overall results of this investigation lead into the same direction as Alakukku et al. (2003) and Keller and Arvidsson (2004) against the establishment of mere axle load limitations. The change in soil physical properties commonly referred to as soil compaction is not a function only being influenced by load, it is rather a function of spreading the load over the contact area. With the same load the author found a range of responses for different carriages for the load, where some caused significantly less soil compaction than others.

## 9 CONCLUSIONS

- 1) The major benefits of the use of "Terra trac" drive systems in comparison to conventional tire systems are:
  - a) a greater increase in penetrometer resistance in the surface layers with a smaller increase in the subsoil layers. This has great advantage as it would be much easier to remove with subsequent tillage operations.
  - b) a reduction in the surface rut depth and the sub surface soil deformation with depth to approximately 50 % of that of a tire system which substantially reduces the soil bulk density increase (from 15 % to 10 %).
  - c) improved crop performance and root development for broadcast oil seed rape crop
- 2) It was not possible to differentiate the changes in soil physical properties with the Terra Trac at 10.5 and 12 t. Previous conclusions are valid for tracks laden to both 10.5 t and 12.0 t
- 3) The three idler track system shows a reduced peak pressure under the rear sprocket, but the effect is not observed in either penetrometer resistance or soil deformation
- 4) Reducing the inflation pressure from 2.5 bar to 1.25 bar for the 800 mm section width tire significantly reduces the penetrometer resistance, surface rut depth, and sub surface soil deformation. Thereby reducing the increase in DBD from 15 % to 11.6 %.
- 5) At the recommended inflation pressure for 10.5 t overall load (2.2 bar for the 680 mm section width tire, 2.5 for the 800 and 1.9 for the 900) the 900 mm section width tire results in significantly lower soil deformation and penetrometer resistance than the 680 and 800 mm section width tires.
- 6) With subsequent passes of the 900/10.5/1.9 both soil deformation and penetrometer resistance increase significantly. However, the effect reduces with the number of passes, after three passes the shape of the penetrometer resistance is similar to the shape of after the pass of a track. Therefore, both track and multi pass wheels may result in similar soil physical properties.

- 7) Soil compaction in a stratified soil (to simulate a dense layer 200/300 mm deep as in field conditions) in the laboratory stops at the plough layer for the track whereas the effect of the tire pushes the dense soil into the weaker subsoil below. These differences can not be detected from surface rut characteristics.
- 8) Soil compaction in field measurements shows the same tendency. Less increase in penetrometer resistance and soil density for the wheeled combine harvester than for the tracked machine.
- 9) The two models (O'Sullivan et al., 1999 and van den Akker, 2004) considered to predict soil compaction show the general principles, but do not agree with measured data.

## 10 FURTHER REQUIREMENTS AND PRACTICAL SUGGESTIONS

It is necessary to account for the interaction of the rear wheel of a combine harvester, especially for a tracked combine harvester in order to avoid causing more soil compaction with the rear wheels than with the tracks. The ideal size of the rear wheels therefore is unknown and should be determined.

Different wheel systems with weight redistribution have the potential to reduce changes in soil physical properties. The influence of the time of contact on changes in soil physical properties should be investigated to determine the effect of the length of time the soil is strained on soil compaction. These two points may lead wheels towards the same compaction behavior as tracks.

A different attachment system for the tracks might be useful in order to evenly balance the tracks under traction, thereby improving their performance in context with soil compaction. A wider track frame and belt might be a further opportunity to improve the track performance.

Determination of the forces on a deep tillage time after the passage of wheels and tracks in uniform and stratified soil conditions would reveal information concerning the required energy input to loosen the soil again.

These results should further be verified using full size combine harvesters in the field and in controlled laboratory conditions. The results should as well be compared to different soil types and soil moisture contents.

The study of two models for predicting soil compaction revealed that they are not appropriate for reliable predictions without modifications to the soil properties. Therefore setting up a soil compaction model and verifying it with the data gained in the soil bin as well as in field will be useful. In particular focus on the high load range of wheel loads and to include tracks as an option would be a significant advantage.

## 11 BIBLIOGRAPHY

Alakukku, L., Weiskopf, P., Chamen, W.C.T., Tijink, F.G.J., van den Linden, J.P., Pires, S., Sommer, C. and Spoor, G., 2003. Prevention strategies for field traffic – induced subsoil compaction: a review. Part 1. Machine / Soil interactions. *Soil & Tillage Res.* 73: 145 – 160.

Arvidsson, J. and Hakansson, I., 1996. Do effects of soil compaction persist after ploughing? Results from 21 long – term field experiments in Sweden. *Soil & Tillage Res.* 39: 175 – 197.

Arvidsson, J., Trautner, A., van den Akker, J.J.H., and Schjonning, P., 2001. Subsoil compaction caused by heavy sugarbeet harvesters in southern Sweden II. Soil displacement during wheeling and model computations of compaction. *Soil & Tillage Res.* 60: 79 – 89.

Bailey, A.C., Raper, R.L., Way, T.R., Burt, E.C., and Johnson, C.E., 1993. Soil stresses under tractor tires at various inflation pressures. *Proceedings of the 11<sup>th</sup> International Conference of the ISTVS* 1: 276 – 285. Incline Village, Nevada.

Bashford, L.L., Jones, A.J., and Mielke, L.N., 1988. Comparison of bulk density beneath a belt track and a tire. *Applied Engineering in Agriculture* 4: 122- 125.

Bashford, L.L. and Kocher, M.F., 1999. Belts vs. tires, belts vs. belts, tires vs. tires. *ASAE Applied Engineering in Agriculture* 15 (3): 175 – 181.

Baumgartl, Th. and Koeck, B., 2004. Modeling volume change and mechanical properties with hydraulic models. *Soil Science of America Journal* 68: 57 – 65.

Beet, F.G., J. Tijink and J.P. van den Linden. 2000. Engineering approaches to subsoil compaction in cropping systems with sugar beet. In *Subsoil Compaction – Distribution, Processes and Consequences*. (R. Horn, J.J.H. van den Akker and J. Arvidsson., Eds.) Cartina Verlag. Germany.

Bekker, M.G., 1956. *Theorie of Land Locomotion*. University of Michigan Press, Ann Arbor Michigan, USA.

Berli, M., Kirby, J.M., Springman, S.M. and Schulin, R., 2003. Modeling compaction of agricultural subsoils by tracked heavy construction machinery under various moisture conditions in Switzerland. *Soil & Tillage Research* 73: 57 – 66.

Birkas M., Dorogi, I. and Szalai, T., 1992. The effects of soil compaction on the quality and energy requirements of tillage. pp 232-235 in *Proceedings of International Conference on Soil Compaction and Soil Management, 8-12 June 1992. Tallin, Estonia*.

Blunden, B.G., McBride, R.A., Daniel, H. and Blackwell, P.S., 1994. Compaction on an earthy sand by rubber tracked and tyred vehicles. *Australian Journal of Soil Research* 32: 1095 – 1108.

Boussinesq, J. 1885. Application des potentiels à l'étude de l'équilibre et du Mouvement des solides élastique. Gauthier-Villais, Paris, cited by Froehlich (1934).

Brown, H.J., Cruse, R.M., Erbach, D.C., Melvin, S.W., 1992. Tractive device effects on soil physical properties. *Soil & Tillage Research* 22: 41 – 53.

Burger, J.A., Perumpral, J.V., Kreh, R.E., Torbert, J.L., and Minaei, S., 1983. The effect of track and rubber – tired vehicles on soil compaction. *ASAE Paper No.* 83 – 1621.

Burger, J.A., Perumpral, J.V., Kreh, R.E., Torbert, J.L., and Minaei, S., 1985. Impact of tracked and rubber – tired tractors on a forest soil. *Transactions of the ASAE* 28: 369 – 373.

Bygden, G., Eliasson, L. and Wasterlund, I., 2004. Rut depth, soil compaction and rolling resistance when using bogie tracks . *Journal of Terramechanics* 40: 179 – 180.

Campbell, D.J., 1994. Determination and use of dry bulk density in relation to soil compaction, pp 113 – 139. In: *Soil Compaction in Crop Production. Developments in Agricultural Engineering 11* (Eds. Soane, B.D. and van Ouwerkerk, C.). Elsevier, Amsterdam, Netherlands.



Campbell, D.J., Dickson, J.W. and Owen, G.M., 1988. Soil compaction, drawbar pull and stability measurements for Hytracker all terrain vehicle. *Dep. Note 14, Scottish Center for Agricultural Engineering, Penicuik.*

Campbell, D.J., 1976. Plastic limit determination using a drop cone penetrometer. *Journal of Soil Science*, 27: 295 – 300.

Casagrande, A., 1936. The determination of pre-consolidation load and its practical significance. *Int. Soil Mech. Found. Eng. Harvard University, Cambridge, MA.* PP 60 – 64.

Chamen, W.C.T. and Audsley, E., 1993. A study of the comparative economics of conventional and zero traffic systems for arable crops. *Soil & Tillage Res.* 25: 399 – 409.

Chamen, W.C.T., Leede, P.R., Howse, K.R. and Goss, M.J., 1988. The effect of different tire/soil contact pressure on soil and crop responses when growing winter wheat: Year 4 – 1985 – 86. *Div. Note DN 1489. AFRC Inst. Engng. Res., Silsoe, UK.*

Chamen, W. C. T., Cope, R. E., Longstaff, D. J., Patterson, D. E. and Richardson, C. D., 1996. The energy efficiency of seedbed preparation following mouldboard ploughing. *Soil & Tillage Res.* 39 (1-2): 13-30.

Culshaw, D., 1986. Rubber tracks for agriculture. *Div. Note DN 1345, Natl. Inst. Agric. Engng., Silsoe. UK.*

Culshaw, D. and Dawson, J.R., 1987. The performance of a simple rubber track for an agricultural vehicle. *Div. Note DN1382. AFRC Inst. Engng. Res., Silsoe, UK.*

Davis, D.B., Finney, J.B. and Richardson, S.J., 1973. Relative effects of tractor weight and wheel slip in causing soil compaction. *Journal of Soil Science* 24 (3): 399 – 409.

Dias Junior, M.S. and Pierce, F.J., 1995. A simple procedure for estimating preconsolidation pressure from soil compression curves. *Soil Technology* 8: 139 – 151.

Dickson, J.W., 1994. Compaction by a combine harvester operating on moist loose soil. *Soil & Tillage Res.* 29 (2-3): 145 – 150.

Eriksson, J., Hakansson, I. and Danfors, B., 1974. Effects of soil compaction on soil structure and crop yields. *Swedish Institute of Agr. Eng. Bull.* 504: 101 p.

Erbach, D.C., Melvin, S.W., Cruse, R.M., 1988. Effects of tractor tracks during secondary tillage on corn production. *ASAE Paper No.* 88 – 1614.

Erbach, D.C., Melvin, S.W., Cruse, R.M., 1991. Low ground pressure equipment fleets for crop production. *ASAE Paper No.* 91 – 1517.

Erbach, D.C., 1994. Benefits of tracked vehicles in crop production. pp 501 – 520. In: *Developments in Agricultural Engineering 11. Soil Compaction in Crop Production*. Soane, B.D. and van Ouwerkerk, C. (Eds), 1994.

Fekete, A., 1972. Studies of the soil compacting effects of tires. *Mezoegazdasagi Gepesitesi Tanulmányok*, 19: 16 – 25.

Froehlich, O.K. 1934. *Druckverteilung im Baugrunde*. Verlag von Julius Springer, Wien.

Gameda, G., Raghavan, G.S.V., Theriault, R. and McKeyes, E., 1983. Effect of subsoil compaction on corn production. *ASAE Paper No* 83 – 2043.

Gassman, P.W., Erbach, D.C. and Melvin, S.W., 1989. Analysis of track and wheel soil compaction. *Transactions of the ASAE* 32 (1): 23 – 29.

Gill, W.R. and Vanden Berg, G.E., 1968. *Soil Dynamics in Tillage and Traction*. Agricultural Handbook 316. *Agricultural Research Service, USDA. Government Printing Office, Washington, DC, USA*.

Godwin, R.J., 1974. An investigation into the mechanics of narrow tines in frictional soils. *Thesis (Ph.D)*. University of Reading.

Godwin, R.J., 1975. An extended octagonal ring transducer for use in tillage studies. *Journal of Agricultural Engineering Research* 20: 347 – 352.

Godwin, R. J. and Dresser, M. L., 2004. Unpublished data.

Godwin, R.J. and O'Dogherty, M.J., 2003. Integrated soil tillage force prediction models. *Proceedings of the 9<sup>th</sup> European Conference of the International Society for Terrain Vehicle Systems*, Harper Adams University College, UK.

Godwin, R.J. and Spoor, G. 1977. Soil failure with narrow tines. *Journal of Agricultural Engineering Research* 22: 213 – 228.

Godwin, R.J. and Spoor, G., 1981. Overcoming Compaction. *Soil and Water* 9 (1): 11 – 13.

Grecenko, A., 2003. Tire load rating to reduce soil compaction. *Journal of Terramechanics* 40: 97-115.

Gruber, W. and Brokjans, T., 1991. Soil compaction caused by heavy agricultural machinery. In: *Proceedings of the ASAE Meeting. Presentation on soil compaction caused by heavy agricultural machinery. International Summer Meeting*, New Mexico, June 23 – 26, 1991, Paper No. 91-1059.

Hadas, A., 1994. Sol compaction caused by high axle loads – review of concepts and experimental data. *Soil & Tillage Res.* 29: 253 – 276.

Hakansson, I. And Medvedev, V.W., 1995. Protection of soils from mechanical overloading by establishing limits for stresses caused by heavy vehicles. *Soil & Tillage Res.* 35: 85 – 97.

Hakansson, I., Voorhees, W.B. and Riley, H., 1988. Vehicle and wheel factors influencing soil compaction and crop response in different traffic regimes. *Soil & Tillage Research* 11: 239 – 282.

Hamza, M.A. and Anderson, W.K., 2005. Review – Soil Compaction in Cropping Systems. A review of the nature, causes, and possible solutions. *Soil & Tillage Research* 82: 121 - 145

Horn, R. and Fleige, H., 2003. A method for assessing the impact of load on mechanical stability and on physical properties of soils. *Soil & Tillage Research* 73: 89 – 99.

Horn, R., van den Akker, J.J. and Arvidsson, J. (Eds), 2000. *Subsoil Compaction. Distribution, processes and consequences*. Catena Verlag, Reiskirchen, Germany.

Janzen, D.C., Hefner, R.E., and Erbach, D.C., 1985. Soil and corn response to track and wheel compaction. Proc. International Conference on Soil Dynamics 5: 1023 – 1038. National Soil Dynamics Laboratory, Auburn, AL.

Johnson, C.E. and Burt, E.C., 1990. A method of predicting soil stress state under tires. *Transactions of the ASAE*, 33: 713 – 717.

Kirchmann, H. and Thorvaldsson, G., 2000. Challenging targets for future agriculture. *European Journal of Agronomy* 12: 145 – 161.

Keller, T. and Arvidsson, J., 2004. Technical solutions to reduce the risk of subsoil compaction: effects of dual wheels, tandem wheels and tire inflation pressure on stress propagation in soil. *Soil & Tillage Res.* 79: 191 – 205.

Keller, T. Trautner, A. and Arvidsson, J., 2002. Stress distribution and soil displacement under a rubber tracked and a wheeled tractor during ploughing, both on land and within furrows. *Soil & Tillage Res.* 68: 39 – 47.

Kinney, G.R., Erbach, D.C. and Bern, C.J., 1992. Soil strain under three tractor configurations. *Transactions of the ASAE* 35 (4): 1135 – 1139.

Lipiec, J., Arvidsson, J. and Murer, E. 2003. Review of modeling crop growth, movement of water and chemicals in relation to topsoil and subsoil compaction. *Soil & Tillage Res.* 73: 15 – 29.

Lipiec, J. and Hatano, R., 2003. Quantification of compaction effects on soil physical properties and crop growth. *Geoderma* 116: 107 – 136.

Maciejewski, J. and Jarzebowski, A., 2004. Experimental analysis of soil deformation below a rolling rigid cylinder. *Journal of Terramechanics* 41: 223 – 241.

McKyes, E., 1985. Soil Cutting and Tillage. *Developments in Agricultural Engineering* 7. Elsevier, Amsterdam, Netherlands.

Melvin, S.W., Erbach, D.C. and Cruse, R.M., 1994. Effects of axle load and subsoiling on maize yields on three Midwestern U.S. soils. pp 179 – 187. In: *International Soil Tillage Research Organization, Proceedings of the 13<sup>th</sup> International Conference, Volume I*. Jensen, H.E., Schjonning, P., Mikkelsen, S.A. and Madsen, K.B. (Eds.). ISTRO Denmark, Aalborg, July 19 – 24 1994. Soil and Tillage for crop production and protection of the environment.

Mouazen, A.M., Dumont, K., Maertens, K., Ramon, H., 2003. Two – dimensional prediction of spatial variation in topsoil compaction of a sandy loam field – based on measured horizontal force of compaction sensor, cutting depth and moisture content. *Soil & Tillage Research* 74: 91 –102.

Nelder, J.A., 1985. Discussion of Dr. Chatfield's paper. *Journal of the Royal Statistical Society*. Series A, 148 (3): 238.

Negi, S.C., McKyes, E., Raghavan, G.S.V. and Taylor, F., 1981. Relationships of field traffic and tillage to corn yields and soil properties. *Journal of Terramechanics*, 18: 81 – 90.

O'Connell, D.J., 1972. The measurement of apparent specific gravity of soils and its relationship to mechanical composition and plant growth, pp 298 – 313. In *Soil Physical Conditions and Crop Production*. Proceedings of a conference organized by the Soil Scientists of the Agricultural Development and Advisory Service. January, 3-5 1972. Technical Bulletin 29. Ministry of Agriculture, Fisheries and Food.

O'Sullivan, M.F., Henshall, J.K., Dickson, J.W., 1998. A simplified method for estimating soil compaction. *Soil & Tillage Res.* 49: 325-335

Pagliai, M., Marsili, A., Servadio, P., Vignozzi, N. and Pellegrini, S., 2003. Changes in some physical properties of a clay soil in central Italy following the passage of rubber tracked and wheeled tractors of medium power. *Soil & Tillage Res.* 73: 119 – 129.

Piepho, H.P., Buechse, A., and Richter, C., 2004. A mixed modeling approach for randomized experiments with repeated measures. *Journal of Agronomy and Crop Science* 190: 230 – 247.

Poodt, M.P., Koolen, A.J. and van den Linden, J.P., 2003. FEM – Analysis of subsoil reaction on heavy wheel loads with emphasis on soil preconsolidation stress and cohesion. *Soil & Tillage Research* 73: 67 – 76.

Raghavan, G.S.V., McKyes, E. and Chasse, M., 1976. Soil compaction patterns caused by off-road vehicles in Eastern Canadian agricultural soils. *Journal of Terramechanics* 13: 107 – 115.

Raper, R.L., Bailey, A.C., Burt, E.C., and Way, T.R., 1993. Inflation pressure and dynamic load effects on soil – tire – interface stresses. *ASAE Paper No.* 931 517.

Raper, R.L., Bailey, A.C., Burt, E.C., Way, T.R. and Liberati, P., 1993. Inflation pressure effects on soil – tire interface stresses. *Proceedings of the 10<sup>th</sup> International Conference of the ISTVS* 781 – 790. Amsterdam, The Netherlands: Elsevier Science.

Raper, R.L., Bailey, A.C., Burt, E.C., Way, T.R. and Liberati, P., 1995. Inflation pressure and dynamic load effects on soil deformation and soil – tire interface stresses. *Transaction of the ASAE*, 38 (3): 685 – 689.

Reaves, C.A. and Cooper, A.W., 1960. Stress distribution in soils under tractor loads. *Agricultural Engineering* 41: 20 – 21, 31.

Rusanov, V.A., 1991. Effects of wheel and track traffic on the soil and crop growth and yield. *Soil & Tillage Research* 19: 131 – 143.

Servadio, P., Marsili, A., Pagliai, M., Pellegrini, S. and Vignozzi, N., 2001. Effects on some clay soil qualities following the passage of rubber – tracked and wheeled tractors in central Italy. *Soil & Tillage Res.* 61: 143 – 155.

Shestak, C.J. and Busse, M.D., 2005. Compaction alters physical but not biological indices of soil health. *Soil Science Society of America Journal* 69: 236 –246.

Smith, D.L.O. and Dickson, J.W., 1990. Contributions of vehicle weight and ground pressure to soil compaction. *Journal of Agricultural Engineering Research* 46: 13 – 29.

Spoor, G., Tjink, F.G.J. and Weisskopf, P., 2003. Subsoil compaction: risk, avoidance, identification and alleviation. *Soil & Tillage Research* 73: 175 – 182.

Spoor, G. and Godwin, R.J., 1978. An experimental investigation into the deep loosening by rigid tines. *Journal of Agricultural Engineering Research* 23: 243 – 258.

Soane, B.D., 1973. Techniques for measuring changes in the packing state and cone resistance of soil after the passage of wheels and tracks. *Journal of Soil Science* 24: 311 – 323.

Soane, B.D., 1980. Compaction by vehicles. Problems and opportunities. *S. A. W. M. A. Soil compaction conference.*

Soane, B.D., 1985. Traction and transport systems as related to cropping systems. A global review of the compaction of soils by vehicles in the production of agricultural and forest products. *International Conference on Soil Dynamics Proceeding*, 5: 863 – 935.

Soane, B.D., Blackwell, P.S., Dickson, J.W., and Painter, D.J., 1980/81. Compaction by agricultural vehicles: A Review I. Soil and wheel characteristics. *Soil & Tillage Research* 1: 207 – 237.

Soane, B.D., Blackwell, P.S., Dickson, J.W., and Painter, D.J., 1981. Compaction by agricultural vehicles: A Review II. Compaction under tires and other running gear. *Soil & Tillage Research* 1: 373-400.

Soane, B.D., Godwin, R.J., and Spoor, G., 1986. Influence of deep loosening techniques and subsequent wheel traffic on soil structure. *Soil & Tillage Research* 8: 231 – 237.

Soane, B.D. and van Ouwerkerk, C. (Eds), 1994. Developments in Agricultural Engineering 11. Soil Compaction in Crop Production. Elsevier, Amsterdam, Netherlands.

Soehne, W., 1953. Druckverteilung im Boden und Bodenverformung unter Schlepperreifen. (Pressure distribution in the soil and soil deformation under tractor tires). *Grundlagen Landtechnik* 5: 49-63.

Soehne, W., 1958. Fundamentals of pressure distribution and soil compaction under tractor tyres. *Journal of Agricultural Engineering* 39: 276 – 281, 290.

Soil Science Society of America, 1996. *Glossary of Soil Science Terms*. Madison, WI, USA.

Taylor, J.H. and Burt, E.C., 1975. Track and tire performance in agriculture. *Transactions of the ASAE* 18: 3 – 6.

Terzaghi, K. and Peck, R.B., 1967. *Soil Mechanics in Engineering Practice*. 2<sup>nd</sup> Edition. John Wiley & Sons, New York, USA.

Tijink, F.G.J., 1994. Quantification of vehicle running gear. pp 391 – 415. In: Developments in Agricultural Engineering 11. Soil Compaction in Crop Production. Soane, B.D. and van Ouwerkerk, C. (Eds), 1994. Elsevier, Amsterdam, Netherlands.

Trautner, A. and Arvidsson, J., 2003. Subsoil compaction caused by machinery traffic on a Swedish Eutric Cambiosol at different soil water contents. *Soil & Tillage Res.* 73: 107 – 118.



Trein, C.R., 1995. The Mechanics of Soil Compaction Under Wheels. *PhD – Thesis in Ag. Eng. Cranfield University, Silsoe College.*

Van den Akker, J.J., 2004. SOCOMO: a soil compaction model to calculate soil stress and subsoil carrying capacity. *Soil & Tillage Research* 79: 113 – 127.

Vanden Berg, G.E., 1966. Triaxial measurements of shear strain and compaction in unsaturated soil. *Transaction of the ASAE* 9: 460 – 463, 467.

Vorhees, W.B. and Lindstrom, M.J., 1983. Soil compaction constraints on conservation tillage in the northern Corn Belt. *Journal of Soil and Water Conservation* 38: 307 – 311.

Vorhees, W.B., 1986. The effect of soil compaction on crop yield. Earth Moving Conference Preoria, Illinois. April 8-10, 1986. *SAE Technical Paper Series* 860729

Way, T. R., Erbach, D.C., Bailey, A.c., Burt, E.C. and Johnson, C.E., 2005. Soil displacement below an agricultural tractor drive tire. *Journal of Terramechanics* 42: 35 - 46.

Way, T.R., Johnson, C.E., Bailey, A.C., Raper, R.L. and Burt, E.C., 1996. Soil stress state orientation beneath a tire at various loads and inflation pressures. *Journal of Terramechanics* 33: 185 – 194.

Weissbach, M., 2003. Landtechnische Untersuchungen zur Wirkung bodenschonender Fahrwerke an Schleppern und Arbeitsmaschinen mit verschiedenen Radlasten. *Habilitationsschrift, Universitaet Kiel. Logos Verlag, Berlin, Germany.*

Yavuzcan, G.H., Matthies, D. and Auernhammer, H., 2004. Vulnerability of Bavarian silty loam soil to compaction under heavy wheel traffic: impacts of tillage method and soil water content. *Soil & Tillage Res.* Article in Press. 1st of September 2005.

Young, R.A., Voorhees, W.B., 1982. Soil erosion and run off from planting to canopy development as influenced by tractor wheel traffic. *Transaction of the ASAE* 25 (3) :708 – 712.

## 12 ACKNOWLEDGEMENTS

At first I want to thank Prof. Dick Godwin for suggesting this interesting topic and his permanent support during the work on this Master Thesis. Discussing the results with him and getting his ideas to make the data comparable was a great experience.

Without the financial support from Dr. Helmut Claas and Dr. Herman Garbers this work would not have been possible and this is very gratefully acknowledged. Christian Hillekes help in carrying out the day – by – day topics was important – thank you very much ☺. Trevor Tyrrell did me an enormous favor by supplying a combine harvester for one week.

Many thanks have to go to Dr. James Brighton for his ideas, help, and questioning of results. The huge computer technical support from Dr. Kim Blackburn was of more than remarkable importance in order to set up such profound measurement devices.

Great thanks have to go to Roy Newland and Simon Stranks for their tremendous support during all my work in the soil bin. Roger Swatlands' help during the runs is acknowledged as well as Phil Riley who always was there in any case of emergency need of a technician. In case the power pack decided once again not to work any more, Ray Chapple was a big help, too. Robert Walkers' ability to get a proper power pack and doing the necessary service with it is highly acknowledged.

The farmers Robert Barnes and Sam Fairs gave a significant contribution towards the in – field verification of my results by letting me do measurements on their fields. Thanks have to go to Dr. Marc Dresser for his help at Sam Fairs' farm.

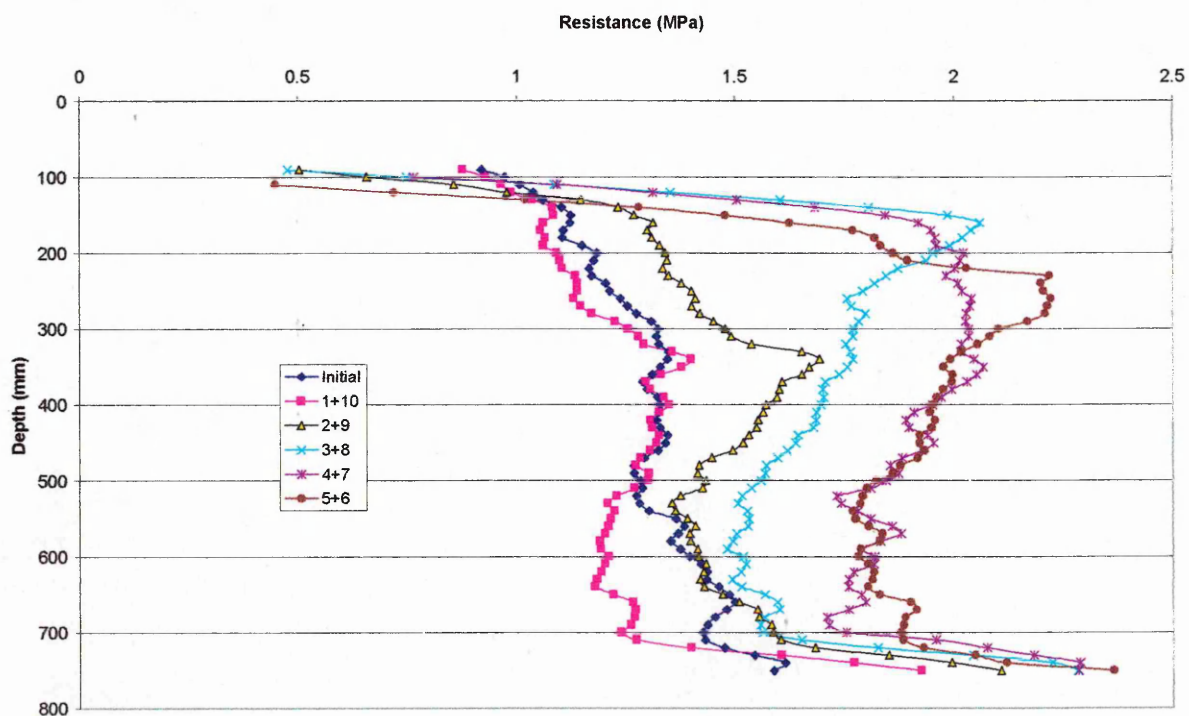
Many thanks as well to all the people I may have forgotten ☺.

Great thanks also to my parents Hiltrud Ansorge and Walter Zuern for their continuous support during the whole work.

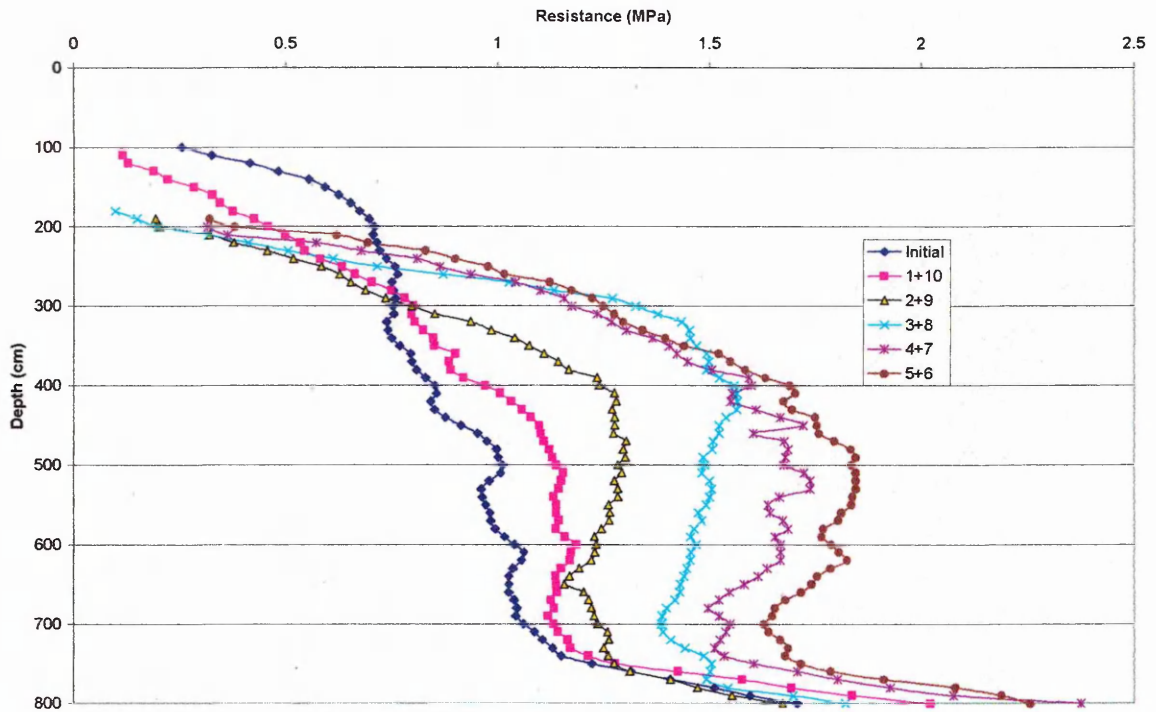
### 13 APPENDIX

#### 13.1 Data of Soil Compaction Studies

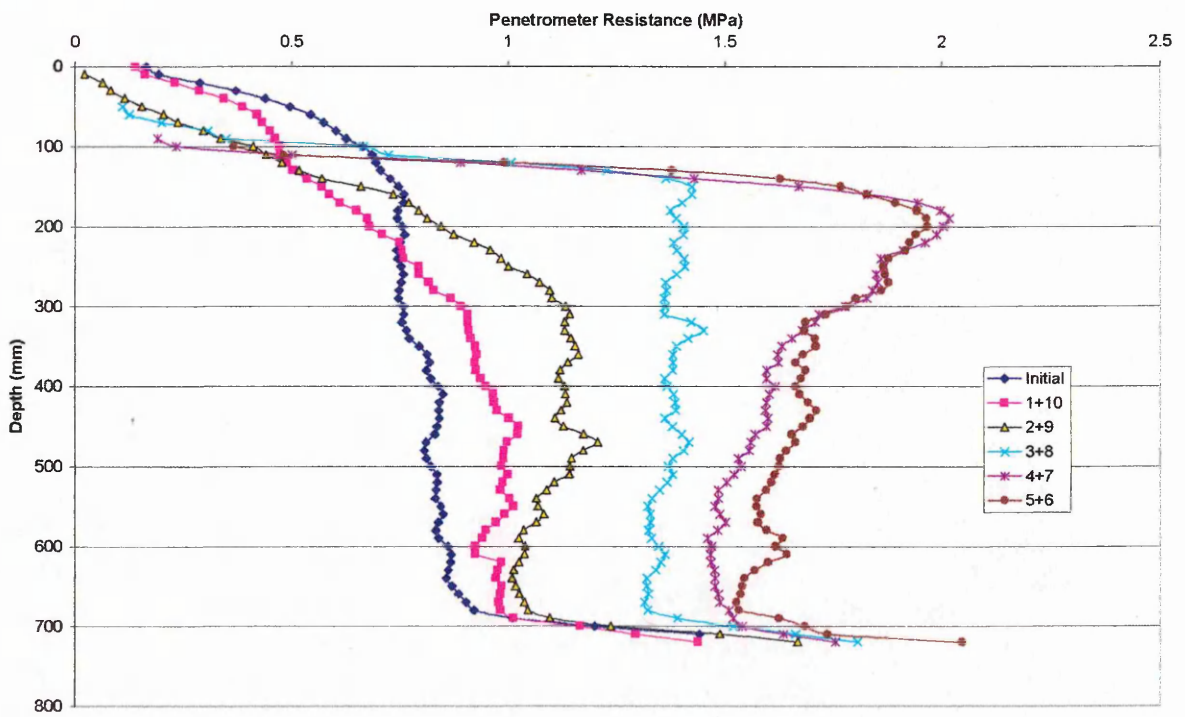
##### 13.1.1 Average Penetrometer Resistance



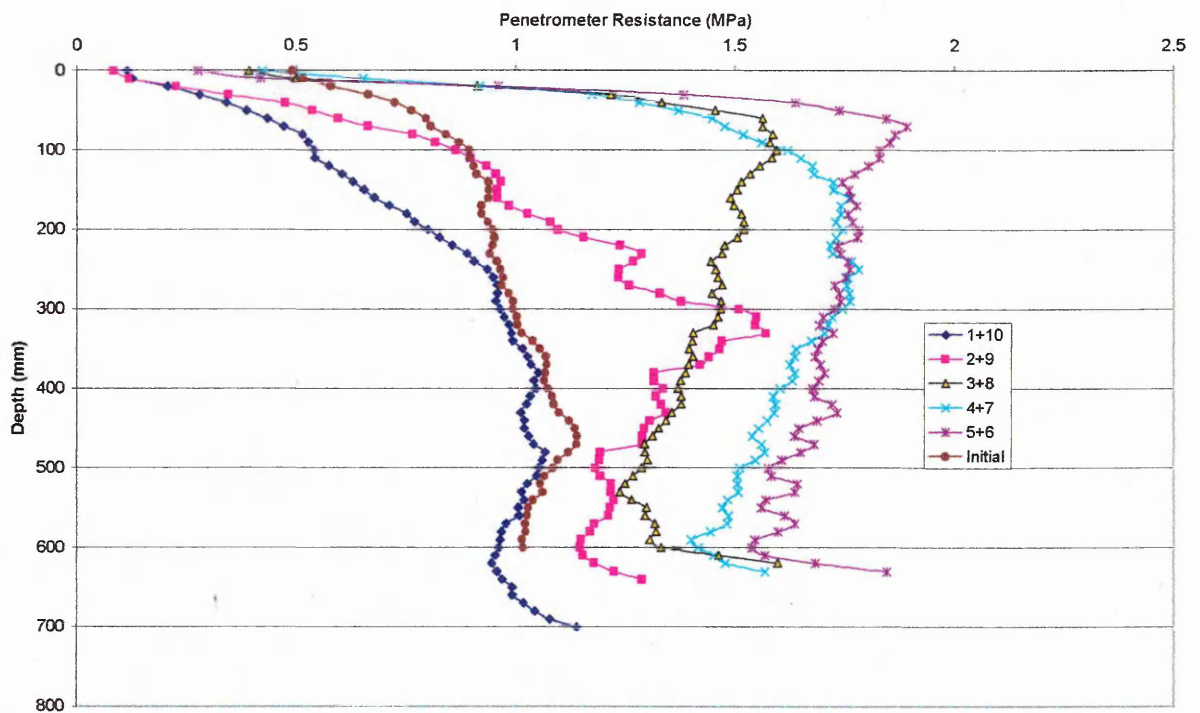
800/8.5/2.5tm



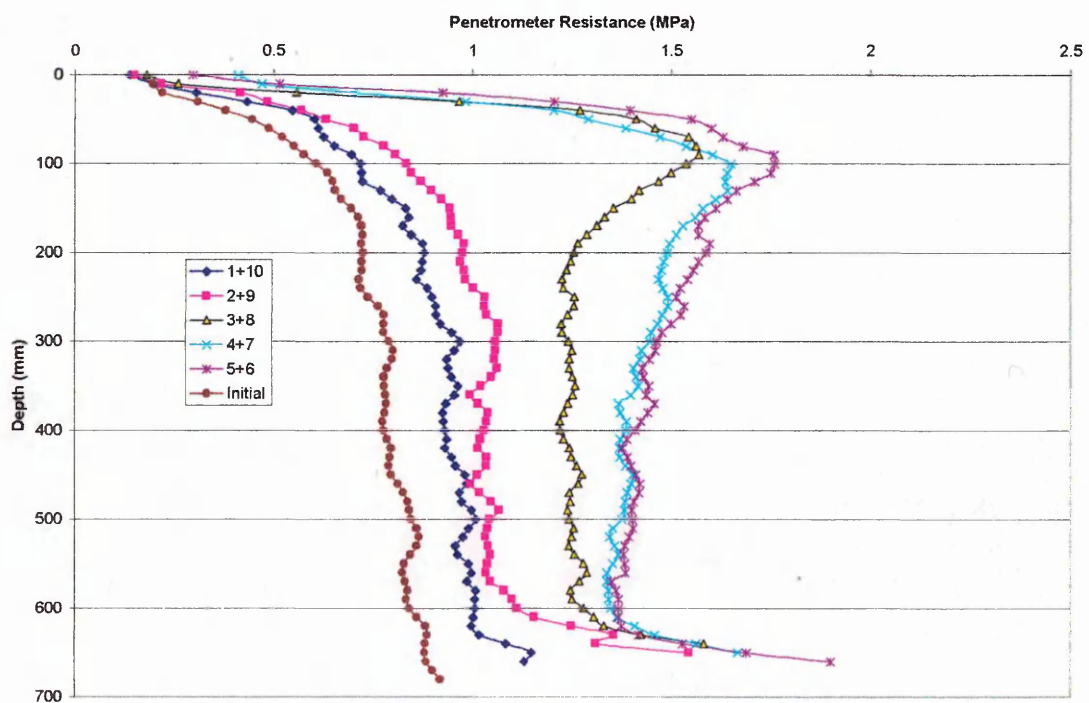
800/8.5/2.5ts



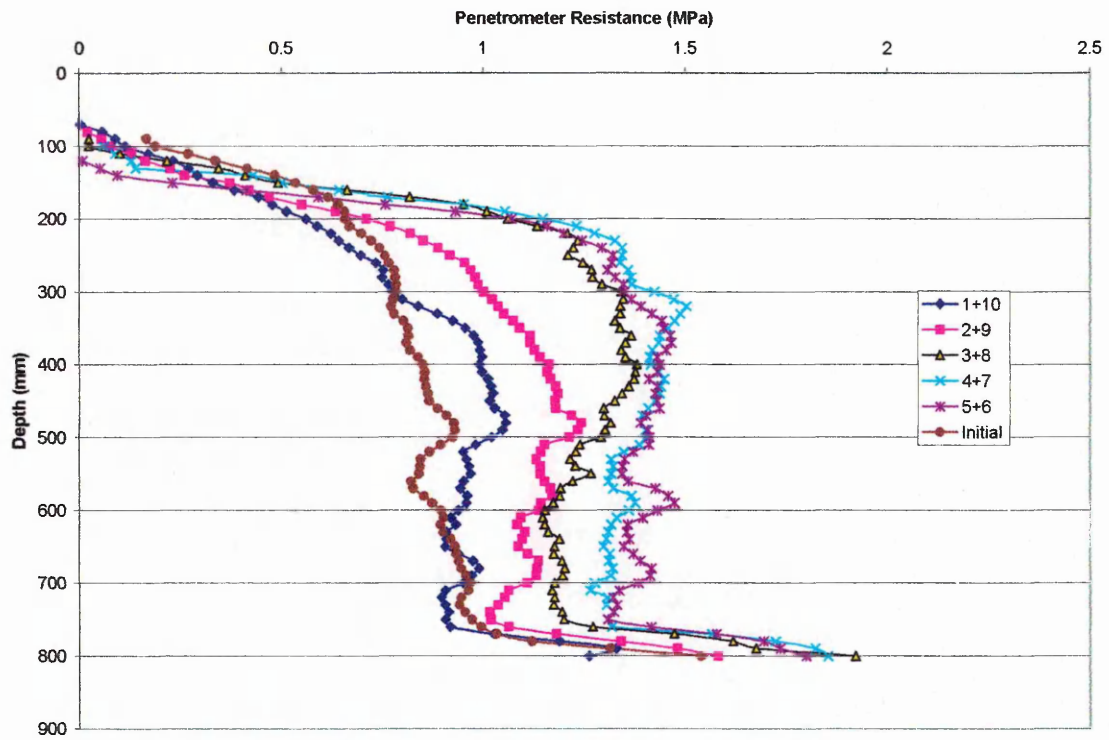
680/10.5/2.2



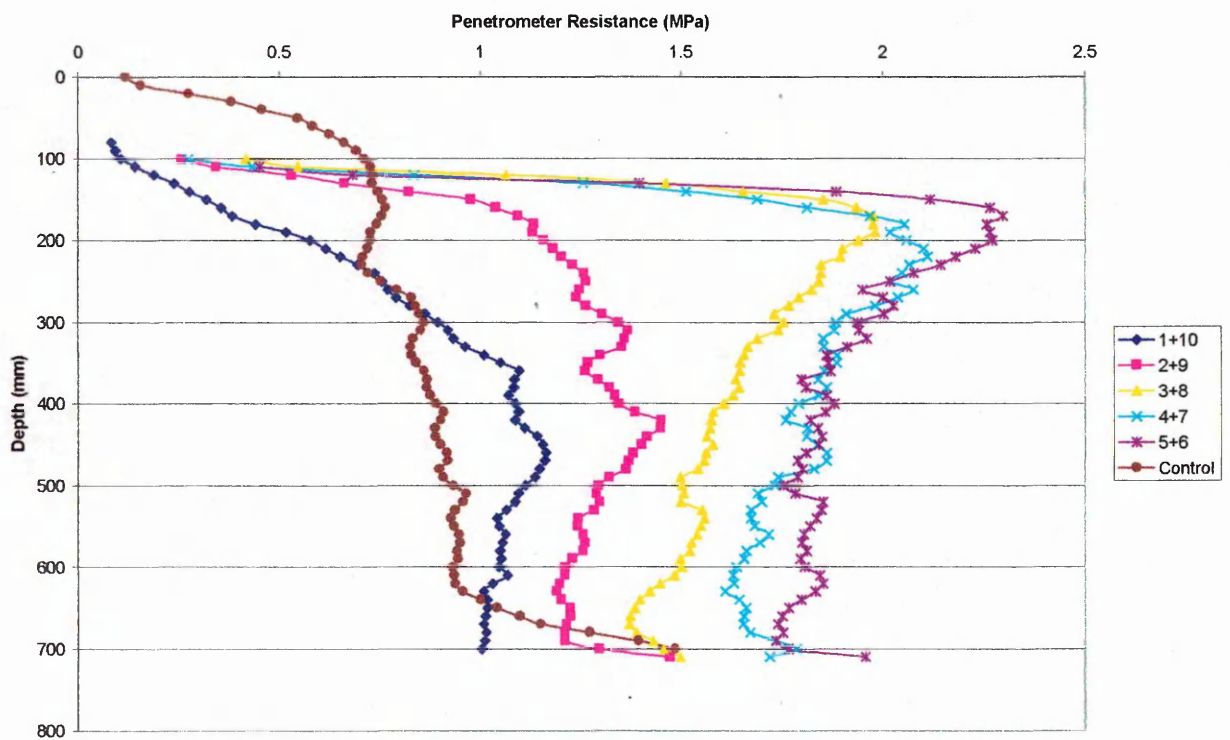
800/10.5/2.5



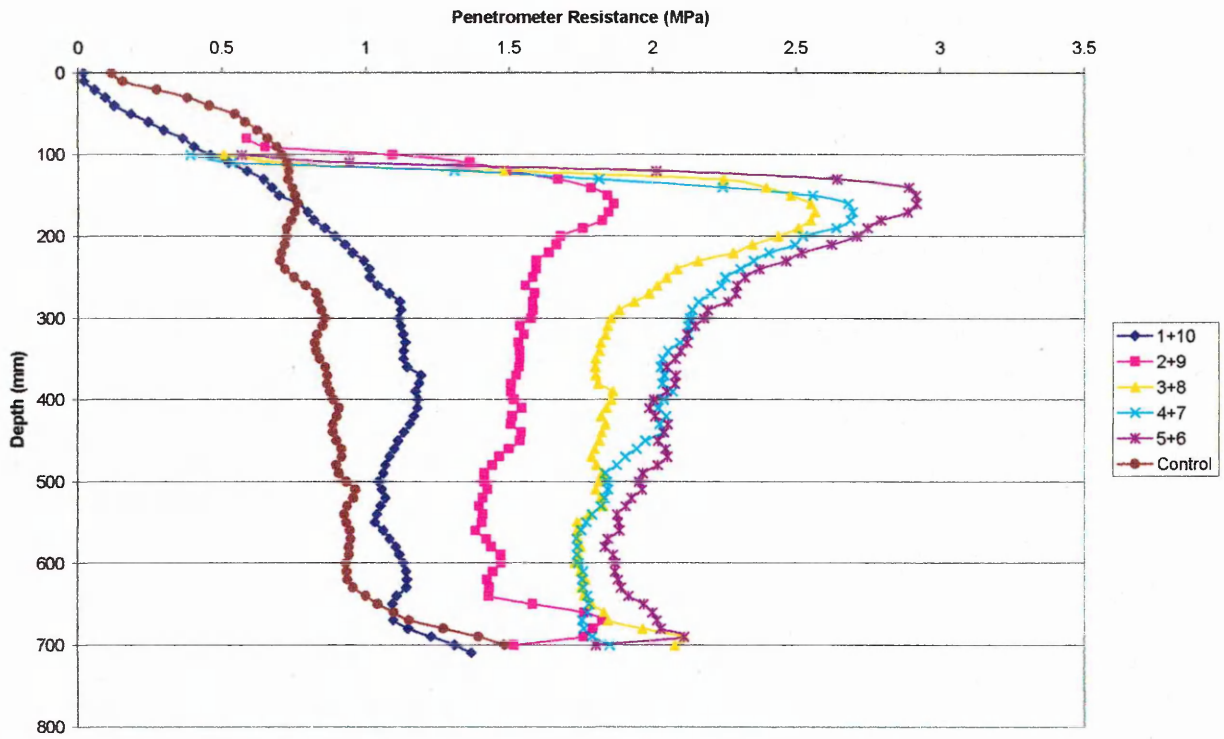
800/10.5/1.25



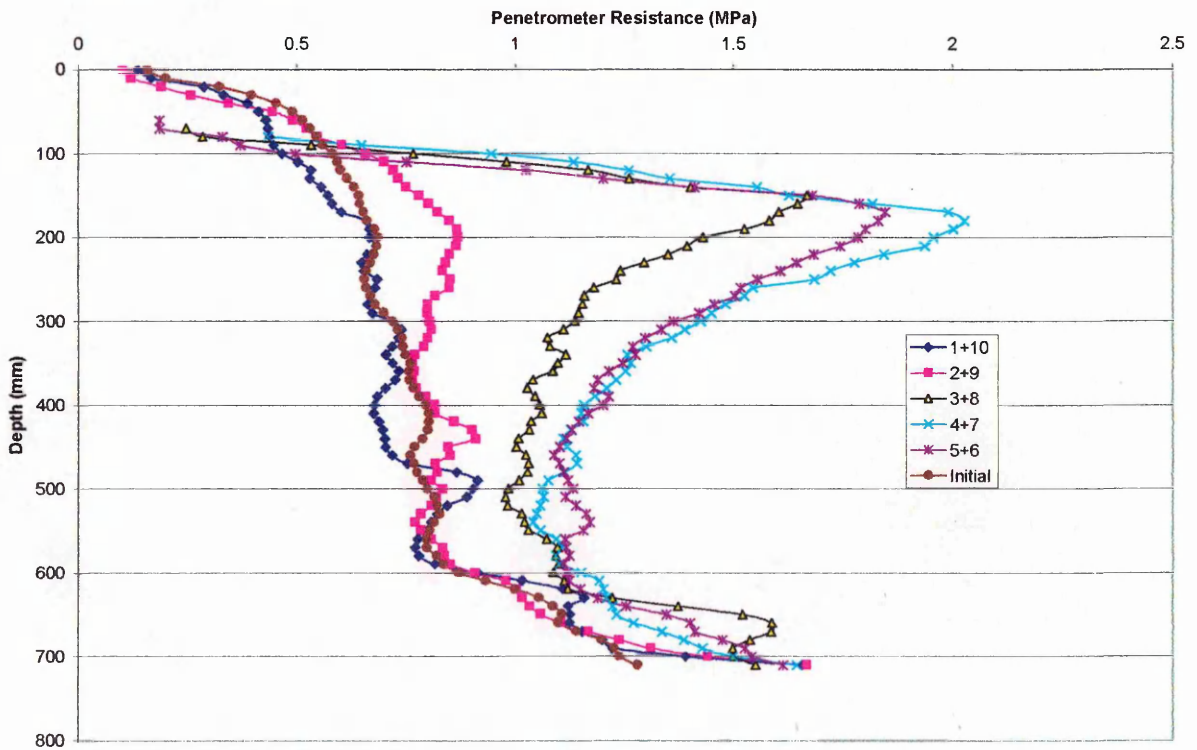
900/10.5/1.9



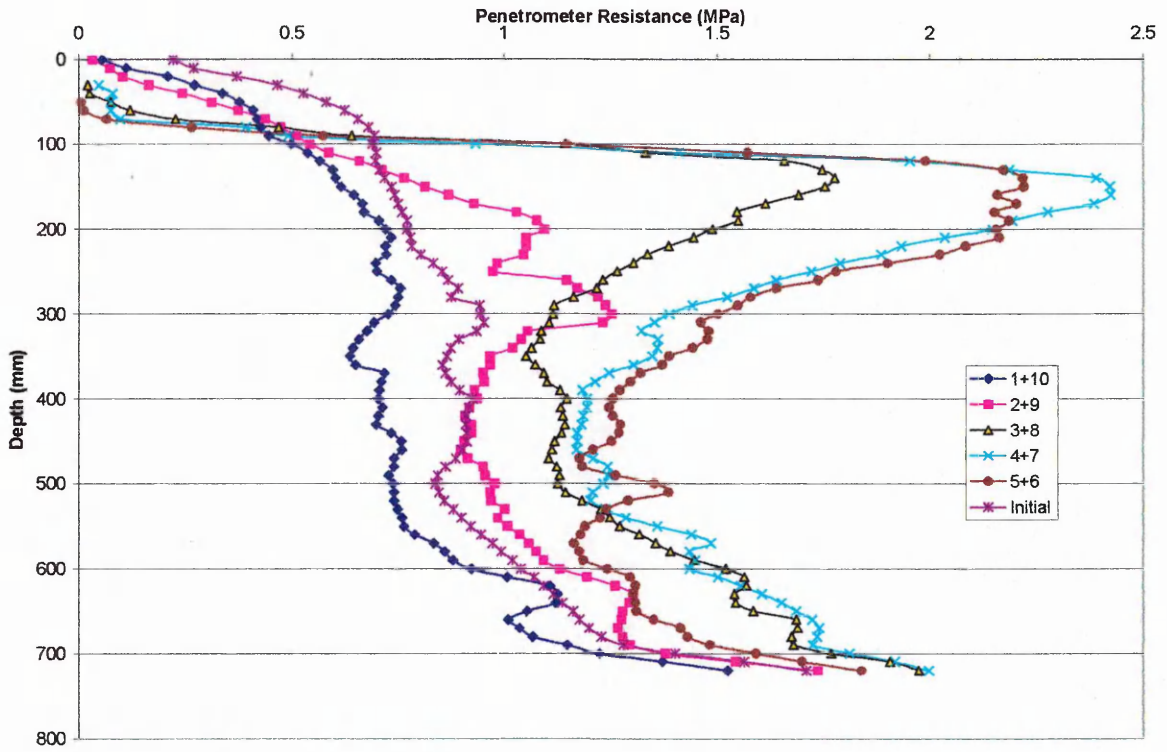
900/10.5/1.9 after two passes



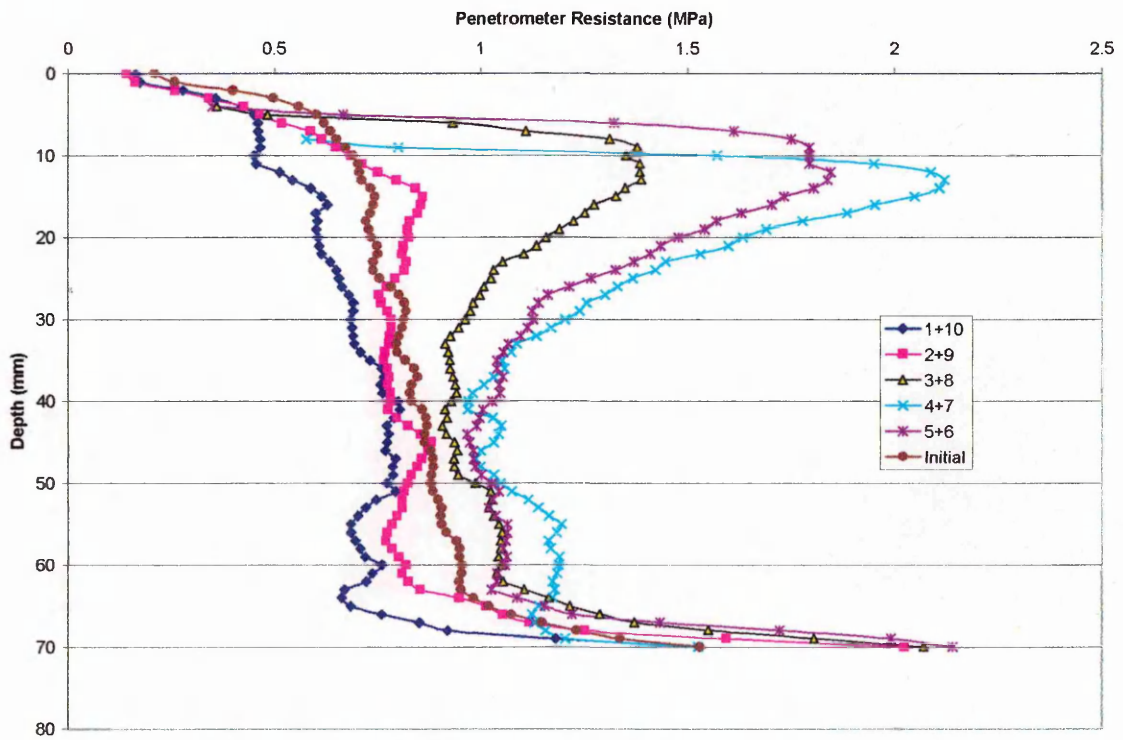
900/10.5/1.9 after three passes



t2/10.5

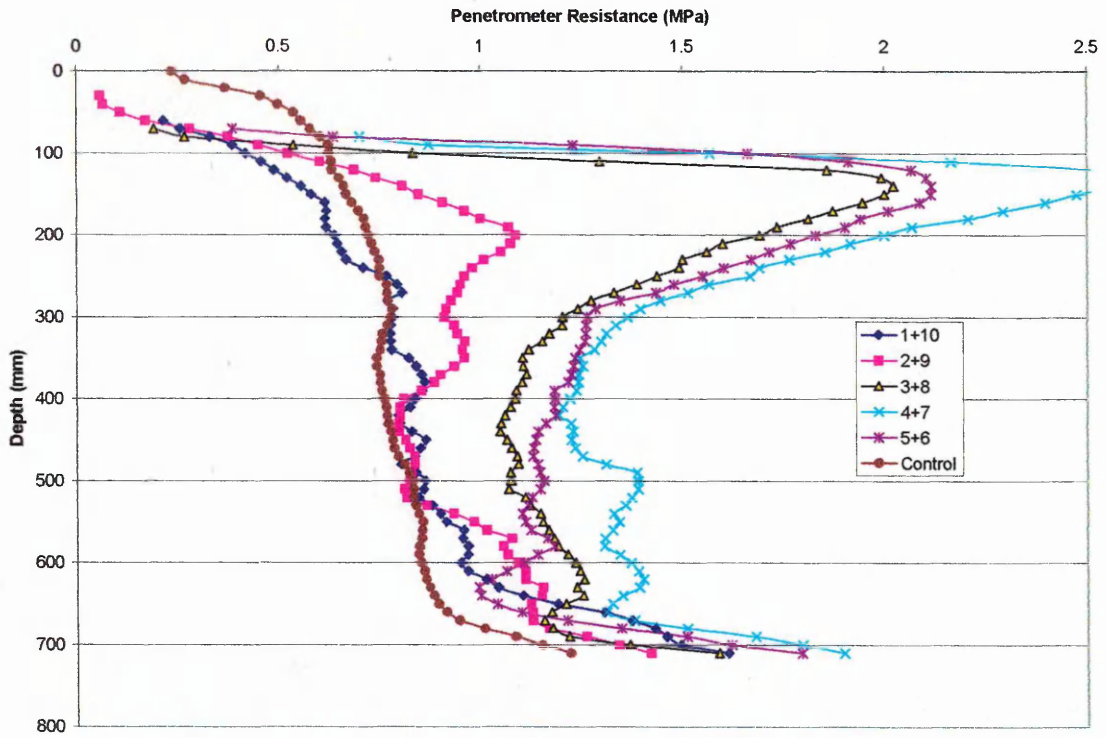


t2/12

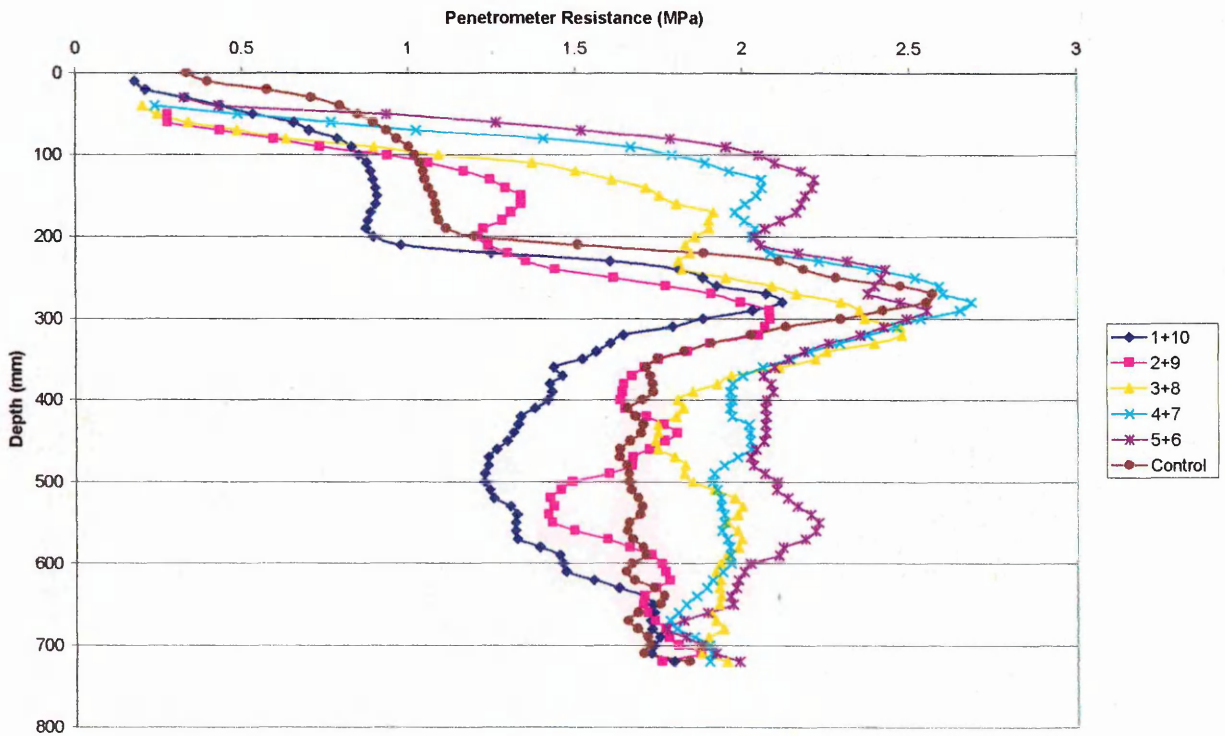


t3/10.5

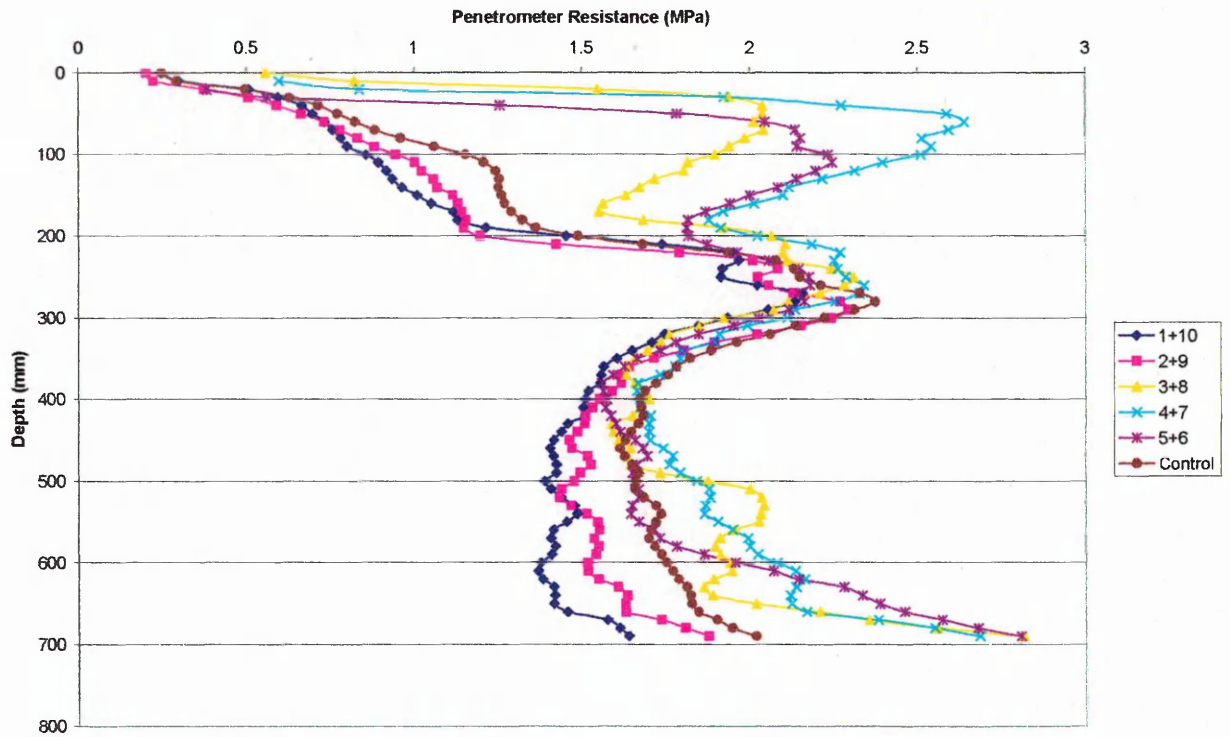




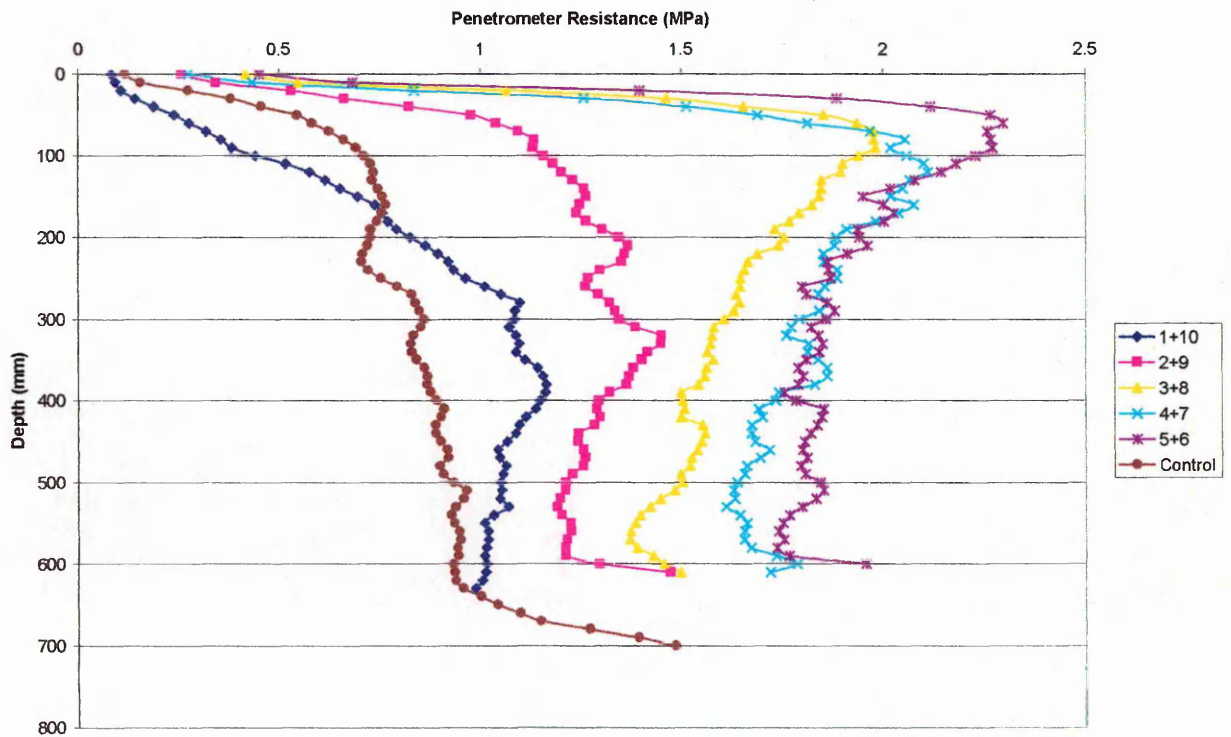
t3/12



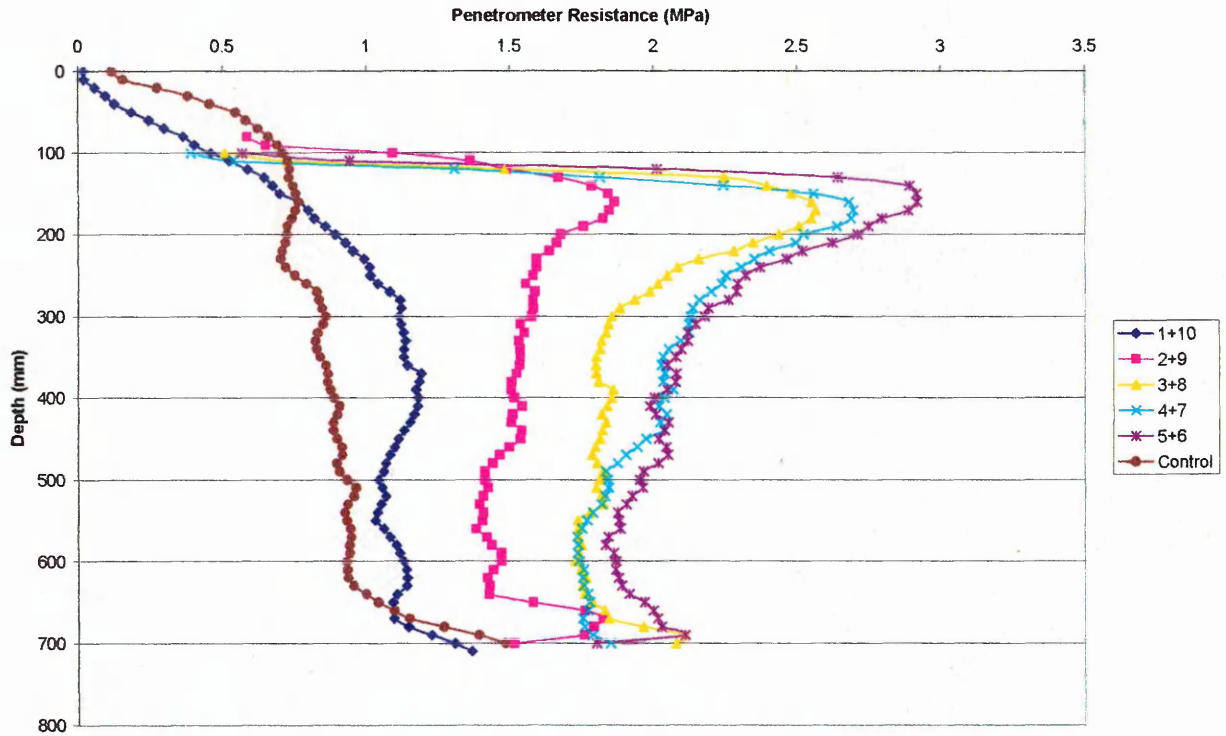
900/10.5/1.9 Stratified Soil



t3/12 Stratified Soil

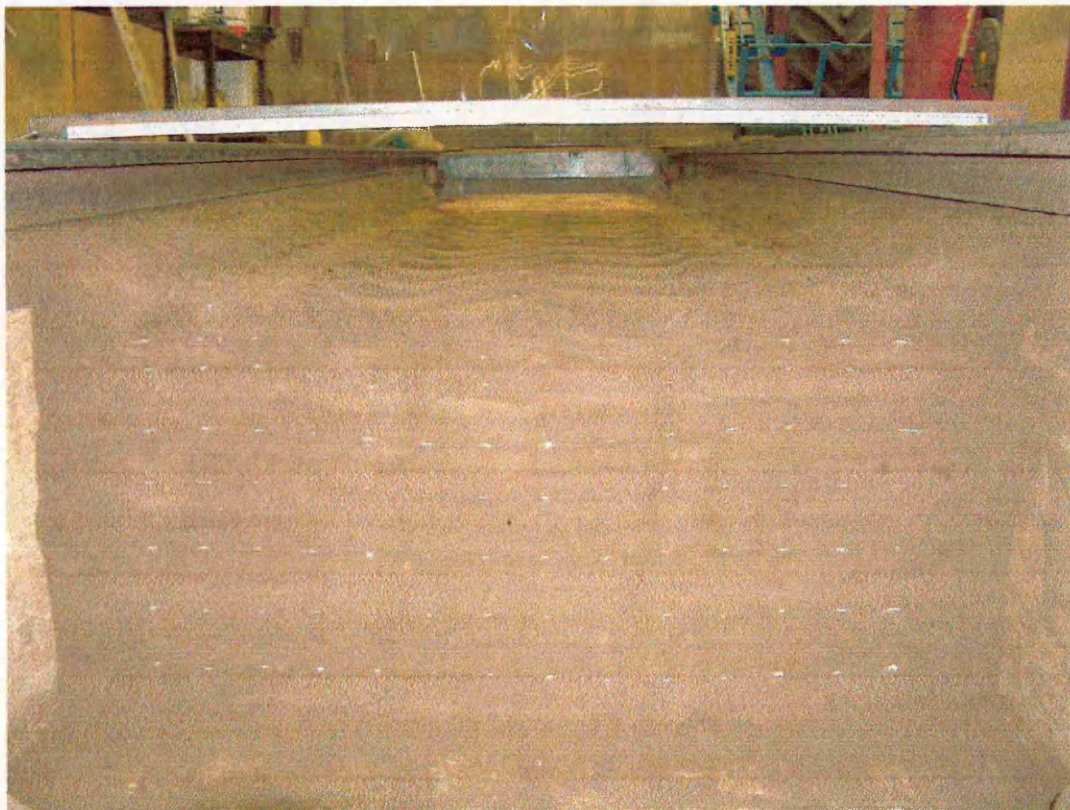


900/10.5/1.9 after two passes

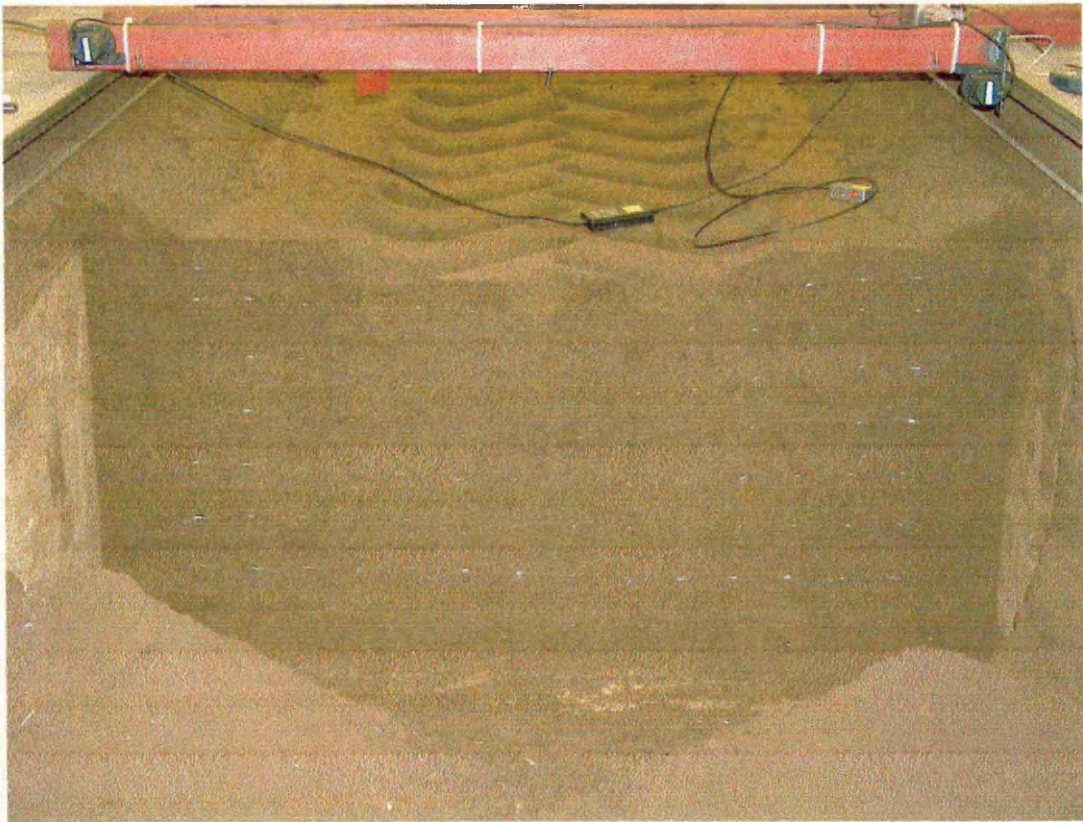


900/10.5/1.9 after three passes

**13.1.2 Soil Profile Pictures**



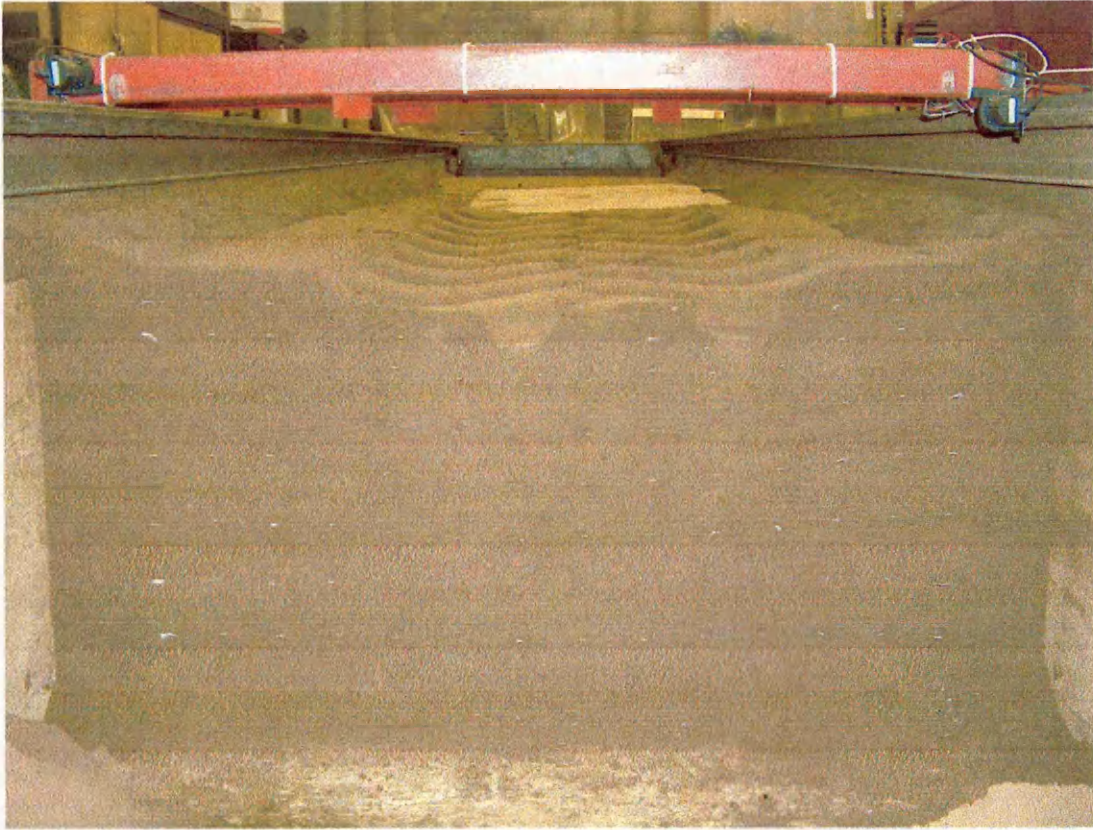
800/8.5/2.5tm



800/8.5/2.5ts



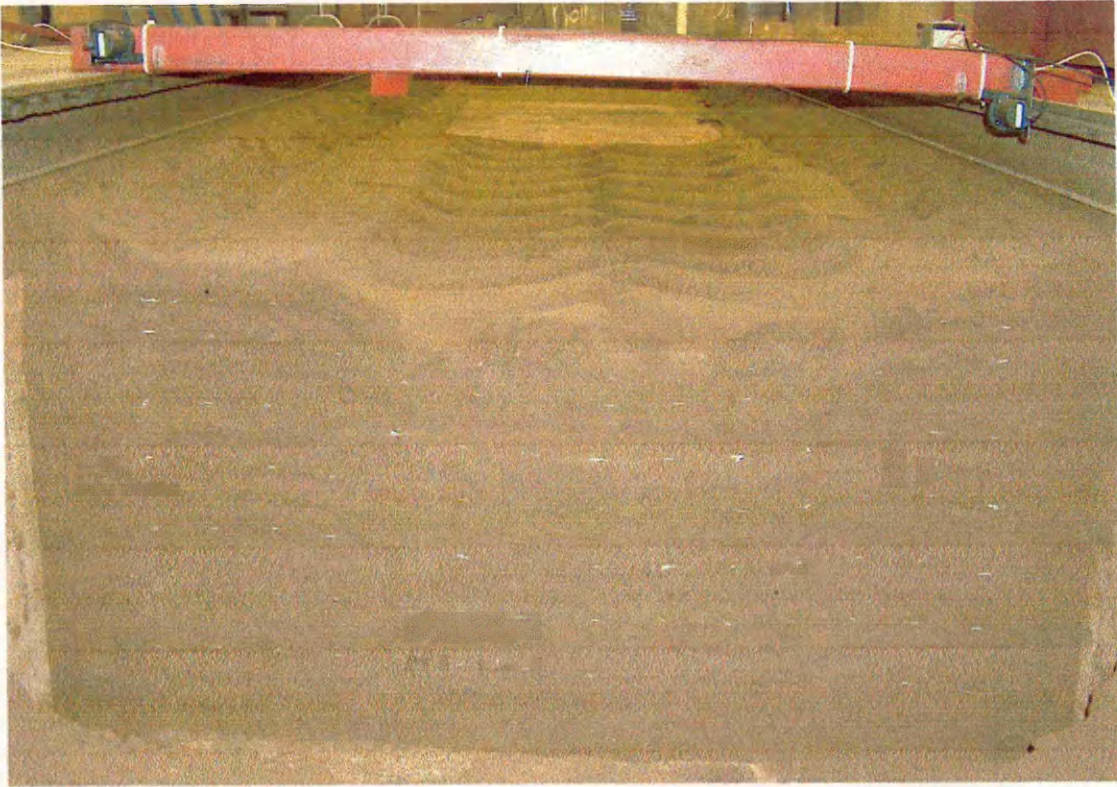
680/10.5/2.2



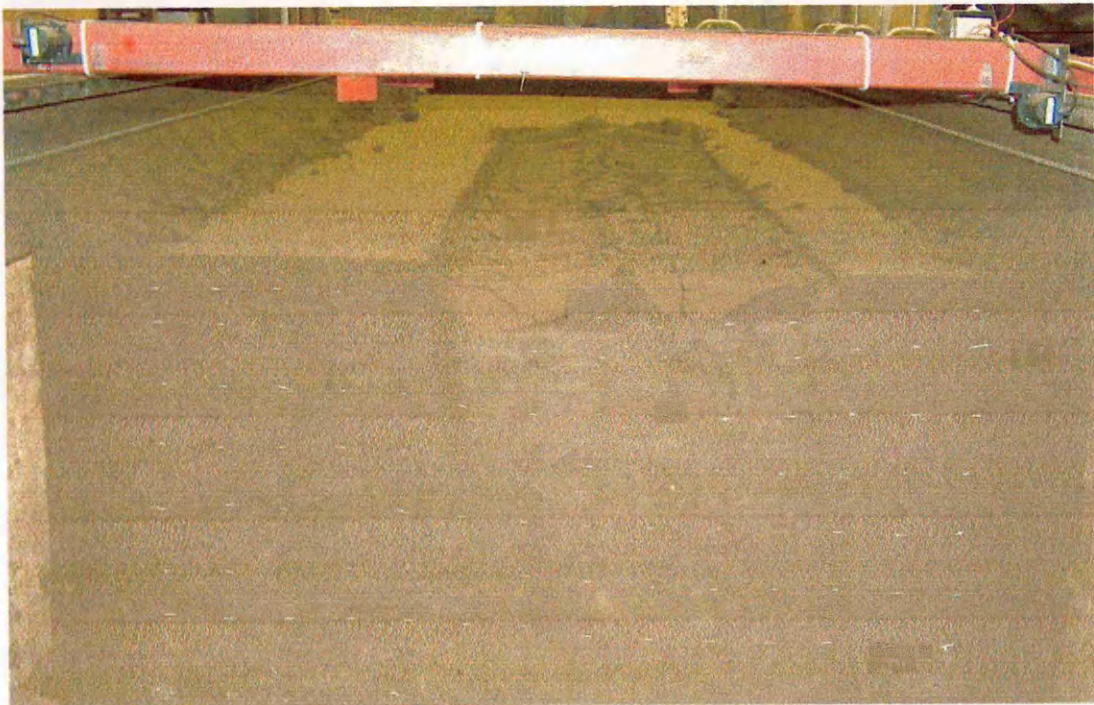
800/10.5/2.5



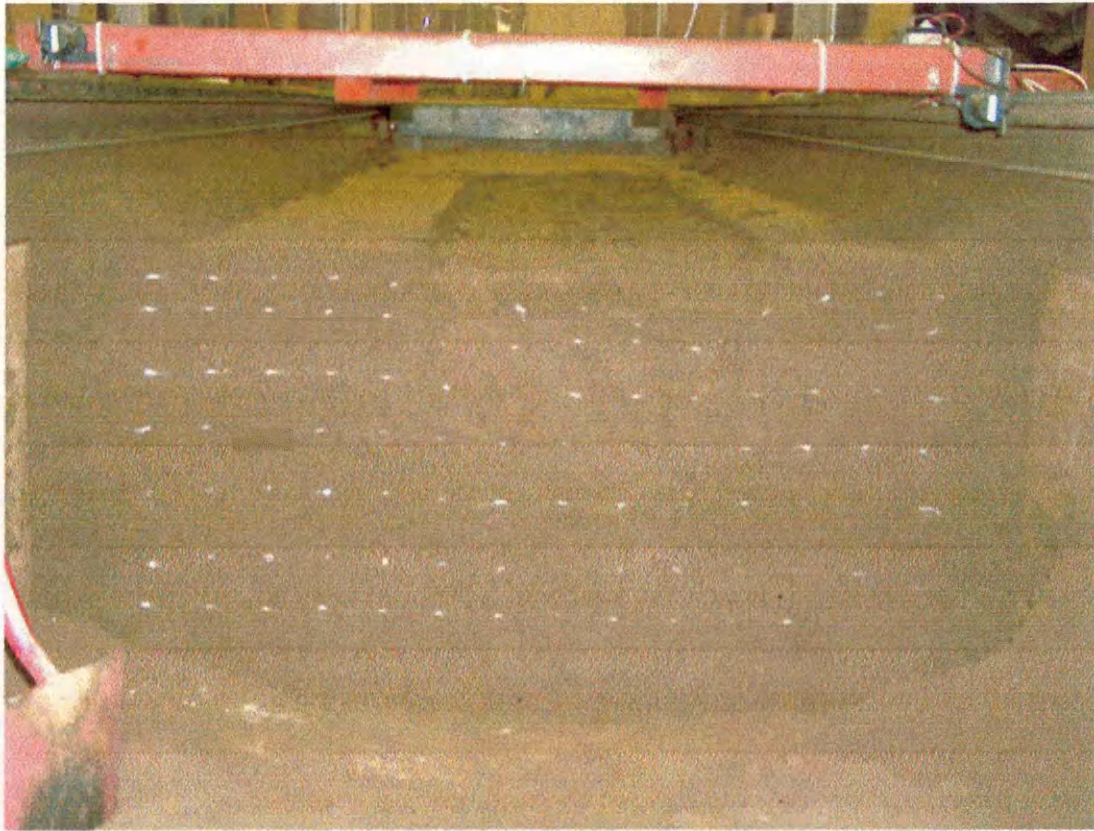
800/10.5/1.25



900/10.5/1.9



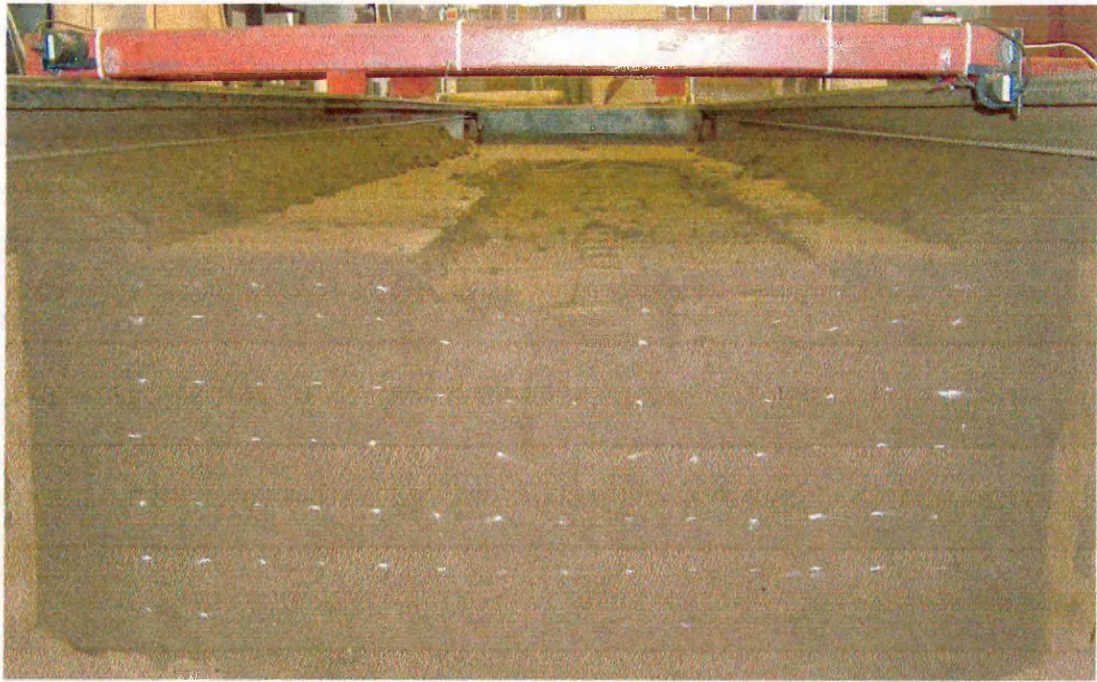
t2/10.5



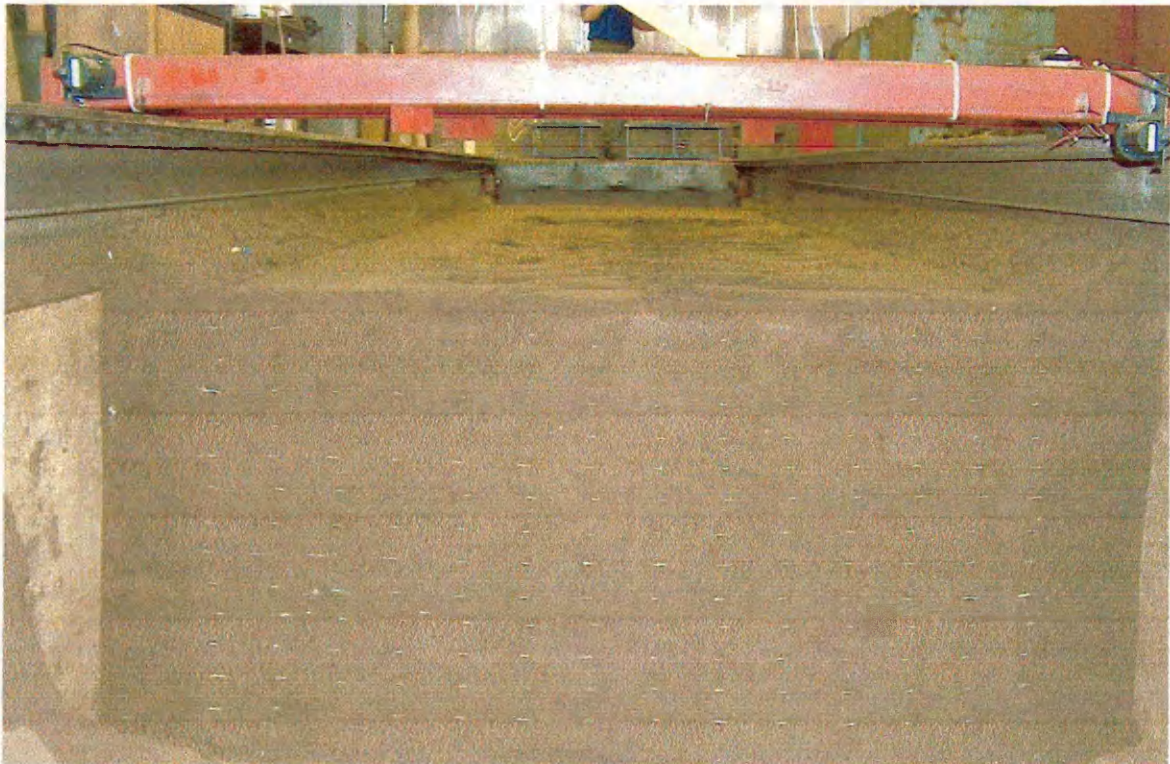
t2/12



t3/10.5

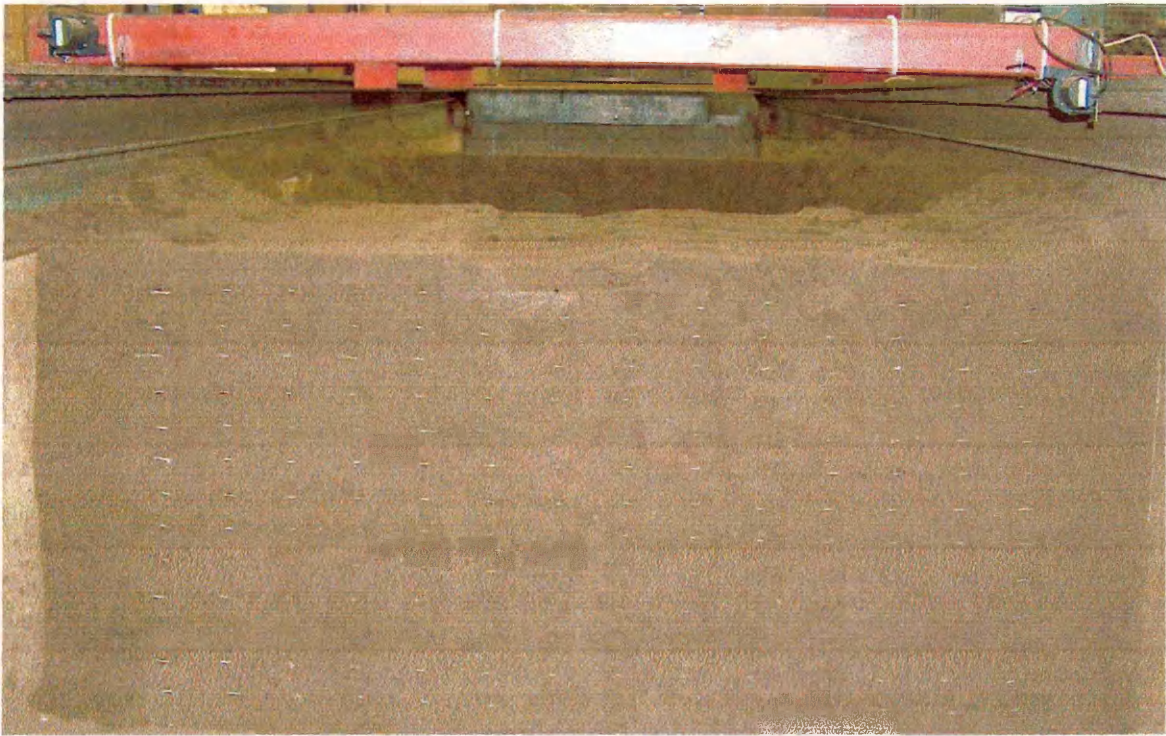


t3/12

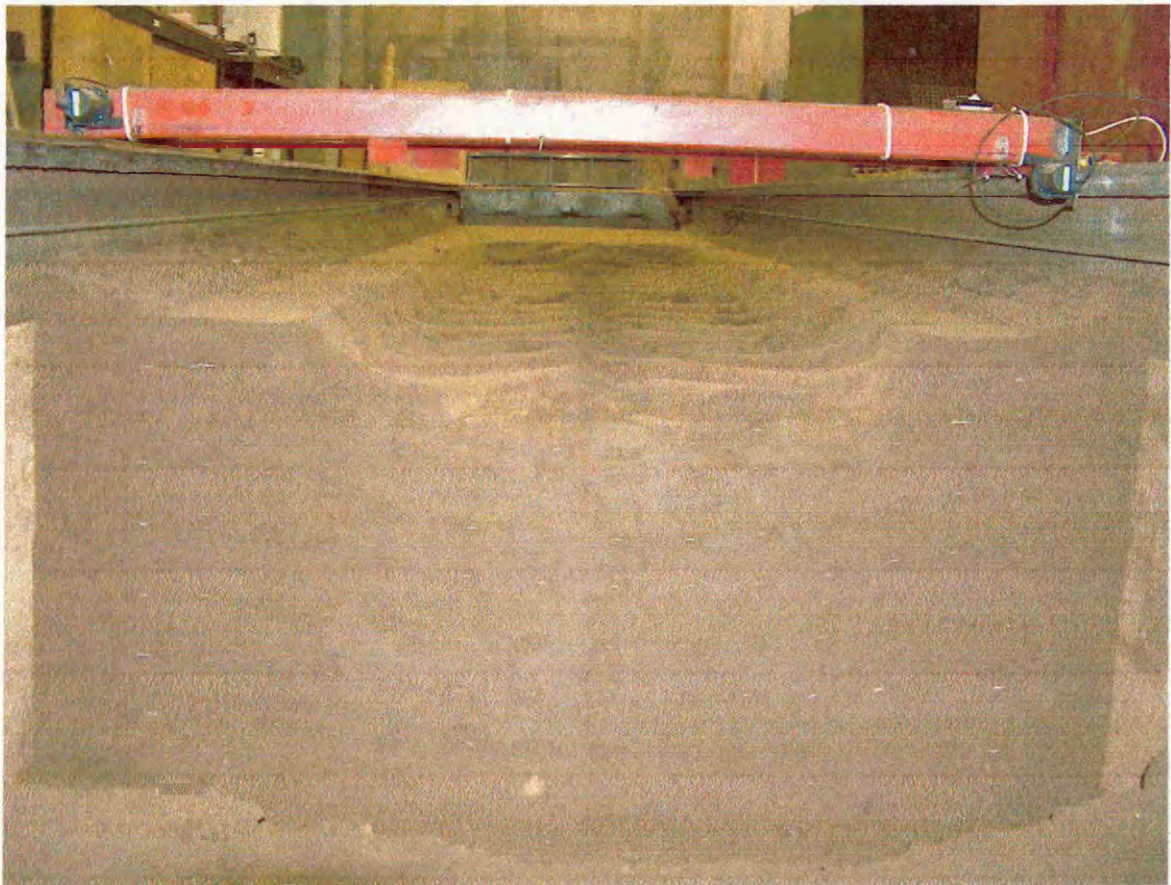


900/10.5/1.9 Stratified Soil



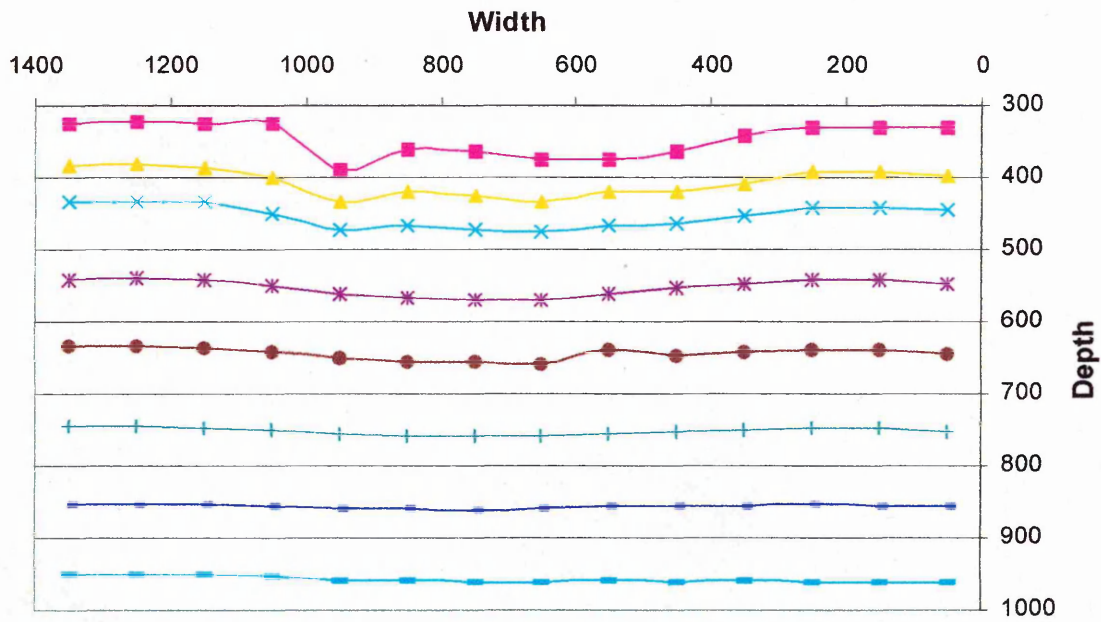


t3/12 Stratified Soil

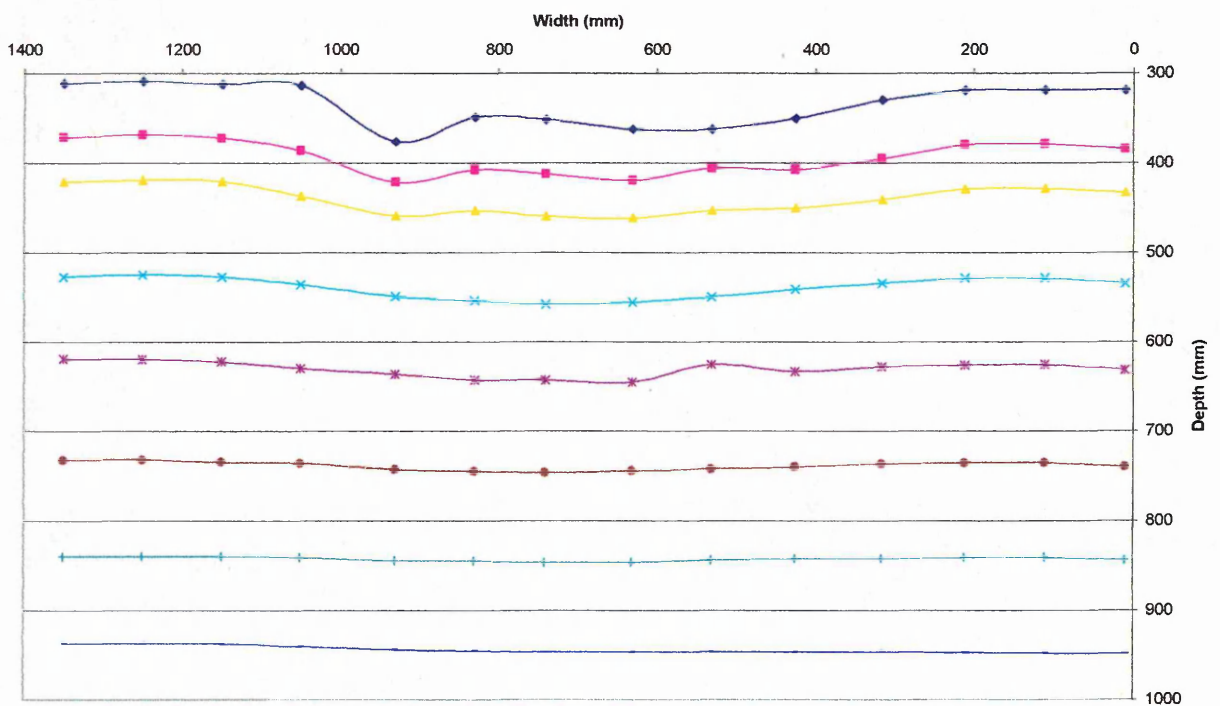


900/10.5/1.9 after three passes

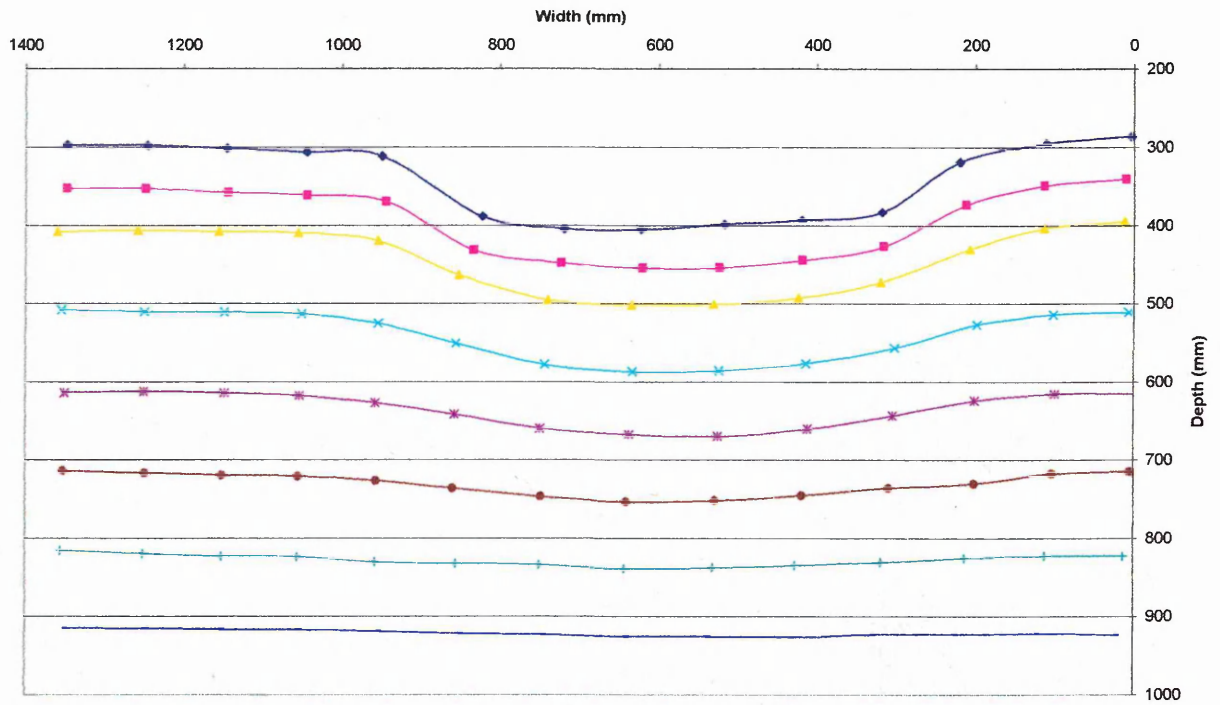
### 13.1.3 Average Soil Displacement Diagrams



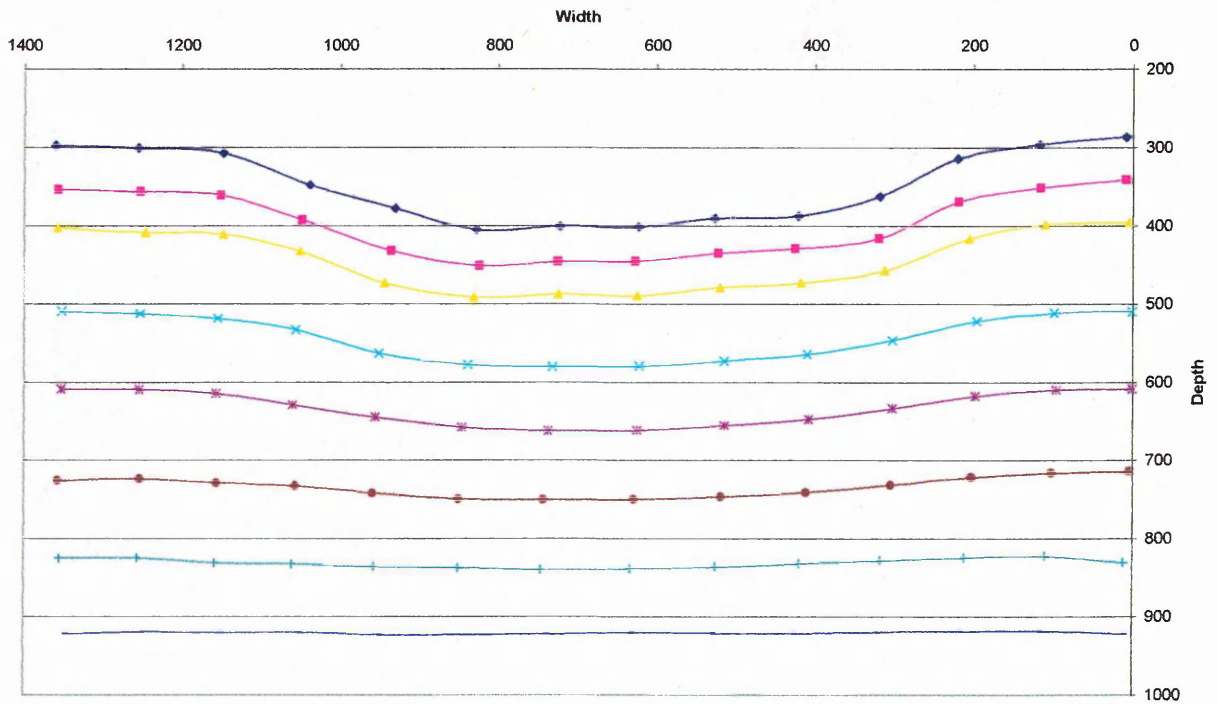
800/8.5/2.5t on medium soil



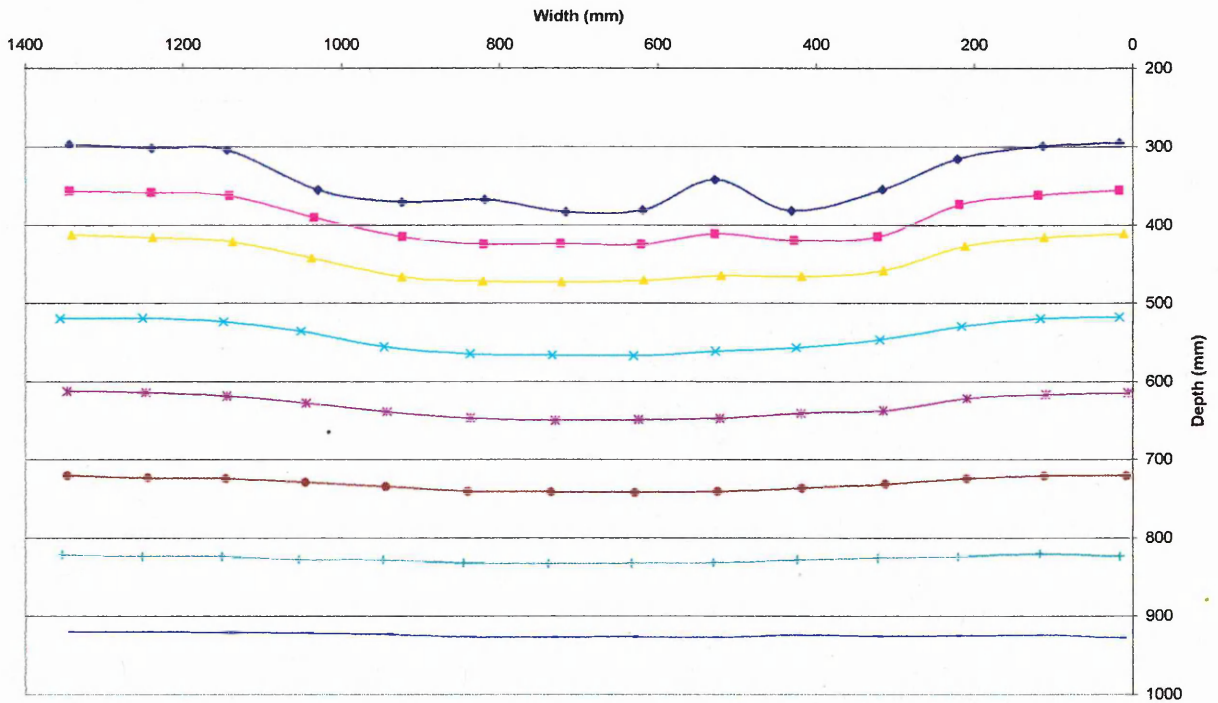
800/8.5/2.5t on soft soil



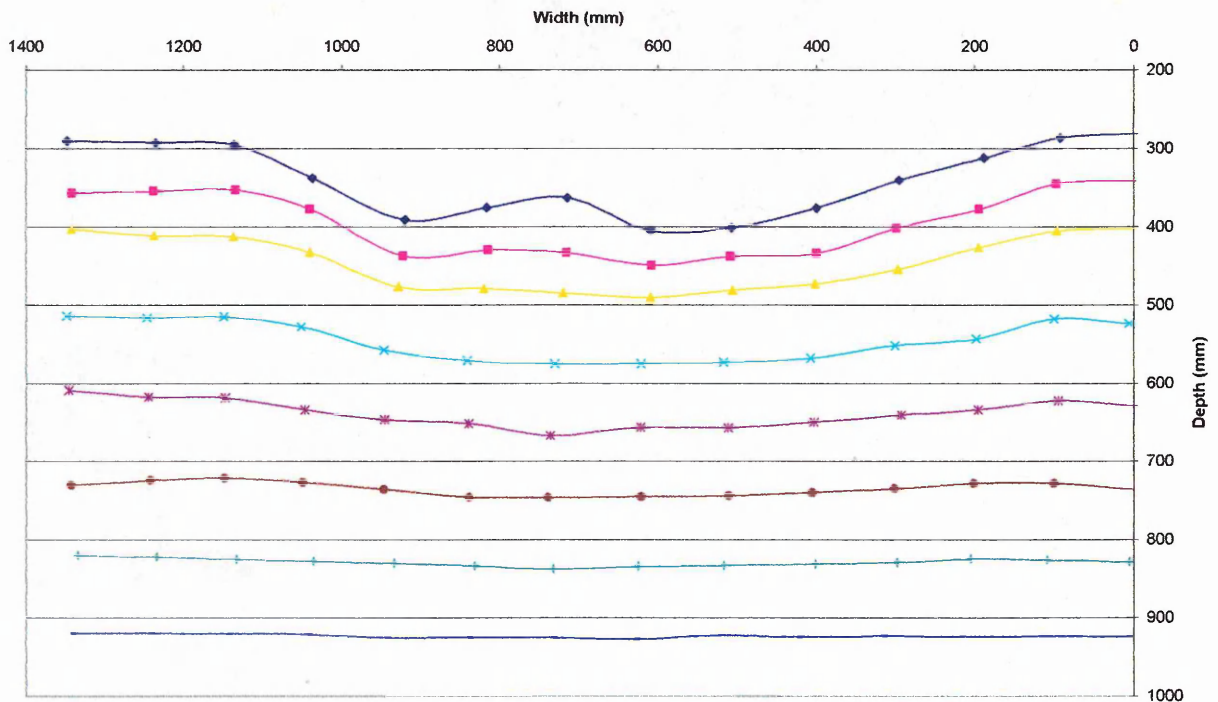
680/10.5/2.2



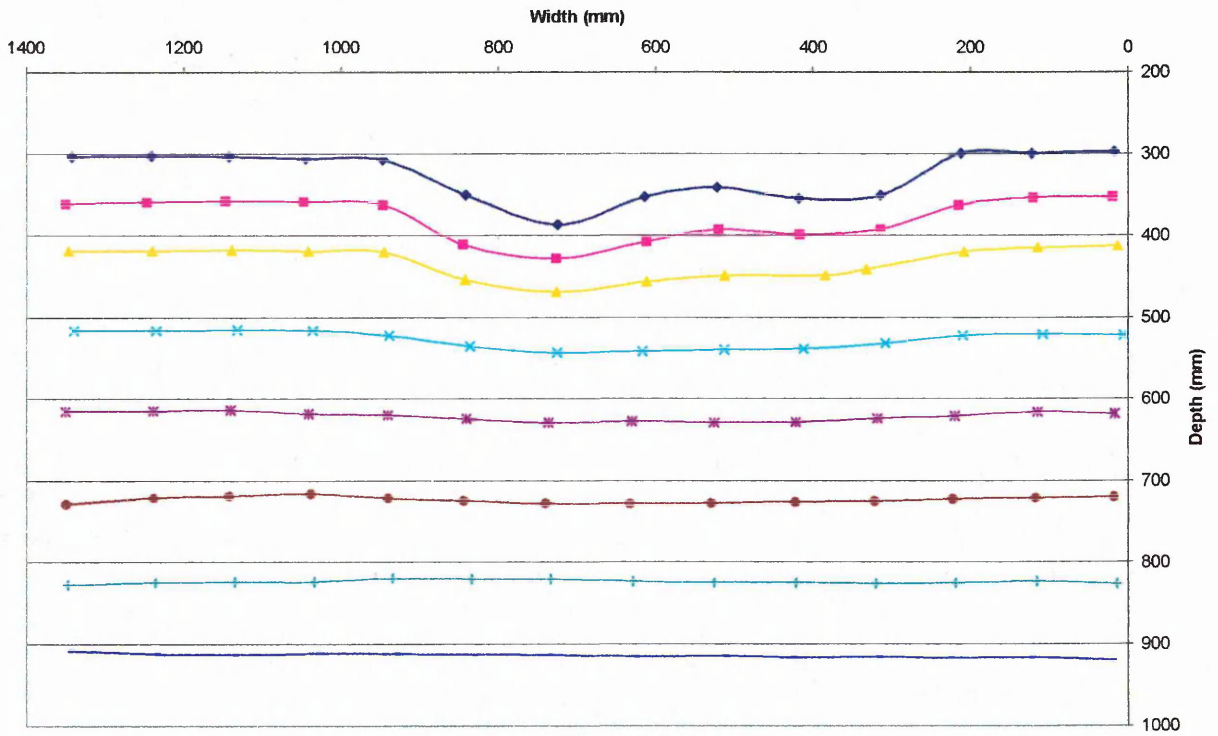
800/10.5/2.5



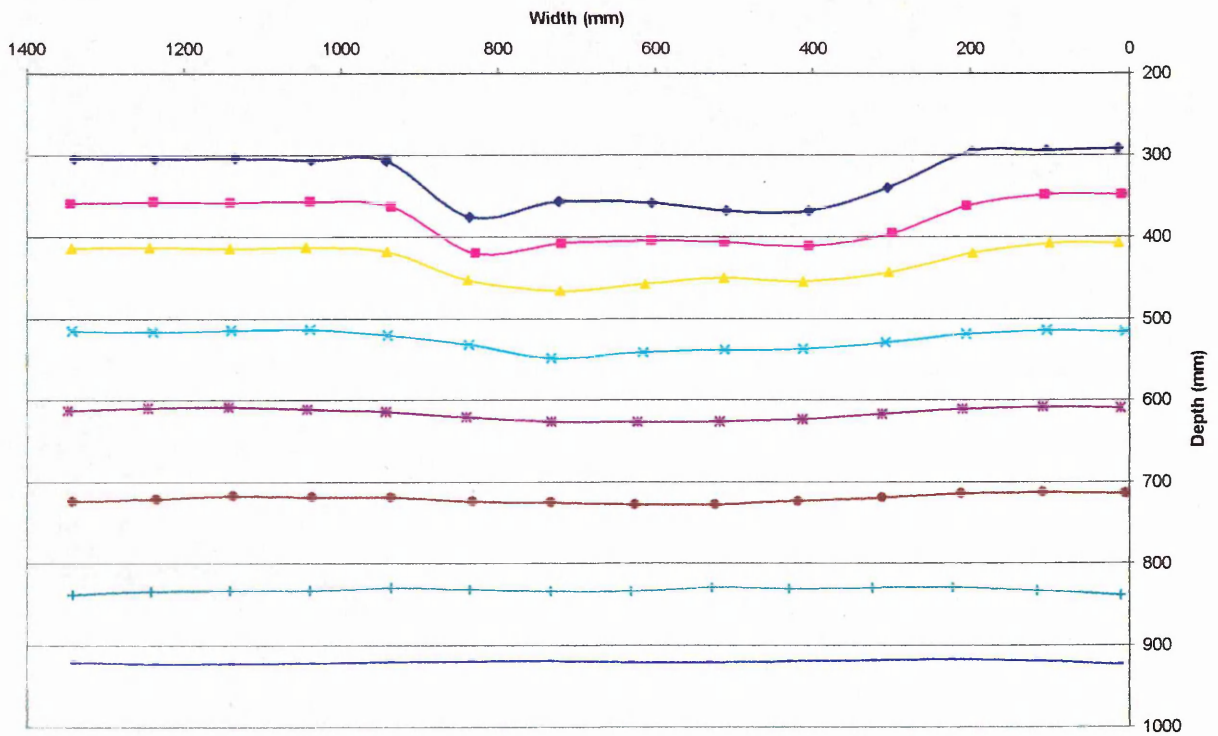
800/10.5/1.25



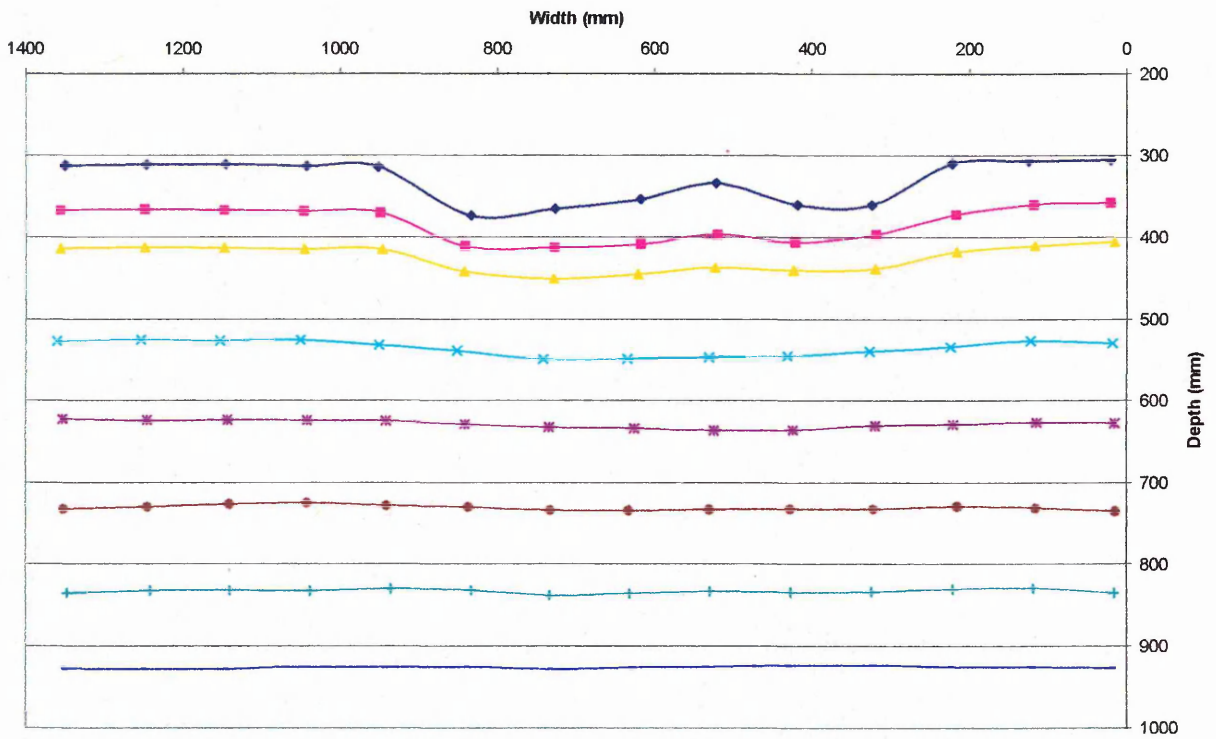
900/10.5/1.9



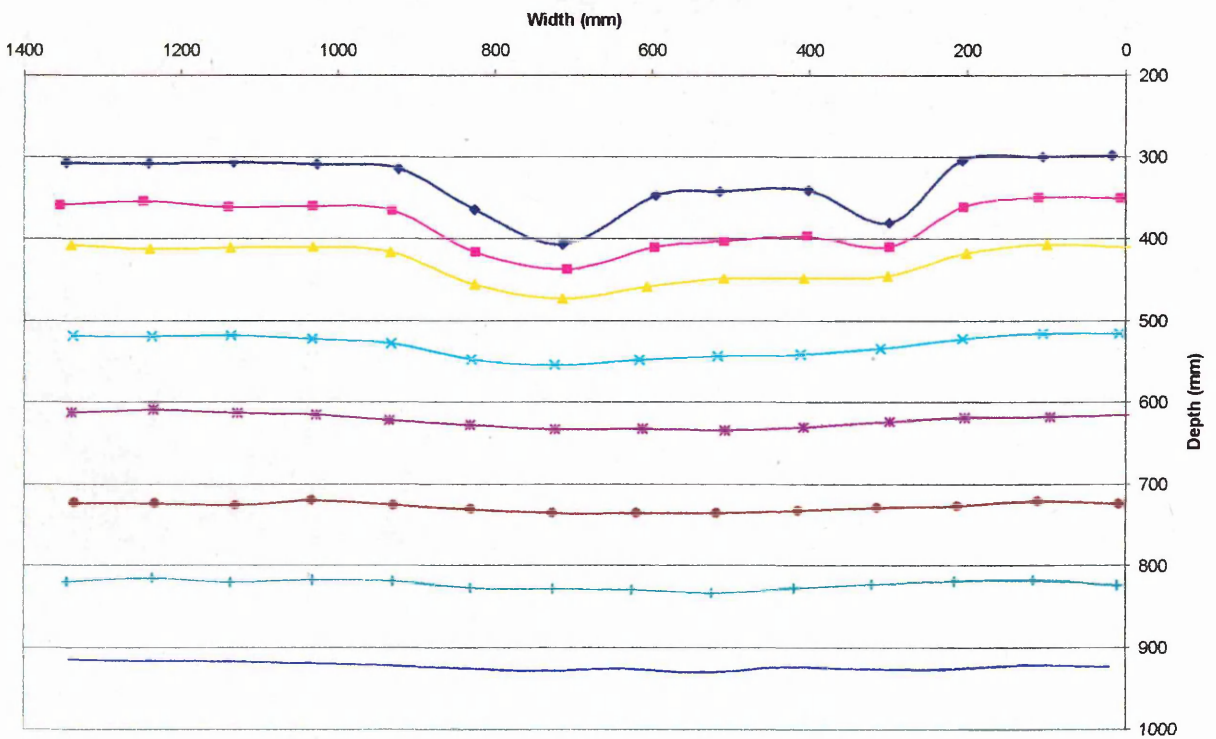
t2/10.5



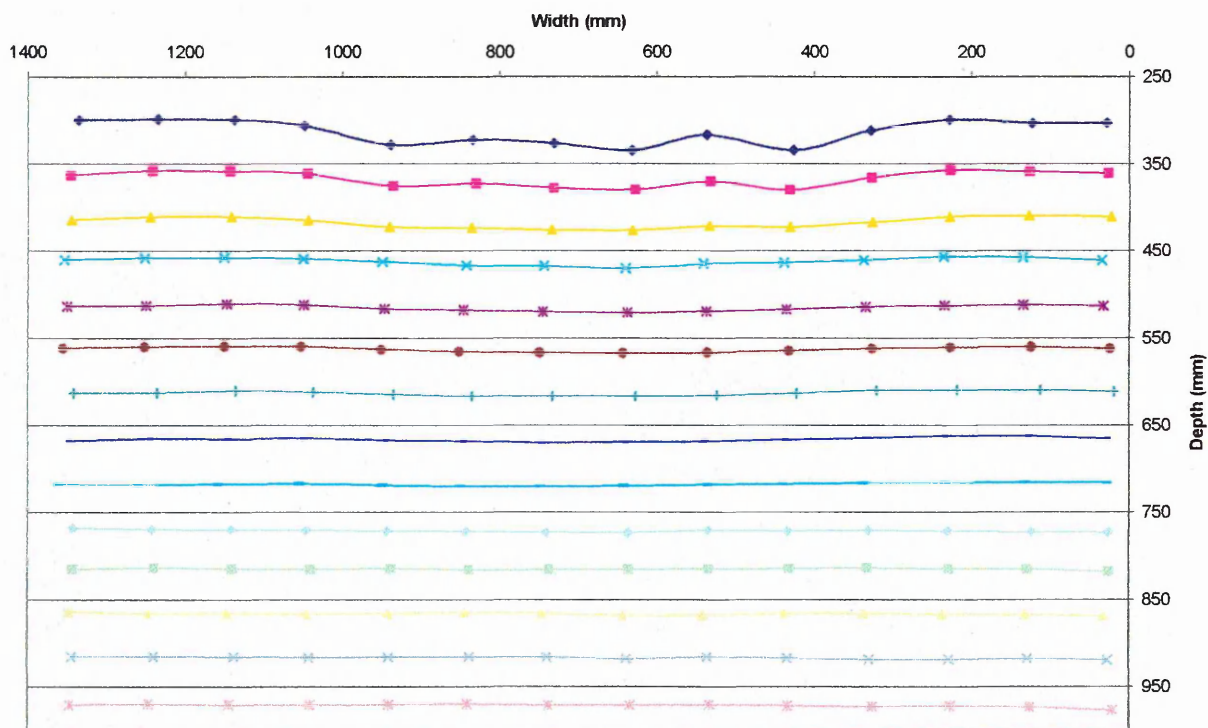
t2/12



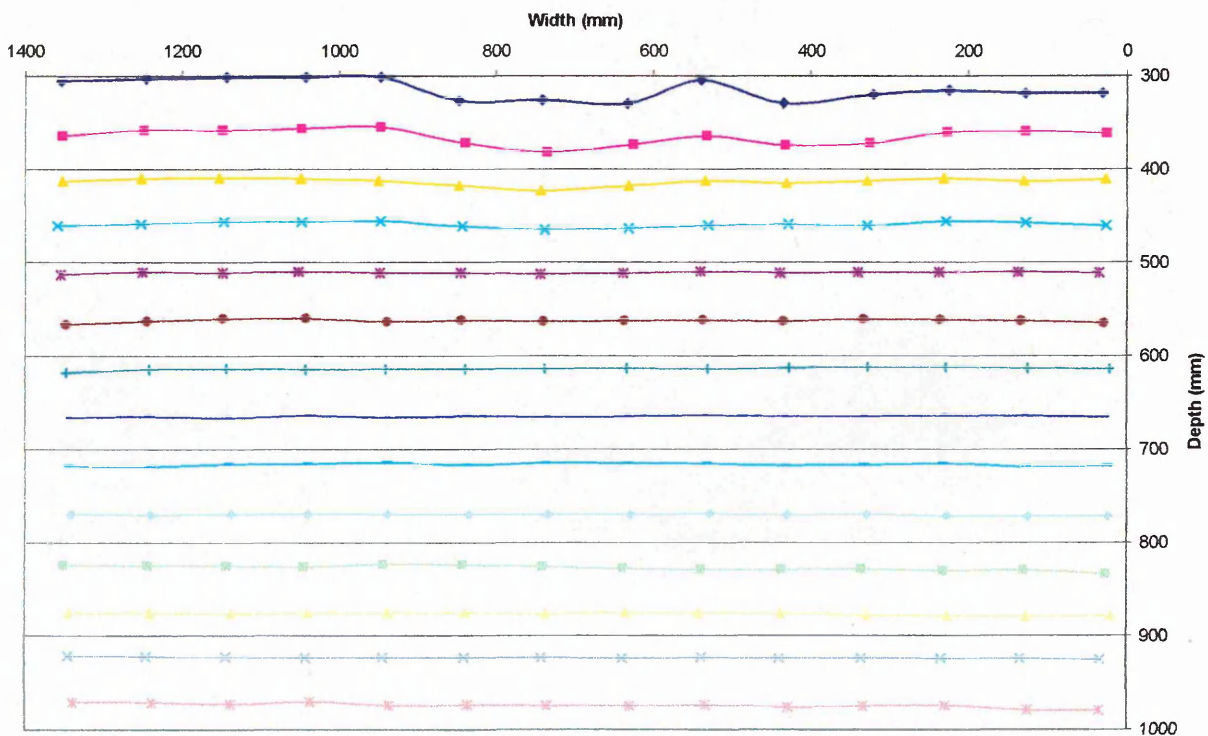
t3/10.5



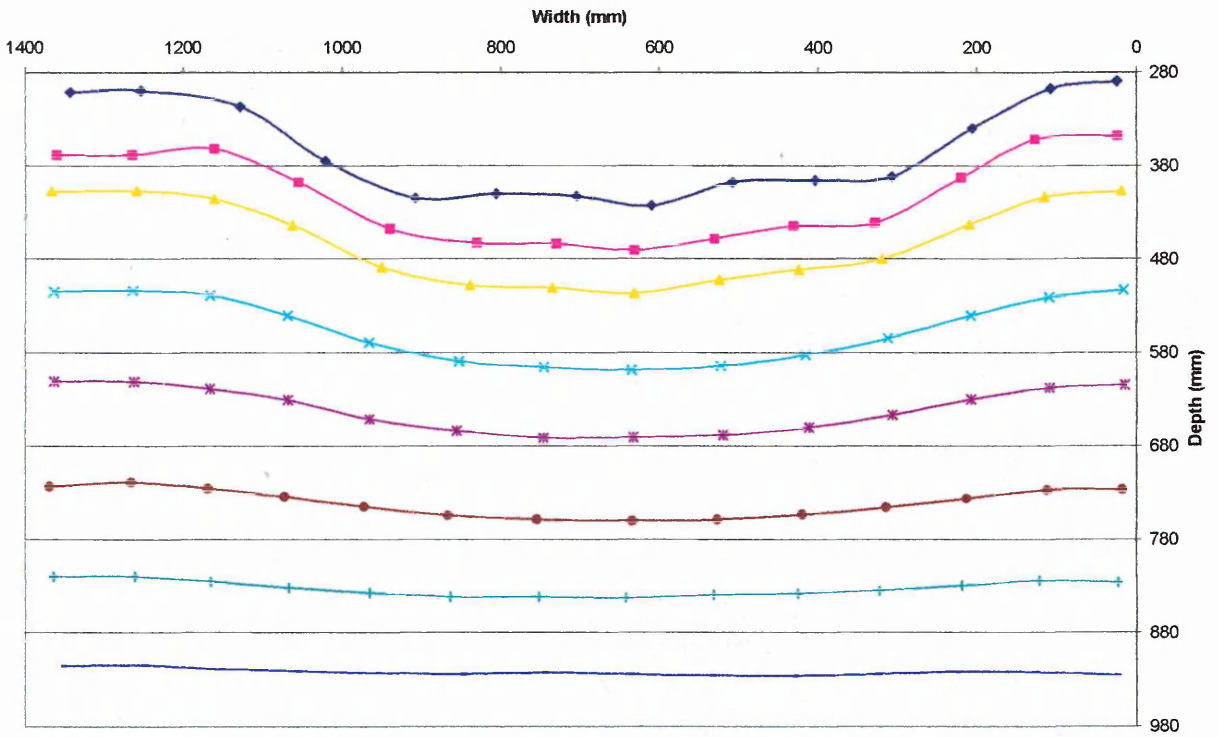
t3/12



900/10.5/1.9 Stratified Soil



t3/12 Stratified Soil



900/10.5/1.9 after three passes



**13.2 Single Wheel and Track Test Frame (submitted as M.Sc. Thesis at University of Hohenheim)**

University of Hohenheim

Master Thesis

Design of a single wheel soil interaction test rig

Dirk Ansorge

Supervisor:  
Prof. Stefan Boettinger

Faculty of Agriculture

Department of Agricultural Engineering

## TABLE OF CONTENTS

LIST OF TABLES .....	133
NOMENCLATURE .....	134
SUMMARY .....	135
1 INTRODUCTION .....	136
2 THE CONCEPT .....	137
2.1 Outline Specifications .....	137
2.2 Single Wheel Testers described in Literature .....	137
2.3 Ideas and Facts Leading to the Present Solution.....	141
3 REQUIREMENTS AND CONDITIONS FOR THE SOLUTION .....	146
3.1 Performance Specifications and Requirements.....	146
3.2 The Solution .....	147
3.2.1 Sinkage.....	147
3.2.2 Weight and its distribution.....	147
3.2.2.1 Hydraulic ram and Torque.....	148
3.2.3 Castors .....	149
3.2.4 Guiders.....	150
3.2.5 Hydraulic System for Load Control.....	150
3.2.5.1 Hydraulic ram .....	150
3.2.5.2 Hydraulic pressure maintaining valve .....	151
3.2.5.3 Hydraulic circuit for the hydraulic ram .....	151
3.2.6 Hydraulic System for Speed Control .....	152
3.2.7 Linear Bearing .....	154
3.2.8 Dimensions .....	156
3.2.9 Track – Wheel Fitting .....	157
3.2.10 Instrumentation .....	159
3.2.10.1 Speed Recording and Slip Calculation .....	159
3.2.10.2 Hydraulic Pressure Recording .....	161
4 STRESS AND STRAIN CALCULATIONS.....	162
4.1 Stress and Strain estimates for choice of Box Sections .....	163
4.2 Stress and Strain in Welds.....	165
4.3 Stress and Strain in Bolts .....	165
4.4 FEA – Results.....	166
4.4.1 Load Box for Plates (759101P04) .....	166
4.4.2 Load Box for Boxes (large) (759102P04) .....	168

4.4.3	Load Box for Boxes (small) (759103P04)	169
4.4.4	Assembly Main Frame (759003A04)	171
4.4.5	Linear Bearing – Axle Bracket (759106/7P04)	172
4.4.6	Wheel – Track Axle Adapter (759108P04)	175
5	DRAWINGS	176
5.1	Main Frame (759002A04)	176
5.2	Main Frame with Load Boxes (759003A04)	178
5.3	Load Box for Plates (759101P04)	179
5.4	Load Box for Boxes (l) (759102P04)	180
5.5	Load Box for Boxes (s) (759103P04)	181
5.6	Guiding Blocks for Back of the Frame (759105P04)	182
5.7	LB – Axle Bracket (759106P04)	183
5.8	Wheel – Track Assembly (759108P04)	184
5.9	Drawbar Bracket (759109P04)	185
5.10	Details of Unequal Ends (759333P04)	186
5.11	Piece to Level Linear Bearing (759111P04)	187
5.12	Piece to level Linear Bearing (759112P04)	188
5.13	Box Section with holes to bolt Linear Bearing on (759113P04)	189
5.14	Wheel Plate to attach Castors (759114P04)	190
5.15	Guiding Blocks (759115P04)	191
5.16	I – Beam (759116P04)	192
5.17	Box Section to close Frame in the Back (759117P04)	193
5.18	Plates to attach Drawbar (759118P04)	194
5.19	Assembly without Linear Bearing and Axle (759003A04)	195
6	PERFORMANCE OF SINGLE WHEEL TESTER	196
6.1	Changing Driving Devices	197
6.2	Applying Loads	198
6.3	Movement	199
7	CONCLUSIONS	201
8	FUTURE RECOMMENDATIONS	202
9	BIBLIOGRAPHY	203
10	ACKNOWLEDGEMENTS	205

## List of Figures

<b>Figure 1:</b>	Mk II Single Wheel Tester at NIAE .....	138
<b>Figure 2:</b>	Non - driven frame attached to soil processor in back .....	139
<b>Figure 3:</b>	Proposed rig solution including wheel and track .....	144
<b>Figure 4:</b>	Endelevation of proposed rig solution .....	145
<b>Figure 5:</b>	Position of load boxes and linear bearing .....	148
<b>Figure 6:</b>	Guider and block to stop castor from swiveling .....	150
<b>Figure 7:</b>	Hydraulic circuit for hydraulic cylinder .....	152
<b>Figure 8:</b>	Power versus time .....	154
<b>Figure 9:</b>	Direction of $M_0$ and $M_x$ on vertical linear bearing rail .....	155
<b>Figure 10:</b>	Front view; lever arm length for moment $M_0$ [Units in m] .....	155
<b>Figure 11:</b>	Top view, lever arm length for moment $M_x$ .....	156
<b>Figure 12:</b>	Axle – Track unit with fitting plate as drawn in 759108P04 .....	158
<b>Figure 13:</b>	PTO Shaft to overcome height difference .....	158
<b>Figure 14:</b>	Encoder for measuring actual wheel speed .....	160
<b>Figure 15:</b>	Fifth wheel for measuring true frame speed .....	160
<b>Figure 16:</b>	Stress 759101P04 [Units in MPa; Deformation scale 1:1] .....	167
<b>Figure 17:</b>	Static displacement 759101P04 [Units: mm; Deformation scale 1:40] .....	167
<b>Figure 18:</b>	Stress 759102P04 [Units in MPa; Deformation scale 1:1] .....	168
<b>Figure 19:</b>	Static displacement 759102P04 [Units in mm; Deformation scale 1:164].	169
<b>Figure 20:</b>	Stress 759103P04 [Units in MPa; Deformation scale 1:1] .....	170
<b>Figure 21:</b>	Static displacement 759103P04 [Units in mm; Deformation scale 1:242].	170
<b>Figure 22:</b>	Stress 759003A04 [Units: MPa; Deformation scale: 1:1] .....	171
<b>Figure 23:</b>	Static displacement 759003A04 [Units: mm; Deformation scale 1:1] .....	172
<b>Figure 24:</b>	Stress 759111P04 before modification .....	173
<b>Figure 25:</b>	Static displacement 759111P04 before modification .....	173
<b>Figure 26:</b>	Stress 759111P04 after modification .....	174
<b>Figure 27:</b>	Static displacement 759111P04 after modification .....	174
<b>Figure 28:</b>	Pressure in hydraulic ram during a typical run .....	198
<b>Figure 29:</b>	A typical speed curve of the wheel (blue) and the frame (pink) in a run ...	199

**List of Tables**

**Table 1:** Sizes of wheels and tracks used in soil bin investigation at CU@S..... 137

**Table 2:** Single Wheel Tester Characteristics ..... 140

**NOMENCLATURE**

## Abbreviations:

a	Acceleration
F	Force
FEA	Finite Element Analysis
I	Moment of Inertia
m	Mass
M	Torque
P	Power
PTO	Power Take Off
t	Time
v	Speed
W	Section Modulus

## Units:

h	Hour
J	Joule
l	Liter
m	Meter
m <sup>2</sup>	Square Meter
m <sup>3</sup>	Cubic meter
N	Newton
Pa	Pascal
s	Second
W	Watt

## Factors:

Mega (M)	10 <sup>6</sup>
Kilo (k)	10 <sup>3</sup>
centi (c)	10 <sup>-2</sup>
milli (m)	10 <sup>-3</sup>
micro (μ)	10 <sup>-6</sup>

## SUMMARY

The task of this thesis work was to design a machine, which allows different loads to be applied onto a wheel or track, which can in turn be used to study soil compaction in the soil bin of the National Soil Resources Institute at Cranfield University at Silsoe, UK.

The rig constructed in this thesis transfers a force onto a wheel or track axle by using a hydraulic ram. Thus wheel or track loads can easily be changed as the load is a function of the pressure applied to the hydraulic ram. The hydraulic ram is also used for lowering the wheel and track down to the surface of the soil in the bin as well as lifting it out again. Wheels and tracks can be exchanged or removed through the back of the frame of the rig. In this rig the loading weights for supplying the counterforce of the ram are spread over the frame and thus can stay there when the wheels are changed.

The wheels and tracks are self propelled using a hydraulic motor and pump driven by a combustion engine placed outside of the soil bin.

Forces and torques developing from the movement of the wheel and track are taken up by the linear bearing. This prevents any weight transfer as the linear bearing is essentially frictionless in the vertical direction.

Changing the equipment from wheels to tracks is achieved by removing the final reduction of the axle and replacing it with an adapter to compensate for the height difference and the different pitch circle diameters of the axle and the track. The height difference occurs as the axle stays in the same position for both wheel and track to ensure the same maximum sinkage for both devices. The PTO shaft from the gear box to the track is also able to overcome the height difference as it can be operated at a maximum angle of 35 degree, whereas only 31 degrees are necessary to adapt to the track.

## 1 INTRODUCTION

Many field investigations have been performed to detect the influence of wheeled farm machinery on soil compaction and particularly subsoil compaction. Some laboratory investigations were carried out, as well. Only a few investigations comparing tracked and wheeled vehicles were done in field. A good summary can be found in Horn et al., 2000. So far, to the knowledge of the author there were no investigations into the effects of loads heavier than 50 kN on soil compaction in controlled laboratory conditions using self propelled wheels and tracks.

A recent discussion in Germany concerning the restriction of maximum wheel load allowed for vehicles on fields with missing data shows the importance and necessity of scientific work in this area. In case wheel load would be restricted to 3000 kg as it is discussed, this would affect the whole agricultural machinery production as many agricultural vehicles exceed this load (Kutzbach, 2000). Soil can be severely compacted when being worked in inappropriate conditions and there is no doubt about the influence of soil compaction on yield (Eriksson et al. 1974). However a mere restriction of wheel load can not be an answer as soil compaction depends on load distribution as well (Grecenko, 2003).

A project at Cranfield University at Silsoe (from now on CU@S) aims to study compaction by such loads in a soil bin using different wheels and tracks, while recording bulk density, soil deformation, and cone resistance during the investigations. In order to be able to analyze and to model the influence of an axle load of 240 kN on subsoil compaction either a rig had to be built or an existing one could be modified. The design or modification of this rig is presented in this Master Thesis. The subsequent investigations will be submitted as Master of Science by Research Thesis at Cranfield University at Silsoe and can be found in Appendix 1. These investigations are done in a controlled soil bin environment as soil inhomogeneities in fields have a significant influence on soil behavior.

Splitting up the project in two master theses is possible due to the existing Double Degree program between the University of Hohenheim and Cranfield University at Silsoe.



## 2 THE CONCEPT

### 2.1 Outline Specifications

The outline specifications are:

- ability to propel wheels and tracks specified in Table 1
- transfer of up to 12000 kg onto the wheel or track unit
- the single wheel tester has to fit in the existing soil bin at CU@S

**Table 1:** Sizes of wheels and tracks used in soil bin investigation at CU@S

	Wheel 1	Wheel 2	Wheel 3	Track length / width
Size	680/85 R32	800/65 R32	900/65 R32	3000mm / 635mm

The conceptual design phase is totally discussed in section 2.3. The final solution is presented in section 3.2.

### 2.2 Single Wheel Testers described in Literature

Single wheel testers have been built at various places, like at the National Institut of Agricultural Engineering, UK (NIAE); at the National Tillage Machinery Laboratory, USA (NTML); at the Department of Agricultural Engineering, University of California, USA; at the Instituut voor Mechanisatie, Arbeid in Gebouwen (IMAG) in the Netherlands; at the National Soil and Resources Institute, CU@S, UK (NSRI), at the University of Hohenheim, Germany, and in Israel.

One of the first single wheel testers with no weight transfer and direct measurement of wheel force and tractive force was the NIAE single wheel tester built in 1952 (Bailey, 1954). Using a parallel linkage to make sure no weight transfer can occur from the tested wheel onto the main frame of the machine was a large step forward and ensured constant weight on the tested wheel. Unfortunately this solution caused instantaneous loadings of the wheel due to the inertial forces when accelerating the tested wheel and the mass ap-

plied to it (Bailey, 1954). Inertial forces result from acceleration of any mass and contribute to the balance of forces during the acceleration. This single wheel tester was surpassed by the NIAE Mk II single wheel tester, shown in **Figure 1**, which allowed using larger tires and applying higher weights (Billington, 1973). Still the inertial force problem was not overcome.



**Figure 1:** Mk II Single Wheel Tester at NIAE

A single wheel tester using a hydraulic ram to apply the vertical load instead of directly placing the weight on top of the wheel/axle was designed at the NTML (Burt et al., 1980). A further single wheel tester applying the vertical load hydraulically was built at the Department of Agricultural Engineering at the University of California (Upadhyaya et al., 1985). These two machines did not have to overcome inertial forces as weight was applied hydraulically.

All rigs built at NSRI for testing agricultural tires were designed for pulling as the non-driven frame shown in **Figure 2**. In the other solutions mentioned before the wheels and tracks were self propelled, using either electrical power or hydrostatic drives.

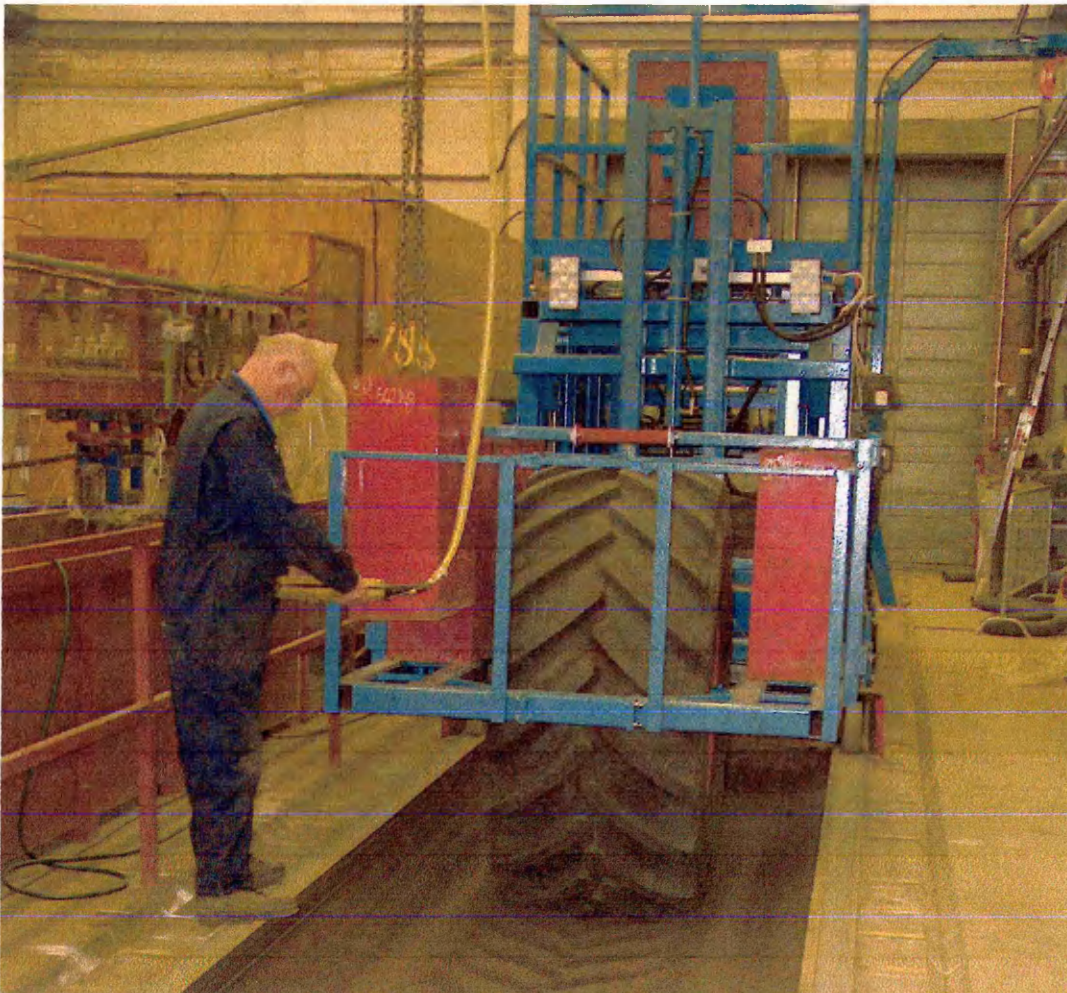


**Figure 2:** Non - driven frame attached to soil processor in back. Soil bin of CU@S

Single wheel testers investigating tire performance with regard to traction and or slip angle were built at the NIAE by Mc Allister (1979) and Lines and Young (1989), at the University of Hohenheim by Armbruster (1991) and Barreilmeyer (1996), in Isreal by Shmulevich et al. (1994) and at the NSRI by Oliver (2002).

A general overview of the single wheel testers reported in this chapter, the author, the place where they were built, the main application, weight transfer and maximum tire diameter as well as width (if known) is given in

**Table 2** (nn = not known).

All mentioned single wheel testers are only useable for application of smaller loads than the ones aimed for in this NSRI project now. Therefore no existing single wheel tester found in literature could have been used without major modifications for these investiga-

tions. One idea for using an existing single wheel tester and modifying it was to use the MK II single wheel tester (**Figure 1**), especially as the NIAE and NSRI are locally close together and share a good relationship. However, as this device would have had to be largely modified as well because the specifications for weight application are not met, the decision was made to construct a new one.

**Table 2:** Single Wheel Tester Characteristics

Author	Place	Application	Max. Weight Transfer [kN]	Max. Tire Diameter / Width (if given) [mm]
Bailey (1954)	NIAE	Traction / Soil Compaction	~ 10	~ 1300
Billington (1973)	NIAE	Traction / Soil Compaction	~ 30	~ 1600 / ~ 500
McAllister (1979)	NIAE	Slip Angle / Traction	35	940
Burt et al. (1980)	NTML	Traction / Soil Compaction	44	~ 1800 / ~ 775
Upadhyaya et al. (1985)	Dep. of Ag. Eng. University of California, USA.	Traction / Soil Compaction	26.7	2000 / 1000
Lines and Young (1989)	NIAE	Suspension of Tires	11	1800 / 500
Armbruster and Kutzbach (1989); Barrelmeyer (1996)	Dep. of Ag. Eng. University of Hohenheim, Germany.	Traction, Soil Compaction, Slip Angle	40	2000 / 1200
Shmulevich et al. (1994)	Israel	Traction / Soil Compaction	Nn	nn
Oliver, 2002	NSRI	Traction	5	600
Brassart, 2005	Michelin, France	Traction	Nn	nn

### 2.3 Ideas and Facts Leading to the Present Solution

The former solutions at NSRI mentioned in 2.2 all place the weight directly onto the wheel axle. The advantage of these solutions are an easily controllable amount of weight which is being applied to the wheel, a simple frame construction, and no hydraulic components.

However, all former rigs using agricultural tires at NSRI have not been self propelled. When the rig is self propelled with the weight placed directly above the axle the disadvantage of the inertial forces of the weight when accelerating the rig appears as mentioned by Bailey (1954). Thereby the position of the center of gravity of the weights also plays a role. A position close to the center of the axle is ideal. Unfortunately under the given conditions the center of gravity of the weight can never be in the center of the axle as this would cause interferences with soil bin depth and expected rut depth. The further the weight is away from the center of the axle, the longer the lever arm will become and in consequence the torques by inertial forces will increase. These reactions will cause an unsteady movement of the rig and thus inhomogeneous soil compaction along the soil bin. The second disadvantage are the additional construction elements being necessary to take out these inertial forces and torques. These problems and their consequences led to the idea of placing the weight onto an independent frame and transferring the load to be applied onto the wheel or track hydraulically. This means using the concept introduced by Burt et al. (1980) and Upadhyaya et al. (1985). Thereby a hydraulic pump supplies a hydraulic cylinder connecting frame and track/wheel axle permanently with the required pressure. Pressure adjustment will take place with a pressure maintaining valve. The accuracy of the particular pressure maintaining valve used is +/- 1% (Riley, 2004). For the required weight of 12000kg this was regarded as sufficient. A further advantage when transferring the load hydraulically is the fact that different loads can be applied easily by varying the hydraulic pressure as long as the main frame weight is not exceeded. Changing wheels and tracks can also be done in a convenient way as compared to former solutions since all the weight can stay on the frame during this process. The weight and frame are supported by castors rolling on the rail of the soil bin during and after the investigations. Castors are used because they can be used on the rails over the soil bin as well as outside.

Power supply for both wheel and track will be achieved with a common combine harvester axle, its hydraulic motor and gear box. This solution was approached after realizing that all other ideas (i.e. putting a hydraulic motor and a gear box to an axle, propelling the wheel somehow with a drive shaft) would result in a new construction doing the same as a common driven axle with these devices. So it was easier to use and modify a standard combine harvester axle. As the axle requires hydraulic power to be driven, a hydraulic power pack has to be added to the system. The obvious solution was to use an available power pack with a Perkins 6354 engine placed outside of the soil bin and being hydraulically connected. In connection with the hydraulic circuit for the ram there is the possibility of having one common or two separated hydraulic systems. In order to keep pressure fluctuations inside the hydraulic ram as small as possible and to be entirely independent of the driving system of the frame it was decided to split it up in two independent systems. So the power pack will drive the frame and a second hydraulic power supply will drive the hydraulic ram.

As the weight is applied only on that side of the wheel where the axle is placed, a torque develops as the vertical input force is not directly above the center of the tire. This torque as well as the forward force have to be taken out of the system. The axle has to be connected somehow to the main frame as well to direct the vertical movement. The use of a linear bearing enables all of these requirements to be met. This linear bearing acts in the same way as a parallel linkage, for example used by Bailey (1954). As the linear bearing moves vertically nearly frictionless no weight transfer from the wheel onto the main frame can happen. The advantage of the linear bearing with respect to a parallel linkage is the reduced space necessary. The only disadvantage of the linear bearing is its cost as it is more expensive than a parallel linkage. However, there is a linear bearing available from a former project thus there are no additional costs. So the decision was made to use the existing linear bearing. The main frame of the linear bearing was placed parallel to the soil bin as placing it orthogonally would require a more rugged component connecting axle and linear bearing to transfer forces and the torque. Fitting the linear bearing into the rig frame would as well be more difficult because of its width and depth.

The loading weight will be split up in several parts and placed at different positions on the rig frame ensuring, that enough mass can be applied in the investigations. As weight existing 500 kg load boxes and existing 1000 kg load plates will be used.

Endelevation of the proposed rig solution is shown in **Figure 4**. **Figure 3** shows a plain view of the proposed rig solution including weight boxes, linear bearing, linear bearing axle connection, axle, engine, and track as well as wheel. For an explanation of placing the weights see 3.2.2. During the process of construction it was decided to take the engine off the rig and place the power pack outside the building. This decision was made due to health and safety issues and the difficulty in waste air removal and as it was easier to realize.

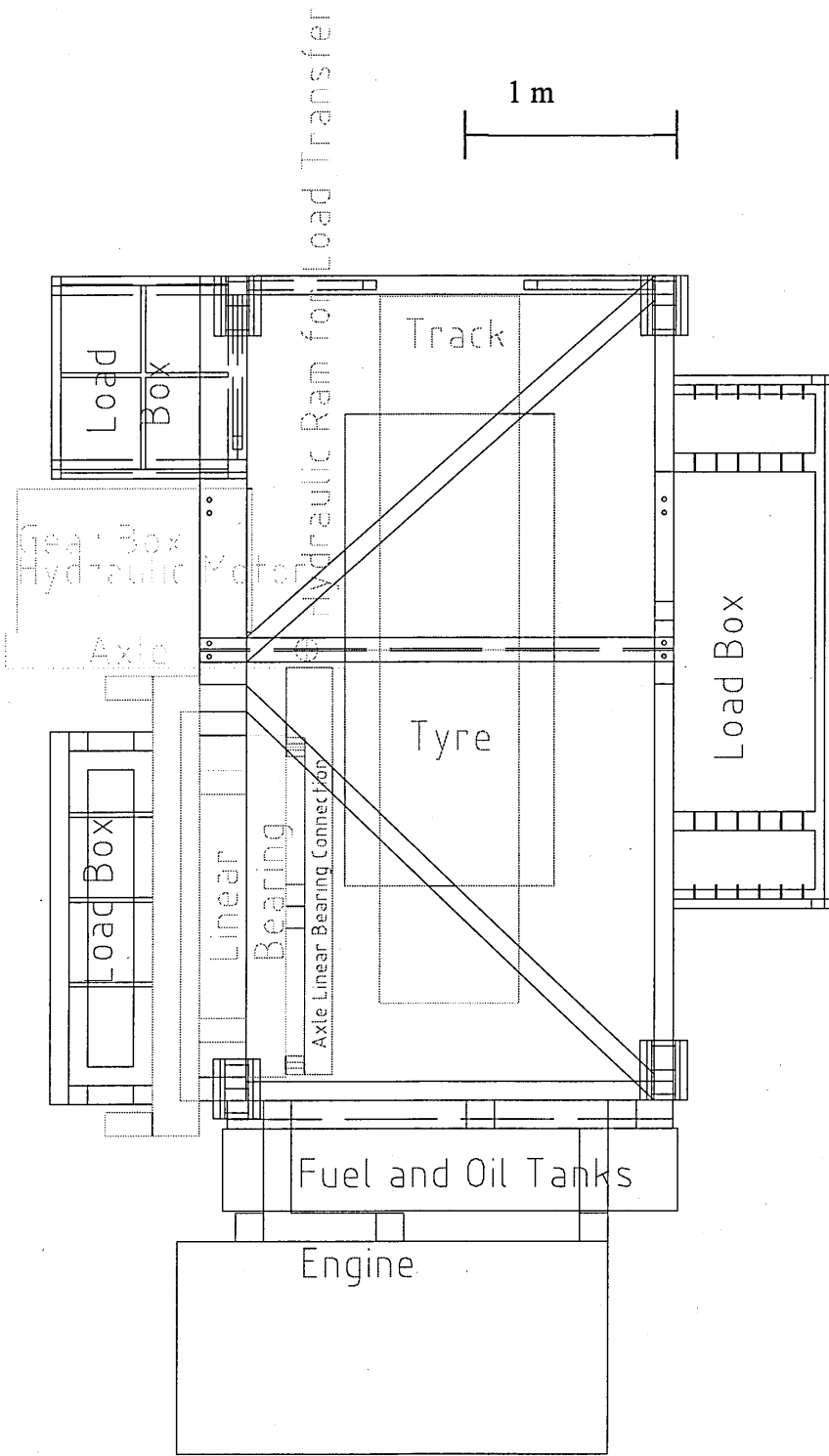


**Figure 3:** Proposed rig solution including wheel and track



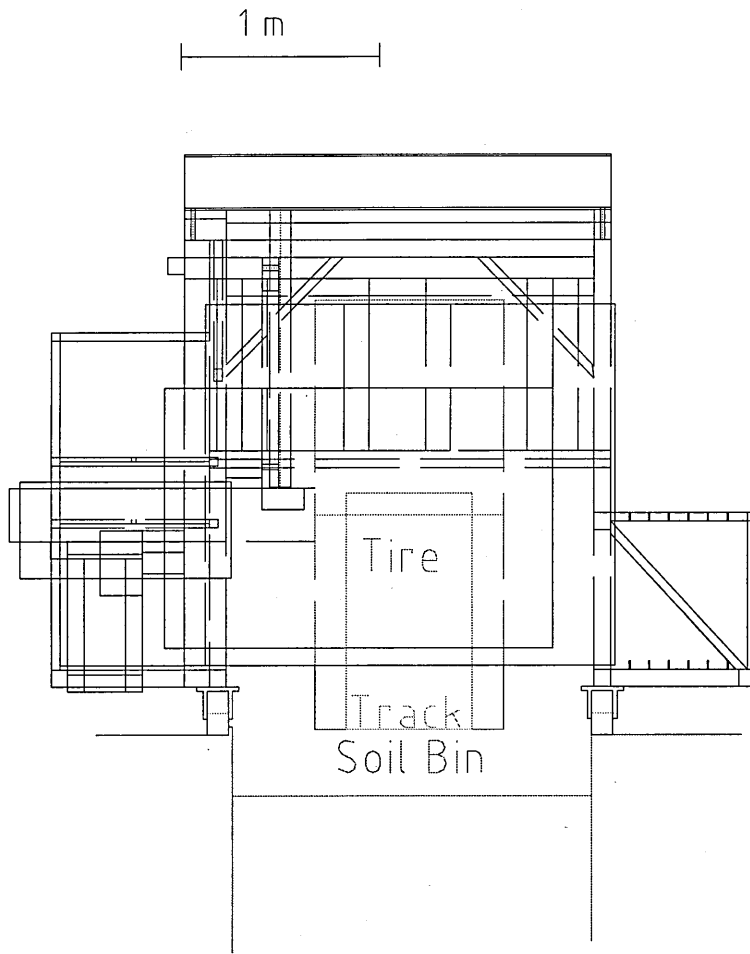


**Figure 4:** Endelevation of proposed rig solution

### 3 REQUIREMENTS AND CONDITIONS FOR THE SOLUTION

#### 3.1 Performance Specifications and Requirements

The frame and rig solution proposed in 2.3 has to meet the following requirements <sup>®</sup> and wishes (w) for this particular investigation:

- Geometry:
  - Wheel and track sizes according to **Table 1** <sup>®</sup>
  - Soil bin width of 1745 mm <sup>®</sup>
  - Rail width of 115 mm <sup>®</sup>
  - Free space around soil bin: 900 mm left hand side; 1200 mm right hand side <sup>®</sup>
  - Axle size and its components: overall axle width 760 mm; height of axle 250 mm; lowest point of gear box below bottom of axle 170 mm <sup>®</sup>
  - Possibility to place the required weight on the main frame <sup>®</sup>
  - Maximum expected rut depth of 400 mm (Godwin and Dresser, 2004) <sup>®</sup>
- Kinematics:
  - Driving speed approximately 1 m/s <sup>®</sup>
- Forces and Moments:
  - Possibility of applying up to 12000 kg onto the axle with tested device <sup>®</sup>
  - Possibility to place the required weight on the main frame <sup>®</sup>
  - Ability to take out the torques caused by weight application <sup>®</sup>
- Energy:
  - Provision of power supply <sup>®</sup>
- Signals:
  - Recording of pressure inside the cylinder <sup>®</sup>
  - Recording of actual frame speed and wheel speed to calculate slip <sup>®</sup>
- Manufacturing:
  - Main frame built outside <sup>®</sup>

- Small pieces built in workshop at CU@S ®
  - Using standard Claas combine axle ®
- Handling:
- Easy manageable load plates (w)
  - Convenient weight adjustment (already achieved using a hydraulic cylinder for applying the vertical load) (w)
  - Ability to move the rig frame outside of the soil bin (castors were chosen) (w)

## 3.2 The Solution

### 3.2.1 Sinkage

The maximum possible sinkage of the tire is given by:

1000 mm height above ground (tire radius)

- 300 mm soil bin depth
  - 125 mm half axle height
  - 170 mm gear box below axle
- resulting in 405 mm sinkage

So the maximum sinkage for the given conditions results in 405 mm, which is slightly larger than the minimal requirement.

### 3.2.2 Weight and its distribution

The weights are distributed as follows (see **Figure 5**):

Frame construction:	1000 kg	
Engine:	1000 kg	(later replaced by load boxes as engine is taken off the rig)
Linear bearing and axle:	1000 kg	(right hand side)
Additional load:	13000 kg	(7000 kg on left; 6000 kg on right hand side)

Thus, the whole equipment weighs approximately 16000 kg. When the operational load limit of 12000 kg is being applied to the wheel/track during the investigations in the soil bin 4000 kg remains as load on the rails (1000 kg for each castor). These 4000 kg allow a safety margin in calculating the torque for the whole system so that the support wheels always have sufficient vertical load to guide the rig.

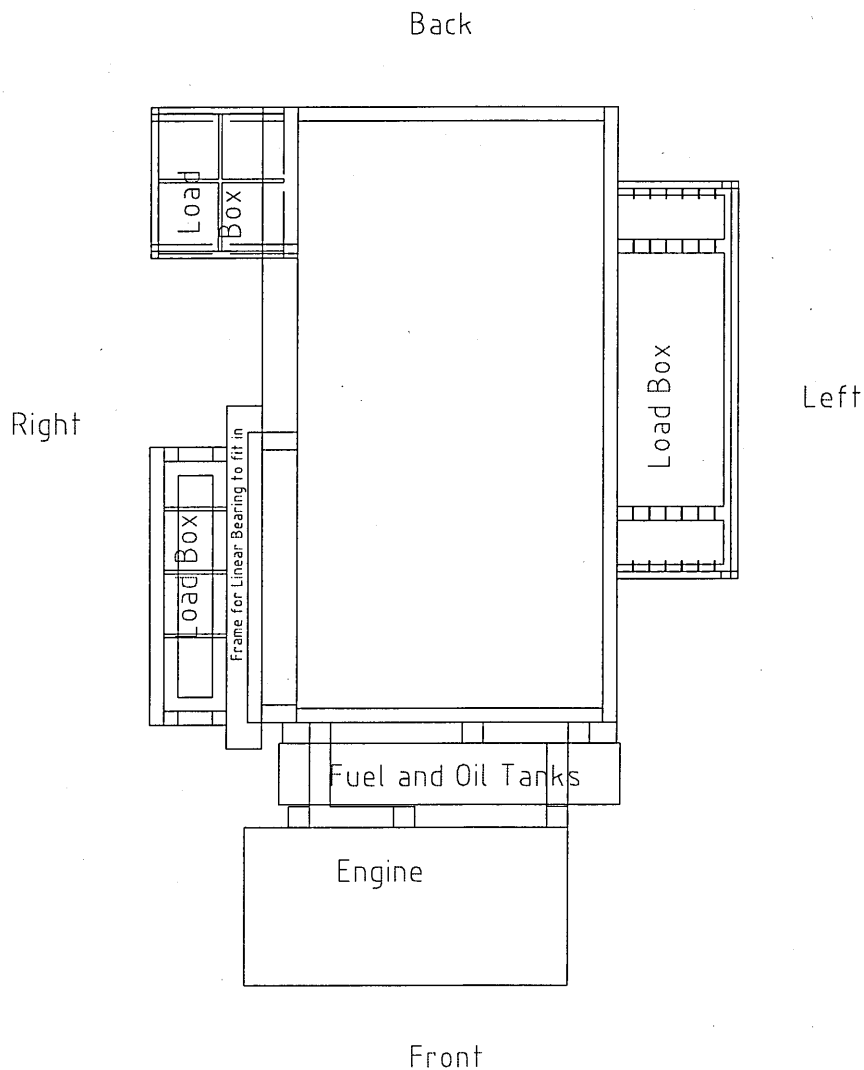


**Figure 5:** Position of load boxes and linear bearing

### 3.2.2.1 Hydraulic ram and Torque

The weight is balanced about the contact patch of the test wheel or track so that all 4 support wheels have approximately the same vertical load which always must remain positive.

The hydraulic ram position was dictated by the length of the linear bearing and its position (1820 mm) and half the axle width (75 mm) as well as 20 mm clearance.

In front of hydraulic ram:

Linear Bearing:	$1000 \text{ kg} * 1000 \text{ mm} * 10 \text{ m/s}^2$
Engine	$1000 \text{ kg} * 2300 \text{ mm} * 10 \text{ m/s}^2$
Frame:	$540 \text{ kg} * 900 \text{ mm} * 10 \text{ m/s}^2$
Weight:	$2000 \text{ kg} * 1000 \text{ mm} * 10 \text{ m/s}^2$

Behind the hydraulic ram:

Frame:	$460 \text{ kg} * 800 \text{ mm} * 10 \text{ m/s}^2$
Weight:	$4000 \text{ kg} * 1300 \text{ mm} * 10 \text{ m/s}^2$

This weight distribution results in a torque of approximately 2000 Nm. Thus the frame is approximately balanced and the position of the center of gravity of the 7000 kg load box can be centered about the position of the hydraulic ram. Essentially the mass of the engine has to be replaced by a “dummy” mass to keep the other specifications.

As it was decided to relocate the engine off the main frame, either the operational load limit of the rig must be reduced or additional weight equal to the engine mass must be attached to maintain acceptable vertical loads on the support wheels.

### 3.2.3 Castors

In order to be able to move the rig outside the soil bin it was decided to mount 4 castors as support wheels on the bottom of the frame (4\*LSDGSPO 125K, Blicke Castors & Wheels). These castors have to fit the rail width as well as to be able to carry the maximum weight of the rig. The chosen castors have a diameter of 125 mm, a width of 110 mm, a total height of 205 mm and are able to carry 3600 kg each. This results in 14400 kg bearing capacity for the four castors compared to an estimated total weight of 16000 kg. The deficit of 1600 kg in total, or 400 kg for each castor was accepted. In order to stop the castors

from swiveling when sitting on the rails, 4 blocks were cut fitting below the castor plate and being bolted onto the same. This stops the castors from swiveling (shown in **Figure 6**).

### 3.2.4 Guiders

To take out any occurring side force during the run, e.g. caused by a small offset of the tire trying to pull in one direction guiders have been fitted inside the frame on each corner. For further information see **Figure 6**. To these guiding blocks plastic bearing plates were bolted to make the surface contact between guiders and the edge of the rail as frictionless as possible.

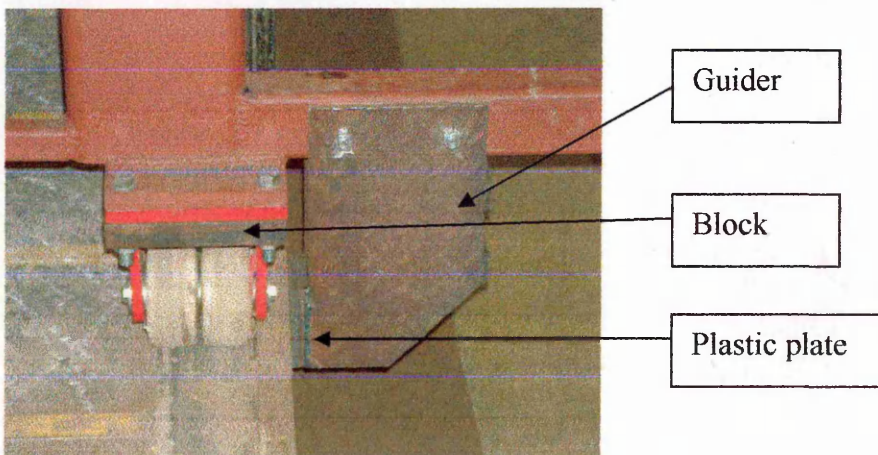


**Figure 6:** Guider and block to stop castor from swiveling

Canting between the front and rear guiders does not occur. The guiders are 3000 mm apart from each other and therefore the twist necessary to cause a sufficient angle between the guiders to in turn cause canting can not be reached.

### 3.2.5 Hydraulic System for Load Control

#### 3.2.5.1 Hydraulic ram

The necessary stroke length of the hydraulic cylinder sums up to 900 mm. This results as follows:

300 mm soil bin depth (distance from rail surface to soil surface)

450 mm possible sinkage

100 mm wheel above ground including frame deformation

50 mm safety

The ram size for applying 15000 kg was chosen according to the buckling load chart and push and pull table of Ewo, 2004 with a safety factor of 2.5. 15000 kg were chosen to allow for possible further investigations with even higher loads. The chosen ram is a SH10060900 of Ewo.

### 3.2.5.2 Hydraulic pressure maintaining valve

The relief valve being used has a flow rate of 95 l/min and a pressure range of 70 – 2100 kPa with an accuracy of better than 1% at full range. This was regarded as exact enough. Maximum speed of the stroke for the given cylinder and a flow rate of 95 l/min is 150 mm/s which is sufficient (Godwin and Dresser, 2004).

### 3.2.5.3 Hydraulic circuit for the hydraulic ram

The hydraulic ram was connected through the pressure maintaining valve to a valve block. Via the valve block it was possible to steer the ram. The circuit was designed to be an open flow in neutral, but unfortunately only a valve being closed in neutral was available. Therefore in neutral all fluid was blown over the relief valve inside the MB – Trac which was being used for supplying the hydraulic power to the ram. For the hydraulic circuit see **Figure 7**. As hose size 12.7 mm hoses were chosen to allow the necessary flow with least friction losses. The pressure in the system was controlled with an electrical pressure transducer ranging from 0 – 600 bar with an output of 0 – 3 V. Details are explained in section 3.2.10.2.

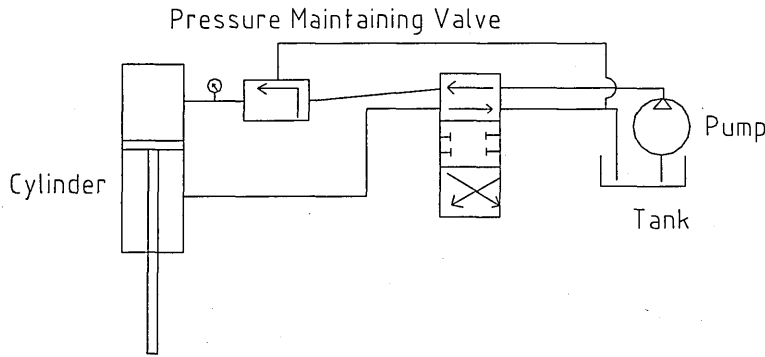


**Figure 7:** Hydraulic circuit for hydraulic cylinder

### 3.2.6 Hydraulic System for Speed Control

The used Perkins 6354 engine is connected to a PM1000 hydraulic pump which is according to its specifications able to supply 60 kW. This hydraulic pump is connected to the hydraulic motor of the axle in order to run the device. Eq. 1 shows the instantaneous power requirement  $P(t)$ :

$$P(t) = (F_A(t) + F_R(t)) * v(t)$$

Eq. 1

where  $F$  is the force and  $v$  is the velocity.  $F_A$  is the force needed to accelerate the assembly up to the required speed and  $F_R$  is the rolling resistance of the particular wheel or track in the soil bin. For motion with constant acceleration starting from rest the following equations hold:

$$t = \frac{v}{a}$$

$$s = \frac{1}{2} * a * t^2$$

Eq. 2

where  $s$  is the distance traveled. According to Eq. 2 for an assumed acceleration of  $1 \text{ m/s}^2$  the resulting distance for speeding up the device to  $6 \text{ km/h}$  is  $1.4 \text{ m}$  and the duration of the acceleration phase is  $1.67 \text{ s}$ .

The force needed to accelerate a mass of  $16000 \text{ kg}$  with  $1 \text{ m/s}^2$  is



$$F_A = m * a$$

Eq. 3

which results in 16 kN.

For the instantaneous power follows:

$$P_A(t) = m * a^2 * t$$

Eq. 4

Thus the maximum power required for acceleration is 26.8 kW, occurring at the end of the acceleration phase.

The mean power during this phase is 13.4 kW:

$$P_{aver} = m * a^2 * \frac{t_{max}}{2}$$

Eq. 5

The rolling resistance force  $F_R$  is

$$F_R = \mu * F_N$$

Eq. 6

with  $F_N$  being the load of 120 kN applied to the wheel or track and  $\mu$  being the coefficient of rolling resistance assumed at 0.3 (Godwin and Dresser, 2004). The power to overcome this rolling resistance at a given speed results from the rolling resistance force of 40 kN times the speed:

$$P_R = F_R * v$$

Eq. 7

For an assumed speed of 1.67 m/s the resulting power to overcome rolling resistance with the given conditions equals 67.2 kW.

Power required as a function of time is compared to the power available in **Figure 8**. For the acceleration phase there is an abundance of power available, while for the period of constant speed in the soil with an assumed rolling resistance coefficient of 0.3 the power barely suffices. However, according to Godwin and Dresser (2004) rolling resistance is expected to be 0.20 – 0.25, in which case 33 to 16% spare power remains.

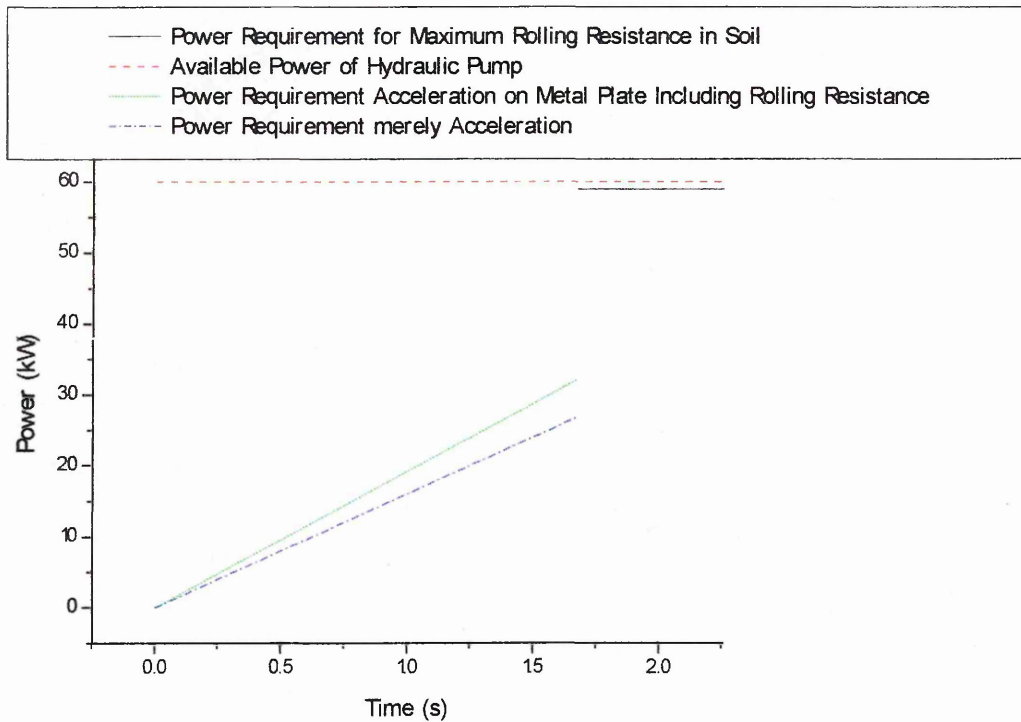


**Figure 8:** Power versus time

### 3.2.7 Linear Bearing

The torques developing during operation should be taken out using a linear bearing. The linear bearing used was available from a former project. Unfortunately the main frame of the linear bearing was mandatory to be used and could not have been taken apart and refitted again. This would have made construction easier as the given conditions of this particular project had had to meet the dimensions of the linear bearing and not vice versa. Thus the main rig frame had to be enlarged and specially designed in order to carry the frame of the linear bearing.

The linear bearing has to vertical rails with three glider blocks each. The rails are fixed to a frame fitting into the main frame of the single wheel tester. The blocks are bolted to a plate which in turn is bolted to the linear bearing axle connection drawn as 759106P04.

Technical specifications of the linear bearing:

890 mm possible vertical movement

$M_0$  : 82.8 kN per piece (totally 6 pieces, split up on two rails)

$M_x$  : 96.9 kN per piece ( “ “ “ “ “ “ “ “ )

For direction of  $M_0$  and  $M_x$  see **Figure 9**.

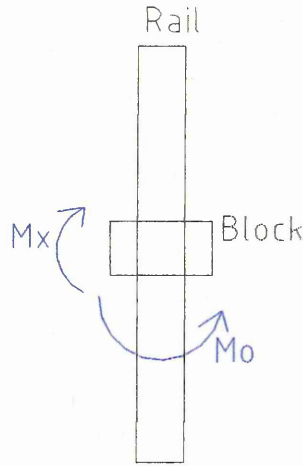


**Figure 9:** Direction of  $M_0$  and  $M_x$  on vertical linear bearing rail

Note: Forces for torques act in drawing plane for  $M_x$  and perpendicular to drawing plane for  $M_0$ . The torque  $M_0$  is highest when the frame comes to a sudden stop and the tire is still trying to pull the frame along. The force pushing is 120 kN if the traction coefficient is 1, worst case assumed. The lever arm of 0.6 m length for this moment is shown in **Figure 10**.

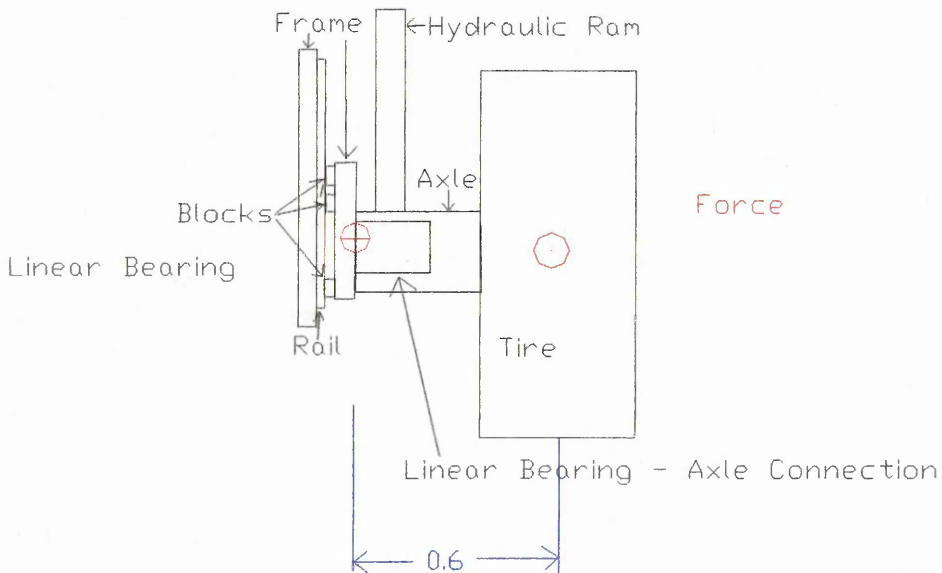


**Figure 10:** Front view; lever arm length for moment  $M_0$  [Units in m]

The torque  $M_x$  develops from applying the load of 120 kN 0.55 m offset to the center of the tire. The lever arm and the principle is shown in **Figure 11**.

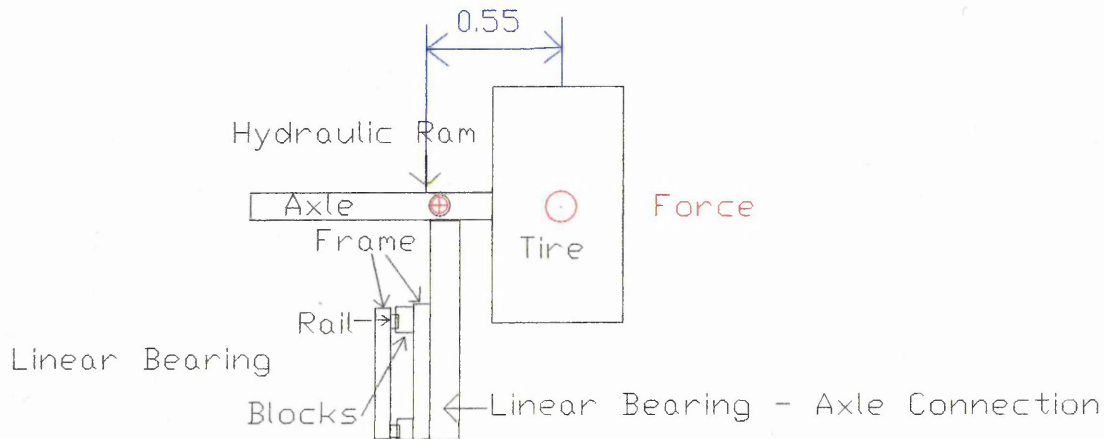


**Figure 11:** Top view, lever arm length for moment  $M_x$  from applying load [Units in m]

Forces:

$M_x$ :

Load Moment:

$$0.55m * 120kN = 66kNm$$

$$66kNm / 0.95m = 69.5kN \text{ divided into two rails.}$$

$M_0$ :

Forward movement; worst case when frame suddenly stops completely but wheel or track still moves forward and all weight force is used:

$$120kN * 0.6m = 72kNm$$

$$72kNm / 0.95m = 76kN \text{ divided onto 3 pieces on one rail.}$$

Resulting torques can be taken up by linear bearing with a safety factor of 2.

### 3.2.8 Dimensions

The dimensions of the frame were adjusted to the requirements as followed:

Clear width within frame: 1750 mm (Main Frame (759002A04))

Clear length within frame: 3340 mm (Main Frame (759002A04))

Position of hydraulics/axle: 1880 mm (measured from beginning of frame to beginning of axle)

The positions of the hydraulics and the axle are determined by the length of the linear bearing plus half the axle width plus additional space to allow the movement of the axle in front of the frame of the linear bearing.

Clear height within frame:  $2220 \text{ mm} + 205 \text{ mm}(\text{castor}) + 20 \text{ mm}(\text{castor plate}) = 2445 \text{ mm}$  (Main Frame (759002A04))

The height of the frame is used for 1290 mm (total hydraulic ram) plus 125 mm (half axle) plus 1000 mm (tire radius) and results in just 30 mm free space below the tire when it is completely lifted up. A tire radius of 1000 mm was assumed here as this is 30.5 mm more than the approximate tire radius of the largest tire in diameter (680 R85 32) being used (Continental, 2004). All other requirements were met when designing the frame rig.

### 3.2.9 Track – Wheel Fitting

A further challenge was the requirement of using both wheels and tracks. For the given conditions a fitting plate as drawn in 759108P04 was chosen to overcome the height difference between the axle-wheel connection and the axle-track connection shown in **Figure 12**. Moreover the different pitch circle diameters had also to be accounted for.

The PTO shaft from the gear box at the axle to the track had to overcome the height difference shown in **Figure 13** as well. As shown in calculations below the maximum working angle of the PTO shaft is not reached. The edge of the soil bin is not being hit by the PTO shaft before the bottom of the gear box hits the ground.

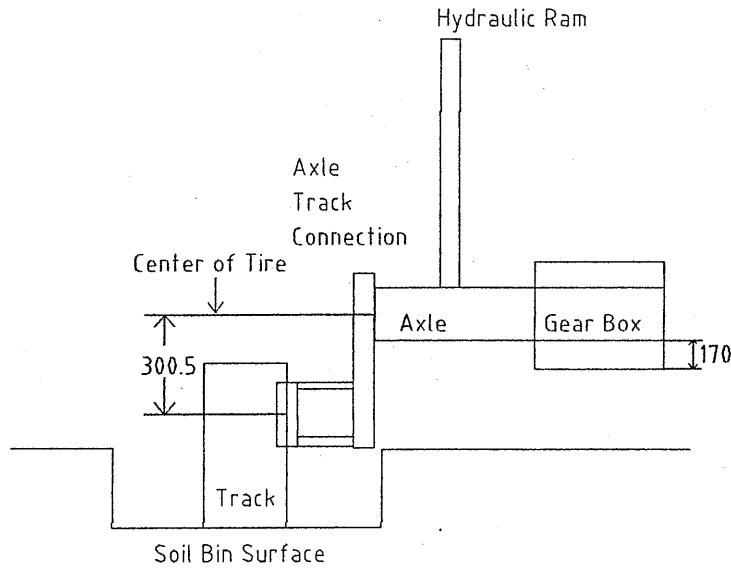


**Figure 12:** Axle – Track unit with fitting plate as drawn in 759108P04 [Units in mm]

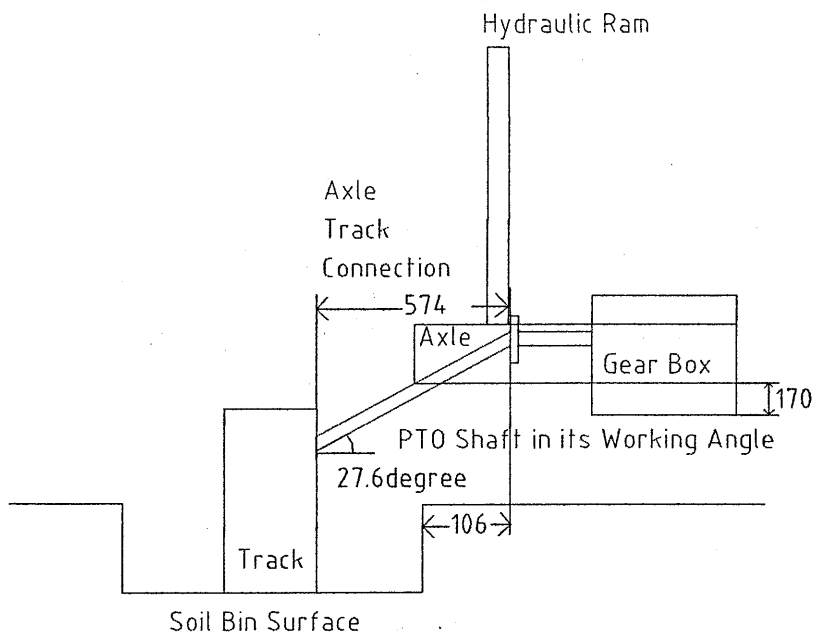


**Figure 13:** PTO Shaft to overcome height difference as occurring from axle to track. For clarity the connection plate is not shown in this figure [Units in mm]

### Specifications of the Track

Max. Working Angle of PTO:	35 degree
Horizontal Distance of PTO:	~574 mm
Length Break – Edge of Soil Bin	106 mm
Height Difference Center Line Axle – Track	300.5 mm

**Angle of PTO:**

$$\tan \alpha = 300.5/574 = 0.534 \Rightarrow \alpha = 27.6^\circ$$

⇒ ok

**Hitting the edge of the soil bin with PTO:**

$$\text{Height} = \tan \alpha * 106\text{mm} = 56\text{mm}$$

⇒ ok, because gear box is 170 mm below axle

This solution takes care of the track – wheel difference in order to obtain the same sinkage for the tracks as for the wheels.

### 3.2.10 Instrumentation

#### 3.2.10.1 Speed Recording and Slip Calculation

In order to be able to calculate wheel slip the actual speed of the tire as well as the true speed of the frame had to be measured and recorded. Actual speed of the wheel was measured mounting a rotary pulse encoder onto the right hand side output drive shaft of the gear box (shown in **Figure 14**).

The true speed of the frame was measured using a second identical encoder mounted onto a standard fifth wheel from the lab of the engineering group. The fifth wheel was clamped onto the main frame in front of it and running on the concrete floor beside the soil bin. So slip of this tire can be neglected. The assembly is shown in **Figure 15**.

The digital outputs of the encoders were recorded during the tests via the Iotech Wavebook onto a laptop computer using Daisy Lab 5.6 Software. In Daisy Lab 5.6 the encoder signal was integrated and transferred into rotations per second. Knowing the rolling circumference of both wheels slip can be calculated from the difference in speed. This data was recorded simultaneously with the pressure described in section 3.2.10.2. So not merely pressure over time curves can be drawn but pressure over actual frame position as well.

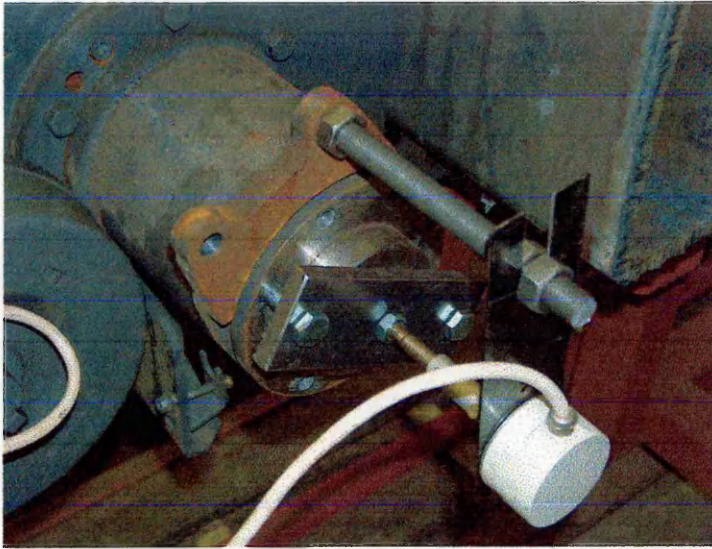


**Figure 14:** Encoder for measuring actual wheel speed

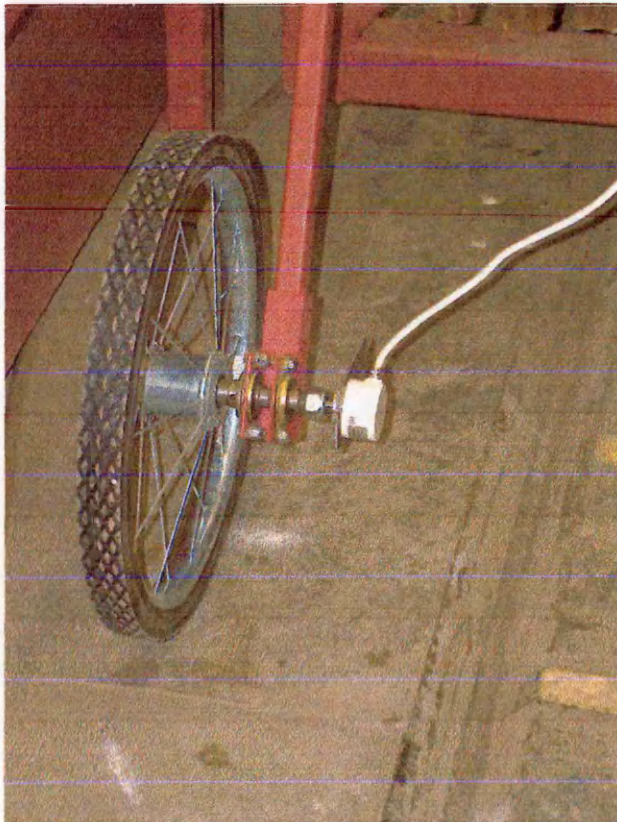


**Figure 15:** Fifth wheel for measuring true frame speed



### **3.2.10.2 Hydraulic Pressure Recording**

The pressure in the hydraulic system of the ram was sensed with an electrical pressure transducer mounted between the pressure maintaining valve and the cylinder. The transducer range was from 0 – 600 bar with an output of 0 – 3 V. Output voltage was independent of input voltage. Input voltage from 12 – 30 V could be used. As power supply a 12 V battery was used. Readings were processed and recorded during the run onto a laptop via a Iotech – Wavebook as an analog digital exchange device and using Daisy Lab 5.6 Software. The pressure transducer was bolted into a socket in the pressure maintaining valve on the pressure restricted outlet. Therefore readings were the actual pressure readings inside the cylinder as the maintaining valve was placed directly in front of the input of the hydraulic ram.

#### 4 STRESS AND STRAIN CALCULATIONS

Stress and strain calculations were carried out for the highly stressed parts in the frame in order to choose the appropriate box section size for these beams. For parts which were anticipated to be less stressed, calculations were not done. After drawing the whole model in Mechanical Desktop the main frame as well as its sub assemblies were evaluated using a finite element analysis package (Cosmos – Star Design). The results of this are given in chapter 4.4.

The moment of inertia (I) was calculated according to Bosch (1986) for all box sections. Although one has to distinguish between torsion and bending cases, the expressions are identical. Section modulus (W) results from (I) divided by the distance (l) between the neutral axis and the extreme cross section fiber.

Stress for both torsion and normal stress is calculated according to:

$$\sigma = \frac{M * l}{I} = \frac{M}{W} = \frac{F}{A}$$

Eq. 8

where A is the cross sectional area and M the applied torque. The deflection (d) is calculated for the case of a cantilever according to the following equation:

$$d = \frac{L^3}{3} * \frac{F}{E * I}$$

Eq. 9

where L is the length of the cantilever and E the coefficient of elasticity. In case of a simply supported beam, the value of 1/3 in Eq. 9 has to be replaced by 5/384 for calculation of deflection (Bosch, 1986).

Buckling is calculated according to the Euler – equation or Tetmajer – equation depending on the slenderness ratio  $\lambda$  with  $l_k$  = buckling length (Bosch, 1986):

$$\lambda = \frac{l_k}{\sqrt{\frac{I}{A}}}$$

Eq. 10

In case  $\lambda$  is larger than 104 (this number depends on material properties, here the mild steel class St 37 is assumed), Euler - equation is used. In case  $\lambda$  is smaller than 104, buckling is calculated according to the Tetmajer – equation (Bosch, 1986). Before calculating the possible buckling,  $\lambda$  has to be identified for each piece using Eq. 10.

In case the buckling tension equation according to Euler applies, the stress is calculated:

$$\sigma_b = \pi^2 * E / \lambda^2$$

Eq. 11

In case Tetmajer – equation does apply for the maximum permissible buckling tension (in MPa) we have for St 37:

$$\sigma_t = 310 - 1.14 * \lambda$$

Eq. 12

$\sigma_t$  is divided by the chosen safety factor to get the permissible buckling tension. Tension caused by the force is calculated according to Eq. 8 (Bosch, 1986).

#### 4.1 Stress and Strain estimates for choice of Box Sections

As material mild steel S235JR (formerly called St37) was chosen with a yield strength of 235 N/mm<sup>2</sup> and a tensile strength of 340 N/mm<sup>2</sup> (Bosch, 1986).

The largest box section was given by the fact that the main frame of the linear bearing had to fit into this construction on one side. Therefore its box section width was used. The beams used were therefore 200 mm \* 100 mm. Their thickness of 10 mm resulted from a torsion analysis of the linear bearing - axle connection (759106P04) which resulted in 200 MPa shear stress for piece No 1. As this is close to yield stress, these particular pieces were strengthened by welding a 10 mm plate on top and bottom of the box section. The stress could thus be reduced to 132 MPa.

The deflection of this box section at the right hand side of the frame where 759102P04 is attached results in 1.5 mm for piece No 9 in 759002A04. The lever arm length of the 4000 kg equals 330 mm and this results in a torque of 12.95 kNm trying to move the arm inwards. This torque is taken up by the two arms with a length of 2000 mm, thus the result-

ing force at the bottom is 3.3 kN. The deflection at the linear bearing can be ignored as the weight is smaller and the lever arm length is shorter.

An “I – Beam” was used for supporting the hydraulic ram as it was available from the work shop. The deflection of the chosen I – Beam (759116P04) would be less than 2 mm when 150 kN would be applied at the center. In reality merely 120 kN are applied outside the center and thus deflection and stress are smaller.

A 80 mm \* 80 mm \* 8 mm box section was chosen for all other parts because of stress and deflection calculations for the left hand side of the rig frame and the results for the weight boxes. The stress and deflection values for the given conditions were as follows:

The total deflection of the right hand side where the 7000 kg of weight (Drawing 759101P04) are being added to sums up to 22 mm as the weight has a lever arm length of 400 mm resulting in 27.5 kNm of torque trying to bend inwards. This results in a force of 13.75 kN as the length of the arm is again 2000 mm (piece No 1 in 759002A04). The force is distributed to 4 box sections, each taking 3.44 kN. The deflection is tolerable in the middle, but not on the sections where the castors are mounted. However, here the deflection is avoided by the connection of the right hand side frame with the left hand side frame in the front part and with a connecting bar in the back (759117P04). This is placed into the structure in which normally the drawbar (759109P04) is placed when the rig has to be moved outside the soil bin. The stress was estimated at 140 MPa and therefore below the limits for plastic deformation. For the 7000 kg load box the weight is transferred to the main frame over 4 80 mm \* 80 mm \* 8 mm box sections (pieces No 2) as well as smaller supporting frames. For these box sections the resulting stress equals 160 MPa. Additional safety is given by the smaller supporting box sections (pieces No 5). All other parts of the frame are subject to smaller forces and torques, which were not calculated.

A 40 mm \* 40 mm \* 4 mm box section was chosen for the stiffening pieces as for the length of 500 mm a load of 850 kg assuming a safety factor of 2 could be applied referring to the yield strength in buckling. In tension this box section can take half the force of the weight in the load box (759101P04; piece No. 5), thereby reducing the torque in the bottom box section (same drawing; piece No. 2) to zero. Half the force in this case was assumed to be 40 kN times square root of two. The factor “square root of two” occurs due to the diagonal direction of the resulting force compared to the vertical direction initially.

Cross section area of this particular box section equals  $576 \text{ mm}^2$  and the resulting stress is only 98 MPa.

#### 4.2 Stress and Strain in Welds

For all box sections a fillet weld with 7 mm leg length was chosen according to the stress and strain calculations at the connection of the large weight box to the main frame. Here this weld is loaded by a stress of 104 MPa whereas 115 MPa are permissible. For the weld in the connecting piece from the axle to the linear bearing a leg length of 20 mm seems appropriate as the maximum stress is 110 MPa (calculated as torsion).

#### 4.3 Stress and Strain in Bolts

The common M = 8.8 class was chosen as the strength class of the bolts with a friction coefficient of  $\mu = 0.16$  was selected which accounts for bolts and nuts both running dry.

The I – Beam where the hydraulic cylinder is attached will be bolted to the main frame. The acting forces on these bolts split up equally although the hydraulic ram does not act in the center of the I – Beam. However, the torque in this case is opposite to the torque arising from the fact that the load is not applied in the center of the tire which is taken out by the linear bearing. Thus the total torque is zero again.

$$F_A + F_B = F_H (=150\text{kN})$$

$F_H$  splits equally up between  $F_A$  and  $F_B$ . Both of those forces split in turn up in half for each of the two bolts, thus the remaining force on each bolt on each side equals 37.25 kN. According to Bosch (1986) for the given conditions a M14 bolt is able to withstand a tension force of 50.6 kN and a M16 bolt is able to withstand 69.7 kN. Thus an M14 bolt was chosen for this connection.

Component No 11 in drawing 759002A04 also has to be bolted onto the main frame as it has to be taken out to fit the linear bearing. However, it is necessary to support the linear

bearing once in place. On this part a force of 63 kN acts in the very worst case when the linear bearing is in its uppermost position and if 12000 kN are applied onto the axle. In reality this will not happen as the wheel /track has to be lowered 330 mm to reach the surface of the soil bin and as this is 1/3 of the total way of the linear bearing the force on the top box section also decreases in reality to 41 kN. Thus the yield tension for the bolts has to be 31.5 kN each as the total force is split up symmetrically and worst case assumed. According to Bosch (1986) for a strength class of  $M = 8.8$  the resulting bolt will be a M12 which can withstand a tension of 36.8 kN.

#### 4.4 FEA – Results

In this section the red arrows in the shown figures indicate the application of load and the green arrows the constraints. Stress and strain is color coded as shown on the right hand side of figures..

##### 4.4.1 Load Box for Plates (759101P04)

The maximum stress and deflection occurring in this part is according to the FEA in piece No 1 with a stress of 100 MPa shown in **Figure 16** and a deflection of 5.6 mm as shown in **Figure 17**. This can be tolerated as the applied force in the FEA is 80 kN, whereas in reality not more than 70 kN will be placed in this part. In **Figure 16** and **Figure 17** of the FEA analysis the influence of a diagonal support beam on stress and strain can be shown. The diagonal support beam is missing on one side, but in reality it is included as well as on the other side. On the side where the beam is missing the deflection as well as the stress is larger and would be intolerable. Yet on the other side the diagonal beam reduces the stress and hereby it is tolerable.

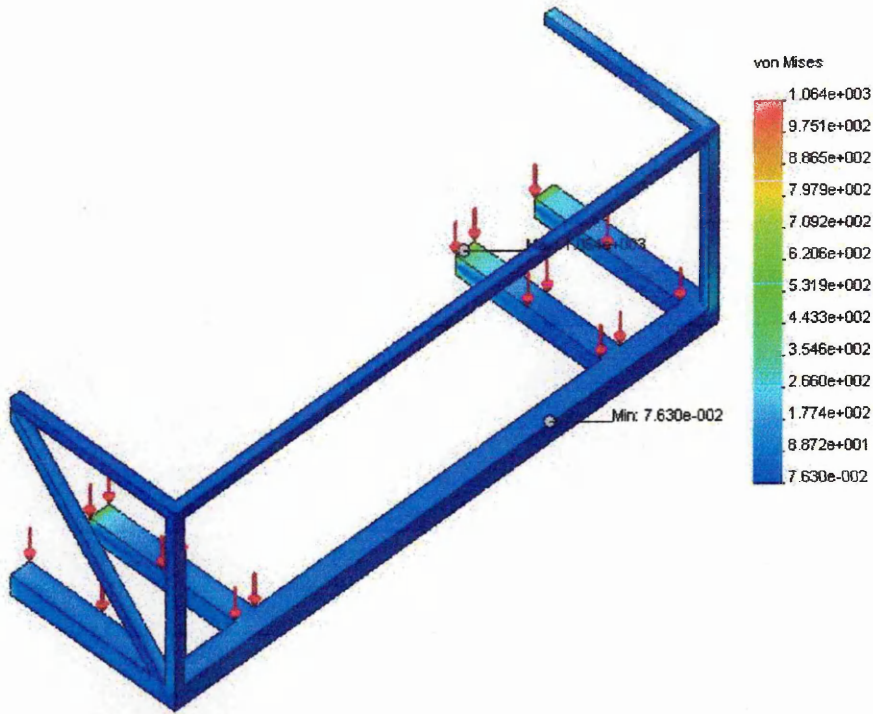


Figure 16: Stress 759101P04 [Units in MPa; Deformation scale 1:1]

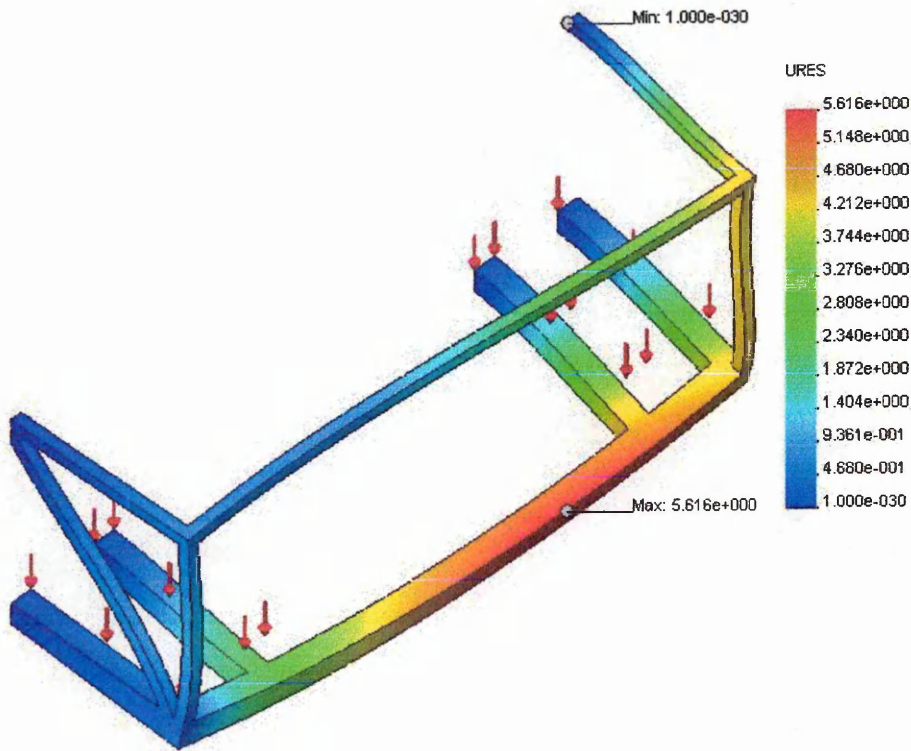
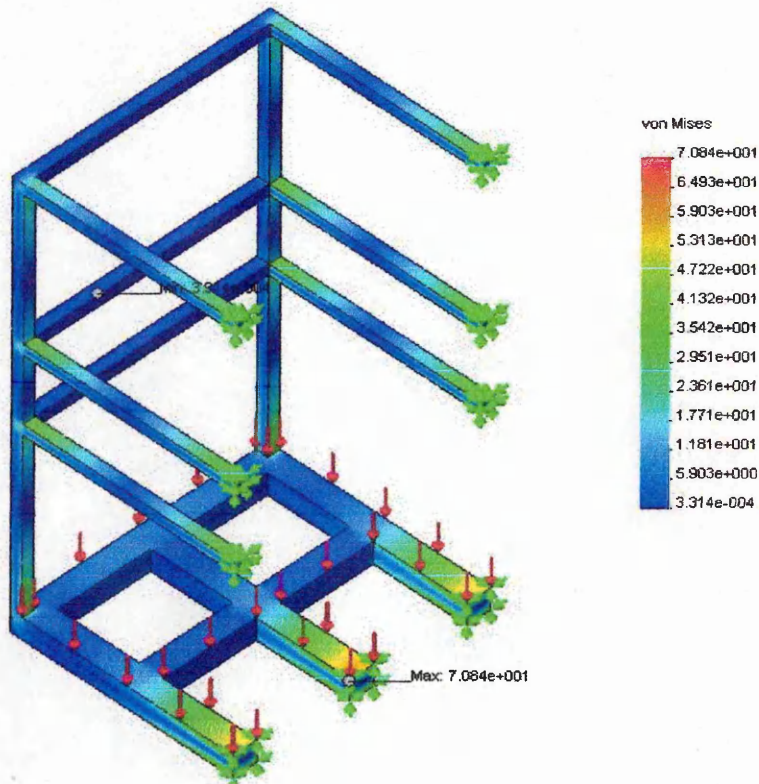


Figure 17: Static displacement 759101P04 [Units: mm; Deformation scale 1:40]

#### 4.4.2 Load Box for Boxes (large) (759102P04)

In this part 50 kN were applied and resulted in a maximum stress of 70 MPa and a maximum deflection of 1mm. Due to the small resulting stress and the application of 10 kN more than in reality one could argue to reduce the size of the chosen box sections. However, due to the dimensions being necessary to support the load boxes this is not possible and would only account for a small amount of box section as well. In **Figure 18** and **Figure 19** the stress and strain results of the FEA are shown, respectively.



**Figure 18:** Stress 759102P04 [Units in MPa; Deformation scale 1:1]



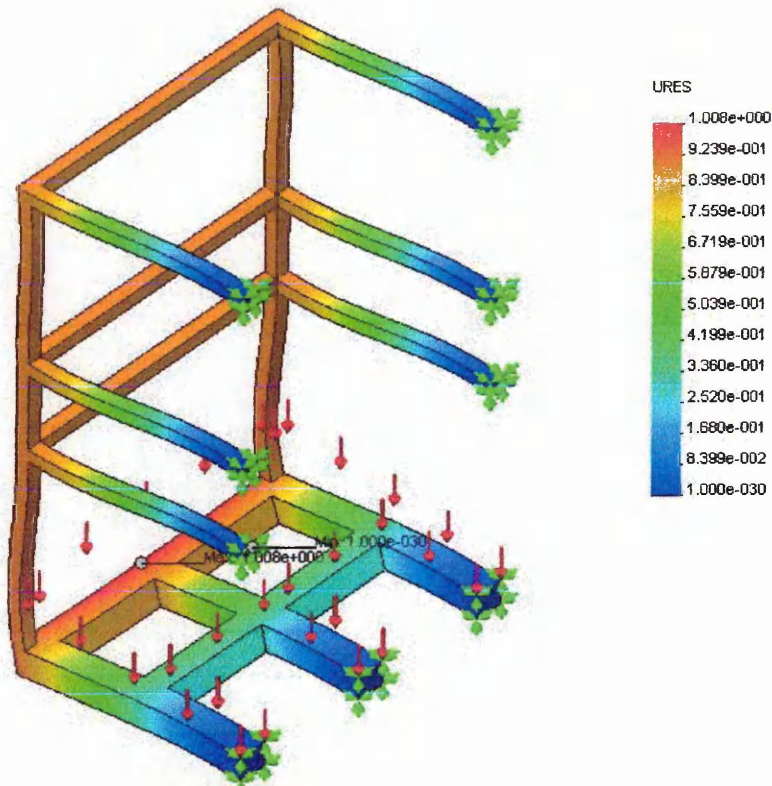


**Figure 19:** Static displacement 759102P04 [Units in mm; Deformation scale 1:164]

#### 4.4.3 Load Box for Boxes (small) (759103P04)

In this part 30kN were applied and resulted in a maximum stress of 41 MPa and a maximum deflection of less than 1mm as shown in **Figure 20** and **Figure 21**, respectively. The size of the chosen box section can not be reduced due to the same reasons mentioned in 4.4.2..

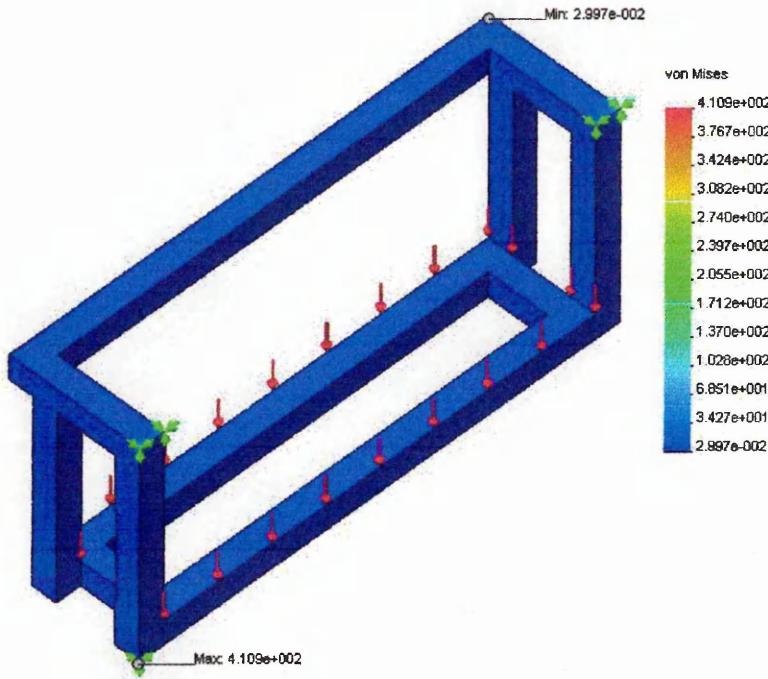


**Figure 20:** Stress 759103P04 [Units in MPa; Deformation scale 1:1]

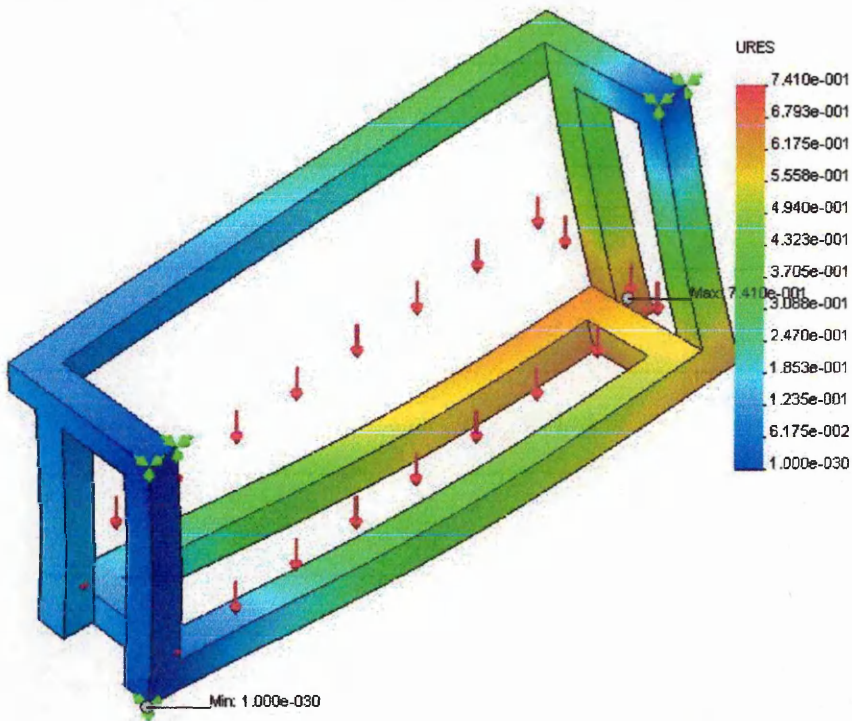


**Figure 21:** Static displacement 759103P04 [Units in mm; Deformation scale 1:242]

#### 4.4.4 Assembly Main Frame (759003A04)

The main frame was tested without the assembled parts mentioned below, however the applied forces were according to the ones in reality and mentioned in each section. Maximum deflection occurred at the side where the load box for the plates is attached with 115 mm deflection to the outside in the middle as shown in **Figure 23**. Maximum stress of 1360 MPa occurred at the attachment of the I-Beam on top of the frame as shown in **Figure 22**. This is very high and could not be tolerated. Yet as in reality the whole weight of 16000 kg will never be attached on top the real stress will be at least 1/3 less. Further on real stress on the load plate side is reduced by two diagonal pieces No 19 and 22 shown in drawing 759003A04, sheet two of two. Across the back stress is reduced by using a connecting beam 759117P04 across the back of the frame. Yet this was not further tested by FEA.

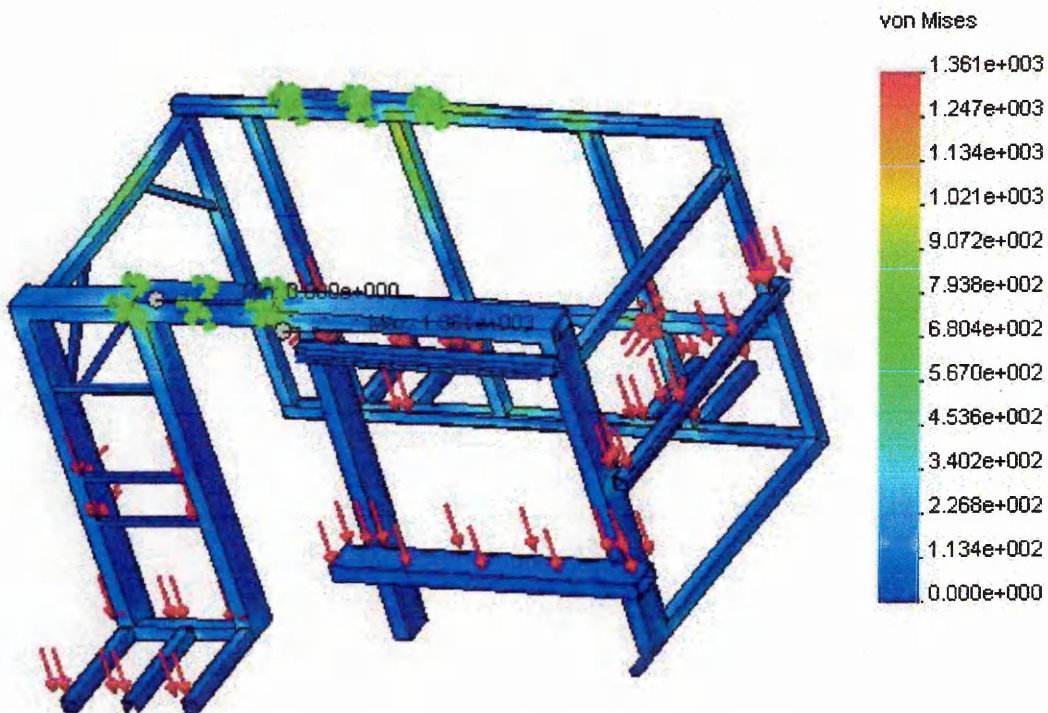


**Figure 22:** Stress 759003A04 [Units: MPa; Deformation scale: 1:1]

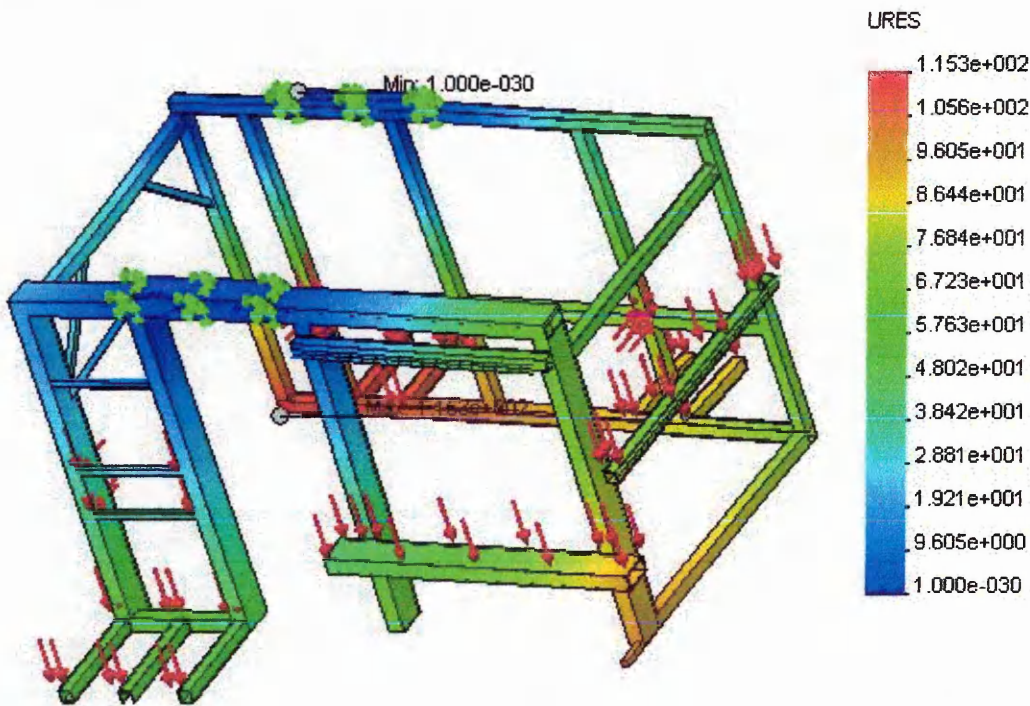


**Figure 23:** Static displacement 759003A04 [Units: mm; Deformation scale 1:1]

#### 4.4.5 Linear Bearing – Axle Bracket (759106/7P04)

As mentioned in 4.1 welding of 10 mm thick plates to the top and bottom of the 200 mm \* 100 mm \* 10 mm box section reduces the maximum stress and deflection to 132 MPa and less than 5 mm, respectively, assuming an applied torque of 66 kN. However, the FEA results shown in **Figure 24** and **Figure 25** for the given part and its constitutions were not tolerable. Maximum deflection was close to 300 mm and maximum stress was far beyond 1200 MPa for most of the part. The problems of these different results originate from the fact that the torsion calculation in 4.1 assumes a box section being restrained over the whole face area as well as applying the torsion over the whole face area. However, the first solution for this part was obtained with the box section restrained merely on its top face as the pieces connecting the 200 \* 100 mm box section to the linear bearing and transferring the torque onto the linear bearing were merely welded on top. In **Figure 24** this construction is shown. There was nothing to support the edges of the box section and the face vertical to the top. Thus the whole torque was taken by the faces not being restrained which tried to transfer it to the restrained face. This led to the enormous stress and deflection. One solution is to weld 20 mm thick plates as shown in drawing 759111P04 and in **Figure 26**

over the edge of the box section and thus restraining the other face as well. Then maximum stress is reduced to 132 MPa and a deflection of 5 mm. When looking at **Figure 26** maximum stress is given as 716 MPa, however this is only a particular point load and in general in crucial parts the mentioned 132 MPa are not exceeded. Using FEA was extremely useful in this case.

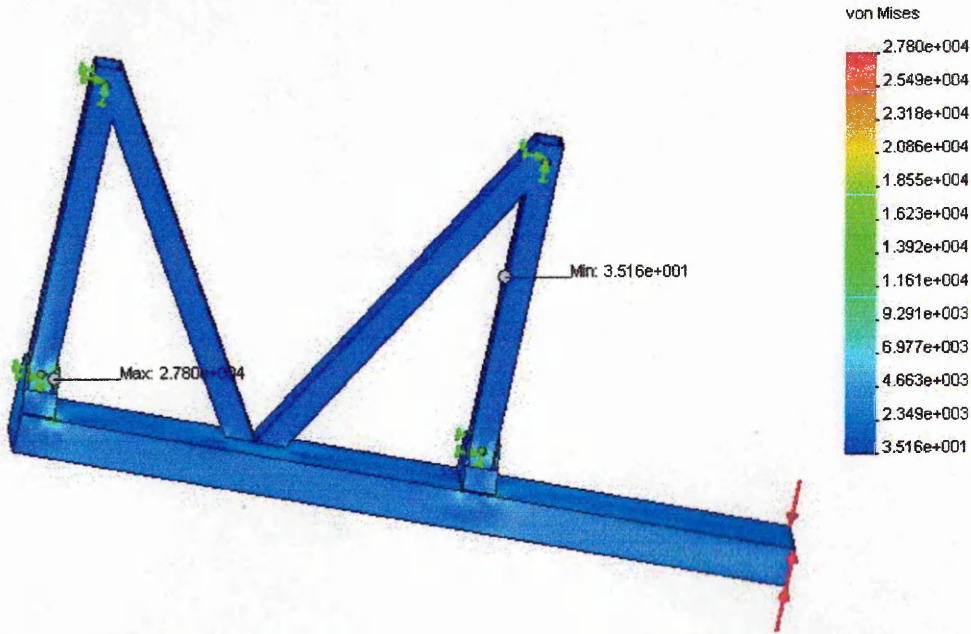


**Figure 24:** Stress 759111P04 before modification [Units: MPa; Deformation scale 1:0]

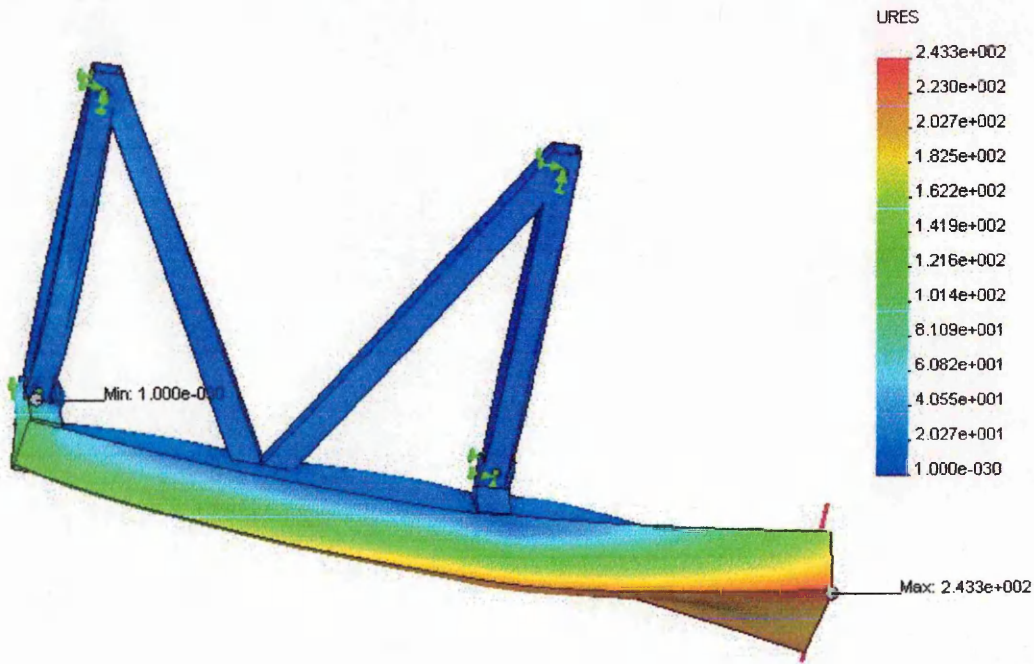


**Figure 25:** Static displacement 759111P04 before modification [Units: mm; Deformation scale 1:1]

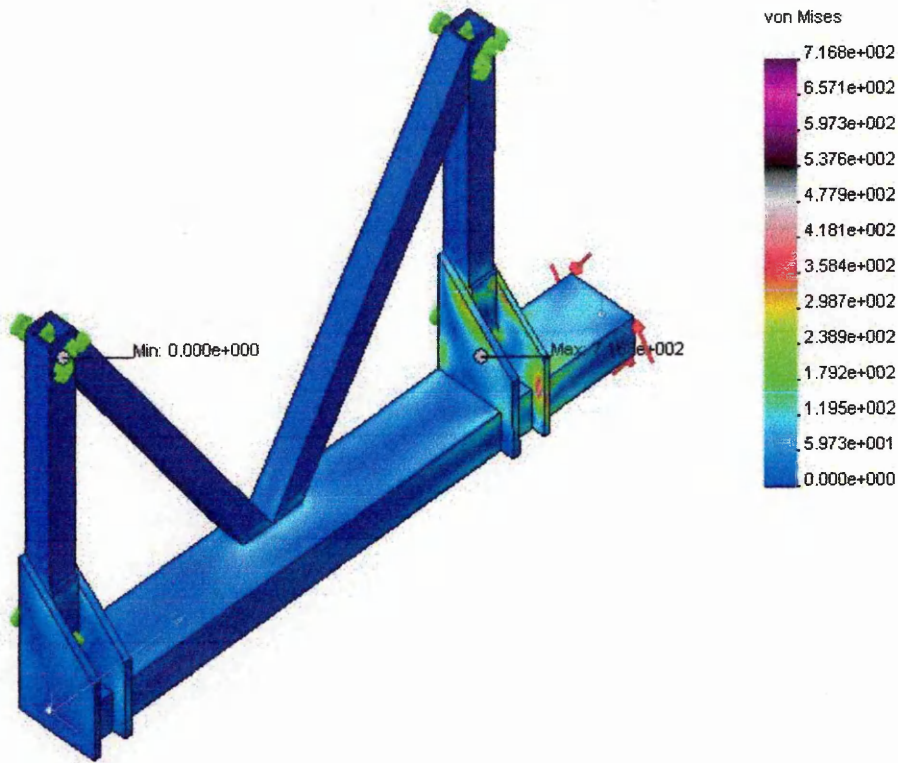


**Figure 26:** Stress 759111P04 after modification [Units: MPa; Deformation scale 1:1]

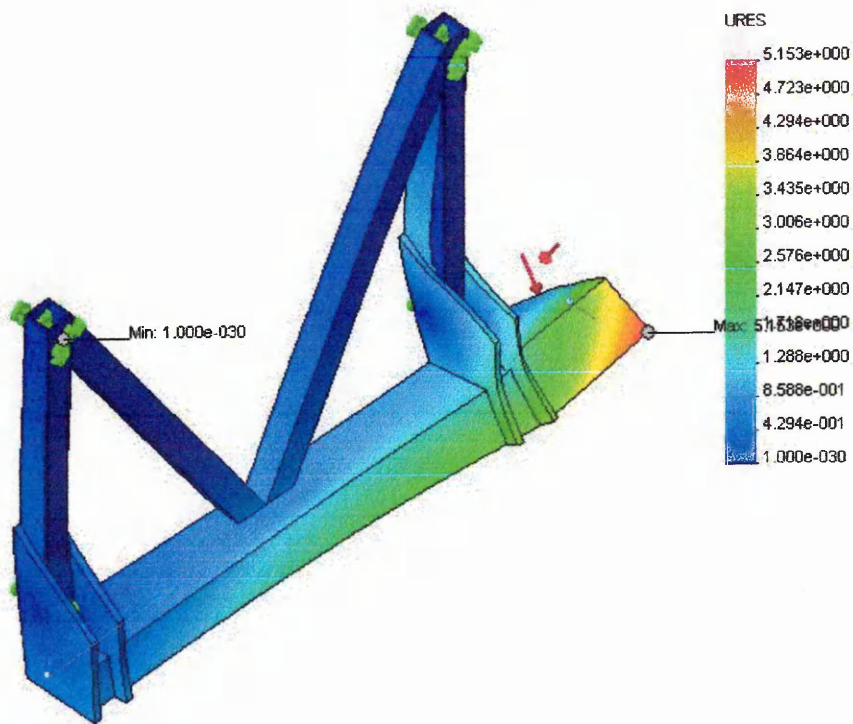


**Figure 27:** Static displacement 759111P04 after modification [Units: mm; Deformation scale 1:46]

#### **4.4.6 Wheel – Track Axle Adapter (759108P04)**

With a shear force of 120 kN being applied to the track over the axle the maximum stress in this part was 140 MPa and a deflection of 4 – 5 mm on the top of the plate. This assumes a 40 mm thick plate as designed originally. However, as this thickness is both heavy and difficult to handle, and in the work shop a plate fitting the appropriate dimensions is available in RQT701 with a thickness of 25 mm this one will be used therefore. RQT701 has a tensile stress of 760 MPa. Thus this plate is used.





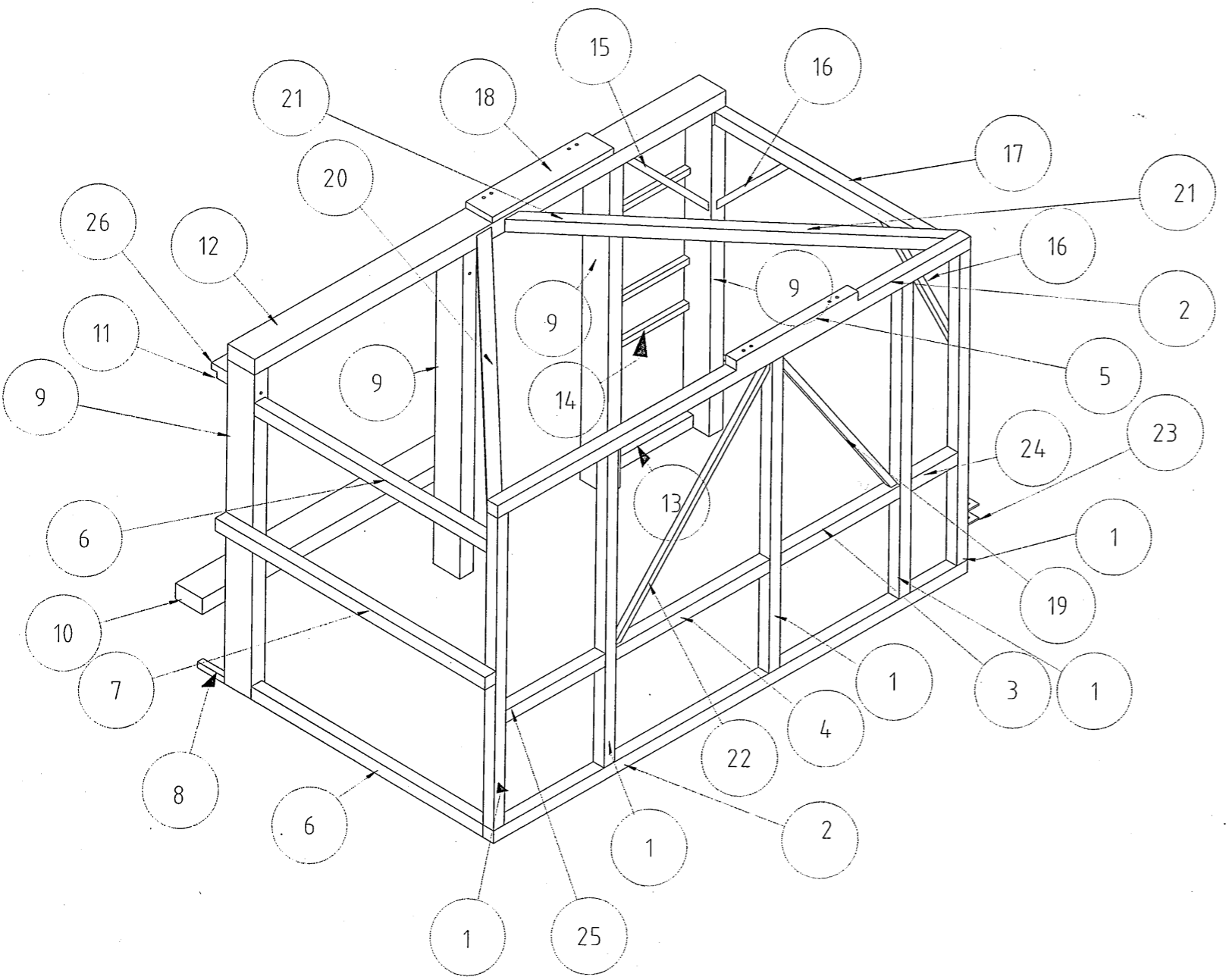
PART No. 759002A04		
ISSUE	CHANGE RECORD	DATE-AUTHY
1	PRODUCTION REL	DA04

Cutting List

Symbol	Part Name	Length	Quantity
1	80x80x6	2000	5
2	80x80x6	3500	2
3	80x80x6	880	1
4	80x80x6	1140	1
5	60x80x900 see 759111P04		1
6	80x80x6	1750	2
7	80x80x5	2030	1
8	40x40x4	200	1
9	100x200x10	2080	4
10	100x200x10 see 759113P04		1
11	80x80x6	1650	1 being bolted!
12	100x200x10	3500	1
13	80x80x6	660	1
14	40x40x4	660	3
15	40x40x4 see 759333P04		1
16	40x40x4 see 759333P04		2
17	80x80x6	1750	1
18	40x200x900 see 759112P04		1
19	40x40x4 see 759333P04		1
20	80x80x6 see 759333P04		1
21	80x80x6 see 759333P04		1
22	40x40x4 see 759333P04		1
23	80x10	80	4
24	80x80x6	345	1
25	80x80x6	735	1
26	40x40x4	1650	1

NOTES:

All joints weld around unless specified otherwise.  
Fillet weld min leg=7mm for 80x80 and 40x40



© CRANFIELD UNIVERSITY 2004. ALL RIGHTS RESERVED. THIS DRAWING IS THE CONFIDENTIAL PROPERTY OF THE ABOVE NAMED COMPANY. WITHOUT WHOSE PRIOR WRITTEN CONSENT, IT MUST NOT BE COPIED, LOANED OR COMMUNICATED TO OTHERS, WHOLLY OR IN PART.

**Cranfield UNIVERSITY**  
Silsoe

SILSOE CAMPUS DESIGN OFFICE  
NS01 ENGINEERING GROUP  
SILSOE CAMPUS, SILSOE,  
BEDFORDSHIRE, MK45 4BT,  
UNITED KINGDOM

TEL: +44 (0) 1525 863000  
FAX: +44 (0) 1525 863001

MATERIAL: **LOW CARBON MILD STEEL** No off **1**

FINISH: **PRIME AND PAINT BLACK**

DIMENSIONS IN MILLIMETRES UNLESS OTHERWISE SPECIFIED

THIRD ANGLE PROJECTION

TOLERANCES ON DIMENSIONS UNLESS OTHERWISE SPECIFIED

NOMINAL SIZE OF DIMENSION: 0-120 120-315 315-1000 1000+

0 DECIMAL PLACES:  $\pm 0.5$   $\pm 1$   $\pm 1.5$   $\pm 3.0$

2 DECIMAL PLACES:  $\pm 0.25$

ANGULAR TOLERANCE:  $\pm 0' 30''$

DRAWN BY: **DIRK ANSORGE** TITLE: **WHEEL & TRACK RIG**

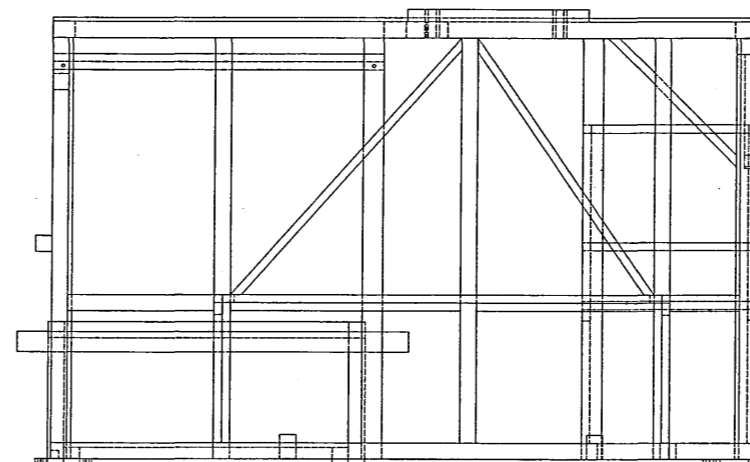
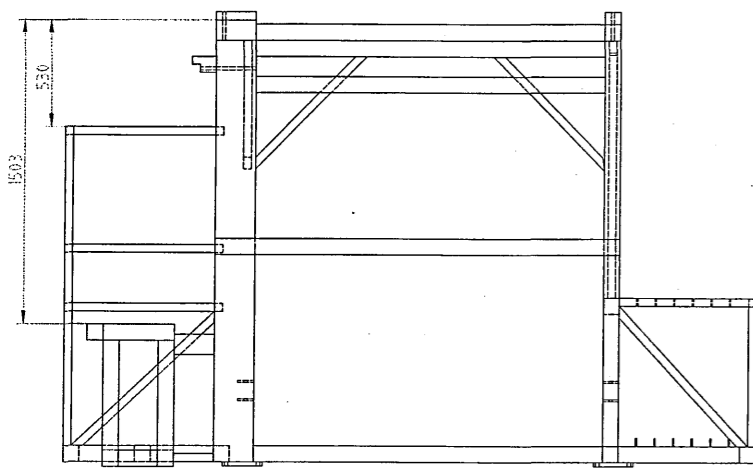
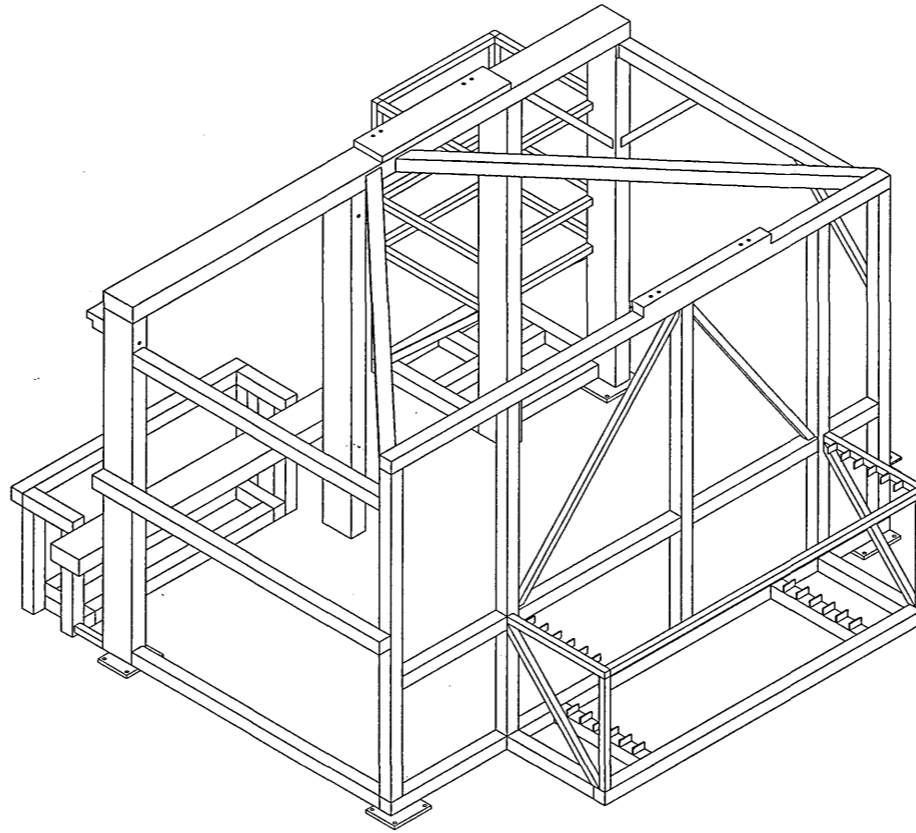
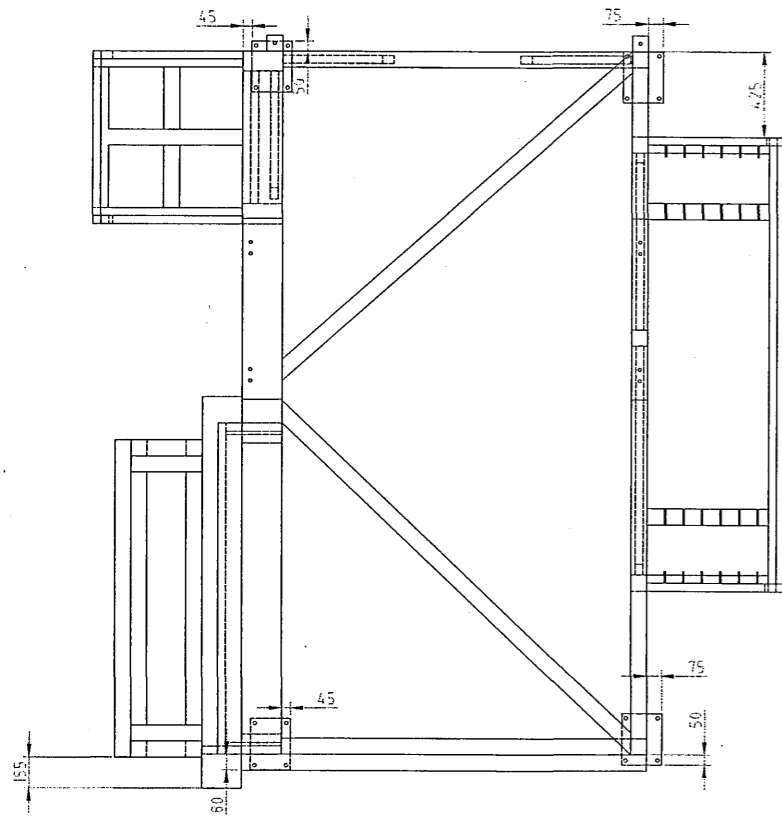
DATE: **10.12.2004** **Pieces of Main Frame**

CHECKED BY: PART No. **759002A04** SH. **2 of 2**

DATE: **759002A04**

DO NOT SCALE

### 5.2 Main Frame with Load Boxes (759003A04)



PART No.		759003A04
ISSUE	CHANGE RECORD	DATE-AUTHY
1	PRODUCTION REL	DA04

NOTES:

All open box sections to be capped with 3mm steel

All joints weld around unless specified otherwise.

Fillet weld min leg=7mm for 80x80 and 40x40

© CRANFIELD UNIVERSITY 2004. ALL RIGHTS RESERVED. THIS DRAWING IS THE EMERENTIAL PROPERTY OF THE ABOVE NAMED COMPANY. WITHOUT WHOSE PRIOR WRITTEN CONSENT IT MUST NOT BE COPIED, USED OR COMMUNICATED TO OTHERS, WHOLLY OR IN PART.

**Cranfield UNIVERSITY**  
Silsoe

SILSOE CAMPUS DESIGN OFFICE  
NEAR ENGINEERING GROUP  
SILSOE CAMPUS, SILSOE,  
BEDFORDSHIRE, MK45 4DT,  
UNITED KINGDOM. TEL +44 (0) 1525 863000  
FAX +44 (0) 1525 863001

MATERIAL: **LOW CARBON MILD STEEL** No off 1

FINISH: **PRIME AND PAINT BLACK**

DIMENSIONS IN MILLIMETRES UNLESS OTHERWISE SPECIFIED

THIRD ANGLE PROJECTION

TOLERANCES ON DIMENSIONS UNLESS OTHERWISE SPECIFIED

NOMINAL SIZE	0-120	120-315	315-1000	1000+
OF DIMENSION	$\pm 0.15$	$\pm 0.2$	$\pm 0.3$	$\pm 0.5$
2 or 3 DECIMAL PLACES	$\pm 0.05$	$\pm 0.1$	$\pm 0.15$	$\pm 0.2$
2 DECIMAL PLACES	$\pm 0.05$	$\pm 0.1$	$\pm 0.15$	$\pm 0.2$
ANGULAR TOLERANCE	$\pm 0' 30''$			

DRAWN BY: DIRK ANSORGE TITLE: WHEEL & TRACK RIG

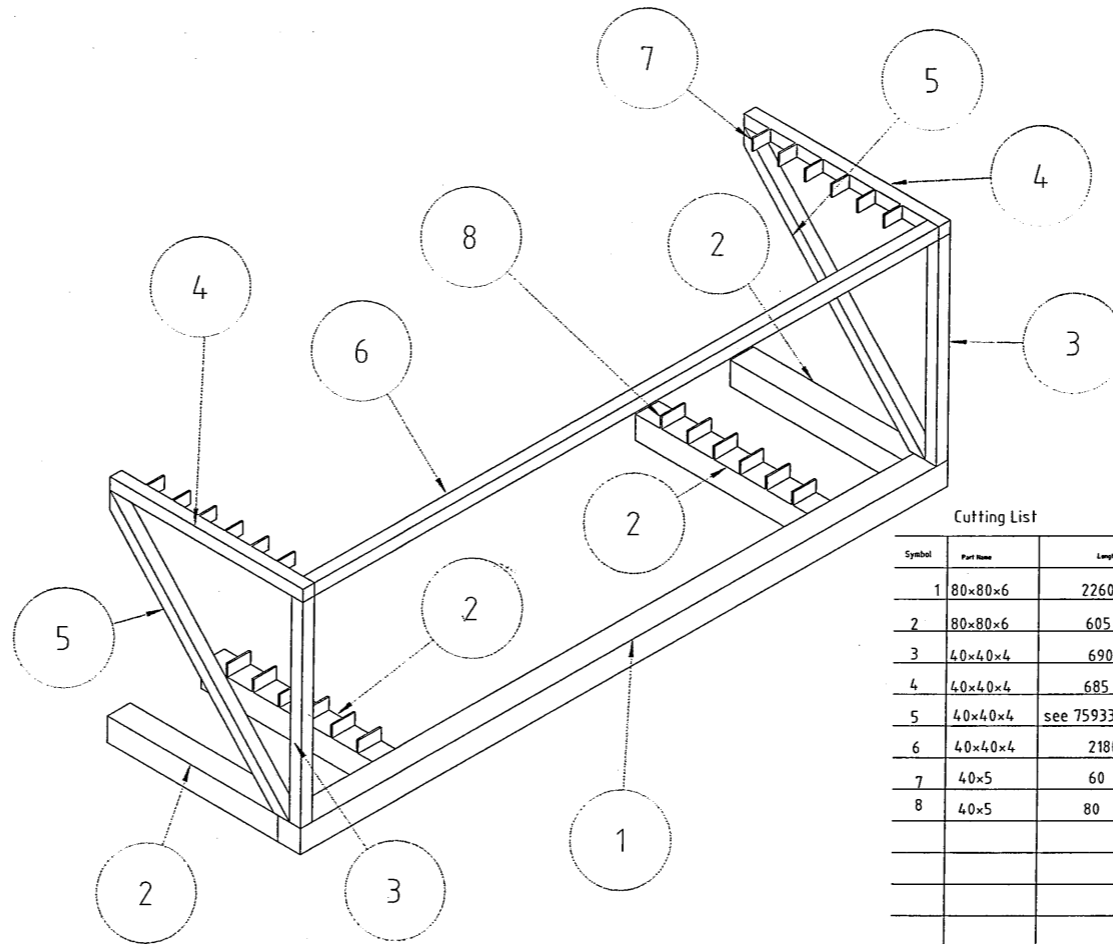
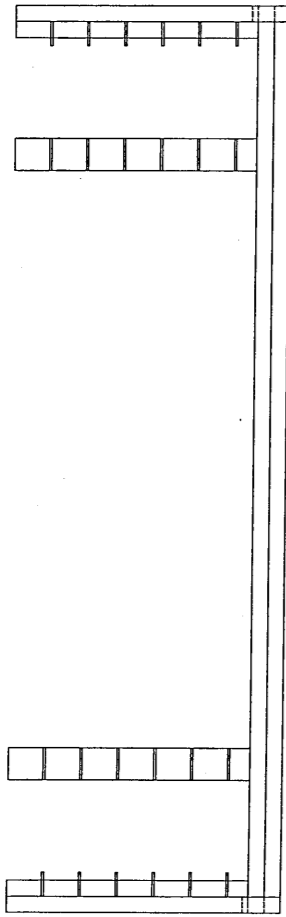
DATE: 10.12.2004 Assembly without LB&Arle

CHECKED BY: PART No. 759003A04

DATE: SHT. 1 OF 1

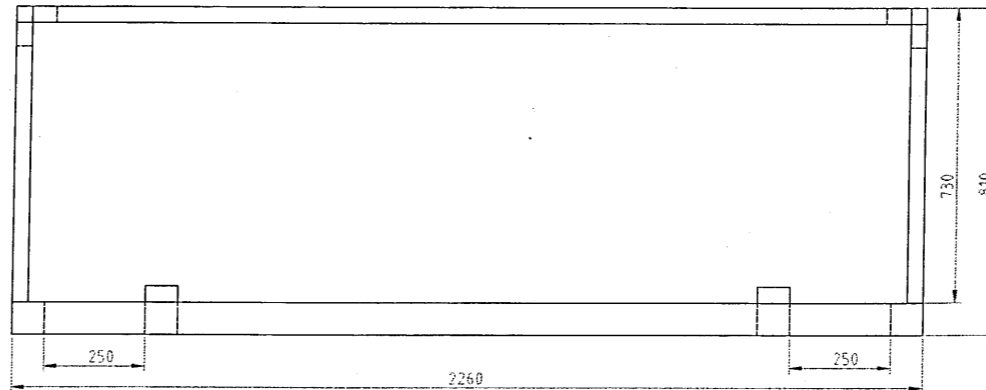
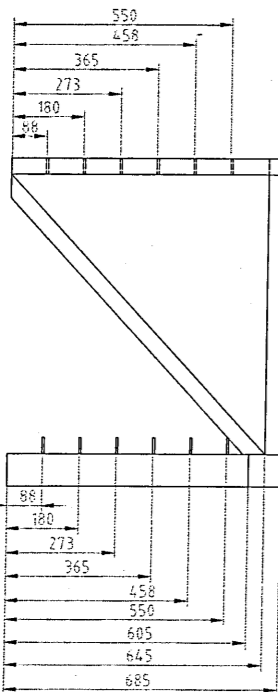
DO NOT SCALE

5.3 Load Box for Plates (759101P04)



Cutting List

Symbol	Part Name	Length	Quantity
1	80x80x6	2260	1
2	80x80x6	605	4
3	40x40x4	690	2
4	40x40x4	685	2
5	40x40x4	see 759333P04	2
6	40x40x4	2180	1
7	40x5	60	12
8	40x5	80	12



PART No. 759101P04		
ISSUE	CHANGE RECORD	DATE-AUTHY
1	PRODUCTION REL.	DA04

NOTES:

All joints weld around unless specified otherwise.  
 Fillet weld min leg=7mm for 80x80 and 40x40

© CRANFIELD UNIVERSITY 2004. ALL RIGHTS RESERVED.  
 THIS DRAWING IS THE CONFIDENTIAL PROPERTY OF THE ABOVE NAMED COMPANY WITHOUT WHOSE PRIOR WRITTEN CONSENT IT MUST NOT BE COPIED, USED OR COMMUNICATED TO OTHERS, WHOLLY OR IN PART.

**Cranfield UNIVERSITY**  
 Silsoe

SILSOE CAMPUS DESIGN OFFICE  
 NRS0 ENGINEERING GROUP  
 SILSOE CAMPUS, SILSOE,  
 BEDFORDSHIRE, MK45 4DT,  
 UNITED KINGDOM. TEL +44 (0) 1525 863000  
 FAX +44 (0) 1525 863001

MATERIAL: **LOW CARBON MILD STEEL**

FINISH: 1

DIMENSIONS IN MILLIMETRES UNLESS OTHERWISE SPECIFIED

THIRD ANGLE PROJECTION

TOLERANCES ON DIMENSIONS UNLESS OTHERWISE SPECIFIED

NORMAL SIZE OF DIMENSION	0-120	120-315	315-1000	1000+
0 or 1 DECIMAL PLACE	±0.5	±1	±1.5	±3.0
2 DECIMAL PLACES	±0.25			
ANGULAR TOLERANCE	±0° 30'			

DRAWN BY: DIRK ANSORGE  
 DATE: 10.12.2004

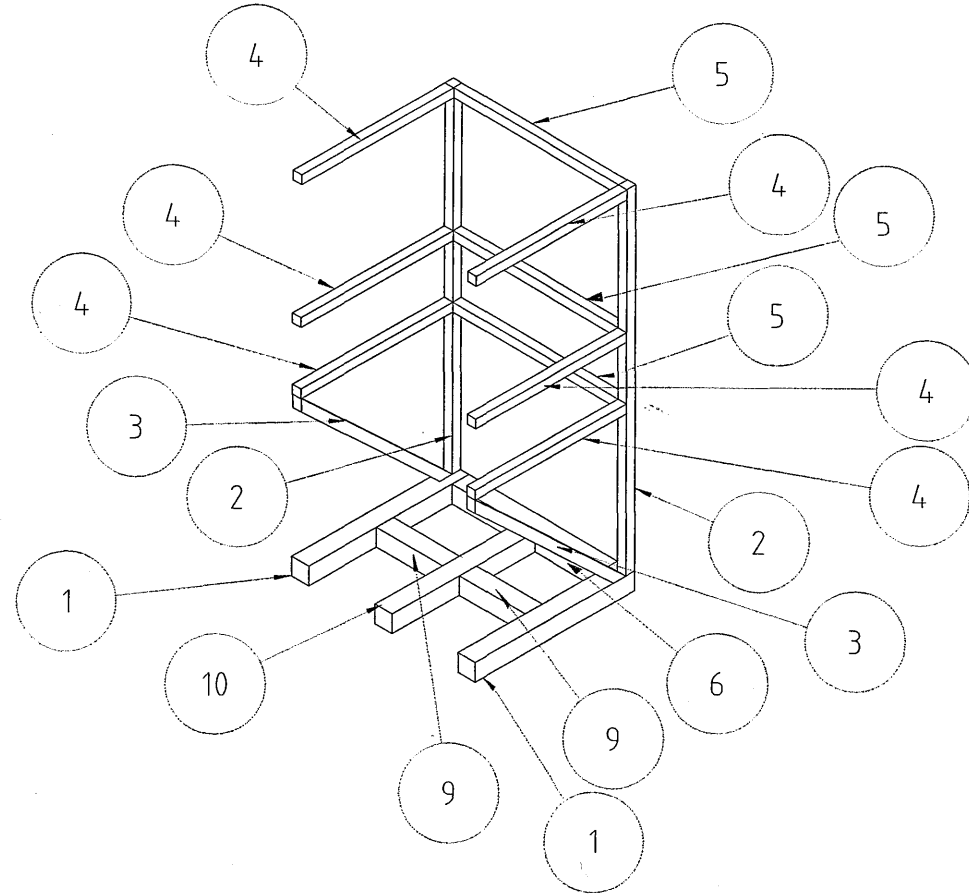
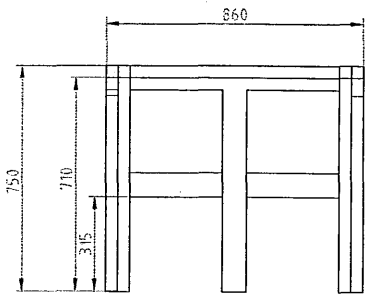
CHECKED BY:  
 DATE:

TITLE: **WHEEL & TRACK RIG Loadbox for Plates**

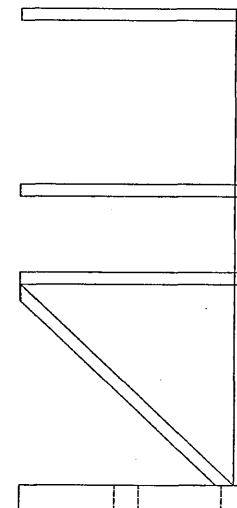
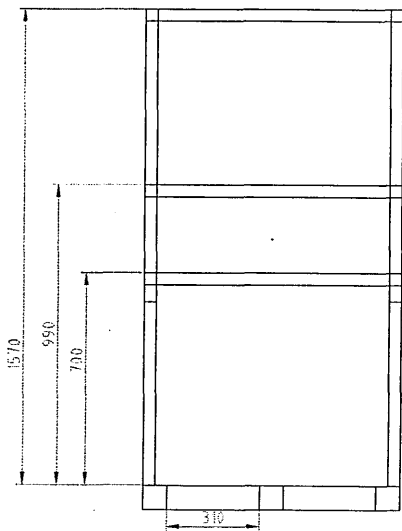
PART No. 759101P04  
 SHT. 7 of 1

DO NOT SCALE

5.4 Load Box for Boxes (I) (759102P04)



Symbol	Part Name	Length	Quantity
1	80x80x6	750	2
2	40x40x4	1570	2
3	40x40x4	see 759333P04	2
4	40x40x4	710	6
5	40x40x4	780	3
6	80x80x6	700	1
9	80x80x6	310	2
10	80x80x6	670	1



PART No. 759102P04

ISSUE	CHANGE RECORD	DATE/AUTHY	
1	PRODUCTION REL	DA04	

NOTES:

All joints weld around unless specified otherwise.  
Fillet weld min leg=7mm for 80x80 and 40x40

© CRANFIELD UNIVERSITY 2004. ALL RIGHTS RESERVED.  
THIS DRAWING IS THE CONFIDENTIAL PROPERTY OF THE ABOVE NAMED COMPANY WITHOUT WHOSE PRIOR WRITTEN CONSENT IT MUST NOT BE COPIED, USED OR COMMUNICATED TO OTHERS, WHOLLY OR IN PART.

**Cranfield UNIVERSITY**  
Silsoe

SILSOE CAMPUS DESIGN OFFICE  
MESH ENGINEERING GROUP  
SILSOE CAMPUS, SILSOE  
BEDFORDSHIRE, MK45 4DT,  
UNITED KINGDOM. TEL +44 (0) 1525 863000  
FAX +44 (0) 1525 863001

MATERIAL: **LOW CARBON MILD STEEL** No off 1

FINISH:

DIMENSIONS IN MILLIMETRES UNLESS OTHERWISE SPECIFIED

THIRD ANGLE PROJECTION

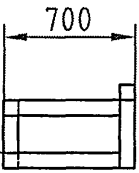
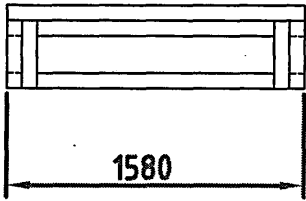
TOLERANCES ON DIMENSIONS UNLESS OTHERWISE SPECIFIED

NOMINAL SIZE	0-120	120-315	315-1000	1000+
OF DIMENSION				
0 OF DECIMAL PLACES	+0.5	+1	+1.5	+3.0
2 DECIMAL PLACES	±0.25			
ANGULAR TOLERANCE	±1° 0' 30"			

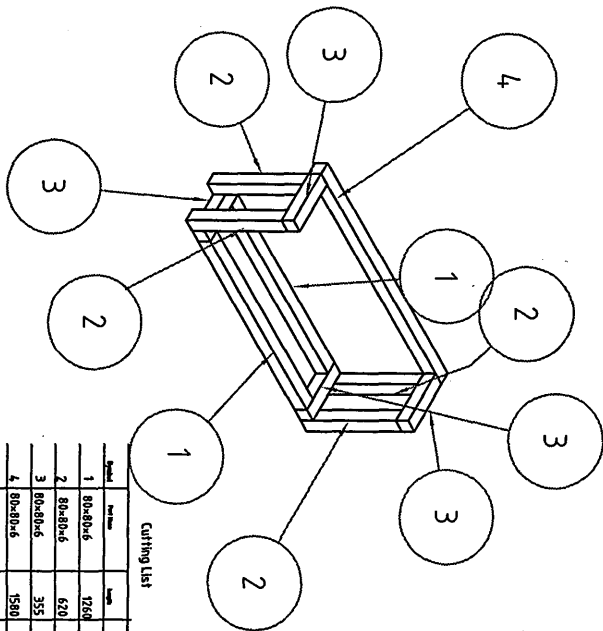
DRAWN BY: <b>DIRK ANSORGE</b>	TITLE <b>WHEEL &amp; TRACK RIG</b>
TELEPHONE: <b>DATE: 10 12 2004</b>	<b>Loadbox for Boxes (I)</b>
CHECKED BY:	PART No. <b>759102P04</b> <span style="float: right;">Sht. 1 of 1</span>
DATE:	

DO NOT SCALE

**5.5 Load Box for Boxes (s) (759103P04)**

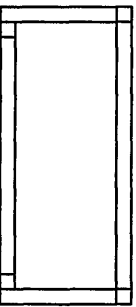


195



Cutting List

Item	Part Name	Qty	Length	Qty
1	80x80x6	2	1760	2
2	80x80x6	4	670	4
3	80x80x6	4	355	4
4	80x80x6	1	1580	1



PART No. **759103P04**

REV	DATE	DESCRIPTION
1	PRODUCTION REL.	DATA

All joints weld around unless specified otherwise.  
 Fillet weld min leg=7mm for 80x80 and 40x40

Consult your local branch office for material specifications and standards. All dimensions are in millimeters unless otherwise specified.

**Camfield**  
 UNIVERSITY  
 Slisoc

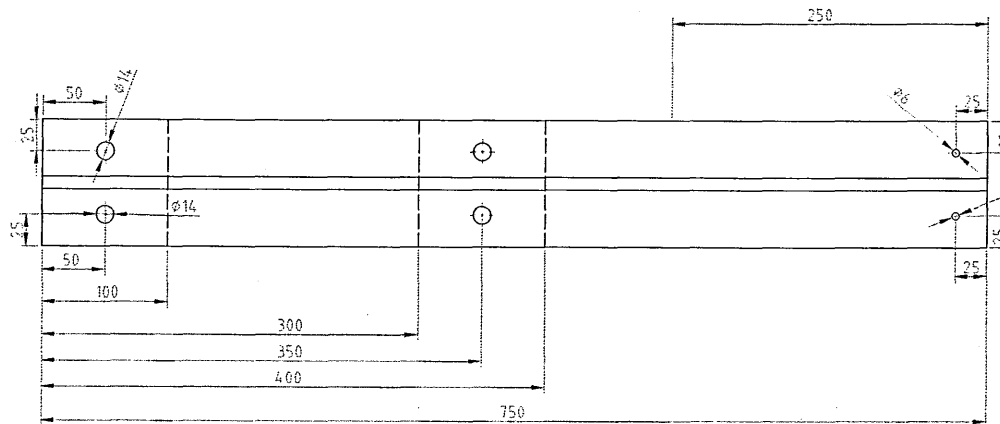
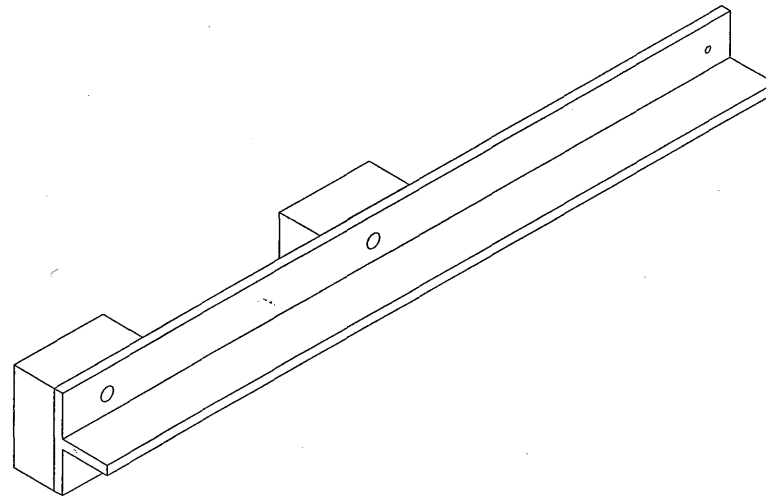
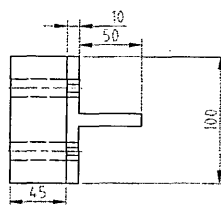
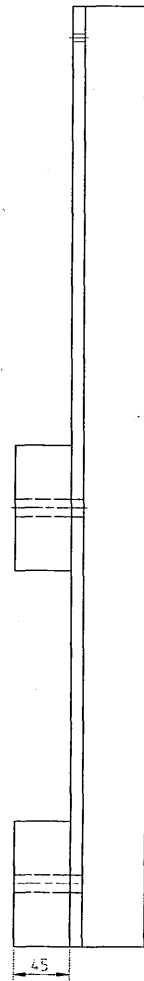
201001010101  
 201001010101

LOW CARBON MILD STEEL

7

PRODUCTION REL. DATA

5.6 Guiding Blocks for Back of the Frame (759105P04)



PART No. 759105P04		
ISSUE	CHANGE RECORD	DATE-AUTHY
1	PRODUCTION REL.	DA04

NOTES:

All joints weld around unless specified otherwise.  
Fillet weld min leg=7mm

© CRANFIELD UNIVERSITY 2004. ALL RIGHTS RESERVED.  
THIS DRAWING IS THE CONFIDENTIAL PROPERTY OF THE ABOVE NAMED COMPANY AND MUST REMAIN UNAVAILABLE TO ANY OTHER PARTY WITHOUT THE WRITTEN CONSENT IN WRITING. IT MUST NOT BE COPIED, USED OR COMMUNICATED TO OTHERS, WHOLLY OR IN PART.

**Cranfield UNIVERSITY**  
Silsoe

SE SOE CAMPUS DESIGN OFFICE  
MSO ENGINEERING GROUP  
SE SOE CAMPUS, SE SOE,  
BEDFORDSHIRE, MK43 4DT,  
UNITED KINGDOM  
TEL +44 (0)1525 863000  
FAX +44 (0)1525 863001

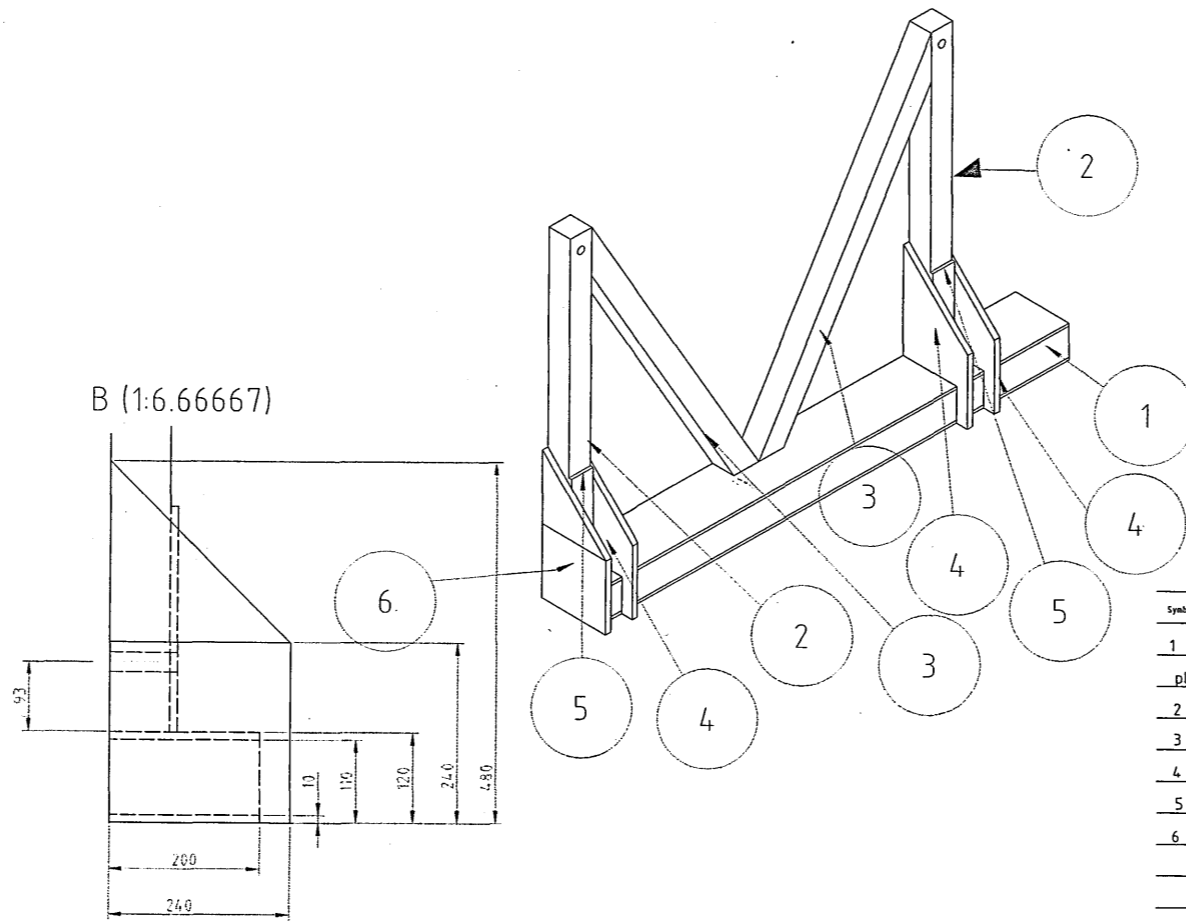
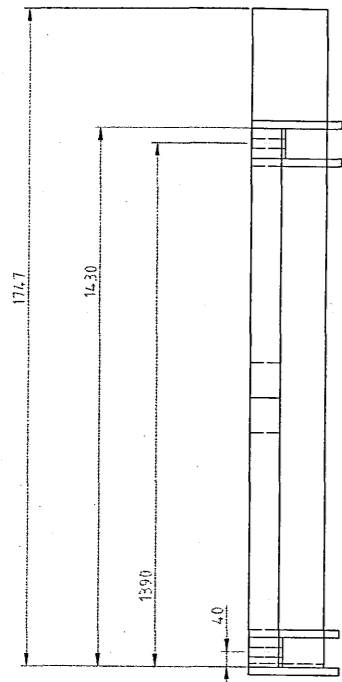
MATERIAL: LOW CARBON MILD STEEL  
FINISH:  
DIMENSIONS IN MILLIMETRES UNLESS OTHERWISE SPECIFIED  
THIRD ANGLE PROJECTION  
TOLERANCES ON DIMENSIONS UNLESS OTHERWISE SPECIFIED  
NOMINAL SIZE OF DIMENSION: 0-100: ±0.15; 100-315: ±0.20; 315-1000: ±0.30  
0 OF DECIMAL PLACES: ±0.15; ±0.20; ±0.30  
1 OF DECIMAL PLACES: ±0.05; ±0.10; ±0.15; ±0.20  
2 OF DECIMAL PLACES: ±0.02; ±0.04; ±0.06  
ANGULAR TOLERANCE: ±0° 30'

DRAWN BY: DIRK ANSORGE  
DATE: 10.12.2004  
CHECKED BY:  
DATE:

TITLE: WHEEL & TRACK RIG  
Plates for Wheels  
PART No. 759105P04  
SHT. 1 OF 1

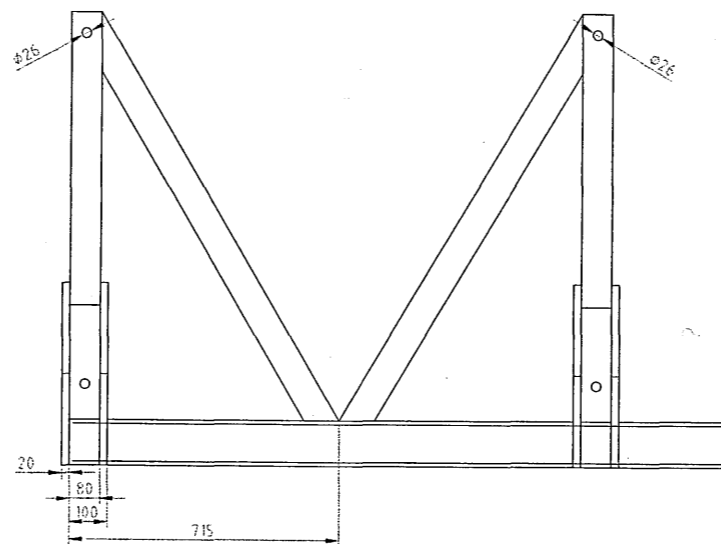
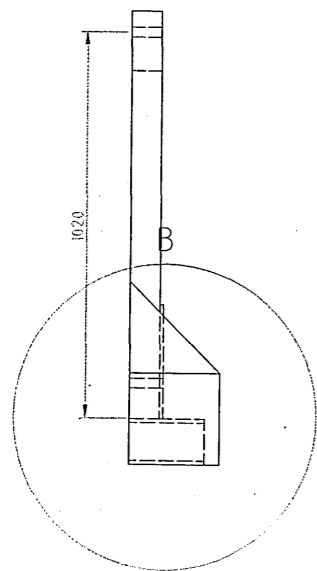
DO NOT SCALE

5.7 LB - Axle Bracket (759106P04)



Cutting List

Symbol	Part Name	Length	Quantity
1	200x100x10 plus a 200x10x174.7 welded on top and below	174.7	1
2	80x80x6	1075	2
3	80x80x6 see 759333P04		2
4	240x480 cut 200x120 20mm thick		3
5	80x300 10mm thick		2
6	240x480 20mm thick		1



PART No. 759106P04		
ISSUE	CHANGE RECORD	DATE-AUTHY
1	PRODUCTION REL.	DA04

NOTES:

All joints weld around unless specified otherwise.  
Fillet weld min leg=7mm for 80x80 and 40x40

© CRANFIELD UNIVERSITY 2004. ALL RIGHTS RESERVED. THIS DRAWING IS THE CONFIDENTIAL PROPERTY OF THE ABOVE NAMED COMPANY WITHOUT WHICH PRIOR WRITTEN CONSENT IT MUST NOT BE COPIED, USED OR COMMUNICATED TO OTHERS, WHOLLY OR IN PART.

**Cranfield UNIVERSITY**  
Silsoe

SILSOE CAMPUS DESIGN OFFICE  
NSM ENGINEERING GROUP  
SILSOE CAMPUS, SILSOE,  
BEDFORDSHIRE, MK45 4DT,  
UNITED KINGDOM. TEL +44 (0) 1525 863000  
FAX +44 (0) 1525 863001

MATERIAL: **LOW CARBON MILD STEEL** No off: **1**

FRESH

DIMENSIONS IN MILLIMETRES UNLESS OTHERWISE SPECIFIED

THIRD ANGLE PROJECTION

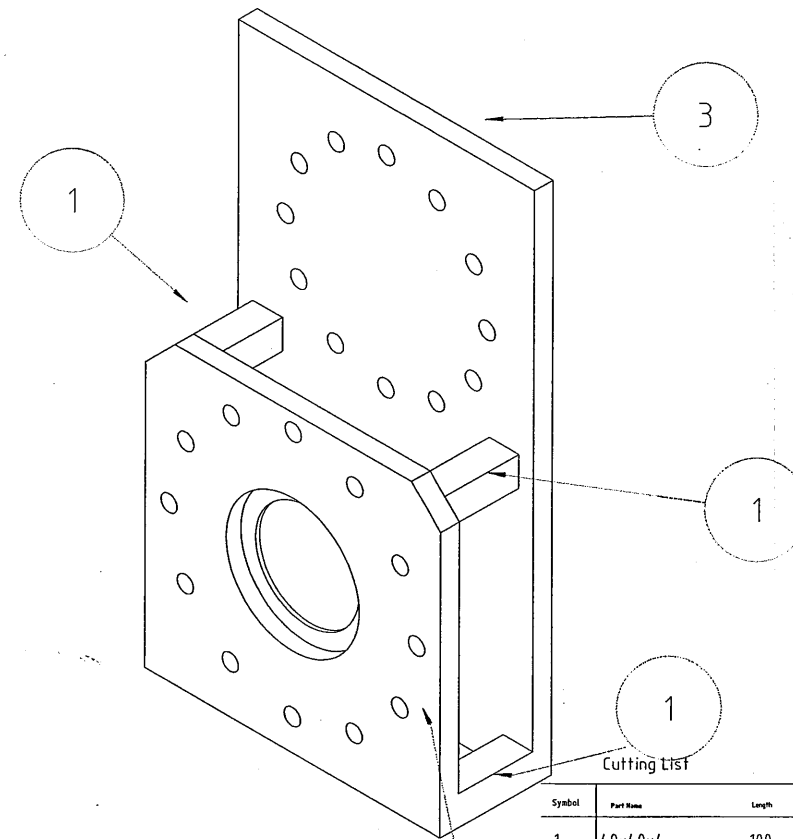
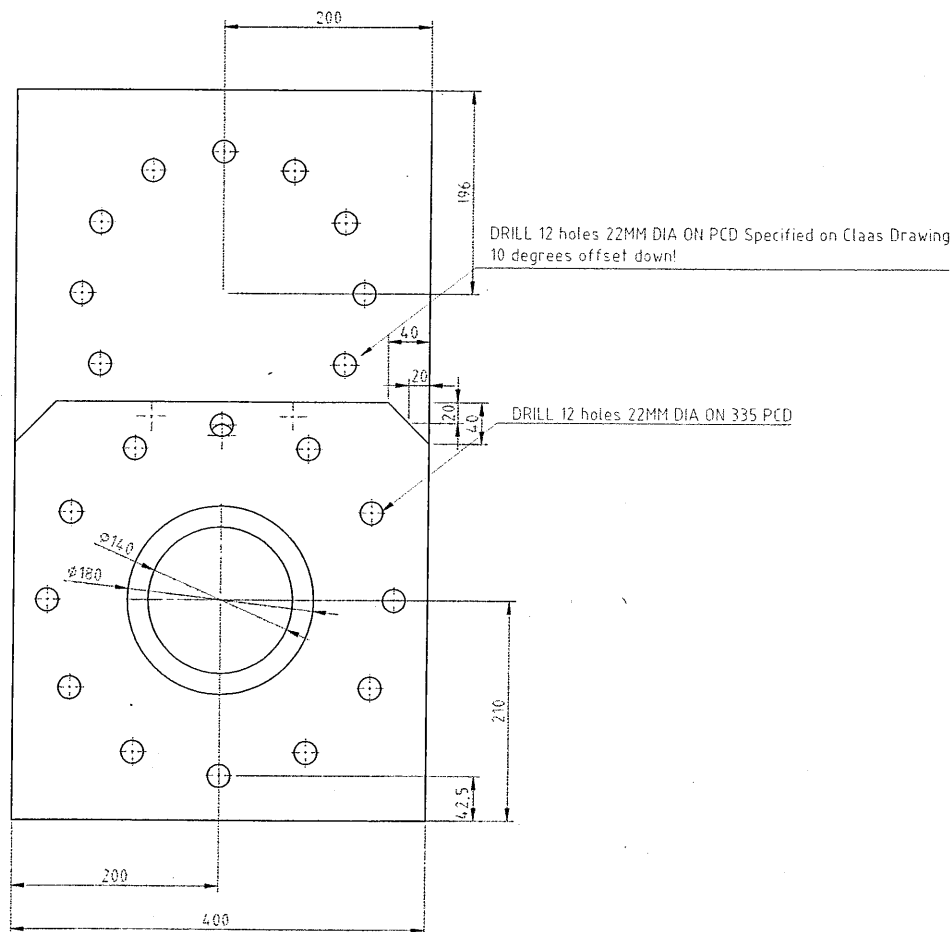
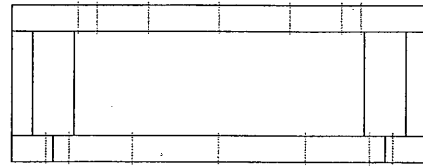
TOLERANCES ON DIMENSIONS UNLESS OTHERWISE SPECIFIED

NOMINAL SIZE	0-120	120-315	315-1000	1000+
OF DIMENSION				
0 or 1 DECIMAL PLACE	+0.5	+1	+1.5	+3.0
2 DECIMAL PLACES			+/- 0.25	
ANGULAR TOLERANCE			+/- 0.30°	

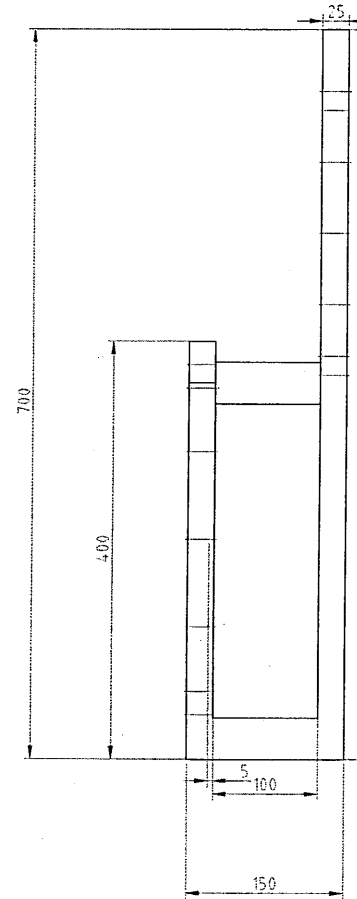
DRAWN BY: DIRK ANSORGE  
TITLE: WHEEL & TRACK RIG  
DATE: 10.12.2004  
LB - Axle bracket  
CHECKED BY: PART No. 759106P04  
DATE: SHEET 1 OF 1

DO NOT SCALE

### 5.8 Wheel – Track Assembly (759108P04)



Symbol	Part Name	Length	Quantity
1	40x40x4	100	4
2	400x400x25 rqt plate		1 xx
3	700x400x25 rqt plate		1
xx two edges cut as specified			



PART No. 759108P04		
ISSUE	CHANGE RECORD	DATE-AUTHY
1	PRODUCTION REL.	DA04

NOTES:  
 All open box sections to be capped with 3mm steel  
 All joints weld around unless specified otherwise.  
 Fillet weld min leg=7mm for 80x80 and 40x40  
 for 20x20 min leg 3mm

© CRANFIELD UNIVERSITY 2004. ALL RIGHTS RESERVED. THIS DRAWING IS THE CONFIDENTIAL PROPERTY OF THE ABOVE NAMED COMPANY WITHOUT WHOLE PRIOR WRITTEN CONSENT IT MUST NOT BE COPIED, USED OR COMMUNICATED TO OTHERS, WHOLLY OR IN PART.

**Cranfield UNIVERSITY**  
 Silsoe

SILSOE CAMPUS DESIGN OFFICE  
 N&R ENGINEERING GROUP  
 SILSOE CAMPUS, SILSOE,  
 BEDFORDSHIRE, MK45 4DT,  
 UNITED KINGDOM. TEL: +44 (0) 1525 863000 FAX: +44 (0) 1525 863001

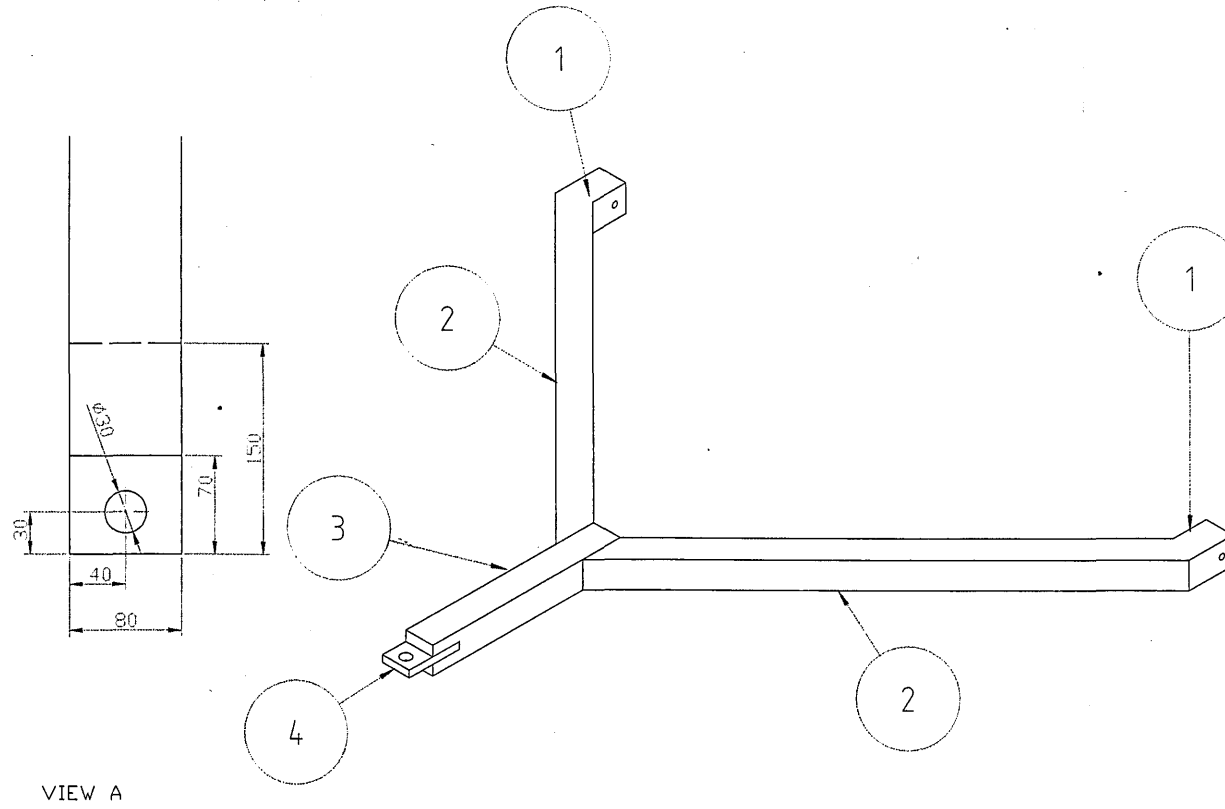
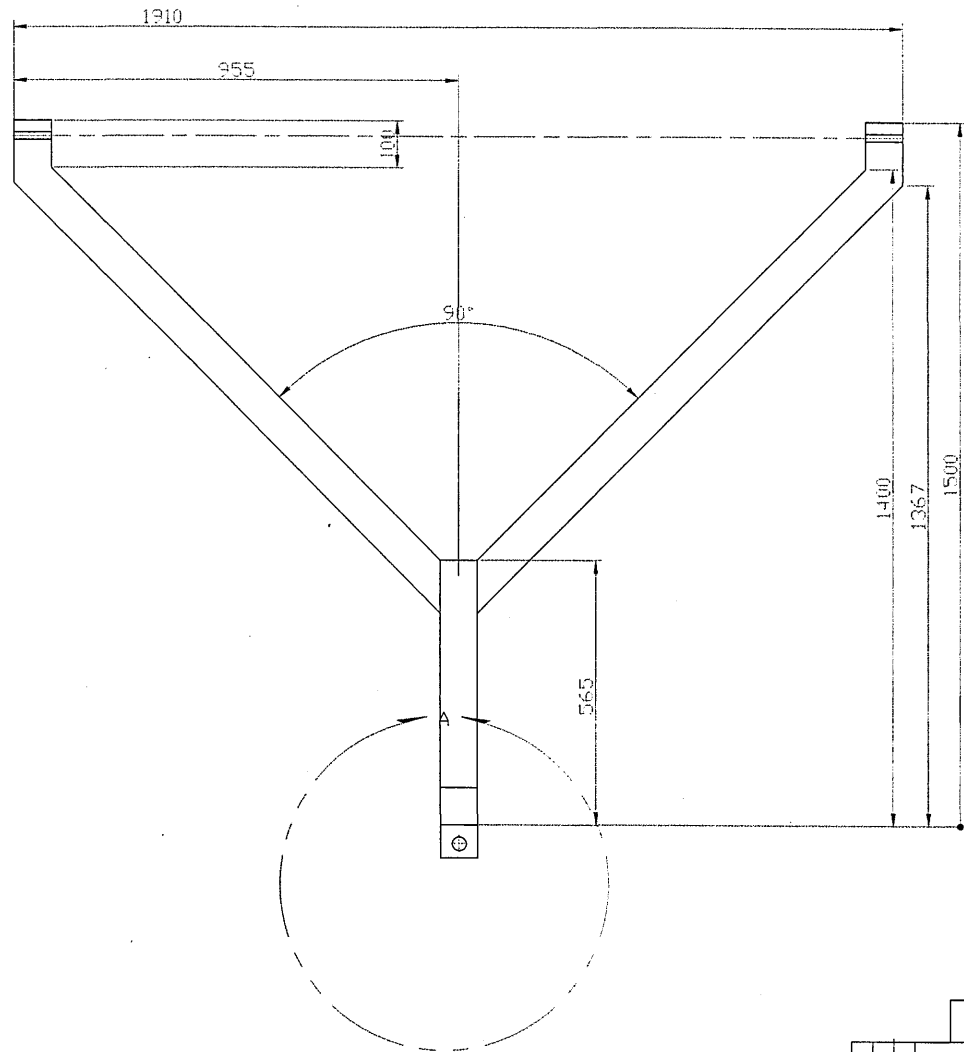
MATERIAL: **LOW CARBON MILD STEEL**  
 FINISH:   
 DIMENSIONS IN MILLIMETRES UNLESS OTHERWISE SPECIFIED  
 THIRD ANGLE PROJECTION

TOLERANCES ON DIMENSIONS UNLESS OTHERWISE SPECIFIED  
 NOMINAL SIZE OF DIMENSION 0-120 120-315 315-1000 1000+  
 0 or 1 DECIMAL PLACE +/-0.5 +/-1 +/-1.5 +/-3.0  
 2 DECIMAL PLACES +/-0.25 +/-0.5  
 ANGULAR TOLERANCE +/- 0°30'

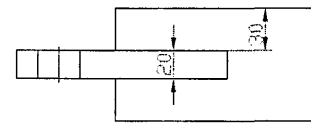
DRAWN BY: DIRK ANSORGE	TITLE <b>WHEEL &amp; TRACK RIG</b> Axle - Track bracket
DATE: 10 12 2004	PART No. 759108P04
CHECKED BY:	SHIT. 1 of 1
DATE:	759108P04
DO NOT SCALE	



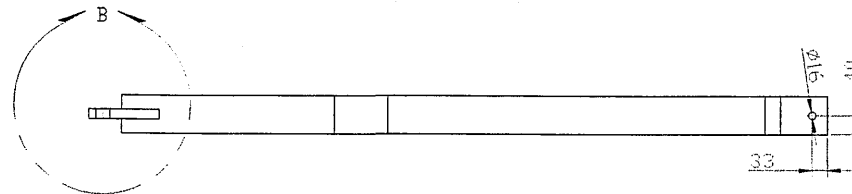
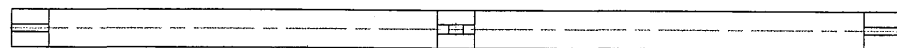
5.9 Drawbar Bracket (759109P04)



VIEW A



VIEW B



Cutting List

Symbol	Part Name	Length	Quantity
1	80*80*5 equal end and 22.5degrees	100/133	2
2	80*80*5 22.5 and 45 degree cut at the end	1217/1181	2
3	80*80*5	565	1
4	80*150 thick 20mm		

PART No. 759109P04		
ISSUE	CHANGE RECORD	DATE+AUTHY
1	PRODUCTION REL.	DA04

NOTES:

All joints weld around unless specified otherwise.  
Fillet weld min leg=7mm for 80\*80 and 40\*40

© CRANFIELD UNIVERSITY 2004 ALL RIGHTS RESERVED.  
THIS DRAWING IS THE CONFIDENTIAL PROPERTY OF THE ABOVE NAMED COMPANY WITHOUT WRITTEN PRIOR WRITTEN CONSENT IT MUST NOT BE COPIED, USED OR COMMUNICATED TO OTHERS, WHOLLY OR IN PART.

**Cranfield UNIVERSITY**  
Silsoe

SILSOE CAMPUS DESIGN OFFICE  
NS301 ENGINEERING GROUP  
SILSOE CAMPUS, SILSOE  
BEDFORDSHIRE, MK45 4DT. TEL +44 (0) 1525 963000  
UNITED KINGDOM. FAX +44 (0) 1525 963001

MATERIAL: LOW CARBON MILD STEEL  
FINISH: PRIME AND PAINT BLACK  
No. off: 1

DIMENSIONS IN MILLIMETRES UNLESS OTHERWISE SPECIFIED  
THIRD ANGLE PROJECTION

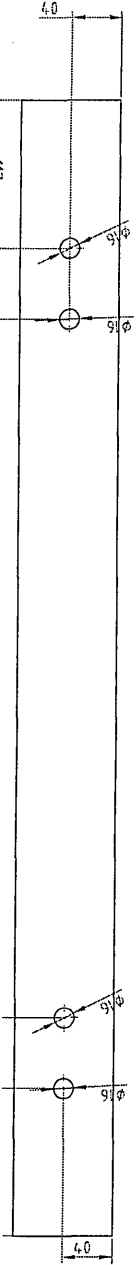
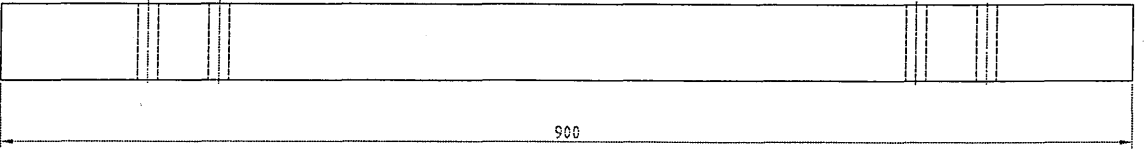
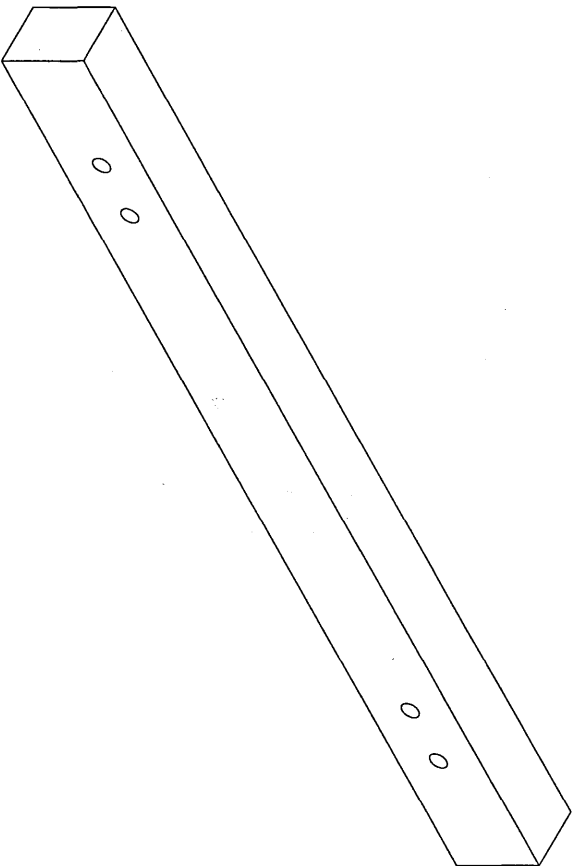
TOLERANCES ON DIMENSIONS UNLESS OTHERWISE SPECIFIED				
NOMINAL SIZE OF DIMENSION	0-120	120-315	315-1000	1000+
0 or 1 DECIMAL PLACE	+0.5	+1	+1.5	+3.0
2 DECIMAL PLACES	+/- 0.25			
ANGULAR TOLERANCE	+/- 0' 30"			

DRAWN BY: DIRK ANSORGE  
TELE:   
DATE: 10.12.2004  
CHECKED BY:   
DATE:   
TITLE: WHEEL & TRACK RIG  
Drawbar  
PART No. 759109P04  
SHT. 1 OF 1

DO NOT SCALE



**5.11 Piece to Level Linear Bearing (759111P04)**



PART No.		<b>759111P04</b>	
SIZE	ORDER CODE	ALT./REV.	DATE
1	PRODUCTION REL.		

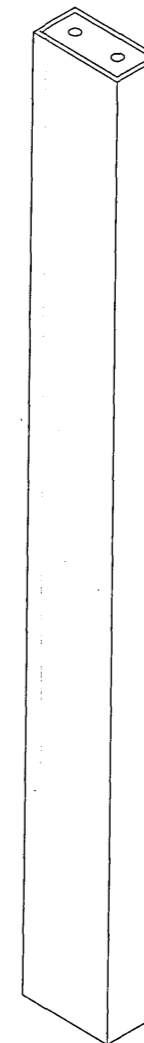
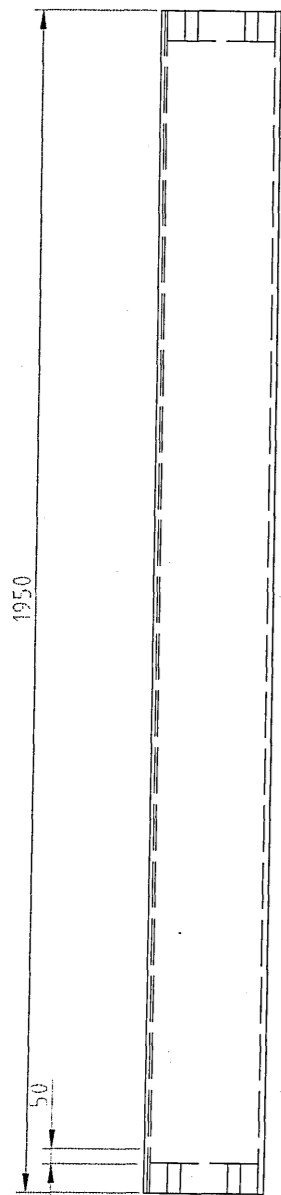
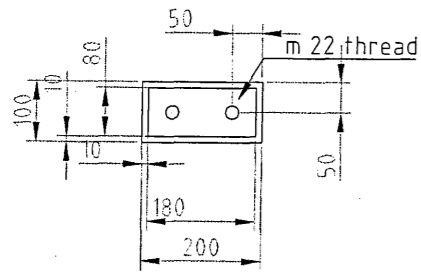
Overall Dimensions are important, not the box section or how it is put together. Just no pieces with less than 4mm wall thickness.

Cambridge UNIVERSITY  
SILSOE  
1752 ENGINEERING AVENUE  
MILTON KEYNES MK15 9JQ  
TEL: 01295 833000  
WWW.CAMBRIDGEUNIVERSITYPRESS.COM

LOW CARBON MILD STEEL  
FINISH: POLISHED  
MATERIAL SPECIFICATION: EN 10088-2  
TENSILE STRENGTH: 500 N/mm<sup>2</sup>  
YIELD STRENGTH: 275 N/mm<sup>2</sup>  
Elongation: 20%  
Surface finish: Ra 0.8



5.13 Box Section with holes to bolt Linear Bearing on (759113P04)



PART No. 759113P04

ISSUE	CHANGE RECORD	DATE-AUTHY
1	PRODUCTION REL.	DA04

NOTES:

All 4 holes have same dimensions.  
 200x100x10 box section as origin.  
 Filled with 50mm on both ends.

© CRANFIELD UNIVERSITY 2004. ALL RIGHTS RESERVED.  
 THIS DRAWING IS THE CONFIDENTIAL PROPERTY OF THE ABOVE NAMED COMPANY  
 WITHOUT WHOSE PRIOR WRITTEN CONSENT IT MUST NOT BE COPIED, USED OR  
 COMMUNICATED TO OTHERS, WHOLLY OR IN PART.

**Cranfield UNIVERSITY**  
 Silsoe

SILSOE CAMPUS DESIGN OFFICE  
 NSRI ENGINEERING GROUP  
 SILSOE CAMPUS, SILSOE  
 BEDFORDSHIRE, MK45 4DT,  
 UNITED KINGDOM

TEL +44 (0) 1525 863000  
 FAX +44 (0) 1525 863001

MATERIAL: **LOW CARBON MILD STEEL** No of 1

FINISH: **F**

DIMENSIONS IN MILLIMETRES UNLESS OTHERWISE SPECIFIED

THIRD ANGLE PROJECTION

TOLERANCES ON DIMENSIONS UNLESS OTHERWISE SPECIFIED

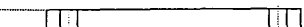
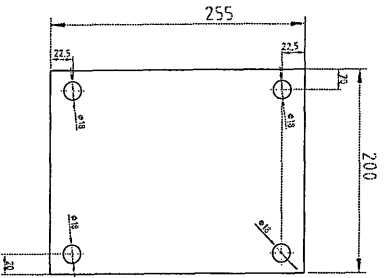
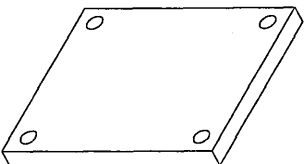
NOMINAL SIZE OF DIMENSION	TOLERANCE
0-120	$\pm 0.25$
120-315	$\pm 0.30$
315-1000	$\pm 0.50$
0 or 1 DECIMAL PLACE	$\pm 0.5$
2 DECIMAL PLACES	$\pm 0.25$
ANGULAR TOLERANCE	$\pm 0' 30''$

DRAWN BY: **DIRK ANSORGE** TITLE: **WHEEL & TRACK RIG**  
 DATE: **10.12.2004** **Linear Bearing Sit**

CHECKED BY: DATE: PART No. **759113P04** SHT. **1** OF. **1**

DO NOT SCALE

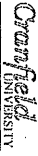
5.14 Wheel Plate to attach Castors (759114P04)



PART No 759114P04

REV	CHANGED BY	AUTHORITY
1	PRODUCTION REL.	DAH

All joints weld around unless specified otherwise.  
Filler weld min leg=7mm

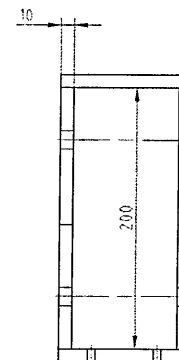
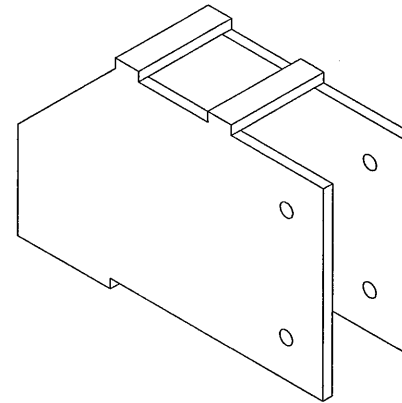
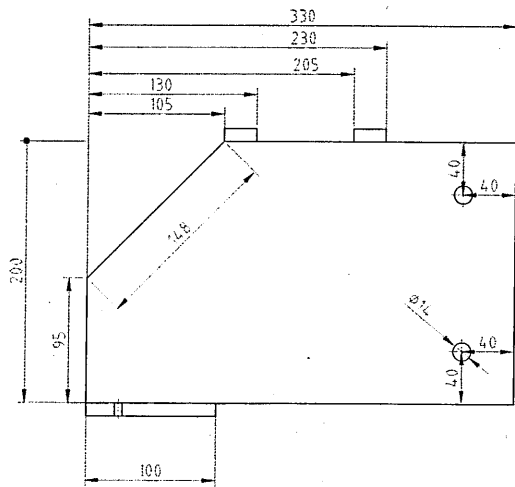
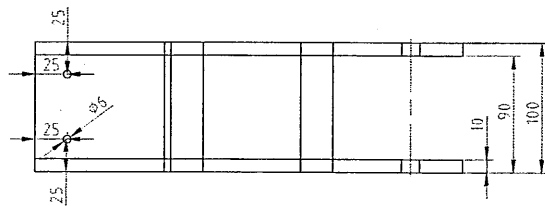
  
 CROWNFIELD  
 UNIVERSITY  
 ST150E  
 ST. ALBANS, HERTS., AL1 1AA, U.K.  
 TEL: 045 89 525 1933  
 FAX: 045 89 525 1933

MATERIAL LOW CARBON MILD STEEL QUANTITY 2

FINISH

SPECIFIC INSTRUCTIONS FOR THE FABRICATOR TO BE ADHERED TO  
 1. WELDING  
 2. ALL JOINTS WELD AROUND UNLESS SPECIFIED OTHERWISE  
 3. FILLER WELD MIN LEG = 7MM  
 4. ALL DIMENSIONS TO CENTRE UNLESS OTHERWISE STATED  
 5. FINISH TO SURFACE UNLESS OTHERWISE STATED  
 6. DIMENSIONS TO SURFACE UNLESS OTHERWISE STATED  
 7. DIMENSIONS TO SURFACE UNLESS OTHERWISE STATED  
 8. DIMENSIONS TO SURFACE UNLESS OTHERWISE STATED  
 9. DIMENSIONS TO SURFACE UNLESS OTHERWISE STATED  
 10. DIMENSIONS TO SURFACE UNLESS OTHERWISE STATED  
 11. DIMENSIONS TO SURFACE UNLESS OTHERWISE STATED  
 12. DIMENSIONS TO SURFACE UNLESS OTHERWISE STATED  
 13. DIMENSIONS TO SURFACE UNLESS OTHERWISE STATED  
 14. DIMENSIONS TO SURFACE UNLESS OTHERWISE STATED  
 15. DIMENSIONS TO SURFACE UNLESS OTHERWISE STATED  
 16. DIMENSIONS TO SURFACE UNLESS OTHERWISE STATED  
 17. DIMENSIONS TO SURFACE UNLESS OTHERWISE STATED  
 18. DIMENSIONS TO SURFACE UNLESS OTHERWISE STATED  
 19. DIMENSIONS TO SURFACE UNLESS OTHERWISE STATED  
 20. DIMENSIONS TO SURFACE UNLESS OTHERWISE STATED  
 21. DIMENSIONS TO SURFACE UNLESS OTHERWISE STATED  
 22. DIMENSIONS TO SURFACE UNLESS OTHERWISE STATED  
 23. DIMENSIONS TO SURFACE UNLESS OTHERWISE STATED  
 24. DIMENSIONS TO SURFACE UNLESS OTHERWISE STATED  
 25. DIMENSIONS TO SURFACE UNLESS OTHERWISE STATED  
 26. DIMENSIONS TO SURFACE UNLESS OTHERWISE STATED  
 27. DIMENSIONS TO SURFACE UNLESS OTHERWISE STATED  
 28. DIMENSIONS TO SURFACE UNLESS OTHERWISE STATED  
 29. DIMENSIONS TO SURFACE UNLESS OTHERWISE STATED  
 30. DIMENSIONS TO SURFACE UNLESS OTHERWISE STATED  
 31. DIMENSIONS TO SURFACE UNLESS OTHERWISE STATED  
 32. DIMENSIONS TO SURFACE UNLESS OTHERWISE STATED  
 33. DIMENSIONS TO SURFACE UNLESS OTHERWISE STATED  
 34. DIMENSIONS TO SURFACE UNLESS OTHERWISE STATED  
 35. DIMENSIONS TO SURFACE UNLESS OTHERWISE STATED  
 36. DIMENSIONS TO SURFACE UNLESS OTHERWISE STATED  
 37. DIMENSIONS TO SURFACE UNLESS OTHERWISE STATED  
 38. DIMENSIONS TO SURFACE UNLESS OTHERWISE STATED  
 39. DIMENSIONS TO SURFACE UNLESS OTHERWISE STATED  
 40. DIMENSIONS TO SURFACE UNLESS OTHERWISE STATED  
 41. DIMENSIONS TO SURFACE UNLESS OTHERWISE STATED  
 42. DIMENSIONS TO SURFACE UNLESS OTHERWISE STATED  
 43. DIMENSIONS TO SURFACE UNLESS OTHERWISE STATED  
 44. DIMENSIONS TO SURFACE UNLESS OTHERWISE STATED  
 45. DIMENSIONS TO SURFACE UNLESS OTHERWISE STATED  
 46. DIMENSIONS TO SURFACE UNLESS OTHERWISE STATED  
 47. DIMENSIONS TO SURFACE UNLESS OTHERWISE STATED  
 48. DIMENSIONS TO SURFACE UNLESS OTHERWISE STATED  
 49. DIMENSIONS TO SURFACE UNLESS OTHERWISE STATED  
 50. DIMENSIONS TO SURFACE UNLESS OTHERWISE STATED  
 51. DIMENSIONS TO SURFACE UNLESS OTHERWISE STATED  
 52. DIMENSIONS TO SURFACE UNLESS OTHERWISE STATED  
 53. DIMENSIONS TO SURFACE UNLESS OTHERWISE STATED  
 54. DIMENSIONS TO SURFACE UNLESS OTHERWISE STATED  
 55. DIMENSIONS TO SURFACE UNLESS OTHERWISE STATED  
 56. DIMENSIONS TO SURFACE UNLESS OTHERWISE STATED  
 57. DIMENSIONS TO SURFACE UNLESS OTHERWISE STATED  
 58. DIMENSIONS TO SURFACE UNLESS OTHERWISE STATED  
 59. DIMENSIONS TO SURFACE UNLESS OTHERWISE STATED  
 60. DIMENSIONS TO SURFACE UNLESS OTHERWISE STATED  
 61. DIMENSIONS TO SURFACE UNLESS OTHERWISE STATED  
 62. DIMENSIONS TO SURFACE UNLESS OTHERWISE STATED  
 63. DIMENSIONS TO SURFACE UNLESS OTHERWISE STATED  
 64. DIMENSIONS TO SURFACE UNLESS OTHERWISE STATED  
 65. DIMENSIONS TO SURFACE UNLESS OTHERWISE STATED  
 66. DIMENSIONS TO SURFACE UNLESS OTHERWISE STATED  
 67. DIMENSIONS TO SURFACE UNLESS OTHERWISE STATED  
 68. DIMENSIONS TO SURFACE UNLESS OTHERWISE STATED  
 69. DIMENSIONS TO SURFACE UNLESS OTHERWISE STATED  
 70. DIMENSIONS TO SURFACE UNLESS OTHERWISE STATED  
 71. DIMENSIONS TO SURFACE UNLESS OTHERWISE STATED  
 72. DIMENSIONS TO SURFACE UNLESS OTHERWISE STATED  
 73. DIMENSIONS TO SURFACE UNLESS OTHERWISE STATED  
 74. DIMENSIONS TO SURFACE UNLESS OTHERWISE STATED  
 75. DIMENSIONS TO SURFACE UNLESS OTHERWISE STATED  
 76. DIMENSIONS TO SURFACE UNLESS OTHERWISE STATED  
 77. DIMENSIONS TO SURFACE UNLESS OTHERWISE STATED  
 78. DIMENSIONS TO SURFACE UNLESS OTHERWISE STATED  
 79. DIMENSIONS TO SURFACE UNLESS OTHERWISE STATED  
 80. DIMENSIONS TO SURFACE UNLESS OTHERWISE STATED  
 81. DIMENSIONS TO SURFACE UNLESS OTHERWISE STATED  
 82. DIMENSIONS TO SURFACE UNLESS OTHERWISE STATED  
 83. DIMENSIONS TO SURFACE UNLESS OTHERWISE STATED  
 84. DIMENSIONS TO SURFACE UNLESS OTHERWISE STATED  
 85. DIMENSIONS TO SURFACE UNLESS OTHERWISE STATED  
 86. DIMENSIONS TO SURFACE UNLESS OTHERWISE STATED  
 87. DIMENSIONS TO SURFACE UNLESS OTHERWISE STATED  
 88. DIMENSIONS TO SURFACE UNLESS OTHERWISE STATED  
 89. DIMENSIONS TO SURFACE UNLESS OTHERWISE STATED  
 90. DIMENSIONS TO SURFACE UNLESS OTHERWISE STATED  
 91. DIMENSIONS TO SURFACE UNLESS OTHERWISE STATED  
 92. DIMENSIONS TO SURFACE UNLESS OTHERWISE STATED  
 93. DIMENSIONS TO SURFACE UNLESS OTHERWISE STATED  
 94. DIMENSIONS TO SURFACE UNLESS OTHERWISE STATED  
 95. DIMENSIONS TO SURFACE UNLESS OTHERWISE STATED  
 96. DIMENSIONS TO SURFACE UNLESS OTHERWISE STATED  
 97. DIMENSIONS TO SURFACE UNLESS OTHERWISE STATED  
 98. DIMENSIONS TO SURFACE UNLESS OTHERWISE STATED  
 99. DIMENSIONS TO SURFACE UNLESS OTHERWISE STATED  
 100. DIMENSIONS TO SURFACE UNLESS OTHERWISE STATED

5.15 Guiding Blocks (759115P04)



PART No			759115P04
ISSUE	CHANGE RECORD	DATE-AUTHY	
1	PRODUCTION REL.		DA04

NOTES:

All joints weld around unless specified otherwise.  
Fillet weld min leg=7mm

© CRANFIELD UNIVERSITY 2004. ALL RIGHTS RESERVED.  
THIS DRAWING IS THE CONFIDENTIAL PROPERTY OF THE ABOVE NAMED COMPANY  
WITHOUT WHOSE PRIOR WRITTEN CONSENT IT MUST NOT BE COPIED, USED OR  
COMMUNICATED TO OTHERS, WHOLLY OR IN PART.

**Cranfield UNIVERSITY**  
Silsoe

SILSOE CAMPUS DESIGN OFFICE  
NEED ENGINEERING GROUP  
SILSOE CAMPUS, SILSOE  
BEDFORDSHIRE, MK45 4GT,  
UNITED KINGDOM

TEL +44 (0) 1525 863000  
FAX +44 (0) 1525 863001

MATERIAL	No of
LOW CARBON MILD STEEL	2
FINISH	

DIMENSIONS IN MILLIMETRES UNLESS OTHERWISE SPECIFIED

THIRD ANGLE PROJECTION

TOLERANCES ON DIMENSIONS UNLESS OTHERWISE SPECIFIED	
NOMINAL SIZE	0-120 120-315 315-1000 1000+
OF DIMENSION	
0 OF 1 DECIMAL PLACE	+0.5 -0.1 -0.15 -0.30
2 DECIMAL PLACES	+/- 0.25
ANGULAR TOLERANCE	+/- 0° 30'

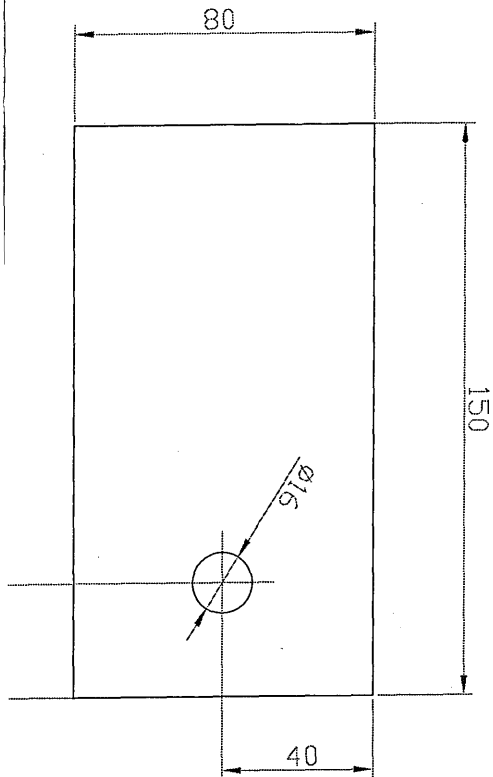
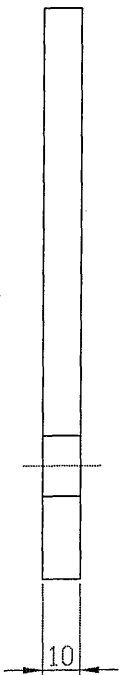
DRAWN BY:	TITLE
DIRK ANSORGE	WHEEL & TRACK RIG
DATE:	Plates for Wheels
10.12.2004	
CHECKED BY:	PART No.
DATE:	759115P04
DO NOT SCALE	SHT. 1 of 1







### 5.18 Plates to attach Drawbar (759118P04)



PART No. 759118P04

ISSUE	CHANGE REASON	DATE/QUANTITY
1	PRODUCTION REL.	DATA

NOTES


All joints weld around  
unless specified  
otherwise.  
File 19027mm  
for 80x80 and 40x40

© Crownfield Engineering Ltd. 1998. All rights reserved.  
This drawing is the property of Crownfield Engineering Ltd. It is to be used for the production of the item specified and is not to be used for any other purpose without the written consent of Crownfield Engineering Ltd.

**Crownfield**  
UNIVERSITY  
SILSOE

1000 CROWNFIELD DRIVE  
SILSOE, BEDFORDSHIRE MK45 2EJ  
UNITED KINGDOM  
TEL: 0456 663 8200  
FAX: 0456 663 8201

MATERIAL: LOW CARBON MILD STEEL

FINISH: PRIMER AND PAINT BLACK

THICKNESS UNLESS OTHERWISE SPECIFIED

SCALE: 1

UNLESS OTHERWISE SPECIFIED  
DIMENSIONS ARE IN MILLIMETERS  
DIMENSIONS IN PARENT BRACKETS ARE IN INCHES

1:19027mm  
2:80x80 and 40x40



## 6 PERFORMANCE OF SINGLE WHEEL TESTER

Normally when not in use the single wheel tester is parked outside the main door leading straight to the soil bin.

After soil bin preparation [as explained in Appendix 1] the single wheel tester is pulled onto the rails over the soil bin to the position where the run is supposed to start using the soil processor inside the building. Once inside the soil bin all 4 guiding brackets have to be bolted onto the frame all the time to ensure a safe ride on the rails. When pulling the frame inside pull the hydraulic hoses at the same time backwards and make sure all the hydraulic hoses are safe and are neither caught below the castors of the soil processor nor by the castors of the single wheel tester at any time.

Then couple the hoses onto the power pack and the MB – Trac. In the next step attach the signal cable flicking the valve to engage the drive inside the power pack to its socket at the power pack. Connect the fifth wheel to the main frame. Then plug the rotary pulse encoders of the fifth wheel and the one mounted to the axle into the IO – Tec wave book. Plug in the cable from the hydraulic pressure transducer, too. Now by pressing the lever arm for the hydraulics upwards lower the wheel/track unit to the top of the soil. Depending on the connection on the MB Trac sometimes flow direction has to be changed.

Make sure the pressure inside the pressure maintaining valve is set to the correct pressure. The weight of the track and axle equals 3 t and the weight of a tire and axle equals 1.5 t. So in case the run should be done at the same working conditions, adjust the pressure in the valve thus that it transfers 9 t. This results in 10.5 t for the tires and 12 t for the track. For the measurement of the pressure inside the pressure maintaining valve use either Daisy Lab Program with the file name dirkrig.dsb on Laptop Engineering 1 or measure the voltage output directly on the pressure maintaining valve. The pressure, corresponding force and voltage output are for 0 bar = 0 kN = 0 Volt and for 115 bar = 90 kN = 0.575Volts. Basically the output of the pressure transducer is 0-600 bar in a 0 – 3 V range. Power supply must be somewhere between 11-30 V for the pressure transducer. During the adjustment of the pressure make sure the hydraulic lever arm is tied upwards and thus the valve is really open. The single wheel tester is ready to drive once the required pressure is set up. Make

sure before you start engaging any driving device the hydraulic lever arm is fixed! Otherwise constant pressure in the cylinder can not be given!

Now switch on the power pack. Turn it to 850 Engine Ref shown (equals 1700 real engine refs). When the tire is run, turn the throttle back in 5 times and the moment the power pack is engaged to drive the frame outwards a further person has to turn the throttle as quick as possible back out 5 times again. This allows a smoother acceleration. In case a track is used turn the power pack again to 850 engine ref shown but then increase it by 5 from there once being engaged. This results in approximately 1m/s forward speed. Now use the button on the control cable to engage the drive and let the device propel itself down the soil bin. Make sure to let the button go early enough to stop where wished. It's good to have a stop line marked with chalk where to let the button go. Read the relevant Health and Safety Instructions of the soil bin and for this project before doing anything on the machinery

## **6.1 Changing Driving Devices**

Due to the width of the 800 mm and 900 mm section tires the final reduction of the axle had to be taken off each time when changing wheels. The tires would not have gone through the space between the hub and the edge of the frame. Therefore a dummy preparation and two large wooden plates were placed on top of the soil in the bin and a pallet placed below the tire. Now pressure from the tire was released to get a larger contact area for the tire to sit on and then the tire was lowered onto the pallet with the hydraulic ram. Afterwards the final reduction was unbolted and the whole assembly was pulled out of the frame using a pallet truck. Once the wheel and the final reduction were outside the frame, the tire was laid down and the final reduction was lifted out using the crane. The tires were placed in using the same procedure vice versa. An advantage of this procedure was the use of the drive shaft for turning the final reduction, keeping the tire fix and thus lining up the holes for the bolts of the axle and final reduction.

In order to attach left hand side tracks the final reduction has to be taken off the axle and then the track – wheel fitting piece (759108P04) has to be bolted onto the axle. Now the track can be placed inside the frame with the crane. Firstly fit the drive shafts together,

then the main axle of the track is bolted to 759108P04. Compared to changing wheels this procedure is easier to accomplish.

## 6.2 Applying Loads

The hydraulic ram and the pressure maintaining valve allowed the application of a constant load onto the axle. Taking the power for the hydraulic ram circuit of the MB – Trac could supply sufficient pressure. Adjusting the load with the pressure maintaining valve and controlling the pressure inside the cylinder with a pressure transducer logging the data via IO - Tec Wavebook and Daisy Lab 5.6 Software onto a laptop was very convenient. A typical pressure curve is shown in **Figure 28**.

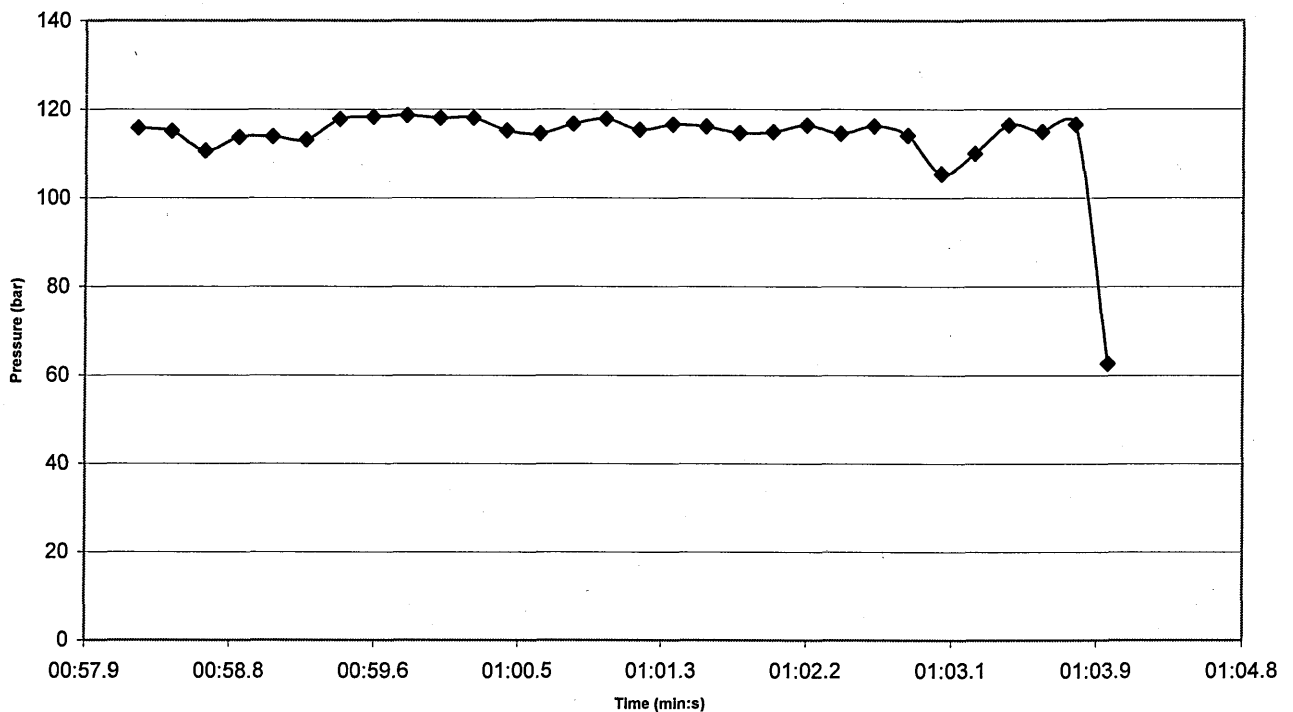


**Figure 28:** Pressure in hydraulic ram during a typical run

The fluctuations in pressure are due to variation in pump performance rather than inaccuracy of the pressure maintaining valve.

### 6.3 Movement

The designed and constructed single wheel tester worked properly. It moved easily up and down the soil bin. Inside the soil bin the soil processor was used to pull and push the frame once not engaged. Outside the soil bin it could be towed with a tractor using a drawbar.

After setting the engine speed of the power pack to  $2/3$  of the required speed at the beginning and winding it up during the acceleration phase of the frame resulted in a very smooth acceleration and driving behavior. This enabled a wheel speed of approximately 1 m/s. A typical speed curve is shown in **Figure 29**. In this figure the actual wheel speed and frame speed is shown. The main frame appears to have a resonant frequency of about 1 Hz.

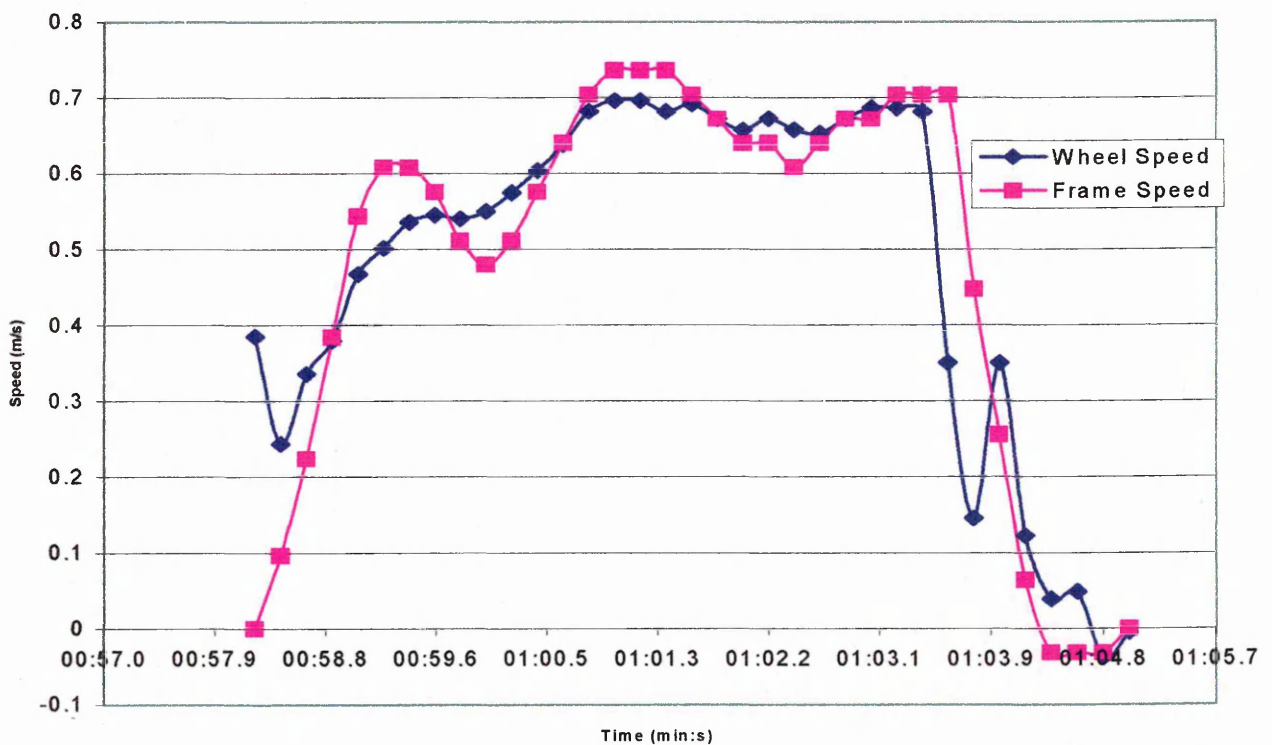


**Figure 29:** A typical speed curve of the wheel (blue) and the frame (pink) in a run

The resonant frequency is due to the elasticity of the driving system as well as the accelerated mass. The 25 m long  $1\frac{1}{2}$  inch hose supplying the axle with the necessary hydraulic power causes most of the elasticity of the driving system. The inertial reaction of the total mass of 16 t of the main frame causes the 2<sup>nd</sup> part of the elasticity.

The high wheel speed for the very first data point shows that most slip occurs right at the beginning and is relatively constant later on. As we are interested in soil compaction and not tire behavior the influence of speed changes within a range of +/- 10 % can be ignored and the velocity profile regarded as satisfying for soil compaction investigations.

## 7 CONCLUSIONS

A useful single wheel tester was built which accomplished all required tasks.

At first the track and wheel sizes specified in **Table 1** fit inside the frame and can be changed without much effort. The whole frame fits into the soil bin onto the rails and the expected rut depth is not exceeded and the combine axle as well as the linear bearing fit into the places where they were planned to fit.

The necessary load (experience up to 9000 kg in these investigations) can be transferred and held constant while sufficient weight remains on all support wheels. The necessary weight for this weight transfer can be put easily on the frame and taken off again using the crane in the soil bin.

The torque emerging from the weight not being applied to the center of the wheel can be taken out by the linear bearing.

Data logging of actual wheel speed, actual frame speed and pressure inside the cylinder worked properly and reliable. Due to the pressure maintaining valve and the pressure gauge the load application onto the wheel / track unit is easily adjustable.

In the context of the Master of Science by Research thesis at CU@S 7 experiments were carried out in the soil bin there. Additional 5 experiments were carried out for the DEFRA project "Trials to Identify Soil Cultivation Practices to Minimise the Impact on Archaeological Sites" project number BD1705 at CU@S. The single wheel tester will at least be used for another two years of soil compaction research at CU@S.



## 8 FUTURE RECOMMENDATIONS

Originally it was planned to be able to place left and right hand side tracks inside the frame. In the process of putting in a right hand track it was realized that merely left hand tracks fitted due to the drive shaft interfering with the linear bearing axle connection piece. In order to avoid a time consuming rebuild the project got another left hand track off a combine harvester to do the work.

The guiders are not precise enough as in the process of the frame moving up and down the soil bin the support wheels (castors) are worn off by 10 mm. So for a future project these should be replaced or a different kind of support wheel chosen.

A convenient storage place and handling device for the hydraulic hoses would be useful as well. So far these are stored in empty load boxes on the frame when not being used.

One problem which occurred with the wheel – track axle adapter (759108P04) was the large deflection. By using RQT 700 instead of mild steel the necessary material thickness could be reduced due to higher tensile strength. However, as both materials have the same elasticity modulus the RQT 700 bends as much as a normal plate would do. So the bottom of the adapter had to be chained back onto the axle to reduced the deflection.

## 9 BIBLIOGRAPHY

Armbruster, K. and Kutzbach, H.D., 1989. Development of a Single Wheel Tester for Measurements on Driven Angled *Wheels*. *Proceedings of the 4<sup>th</sup> European Conference of ISTVS*, Wageningen. Wageningen 1: 8–14.

Bailey, P.H., 1954. The N.I.A.E. Single Wheel Tester. *N.I.A.E. Report* No 40.

Barrelmeyer, T., 1996. Untersuchung der Kraefte an gelenkten und angetriebenen Acker-schlepperraedern bei Gelaende – und Strassenfahrt. PhD – Thesis. University of Hohenheim, Department of Agricultural Engineering. Published in: *Fortschrittberichte VDI, Reihe 14: Landtechnik/Lebensmitteltechnik* Nr. 79. VDI - Verlag, Duesseldorf.

Billington, W.P., 1973. The N.I.A.E. MKII Single Wheel Tester. *J. agric. Engng. Res.* 18: 67-70.

Bosch, Robert GmbH, 1986. *Automotive Handbook*. 2<sup>nd</sup> edition. Ed. U. Adler.

Brassart, F.P., 2005. Evolution of agricultural tyres. Michelin's answer to Farmers needs. Paper No 051108, Section 112 *Innovation in Traction and Tractor Design, ASAE Summer Meeting 2005*, Tampa, Florida.

Burt, E.C., C.A. Reaves, A.C. Bailey and W.D. Pickering, 1980: A Machine for Testing Tractor Tires in Soil Bins. *Transactions of ASAE* – 1980 pp. 546-547 + 552.

Continental Technical Databook. Agricultural Tires, 2005. [http://www.cgs-tires.com/databook\\_en.pdf](http://www.cgs-tires.com/databook_en.pdf) . Accessed on 24.01.2005.

Eriksson, J., I. Hakansson and B. Danfors, 1974: Effect of Soil Compaction on Soil Structure and Crop Yields. *Swedish Institute of Agr. Engng. Bull.* 544, 101p.

Ewo, Fluid Power. Product Catalog, 2004. [http://www.ewo-fluid-power.de/katalog\\_ewo2003/ewo2003.pdf](http://www.ewo-fluid-power.de/katalog_ewo2003/ewo2003.pdf), Accessed on 20.11.2004.

Godwin, R. J. and M.L. Dresser, 2004. Unpublished data.

Grecenko, A., 2003. Tire load rating to reduce soil compaction. *Journal of Terramechanics* 40: 97 – 115.

Hilleke, C., 2004. Personal communication, November 2004.

Horn, R., van den Akker, J.J., and Arvidsson, J., 2000. Subsoil - compaction. Distribution, Processes and Consequences. Catena Verlag, Reiskirchen, Germany.

Kutzbach, H.D., 2000. Trends in power and machinery. *J. agric. Engng. Res.* 76: 237 – 247.

Lines, J.A. and Young, N.A., 1989. A machine for measuring the suspension characteristics of agricultural tires. *J. Terramechanics* 26: 201 – 210.

McAllister, M., 1979. A rig for measuring the forces on a towed wheel. *Journal of Agricultural Engineering Research* 24: 259 – 265.

Oliver, M.J., 2002. Contact patch dynamics of pneumatic tyres in pure sand. Eng.D. Thesis, Cranfield University at Silsoe, classified.

Riley, P. 2004. Personal communication, 8<sup>th</sup> of December 2004.

Shmulevich, I., Mussel, U. and Wolf, D., 1994. A new field single wheel tester. *Ag. Eng.* 94 – D – 034 pp 1-8.

Upadhyaya, S.K., J. Mehlschau, D. Wulfsohn and J.L. Glancey, 1985: Development of a Unique, Mobile, Single Wheel Traction Testing Device. *ASAE Paper* No. 85-1554.

## 10 ACKNOWLEDGEMENTS

The help, support, and agreement of acting as 1<sup>st</sup> referee in this Thesis by Prof. Dr. Boettinger is gratefully acknowledged as well as his cooperation in the double degree program with Cranfield University. Many thanks have to go to Prof. Dr. Kutzbach for his terrific idea of using an existing axle instead of building a new one, acting as a 2<sup>nd</sup> referee for this thesis, and for all his help concerning the University of Hohenheim. I want to thank Prof. Dr. Dick Godwin for suggesting this interesting topic, enabling the project and his great support during the work on this Master Thesis.

Without the financial support from Dr. Helmut Claas and Dr. Hermann Garbers this work would not have been possible and this is very gratefully acknowledged. Christian Hillekes help in carrying out the day – by – day topics was important – thank you very much ☺. Trevor Tyrrell did me a huge favor by supplying a combine harvester for one week.

Very special thanks must go to Dr. James L. Brighton for his enormous support in the construction process and his patience as well as his availability for questions in half hour intervals on several days.

Dr. Terence Richards helped me tremendously without any hesitation in the scientific understanding and analysis of the problems and also gave me important hints and ideas. The remarks of Dr. Peter Crossley are deeply acknowledged as well. Although I did not always like them when they were formulated, they were always correct and true. ☺. Without the help of Phil Trolley and one particularly important hint in manufacturing one of the smaller bits in the workshop at CU@S the whole work would have taken much longer.

I found the help of Christian Brinkmann concerning the day by day business with the University of Hohenheim and his advices on handing in this thesis for Hohenheim very beneficial.

Great thanks also to my parents Hiltrud Ansorge and Walter Zuern for their continuous support during the whole work.